ARC8

ON THE CHARACTERIZATION OF IMPACT PROPERTIES OF ENGINEERING MATERIALS. AN ACOUSTO-ULTRASONICS PATTERN RECOGNITION APPROACH

Gustavo José Molina

A thesis submitted to the Faculty of Graduate Studies and Research in partial fulfillment of the requirements of the degree of Master of Applied Science in Mechanical Engineering.

Department of Mechanical Engineering
University of Ottawa

Ottawa-Carleton Institute for Mechanical and Aerospace Engineering

Ottawa, Canada.
September, 1994.

"...I clung to my notion, ill-defined though it was, that a serious study of any important body of human knowledge, or theory, or belief, if undertaken with a critical but not a cruel mind, would in the end yield some secret, some valuable permanent insight, into the nature of life and the true end of man." (Robertson Davies, 'Fifth Business', Macmillan of Canada, Toronto, 1970).

To my parents and my fiancée Gabriela.

ABSTRACT

This thesis describes the experimental work carried out at the University of Ottawa for the characterization of the residual impact properties of polymeric material systems; namely, Polyvinylchloride and graphite/polycarbonate composite. In this context, the nondestructive Acousto-Ultrasonics (AU) technique in conjunction with Pattern Recognition and Classification methods were used. The material specimens, which present different levels of controlled low-energy repeated impact damage, were also evaluated destructively by Falling Weight Impact and Uniaxial Tensile tests. The results of these destructive tests were used to correlate and verify the AU measurements.

A review of nondestructive evaluation methods, with a focus on the Acousto-Ultrasonics technique used in this thesis is presented. Analysis techniques of AU data are introduced. The Pattern Recognition and Classification methodology is reviewed for its application to identify AU signals. Fundamentals of the Falling Weight Impact Test used are also presented.

The values of the Mean Failure Energy for the samples of the mentioned two materials, as obtained from Falling Weight Impact Test, were found to correlate with the damage states of these samples, as measured by the applied number of controlled repeated-impacts. Also, the values of the Acousto Ultrasonics Parameter, calculated from the retrieved AU signals, were found to correlate with the Mean Failure Energy and Ultimate Tensile Strength values that were obtained from the destructive tests. Identification of the AU signals pertaining to the considered levels of impact damage was performed by means of Pattern Recognition and Classification techniques.

The results obtained indicate that a characterization of low-energy repeated impact conditions in the mentioned two polymeric materials can be based on measurements of the Mean Failure Energy, obtained from Falling Weight Impact testing of samples of specimens. Further, the predictions of the residual impact properties of the two materials can be made by Acousto Ultrasonics, in conjunction with Pattern Recognition and Classification techniques.

ACKNOWLEDGEMENTS

I would like to express my sincere gratitude to my supervisor Professor Y.M.Haddad for his valuable suggestions, guidance, continuous encouragement, and generous help during the course of this study. The design of the Acousto-Ultrasonics System used in this research is based primarily on his ideas, which were implemented in cooperation with Tektrend International Inc., Montréal, Canada.

I am grateful to the Natural Sciences and Engineering Research Council of Canada for the financial support provided for this research through the operating grant of my reseach supervisor. The tuition and fee waiver as well as the entrance scholarship granted to me by the School of Graduate Studies and Research of the University of Ottawa during my master program are sincerely appreciated.

I also thanks the CIMM-INTI (Materials and Metrology Research Centre-National Institute for Industrial Technology) of Argentina, for granting me the study leave to pursue this research work.

I would like also to express my acknowledgements to the staff of the Department of Mechanical Engineering of the University of Ottawa. Finally, I wish to thank the Centre des Matériaux Composites-CEGEP de Saint Jérôme for the supply of the composite material needed for this research.

TABLE OF CONTENTS

ABSTRACT	i
ACKNOWLEDGEMENTS	ii
TABLE OF CONTENTS	iii
LIST OF SYMBOLS	xi
LIST OF TABLES	xv
LIST OF FIGURES	xviii
CHAPTER 1	
INTRODUCTION	1
1.1. General	1
1.2. Statement of the Problem	2
1.3. Objectives and Plan of the Research	4
1.4. Presentation of the Research Work	6

CHAPTER 2

REVIEW OF NON-DESTRUCTIVE TESTING TECHNIQUES BASED ON WAVE PROPAGATION 9

2.1. Introduction 9

2.2. Wave Propagation QNDE Techniques 12

2.2.1. Wave Propagation in Non-Destructive Testing 12

2.2.2. Pulse Echo NDE Techniques 18

2.2.3. Through-Transmission Techniques 21

2.2.4. Surface and Lamb Wave Techniques 23

2.2.5. Resonance Methods 25

2.2.6. Ultrasonic Spectroscopy Techniques 27

2.2.7. Acoustic Emission Technique 28

2.3. Acousto-Ultrasonics Technique 32

2.3.1. Introduction 32

2.3.2. Acousto-Ultrasonics Hypothesis 33

2.3.3. Acousto-Ultrasonics Transducer Configuration and Instrumentation 34

2.3.4. Acousto-Ultrasonics Signals 37

2.4. Conclusions 40

CHAPTER 3

REVIEW OF SIGNAL ANALYSIS TECHNIQUES FOR ACOUSTO-ULTRASONICS 43

3.1. Introduction 43

3.2. Acousto Ultrasonic Wave-Propagation Measurements 45

3.3. Acousto-Ultrasonic Waveform Parameters 46
3.3.1. Peak Voltage Stress Wave Factor 48
3.3.2. Ringdown Stress Wave Factor 49
3.3.3. Acousto-Ultrasonics Parameter (Weighted Ringdown SWF) 51
3.3.4. Energy Integral Stress Wave Factor 53
3.3.5. Homomorphic Signal Processing 54
3.3.6. Partition-Regression Method 55

3.4. Stress Wave Factor Normalization 56

3.5. Acousto-Ultrasonics Data Acquisition 57
3.5.1. External Factors affecting AU Data Acquisition 58
3.5.2. Internal Factors affecting AU Data Acquisition 62

3.6. Conclusions 64

CHAPTER 4
REVIEW OF PATTERN RECOGNITION AND CLASSIFICATION APPROACH 66

4.1. Introduction 66

4.2. Fundamentals for the Design of Pattern Recognition Systems 67

4.3. Pattern Preprocessing and Feature Selection of AU Signals 74

4.4. Pattern Classification by Distance Functions 77
4.4.1. Linear Discriminant Pattern Classifier 78
4.4.2. Minimum-Distance Pattern Classifier 85
4.4.3. Nearest Neighbour Pattern Classification 86
4.4.4. K-Nearest Neighbour Pattern Classifier 88

4.5. Pattern Classification by Likelihood Functions 89
4.5.1. Bayes Classification for minimum risk 91
4.5.2. Bayesian Classifier for normal distributed patterns 92

4.6. Pattern Recognition System Design for Acousto-Ultrasonic Signals 93
4.6.1. AU-Signal Transformation and Feature Extraction 95
4.6.2. AU-Signal Feature Selection 97

4.7. Conclusions 99

CHAPTER 5
REVIEW OF IMPACT-PROPERTY TESTING TECHNIQUES FOR POLYMERIC BASE MATERIALS 101

5.1. Introduction 101

5.2. Impact Testing of Polymers 103
5.2.1. Standard Impact-Tests for Polymeric Materials 104
5.2.1.1. Standard Izod and Charpy Tests for Polymeric Materials 106
5.2.1.2. Standard Tensile Impact Test for Polymeric Materials 108

5.2.1.3. Standard Falling-Weight Impact Tests for Polymeric Materials 109
5.2.1.4. Instrumented Impact Testing 114

5.3. True Sensitivity Experiments 115
5.3.1. The Probit Method 117
5.3.2. The Up-and-Down Method 117
5.3.3. Modified Up-and Down Method for Small Samples 119

5.4. Conclusions 123

CHAPTER 6
EVALUATION OF REPEATED-IMPACT DAMAGE IN SOLID POLYMERS 126

6.1. Introduction 126

6.2. Material and Test Specimens 129

6.3. Controlled Repeated-Impact Procedure 129

6.4. Acousto-Ultrasonics data acquisition 131

6.5. Falling-Weight Impact Testing 133

6.6. Experimental Results 135
6.6.1. Characterization of Polymer Repeated-Impact Properties by Falling-Weight Impact Test 135

6.6.2. Characterization of Polymer Repeated-Impact Properties by Acousto-Ultrasonics 136
6.6.3. Characterization of Polymer Repeated-Impact Properties by Uniaxial Tensile Testing 139
6.6.4. Correlation of Uniaxial Tensile Test Results and Acousto-Ultrasonic Data 139

6.7. Discussion of the obtained characterizations 141

6.8. Conclusions 143

CHAPTER 7
PATTERN RECOGNITION APPROACH TO THE EVALUATION OF REPEATED-IMPACT DAMAGE IN SOLID POLYMERS 147

7.1. Introduction 147

7.2. Experimental Pattern Recognition and Classification of AU-Signals 148

7.3. Experimental Feature Extraction and Normalization 150

7.4. Feature Selection and Classifier Building 154

7.5. Training and Evaluation Performances of the Classifiers 158

7.6. Testing of the Classification Performances 159

7.7. Experimental Results of Pattern Recognition and Classification 160
7.7.1. Material and Test Specimens 160
7.7.2. Experimental Training and Evaluation Performances 161
7.7.3. Experimental Classification Performances 163
7.7.4. Discussion of the obtained Classification Performances 164

7.8. Conclusions 166

CHAPTER 8
EVALUATION OF REPEATED-IMPACT DAMAGE IN
POLYMERIC-MATRIX COMPOSITES 168

8.1. Introduction 168

8.2. Material and Test Specimens 170

8.3. Controlled Repeated Impact Damage 171

8.4. Acousto-Ultrasonics Data Acquisition 172

8.5. Experimental Results 174
8.5.1. Characterization of Composite Repeated-Impact Properties by Falling-Weight Impact Tests 174
8.5.2. Characterization of Composite Repeated-Impact Properties by Acousto-Ultrasonics 175
8.5.3. Characterization of Composite Repeated-Impact Damage by Uniaxial Tensile Test 176
8.5.4. Discussion of the obtained characterizations of Polymer-Matrix Composites 177

8.6. Pattern Recognition and Classification Analysis of Composite Repeated-Impact Damage 180

8.6.1. Classifier Design 180

8.6.2. Performances of Classifiers for Training, Evaluation and Testing of Classification 183

8.7 Conclusions 187

CHAPTER 9

CONCLUSIONS AND REMARKS 190

9.1. Conclusions 190

9.2. Remarks 192

REFERENCES 195

APPENDIX A DECISION RULES FOR PATTERN CLASSIFICATION 206

A.1. Linear Discriminant Decision Rule 206

A.2. Bayes' Decision Rule of Classification for minimum risk 209

A.3. Bayes' Decision Rule for normally distributed patterns 218

APPENDIX B FALLING WEIGHT IMPACT TEST RESULTS AND ESTIMATES OF MEAN FAILURE ENERGY FOR THE TESTED SAMPLES 223

FIGURES 235

LIST OF SYMBOLS

AUP	Acousto-Ultrasonics Parameter.
AUP_N	Normalized Acousto-Ultrasonics Parameter.
C	Digital count of oscillations per waveform.
c_i	Number of counts at the i-th voltage level.
C_S	Classification Space.
C_i	Covariance matrix of the class ω_i.
$\vert C_i \vert$	Determinant of the covariance matrix of the class ω_i.
D	Thickness of a plate or specimen.
d	Variable-Level Interval for a trial in the Up-and-Down Method.
D_i	Euclidean distance between a pattern vector and the prototype pattern of class ω_i.
d_i	i-th decision function.
$d^*(x_j)$	Optimum decision function.
d_{kl}	Decision function for the particular case defined in Equation (4.14).
E	Young's Modulus.
E_V	Maximum voltage oscillation.
$E_i\{\quad\}$	Expectation operator.
f	Frequency of the waveform.
F_S	Feature Space.
F	Frequency interval.
F_{j12}	Fisher Discrimination Ratio for feature j between two classes 1 and 2.

f_D	Frequency of a resonance standing wave.
G	Modulus of Rigidity.
h_i	Measured value of the variable h for the i-th trial carried under the Up-and-Down Method.
K	Number of sample patterns under consideration in a K-Nearest Neighbour Classification.
k	Function defined in equation (5.3).
L	Loss function associated with the risk of misclassification.
M	Number of classes under consideration.
MFE	Mean Failure Energy.
MFE_N	Normalized Mean Failure Energy.
N	Nominal number of trials of the Up-and-Down Method.
n	Number of features under consideration.
N'	Total number of trials of the Up-and-Down Method.
n_o	Number of passes for an Up-and-Down Method test.
n_x	Number of fails for an Up-and-Down Method test.
P_{50}	Value of a variable P for the probability of fail of 50% of the sample.
$p(\omega_i)$	Probability of ocurrence of class ω_i.
$p(x\|\omega_i)$	Multivariate probability density function of the feature x in the class ω_i.
$p(\omega_i, x_j)$	Joint probability density function of the feature x_j ocurring and being represented by the values of feature j in the class ω_i.
P_S	Pattern Space.
R	Average loss of taking the decision of assigning a pattern to a class.
R_P	Repetition rate of the ultrasonic pulse.
r	Risk of taking the decision of assigning a pattern to a class.

SWF	Stress Wave Factor.
s	Estimate of the standard deviation.
s_f	Waveform voltage in frequency domain.
T	Time interval.
T_R	Totalizer reset time.
U	Measured energy for either a Charpy or an Izod test.
U_A	Energy to accelerate the specimen from rest in either a Charpy or an Izod test.
U_{SD}	Energy to bend the specimen in either a Charpy or an Izod test.
U_B	Energy consumed by Brinnel deformation under the nose of the hammer in either a Charpy or an Izod test.
U_{MV}	Energy absorbed by the machine through vibration after initial contact in either a Charpy or an Izod test.
U_M	Energy stored by the machine in either a Charpy or an Izod test.
UTS	Ultimate Tensile Strength.
UTS_N	Normalized Ultimate Tensile Strength.
V	Time varying waveform voltage.
v	Speed of either longitudinal or transverse wave.
v_L	Speed of propagation of a longitudinal wave.
v_T	Speed of propagation of a transversal wave.
V_i	Voltage at the i-th level above the voltage threshold.
V_P	Voltage peak amplitude in time domain of the waveform.
w_{ij}	Matrix arrangement for i pattern-vectors of j feature values.
$w_{i,n+1}$	Constant vector defined in Equation (4.11).
x	Normalized pattern vector.

x_j	Value of feature j for the pattern vector x.
X_n	n-feature space.
z_i	Prototype pattern of the class ω_i.
α	Pattern vector pertaining to the measured values of time-varying waveform.
δ_{ij}	Kronecker delta function.
λ	Likelihood Ratio.
λ_D	Wavelength of a resonance standing wave.
μ	Estimate of the arithmetic mean.
μ_i	Mean vector for the class ω_i.
ν	Poisson's ratio.
ξ_j	Normalized value for feature j.
ρ	Mass Density.
ω_i	i-th pattern class.

LIST OF TABLES

Table 3.1.	Repeatability of Acousto-Ultrasonics Parameter measurements pertaining to three polyvinylchloride specimens for the transducer setup of Figure 3.4. Threshold value: 32 mVolts. Input Frequency: 750 KHz	61
Table 7.1.	Ranking based on Fisher Discrimination Ratio of the twelve best discriminating features for the classification of polyvinylchloride specimens.	156
Table 7.2.	Average of Training and Evaluation perfomances in % of correctly classified AU signals for polyvinylchloride specimens.	161
Table 7.3.	Classification perfomances in % of correctly classified AU signals for polyvinylchloride specimens.	163
Table 8.1.	AU controlled parameters for graphite/polycarbonate composite specimens.	172
Table 8.2.	Ranking based on Fisher Discrimination Ratio of the twelve best discriminating features for the classification of graphite/polycarbonate composite specimens.	182
Table 8.3.	Average of Training and Evaluation perfomances in % of correctly classified AU signals for graphite/polycarbonate composite specimens.	184
Table 8.4.	Classification performances in % of correctly classified AU-signal for graphite/polycarbonate composite specimens.	185
Table B.1.	Values of the coefficient k to estimate P_{50} from an Up-and-Down sequence of trials of nominal number N.	223

Table B.2. Values of the coefficients A and C to estimate P_{50} from an Up-and-Down sequence of trials of nominal number N, for $N > 6$. 224

Table B.3. Results of Falling-Weight Impact Test for the sample of polyvinylchloride specimens of non-impact damage level. 225

Table B.4. Results of Falling-Weight Impact Test for the sample of polyvinylchloride specimens of five-impact damage level. 226

Table B.5. Results of Falling-Weight Impact Test for the sample of polyvinylchloride specimens of ten-impact damage level. 227

Table B.6. Results of Falling-Weight Impact Test for the sample of polyvinylchloride specimens of fifteen-impact damage level. 228

Table B.7. Results of Falling-Weight Impact Test for the sample of polyvinylchloride specimens of twenty-impact damage level. 229

Table B.8. Results of Falling-Weight Impact Test for the sample of graphite/polycarbonate composite specimens of non-impact damage level. 230

Table B.9. Results of Falling-Weight Impact Test for the sample of graphite/polycarbonate composite specimens of one-impact damage level. 231

Table B.10. Results of Falling-Weight Impact Test for the sample of graphite/polycarbonate composite specimens of three-impact damage level. 232

Table B.11. Results of Falling-Weight Impact Test for the sample of graphite/polycarbonate composite specimens of four-impact damage level. 233

Table B.12. Results of Falling-Weight Impact Test for the sample of graphite/polycarbonate composite specimens of six-impact damage level. 234

LIST OF FIGURES

2.1. Instrumentation setup for NDE Pulse Echo technique. 235

2.2. Instrumentation setup for NDE Trough Transmission technique. 236

2.3. Instrumentation setup for NDE Surface and Lamb Wave technique. 237

2.4. Instrumentation setup for NDE Acousto-Ultrasonics technique. 238

2.5. Diagram of some reflections paths of ultrasonic waves in a flat homogeneous solid. (From Vary, A., ref. [33]). 239

2.6. Ultrasonic pulse input and retrieved Acousto-Ultrasonics signal for a flat polyvinylchloride specimen. Input frequency: 750 KHz. Distance between transducers: 3/4". 240

3.1. Instrumentation setup for the measurement of Ringdown Stress Wave Factor. (From Henneke,E.G., ref. [3]). 241

3.2 Schematics for the calculation of Acousto-Ultrasonics Parameter. 242

3.3. Transducer setup for the experimental evaluation of the factors affecting Acousto-Ultrasonics data acquisition. 243

3.4. Sensitivity of AU measurements to distance between transducers. Acousto Ultrasonics Parameter versus distance between emitter and receiver transducers for polyvinylchloride specimens. 244

3.5. Sensitivity of AU measurements to contact pressure applied to transducers. Ringdown Stress Wave Factor versus contact pressure applied to emitter and receiver transducers. (From Russell-Floyd,R. and Phillips,M.G., ref. [45]). 245

3.6. Sensitivity of AU measurements to contact pressure applied to transducers. Coefficient of variation of Ringdown Stress Wave Factor, as the ratio of standard deviation to mean of the measured values, versus contact pressure. (From Russell-Floyd,R. and Phillips,M.G., ref. [45]). 246

3.7. Constant-force clamp configuration to apply relative contact pressure between transducers and the specimen in an Acousto-Ultrasonics experiment. 247

3.8. Sensitivity of AU measurements to the ultrasonic input frequency. Acousto Ultrasonics Parameter versus frequency of the emitted ultrasonic pulse for polyvinylchloride specimens. 248

4.1. Linear Discriminant Decision Function d(x) for two classes in a two-dimension feature-space. Each class is characterized by a single prototype pattern. 249

4.2. "First Case" of linearly separable classes in a two-dimension feature space. The three classes are separated by linear boundaries pertaining to linear discriminant decision functions $d_i(x)$. Each class is characterized by a single prototype pattern. 250

4.3. "Second Case" of linearly separable classes in a two-dimension feature space. Each of the three classes is separated by two linear boundaries pertaining to linear discriminant decision functions $d_i(x)$. Each class is characterized by a single prototype pattern. 251

4.4. "Third Case" of linearly separable classes in a two-dimension feature space. Each of the three classes is separated by two linear boundaries pertaining to linear discriminant decision functions $d_i(x)$. Each class is characterized by a single prototype pattern. 252

4.5. One-Nearest Neighbour Classification of pattern 'x' for two classes ω_1 and ω_2 in a two-dimension feature-space. 253

4.6. Three-Nearest Neighbour Classification of pattern 'x' for two classes ω_1 and ω_2 in a two-dimension feature-space. 254

6.1. Polyvinylchloride specimen for the evaluation of repeated impact damage. 255

6.2. Experimental apparatus for controlled repeated-impact procedure. 256

6.3. Transducer setup for the Acousto-Ultrasonics evaluation of repeated impact damage in polyvinylchloride specimens. 257

6.4. Acousto-Ultrasonics equipment and setup for AU data acquisition. 258

6.5. Ultrasonic pulse input and Acousto-Ultrasonics readings for different levels of repeated-impact damage in polyvinylchloride specimens.
From top to bottom: - Ultrasonic pulse input
- AU reading for five-impact damage level
- AU reading for ten-impact damage level
- AU reading for twenty-impact damage level 259

6.6. "Mean Failure Energy" versus number of repeated impacts for polyvinylchloride specimens. 260

6.7. "Normalized Acousto-Ultrasonics Parameter" versus "Normalized Mean Failure Energy" for polyvinylchloride specimens. 261

6.8. Ultimate Tensile Strength versus number of repeated impacts for polyvinylchloride specimens. 262

6.9. "Normalized Acousto Ultrasonics Parameter" versus "Normalized Ultimate Tensile Strength" for polyvinylchloride specimens. 263

6.10. Comparison of the two expressions (6.6) and (6.7) relating "Normalized Mean Failure Energy" and "Normalized Ultimate Tensile Strength" in polyvinylchloride Specimens. 264

7.1. Schematics of the feature extraction, feature normalization and feature-value splitting for Acousto-Ultrasonics data. 265

7.2. Classifier Tree. Arrangement of Acousto-Ultrasonics data files pertaining to repeated-impact damage classes of polyvinylchloride specimens. 266

7.3. Normalization Tree file-arrangement for feature extraction and normalization of Classifier Sets pertaining to polyvinylchloride specimens. 267

7.4. Schematics of the building and testing of the AU-Classifiers from files of normalized feature-values. 268

7.5. Classification performances for Empirical Bayesian Classifiers pertaining to the number of features used for Classifier building. 269

7.6. Classification performances for Linear Discriminant Classifiers pertaining to the number of features used for Classifier building. 270

7.7. Classification performances for K-Nearest Neighbour Classifiers pertaining to the number of features used for Classifier building. 271

7.8. Classification performances for Minimum Distance Classifiers pertaining to the number of features used for Classifier building. 272

7.9. Training and Evaluation performances for the four designed classifiers of Acousto-Ultrasonics signals pertaining to repeated-impact damage classes of polyvinylchloride specimens. 273

7.10. Normalized values of the two best-ranked features for Training and Evaluation Sets of Acousto-Ultrasonics data pertaining to repeated-impact damage levels in polyvinylchloride specimens. 274

7.11. Classification Performances in % of correctly classified AU-signals for the four designed classifiers of Acousto-Ultrasonics signals pertaining to repeated-impact damage classes of polyvinylchloride specimens. 275

7.12. Probability Density Functions of the first ranked feature for Acousto-Ultrasonics data pertaining to repeated-impact damage classes of polyvinylchloride specimens. 276

7.13. Probability Density Functions of the second ranked feature for Acousto-Ultrasonics data pertaining to repeated-impact damage classes of polyvinylchloride specimens. 277

7.14. Normalized values of the two best-ranked features for Testing Sets and Classifier-Set boundaries for Acousto-Ultrasonics signals pertaining to repeated-impact damage levels of polyvinylchloride specimens. 278

8.1. "Mean Failure Energy" versus number of repeated impacts for graphite/polycarbonate composite specimens. 279

8.2. "Normalized Acousto-Ultrasonics Parameter" versus "Normalized Mean Failure Energy" for graphite/polycarbonate composite specimens. 280

8.3. Ultimate Tensile Strength versus number of repeated impacts for graphite/polycarbonate composite specimens. 281

8.4. Ultimate Tensile Strength versus number of repeated impacts for "failed" and "surviving" graphite/polycarbonate composite specimens. 282

8.5. "Training" and "Evaluation" performances in % of correctly classified AU-signals for the four designed classifiers of Acousto-Ultrasonics signals in graphite/polycarbonate composite specimens. 283

8.6. "Classification" performances in % of correctly classified Acousto-Ultrasonic signals for the four designed classifiers in graphite/polycarbonate composite specimens. 284

8.7. Normalized values of the two best-ranked features from Acousto-Ultrasonic signals pertaining to repeated-impact damage levels in graphite/polycarbonate composite specimens. 285

8.8. Normalized values of the second and third best-ranked features from Acousto-Ultrasonic signals pertaining to repeated-impact damage in graphite/polycarbonate composite specimens. 286

CHAPTER 1

INTRODUCTION

1.1. General

Polymeric base materials are increasingly used as structural components in industrial applications where metals were the major choices until recent years. Their advantages over metals in weight, cost and ease of fabrication and shaping have been recognized since early times. A growing industrial application of solid polymers is observed when they are used in structural components as part of the so-called polymeric-matrix composite systems.

Structural worthiness of polymeric base material systems may be, however, affected by a variety of damaging conditions under ordinary service loading conditions. Understanding of the mechanisms by which those damaging conditions relate to the mechanical properties of the polymeric base materials is essential.

Both design with existing polymeric base materials and development of new polymeric systems of improved or new properties will benefit from this knowledge. Also, techniques to evaluate the deterioration states affecting in-service polymeric base structural components should complete this understanding. In this, quantitative non-destructive testing techniques are seen as the appropriate approach.

1.2 Statement of the Problem

Impact loading may degrade the mechanical properties of polymeric base materials without changes in visual appearance or the presence of overt flaws. The conditions that are revealed in the reduction of the impact strength of these materials may consist of, for instance, dispersed microstructural damage. Low-energy impact, when applied in a repeated manner, may reduce the impact-resistance of pure polymers and polymeric composite systems. Hence, it is important at the design stage to predict the impact-strength reduction of these materials for a given low-energy repeated-impact loading. Moreover, when an in-use polymeric base component has undergone repeated-impact loading, it is necessary to quantify how much its structural ability to withstand subsequent impacts may have been affected.

The impact strength of engineering materials is customarily measured by standard destructive impact tests, e.g., Charpy and Izod impact tests, which require the use of strict-dimension specimens. However, polymeric base material sensitivity to the method of specimen machining and/or fabrication significantly affect specimen properties. Therefore, the structural worthiness of polymeric base material parts presenting low-energy repeated-impact conditions will hardly be assessed or predicted by these tests. Instead, the standard Falling-Weight Impact Test is indicated to test solid polymer parts and may be the most appropriate to evaluate the impact-strength reduction of polymeric-base material parts due to low-energy repeated impact loading.

Since standard impact tests are essentially destructive, Non-Destructive Examination (NDE) techniques are called upon to assess impact-strength reduction of pure polymers and polymeric base composite systems when degrading conditions are likely to affect the mechanical properties of in-service structural components. Although most of the NDE techniques are sensitive to flaws or voids in the tested material, few of them can quantitatively evaluate overall degradation of mechanical properties.

Acousto-Ultrasonics (AU) is a relatively new NDE technique that has been successfully used to nondestructively quantify mechanical properties in materials showing high attenuation of ultrasonic waves, e.g., pure polymers and polymeric-base composite systems, for which traditional non-destructive techniques have proven to be unsuccessful.

Acousto-Ultrasonics signals are usually quite difficult to analyse. A recently introduced approach to ultrasonic-signal analysis is the Pattern Recognition and Classification methodology. It leads to the evaluation of a material state by the identification of the signal data as belonging to a class. In this, a so-called Pattern

Classifier may be designed for this purpose using AU data from different material samples, where each material sample represents a state of the material property.

1.3. Objectives and Plan of the Research

The main objective of the present research is to assess the feasibility of evaluating low-energy repeated-impact damage in polymeric base material systems. In particular, characterizations of the residual impact properties of solid polymer and polymeric-matrix composite specimens presenting low-energy repeated-impact conditions are carried out.

To this purpose, controlled repeated-impact is performed on the material specimens by dropping onto each standard specimen a constant weight from a fixed height a predefined number of times. Discrete levels of impact damage, determined by the final number of controlled repeated impacts applied to each material specimen, are obtained.

Characterization of the obtained levels of impact damage of the specimens is carried out by means of both nondestructive and destructive evaluation techniques. In the nondestructive approach, Acousto-Ultrasonics technique is used. In this, analysis of the retrieved AU signals is carried out by both a single-parameter description and a multivariate recognition and classification method. The former is based on the calculation of the ultrasonic-wave energy transmitted through the material, while the latter makes use of the Pattern Recognition and Classification methodology.

In the destructive evaluation approach, the residual impact strength is quantified by using Falling-Weight Impact testing of samples of material specimens, where each sample comprises the material specimens pertaining to one of the considered levels of repeated impact. Also, the residual tensile strength of the material specimens is quantified by using uniaxial tensile test.

The values obtained by the Falling Weight Impact testing of the material specimens are correlated with the considered levels of repeated impact, as measured by the final number of impacts pertaining to each level. Also, the values obtained by the uniaxial tensile testing of the material specimens are correlated with the final number of impacts of the considered levels of impact. The values of both destructive tests are, then, aplied to correlate with and to verify the Acousto-Ultrasonics measurements.

Appropriate software and hardware environments provide the capabilities of extracting values of characteristic features from the Acousto-Ultrasonics data. For the purposes of Pattern Recognition and Classification, multiple-feature descriptions of the AU signals are grouped as belonging to different classes pertaining to the considered levels of repeated-impact. This process leads to a Pattern Classifier for the identification of the repeated-impact damage state of a given material specimen.

1.4. Presentation of the Research Work

The non-destructive characterization carried out in the experimental work of this thesis is performed by an ultrasonic-wave based technique. Chapter 2 presents a review of some non-destructive techniques based on wave mechanical propagation with a focus on the Acousto-Ultrasonics (AU) technique used. A literature review on previous research work, concerning the applications of AU to evaluate impact-properties in polymeric base materials, is also presented. Chapter 3 presents some of the parameters used for the quantitative analysis of Acousto-Ultrasonics signals. A literature review on the factors that affect Acousto-Ultrasonics data acquisition is also presented. The experimental results of the preliminary experiments carried out on the influence of these factors in the thesis experimental work are included.

Chapter 4 deals with the concept of Pattern Recognition and Classification technique as an approach to the identification and classification of AU data. Its mathematical basis are presented. The available software environment to perform such analysis approach is described.

Chapter 5 presents a review of impact-property testing techniques. Testing methodology and standard tests to characterize impact strength of polymeric materials is discussed. A literature review on the statistical methods that apply to impact testing of polymeric base materials is also included.

Chapter 6 presents the experimental work carried out to evaluate the residual impact-properties of specimens of the solid polymer Polyvinylchloride presenting low-energy repeated-impact damage. Both destructive and nondestructive testing methodologies are used. Different levels of impact damage are obtained by controlled low-energy repeated impact of standard specimens. Acousto-Ultrasonics signals are retrieved from these specimens. The residual impact strength is then evaluated destructively by means of both Falling Weight Impact and Uniaxial Tensile tests. The values from these destructive tests are correlated with the considered levels of impact, as measured by the final number of controlled repeated impacts applied onto each specimen. Also, a parameter of the efficiency of ultrasonic-energy transmission through the test specimens is correlated with the results of the mentioned two destructive tests for the considered levels of impact.

Chapter 7 presents an application of the Pattern Recognition and Classification analysis of AU data to identify the repeated-impact damage states of the polymer specimens. Pattern Recognition classifiers are designed for the considered levels of repeated-impact damage taken as classes of the pertaining AU signals,which were previously retrieved from the Polyvinylchloride specimens. Finally, the identification ability of each classifier is tested by means of AU data obtained from specimens different to those used in the classifier design. The classifier performances from this testing are compared.

Chapter 8 presents the experimental work carried out on the application of the techniques developed in the Chapters 6 and 7 to evaluate the residual impact-properties of a graphite fibre/polycarbonate matrix composite system. An assessment is carried out of the possibility to characterize the low-energy repeated impact states in the composite specimens by means of destructive testing, Acousto-Ultrasonics methods and Pattern Recognition and Classification of AU signals.

Conclusions and remarks are presented in Chapter 9.

Chapter 2

REVIEW OF NON-DESTRUCTIVE TESTING TECHNIQUES BASED ON WAVE PROPAGATION

2.1. Introduction

The traditional purpose of Non-Destructive Examination (NDE) of engineering materials and structures is to provide a basis for determining whether they will perform reliably when placed in service. Hence, NDE's main interests are conventionally focused on the detection, orienting and sizing of flaws, as well as on the determination of which flaws would constitute critical defects and could be harmful to the performance and/or safety of the structural component.

This use of NDE techniques for the assessment of uniformity, serviceability and quality control of materials and components is a well-established practice in both industrial and research fields. The majority of NDE techniques are to detect and size material imperfections so that a decision about expected performance can be made. Few NDE techniques have been directed towards the quantitative evaluation of mechanical properties of materials.

Development of new materials constantly creates needs for new NDE methods. Such NDE methods have to answer not only the incoming problems of flaw detection and characterization of new materials but also those of the application of NDE to quantitatively characterize new-material properties.

Also, the use of traditional and new materials for new purposes poses strict requirements on the non-destructive assessment of component serviceability. Metals, ceramics, polymers and their combined composites may appear free of critical-size defects but would still be susceptible to failure under design loads due to diminished mechanical properties. By similar rationale, structural components with defective conditions may still be suitable for their intended use.

New NDE techniques as well as new analysis approaches are needed to verify the design requirements in a variety of engineering applications and particularly the critical ones. In the latter, the risk cannot be taken of having a structural component in a batch or an in-service structural part whose mechanical properties are below a minimum acceptance limit. In these circumstances, it is no longer sufficient to devise new methods for revealing actual flaws. An additional requirement is now imposed that NDE techniques must be able to detect nonuniformity in the properties of materials and to assess the significance of such nonuniformity in terms of its effects on the mechanical properties of the structural component. Therefore, needs are posed for new techniques pertaining to the so-called non-destructive quantitative evaluation of material properties. The ultimate purpose of these techniques is the assessment of the variations in material properties by nondestructive measurements.

When NDE is used to quantify material properties, it is referred to as Quantitative Non-Destructive Examination (QNDE); see, e.g., ref. [1]. When referring, however, to the broader field of NDE, the name Non-destructive Testing (NDT) applies.

At present, QNDE techniques are usually performed by means of some layout and equipment that are derived from those of NDT. However, their use as a non-destructive alternative to the traditional destructive testing often needs more sophisticated methodologies. Also, analysis techniques based on new concepts are increasingly used to relate the nondestructively retrieved data to the material properties of the inspected specimen; see, for instance, ref. [2].

The present chapter reviews the fundamentals of some QNDE that are based on sonic and ultrasonic wave propagation. A relatively new technique that applies to the experimental work of this thesis is the so-called Acousto-Ultrasonics Technique. Aspects relating to the application of this technique are particularly dealt with.

2.2. Wave-Propagation QNDE Techniques

The broad field of wave-propagation NDE includes a variety of testing methods. They are based on the principle of investigating the material by means of interactions of mechanical waves with the material microstructure and on the analysis of the retrieved data by considering such interactions. Wave-propagation NDE practice is generally performed by high-frequency mechanical vibrations above the audible range, which are input into the material specimen. This characteristic gives the more usual name of "ultrasonic" to the nondestructive techniques based on ultrasonic wave propagation that are used in practice.

As mentioned earlier, most of the present QNDE techniques and equipment are derived from well-established NDE methodologies. Because of the complex wave-interactions QNDE has to deal with, understanding of the different types of propagating waves that may be found when performing QNDE is necessary.

2.2.1 Wave Propagation in Non Destructive Testing

A wave can be defined as a transient phenomenon that conveys energy through space. Mechanical waves must have a propagating medium for transmission to occur. A mechanical wave may be understood as a sharp discontinuity of either stress, strain, particle velocity, particle acceleration or any other mechanical quantity that travels through a propagating medium at a finite velocity. Hence, a suitable description of a mechanical wave may be based on its physical attributes such as displacement, strain, stress and mass density and their derivatives with respect to time; see, e.g., ref. [3].

Propagating-wave characteristics depend on the input-wave frequencies and amplitudes, as well as on the mechanical properties and geometry of the propagating medium. Some classifications of mechanical waves in solids are conventionally established, for instance, by consideration of the propagating medium geometry and its extent. Two broad classifications of mechanical waves in solids, for instance, are:

- Waves in infinite media;
- Waves in semi-infinite and finite media.

Waves in infinite media, also called "bulk waves," propagate through a medium which is large enough to be considered infinite when compared with the wavelength. In this case, interactions of the wave with material boundaries do not affect the major characteristics of the wave propagation. On the other hand, waves in semi-infinite and finite media include the whole variety of waves resulting from interactions of input waves with matter in media of relatively finite sizes.

When waves in infinite media are dealt with, they may be classified into two classes with respect to the relative direction of their particle and wave displacements:

- When the particle displacement is in the same direction of that of the propagation, the resulting wave is referred to as "longitudinal."
- When particle displacement is perpendicular to the direction of propagation of the wave that originates it, the wave is termed "transverse" (also, shear or distortional).

Although in practice both types of waves are always present, either from the starting incidence-angle effect or because of following reflections within the medium, a description of the occurring wave propagation phenomenon in terms of only one type of waves is often possible.

The speed of propagation of a longitudinal wave in an isotropic, elastic material is given by the following expression

$$v_L = \left[\frac{E}{\rho} \frac{1 - \nu}{(1 + \nu)(1 - 2\nu)} \right]^{\frac{1}{2}} \qquad (2.1)$$

while the speed of propagation of a transverse wave in the same type of material is expressed as follows

$$v_T = \left[\frac{G}{\rho} \right]^{\frac{1}{2}} = \left[\frac{E}{\rho} \frac{1}{2 (1 + \nu)} \right]^{\frac{1}{2}} \qquad (2.2)$$

where in the equations (2.1) and (2.2) above, E, G, ρ and ν are respectively the Young's Modulus, Modulus of Rigidity, mass density and Poisson's ratio of the propagating material medium; see, e.g., ref. [3].

These expressions of the speed of longitudinal and transverse waves in terms of the basic mechanical properties of isotropic, elastic materials suggest a method to determine these properties by measurements of the so-called "time-of-flight" of a wave in the material. If the distance traveled by the pulse is known, and the time-of-flight is measured by timing the signal during its travel, the velocity of propagation of the ultrasonic wave can be calculated for both longitudinal and transverse waves. Combining the latter two values of velocity with formulae (2.1) and (2.2), information pertaining to the mechanical properties of the isotropic, elastic medium can be obtained. A discussion concerning the applications and limitations of this simple approach is presented in Chapter 3 of this thesis.

Classifications of waves in semi-infinite and finite-media result from some issues of convenient simplification of the analysis. Some definitions of particular wave types, on which an analysis of the complex wave structure may be based, are presented below.

Surface (or Rayleigh) waves appear when bulk waves propagate parallel to the boundary of a semi-infinite medium. A surface wave is composed of one longitudinal and one transverse oscillation; hence, surface-wave velocity can be defined in terms of its longitudinal and transverse components. For an isotropic elastic medium, these components of a surface wave are in turn determined in terms of the mechanical properties of the propagating medium, according to the previously presented equations (2.1) and (2.2).

When the propagating medium is a thin plate with parallel boundaries to the direction of propagation, Plate (or also, Lamb) waves may develop. They are transverse waves that propagate in a direction parallel to the mid-plane of the plate.

Lamb waves develop when transverse waves propagating parallel to the plate mid-plane present particle displacements perpendicular to this plane. In this case, two types of particle displacements are possible:

- If the displacement fields are symmetric with respect to the mid-plane of the plate, the wave structures are called symmetric Lamb waves. They correspond to expansions and contractions of the thickness of the plate.
- If the displacement fields are antisymmetric with respect to the mid-plane, the wave structures are termed as antisymmetric (also flexural) Lamb waves. They correspond to flexing vibrations of the plate.

Dispersive effects are important in ultrasonic experimental studies. A propagating medium is dispersive if each frequency component of an input wave travels through the medium with a different speed. This may be an effect of either geometric or physical properties.

Most ultrasonic techniques rely upon the transmission and detection of short broadband pulses. If each frequency component of an ultrasonic pulse propagates at its own velocity, the wave envelope, which results of the composition of these frequency components, will distort with time. Therefore, a very complicated waveform may develop after a broadband ultrasonic pulse travels through a dispersive material; see, e.g., ref. [1].

Heterogeneous materials show an additional phenomenon. When a medium is composed of two material phases, or is a polycrystalline material with grain sizes of the order of the wavelength, the energy of the wave that propagates through the matrix phase is scattered in all directions because of the wave interactions with the second phase. This phenomenon, called wave-scattering, can produce a strong reduction in wave-energy as it propagates. Therefore, the amount of wave-energy that can be detected after its interactions with the material microstructure may be critically reduced.

Wave-energy loss is ultimately due to absorption mechanisms through some intermediate wave scattering phenomena, each depending on an average defect size (For instance, grain size in polycristalline solids) and its ratio to the wavelength; see, e.g., ref. [3].

Further characteristics of the described types of waves will be discussed when they pertain to any of the following wave-propagation NDT techniques.

2.2.2 Pulse Echo NDE Techniques

The phenomenon of ultrasonic-pulse reflection on any void in the material specimen and on the back surface of such specimen is the principle of Pulse Echo Techniques. In this technique, a repetitive ultrasonic pulse is emitted into the tested specimen by a sending transducer and the pertaining echoes are received by the same transducer, as represented in Figure 2.1. Since the emitter inputs compressive waves into the material specimen, propagating and received signals are mostly composed of longitudinal waves; see, e.g., ref. [3].

A transducer is a device for converting electrical energy into mechanical motion or waves. The piezoelectric crystals and poled ferroelectric ceramics form the basis of most ultrasonic piezoelectric-transducer designs. In the "piezoelectric effect" there is a linear relationship between the applied stress or strain and the generated electric field. Conversely, when an electric field is applied, stress and strain result from the so-called "converse piezoelectric effect." The latter effect is used for transducer emission by applying alternating electric fields to the transducer crystal, while the former is the basis for receiving mechanical-wave signals on the same or a separate transducer.

The equipment setup for a Pulse Echo technique derives from the setup used on reflected ultrasonic-signal NDE. A typical NDE setup pertaining to a Pulse Echo technique is shown Figure 2.1. and briefly described below.

A single transducer, usually a piezoelectric-type transducer is coupled to the test specimen through a suitable couplant medium. The purpose of the couplant medium is to provide adequate wave-transmission through the interface between the transducer and the specimen. An ultrasonic signal is transmitted to the transducer by a Signal Generator at a particular repetitive rate, which has been provided by a Pulse Generator. The same pulse triggers a Time Base Generator, which sends the input for the x-axis across a cathode ray tube (CRT) display-screen in a Digitizing Oscilloscope.

The reflected portion of the ultrasonic pulse returning back to the transducer is of different magnitude of voltage. Such variations in voltage are passed to a preamplifier and shown on the Y-axis of the CRT. The obtained signal represents the wave reflections from the bottom surface and from any overt flaws in the pathway of the propagating wave.

The described equipment is usually designed to use ultrasonic probe frequencies from 250 KHz to 20 MHz, though narrower ranges are adequate for testing most engineering materials.

In addition to the analogical display of the signal, retrieved data may be digitized and processed under computer control. Principal and secondary echoes may then be analysed in time and frequency domains. Extraction of some describing features from the data may be performed if these features may be suitable to characterize material properties.

Among others, wave velocity and wave attenuation measurements taken for various probe positions on the test-specimen surface may document material variations concerning such specimen. When analysed for selected frequencies they may give experimental correlations with some material properties.

Some material properties were successfully correlated with some features of the captured pulse-echo signals. Chiou and Hahn [4] studied the relation between the complex elasticity modulus and viscosity in glass-based viscoelastic systems and the pulse-echo wave velocity and attenuation. Reynolds et al. [5] determined some relations between moisture-degradation states and pulse-echo attenuation in epoxy resin. Properties of bonded joints were largely examined by Pulse Echo techniques. Dickstein et al. [6], for instance, measured thickness of adhesive layers in aluminium-to-aluminium bond plates by interpreting the highest peaks of the pulse-echo spectrum. Alers et al. [7], also, set correlations between the cohesive shear strength of an aluminium lap joint and the longitudinal wave-velocity in the adhesive bond line.

2.2.3 Through Transmission Techniques

In the Through Transmission Techniques, two transducers, one emitting the ultrasonic pulse while the other receiving it, are aligned on opposite sides of the specimen. Since the emitter inputs compressive waves, propagating and received signals are mainly composed of longitudinal waves; see, e.g., ref. [3].

Figure 2.2. represents an experimental setup for the Through Transmission Technique. This experimental setup may be of the same configuration that is used for the Pulse Echo Technique, but with Through Transmission two-transducer configuration. Hence, for a description of signal instrumentation of this technique as shown in Figure 2.2., the reader is referred to the foregoing section 2.2.2.

The main limitation of the Trough-Transmission Technique may be that the ultrasonic wavelength must always be less than the through-thickness of the smallest defect to be detected. In addition, some experimental difficulties may be encountered when Through Transmission Techniques are used. Probe alignment and establishing good coupling (i.e., between the transducers and the test specimen) on both sides of the specimen could prove to be difficult.

Use of immersion-bath coupling may greatly ease the implementation of this technique. With the incorporation of an automatic C-scan, by which a 2-D image of the inspected defect can be displayed, the Through Transmission Technique is often seen as common practice in material-research laboratories.

Some relations between polymer and polymer-based composite properties were obtained by correlations with features extracted from through-transmission signals. Williams and Lampert [8], for instance, established an experimental relation between residual tensile strength after repeated drop-weight impact damage and the through-transmission wave attenuation in graphite-fiber/epoxy composites. Lee and Williams [9], also, studied correlations between temperature-states in polymers and through-transmission wave attenuation and phase velocity. The latter authors proposed a numerical procedure to determine relaxation functions of polymers for different temperatures from through-transmission data.

2.2.4 Surface and Lamb Wave Techniques

If the incidence of the ultrasonic pulse is purposely at an oblique angle with respect to the specimen surface, surface and Lamb waves result. For a description of the differences between these two types of waves, the reader is referred to the foregoing section 2.2.1. Oblique incidence may be obtained by using a wedge of angle θ_0 between the emitting transducer and the specimen.

Figure 2.3. represents an experimental setup that can be used for the Surface and Lamb Wave Techniques. The experimental set up for these techniques may be the one presented earlier in Figure 2.2. for the Through Transmission Technique, but for the use of the oblique incidence. Hence, for a description of the instrumentation of Figure 2.3., the reader is referred to section 2.2.2.

Surface waves propagate on the surface of an elastic isotropic solid without dispersion down to a half-wavelength-depth. However, the surface-wave amplitude for a fixed depth diminishes with the increase of input frequency. In practice, surface-wave penetration is of the order of the wavelength. See, for instance, ref. [10].

Ultrasonic Lamb waves propagate in a plate or a tube as mode vibrations of the plate or tube. They may be understood as complex resonances modes for given frequencies that are functions of the thickness and mechanical properties of the material and of the input-signal wavelength; see, e.g., ref. [11].

In solid plates with free-boundaries, Lamb waves result in two groups of symmetrical and antisymmetrical modes. For an increasing ratio of plate thickness to wavelength, the half-amplitudes of the lowest symmetric, the lowest antisymmetric modes and a surface wave of the same wavelength become very similar. Interference of both Lamb-wave modes gives a quasi-surface wave; see, for instance, ref. [11]. Although choosing of an appropriate working point might lead to only one mode, both modes are always present in general testing practice. This explains why both surface and Lamb waves are usually referred to as a single method.

Lamb waves require a plate or a tube of uniform thickness and constant mechanical properties in order to propagate. A change in any of such parameters may cause the wave to be strongly reflected. Dumcumb and Keighley [12] concluded that Lamb wave attenuation may change as a consequence, depending on the overall effect to the resonance phenomenon. Interactions of propagating surface waves with the inspected specimen can be used in characterizing and quantifying material properties.

Kline and Hashemi [13] monitored the fatigue damage in single lap aluminium specimens by this technique. Chapman [14] used Lamb waves to evaluate the bond quality of bonded joints in fibreglass reinforced plastic. Pilarski et al. [15] studied experimental relations between interfacial weakness and bond integrity in adhesive bonded structures, and porosity and elastic moduli in composites by using Lamb wave evaluation.

2.2.5 Resonance Methods

The phenomenon of mechanical resonance for some exciting frequencies and its dependence on the specimen dimensions is the principle of NDE-Resonance Methods. In these methods, the frequency of the injected ultrasonic wave is varied until specimen resonance is obtained. When such a condition is reached, the so-called "resonance standing waves" are generated in the material.

The wavelength of a resonance standing wave λ_D and the corresponding resonance frequency f_D is related to the thickness D of a plate (in general, to the local thickness of the tested specimen) by the following expression (see, e.g., ref.[3]):

$$\lambda_D = 2\,n\,D = \frac{n\,v}{f_D} \qquad (2.3)$$

where v is the velocity of either the longitudinal or transverse wave in the medium;

n is an integer index equal or greater than zero. When it is one, the lowest resonance frequency for standing waves applies.

A void in the material results in a reduction of the "seen" thickness, where the resonance frequency changes, indicating the presence of a gap. Hence, experimental methods to apply the resonance principle are based on a continuous changing of the ultrasonic-wave frequency until a resonance condition is reached.

Resonance-test signals are conventionally carried out for thickness or velocity measurements. Measurements of thickness variations are based on the assumption of fixed wave-velocity. Velocity measurements may be based on the obtaining of a resonance condition in a specimen of known thickness.

Resonance methods have traditionally been used for measurements of the elastic modulus, especially in fundamental studies concerning single crystals. They were seldom applied to the traditional NDE purpose of material-flaw detection. However, some applications were worked out to address the quantitative testing of some material properties by this technique. Boser et al. [16], for instance, used resonance methods to measure density in ceramic capacitors.

2.2.6 Ultrasonic Spectroscopy Techniques

Ultrasonic Spectroscopy Techniques comprise some methods of frequency-component analysis of ultrasonic signals which originate from wideband pulses. They are based on the principle of constructive and destructive wave interference; see, for instance, ref. [17]. To perform Ultrasonic Spectroscopy, an ultrasonic signal in time domain is needed; it may be obtained by any of the previously presented ultrasonic techniques.

To obtain the maximum occurrence of such phenomena, a broadband of ultrasonic frequencies is desirable. In the field of ultrasonic testing, the terms "broadband pulse", "highly damped pulse" and "short pulse" are synonymous. The shorter the pulse, the broader is the respective frequency spectrum. Meantime, short pulses are generated by strong damping of the oscillations. Therefore, it follows that the necessary broadband pulses are highly-damped short pulses. An appropriate transducer for ultrasonic spectroscopy experiments is a broadband ultrasonic emitter-receiver. A complete discussion on this issue is presented in ref. [18]. Used frequencies for this method are in the 0.5 to 10 MHz interval.

When an ultrasonic signal travels through a material, the frequency components associated with the input signal may be altered. Although this may be seen in time domain, it is more clearly revealed in frequency domain. Either analog or discrete transformations respectively implemented by spectrum analysers or digital computers are used to produce frequency domain information.

By subjecting the captured echoes to frequency-spectrum analysis, it is possible to compare the effects of varying material states. Correlations may be established between levels of a material property and frequency intervals of the wave spectrum. Ultrasonic spectroscopy techniques have proven to be useful in determining the quality variations of bonded joints in aluminium alloys due to both fabrication processes (see, e.g., refs. [19] and [20]) and hydrothermal degradation (e.g., ref. [21]).

2.2.7 Acoustic Emission Technique

The principle of the Acoustic Emission (AE) Technique is the spontaneous emission of sound and ultrasound pulses from a material specimen subjected to external loadings. The experimental set up for AE technique is based on a conventional loading machine, a pickup piezoelectric transducer and a signal processing system.

The obtained sound level is very low and depending only on the stress level. Therefore, general noise from the experimental layout must be minimized. Practical applications of the method call for careful experiment designs. The captured signal needs a preprocessing treatment of amplification and filtering. Signal processing is then needed, since the data must be put in an appropriate format allowing the discrimination of some describing features.

When studied from the microstructure point of view, AE represents an actual destructive testing method. Certain level of damage, though very low, must be generated to obtain the emission of sound. Emitted waves consist of a low-level high-frequency signal which composes with a discontinuous pulse-type component of varied frequency. The former seems to be rate-strain dependent, while the latter is thought to correspond, at its highest frequencies, to brittle fracture at the microstructure level.

If any sudden relaxation of stress occurs into a limited portion of the microstructure of the material, a new equilibrium state has to be reached. A sudden change of stress or, in general, of forces acting over a particle implies a change of the particle velocity (see, for instance, ref. [22]). At the location of this phenomenon, discontinuities of both stress field and particle velocity field appear. Both field discontinuities propagate through the material as a single wave until equilibrium is reestablished.

AE waves are generated by time-dependent stress and strain fields in a solid. Scruby [23] proposed that the most important source of such fields is a stressed defect, because its growth to open up new crack surfaces leads to the above mentioned redistribution of local stress and strain. Sudden local-stress relaxation may occur because of any the following microstructure processes:

- Nucleation and propagation of cracks;
- Slip of dislocations in metals;
- Activation of dislocation sources;
- Twining and slip of grain boundaries.

Scruby [23] showed that the growth speed of these defect, is one factor controlling the amplitude of the emitted wave. Thus, a slow growing crack will, on the average, produce a weaker signal than the one produced from a rapid growing defect. Understanding of this time dependence may be very helpful for the correlation of AE signals with material properties.

If a metal is stressed to a value near or above its yield stress, then unloaded and stressed again, acoustic emissions that were observed during the first loading will be absent or very much reduced on the second loading up to the previous maximum level. When this level is exceeded, AE would be apparent again. This is the so-called 'Kaiser Effect' (see, e.g., ref. [24]).

Analysis of AE describing-features was used to characterize and quantify some material properties. Nixon et al. [25] studied the relation of drop-weight impact states in carbon fibre/PEEK laminates and the onset of constant acoustic-emission rate. Hill et al. [26] evaluated residual strength in E-glass/polyester chopped strand-material subjected to notch-initiated corrosion cracking and the count of total AE signals. Liu and Xi [27] set a relation between deformation states of AISI 4340 steel in both tensile and creep-fatigue testing and the total AE energy.

The techniques of Clustering Analysis and Statistical Pattern Recognition, which will be presented in Chapter 4, can be used to relate microstructural states to the obtained AE signals. A single-parameter method of clustering analysis was early used by Mihovsky et al. [28] to obtain different clusters for three-point bending-test parameters during the first hydrotest of pressure vessels. Multivariate analysis of AE signals was applied by Cherfaoui and Roget [29] during the initiation and fatigue crack propagation in two aluminium alloys and standard grade steel. The latter authors analysed how the following AE features: peak amplitude, rise time, signal duration and ringdown-count were associated with four populations corresponding to the following states: monotonic plastic deformation, cyclic plastic deformation, phenomena associated with crack closure, and crack extension.

A recent trend has been the application of artificial neural networks to the classification of acoustic emission signals. Maslouhi et al. [30] investigated this alternative analysis of AE signals for the initiation and progression of fatigue damage in graphite-epoxy laminates.

2.3 Acousto-Ultrasonics Technique

2.3.1 Introduction

Acousto-Ultrasonics (AU) may be taken as standing for "acoustic emission simulation with ultrasonic sources" (see, e.g., ref. [31]). Instead of loading the specimen to excite spontaneous stress waves as in Acoustic Emission methods, AU uses external ultrasonic sources to resemble AE waves without destructively disrupting the material.

Early called the stress-wave factor method, AU was developed to detect and quantify damage condition states and variations of mechanical properties in fibre-reinforced composites (see, for instance, references [32-34]).

The AU approach of simulating stress waves was first proposed in the work of Egle and Brown [35]. They investigated the simulation of acoustic-emission signals and sources to improve the methods of spontaneous acoustic emission under stress loading. Vary et al. (e.g., references [36] and [37]) developed the idea of using external-input ultrasonic-waves to interrogate the material for the combined factors which may affect material properties as strength, stiffness, toughness and dynamic response in composites. The rationale for that development was the fact that effects of these distributed and combined factors were seldom easy to assess analytically.

Some alternative methods of simulating acoustic emission signals were proposed and have been used mostly in the material research field, such as excitation of ultrasonic waves by pulse-energy laser. (see, e.g., ref. [38]).

Unlike the usual NDE approaches, AU is less concerned with overt-flaw detection than with the evaluation of the integrated effects from populations of subcritical flaws, thermomechanical degradation and diffuse states in materials. Vary [33, 34] showed that these are factors that both singly and collectively influence Acousto-Ultrasonics measurements as related with mechanical property variation.

2.3.2 Acousto-Ultrasonics Hypothesis

The working hypothesis of the AU technique is that more efficient strain energy transfer and strain redistribution during mechanical loading correspond to increased mechanical strength of the material. This hypothesis is based on the stress-wave interaction concept. It holds that stress waves at the onset of a material fracture will promote rapid cracking unless their energy is promptly and efficiently transmitted away.

If stress-wave energy is dissipated on an existing micro-fracture, propagating stress-waves show energy attenuation. The important implication of this starting hypothesis is that the stress-wave energy loss may be related to the collective effects of microstructural factors which determine overall mechanical properties. Stress-wave energy loss after interactions with matter may be shown in the variation of several wave-describing parameters. These parameters and its analysis are presented in the following Chapters 3 and 4.

Experimental results have largely confirmed this relation when external sources of ultrasonic waves are used. However, complete understanding of the connection between the attenuation of non-destructive ultrasonic-waves and that of spontaneous stress loading has not yet been reached. No satisfactory microstructural or constitutive models to describe ultrasonic wave interactions with the factors that govern mechanical properties are available; see, for instance, ref. [39].

2.3.3 Acousto-Ultrasonics Transducer Configuration and Instrumentation

Unlike both Pulse Echo and Through Transmission techniques, the AU approach imposes no demand on having particularly well-defined signal paths. On the contrary, maximization of the interactions between the interrogating signal and material microstructure that result from multiple wave-paths is desirable.

AU relies on so-called stochastic wave propagation rather than on well-defined interactions between the propagating wave and specimen microstructure. Depending on the material specimen and its geometry, this means that multiple, reflected, scattered and mode-converted waves form the output signal. The result of this stochastic wave propagation is, therefore, a highly modulated signal that usually consists of numerous superimposed components.

Since AU is not concerned with detection, location or sizing of defects, the nature and location of the ultrasonic source are known and fixed. Hence, AU waves are launched periodically at specific times with predetermined repetition rates and a receiving probe is placed at a specific distance from the emitter transducer. Both transducers are fixed while the output-signal data is taken. Depending on experimental layouts, transducers may be then removed and re-positioned on new locations or specimens, or held in their position while the tested material-property is modified by any input. The latter approach was applied by Iyer and Haddad (see, e.g., ref. [40, 41]) for the characterization of the viscoelastic-response of polymers subjected to stress-relaxation under uniaxial loading.

Although any of the transducer configurations from AE, Through Transmission and Ultrasonic Detection of overt-flaws addresses the above-stated requirements, two transducers located at a specific distance on the same side of the specimen are preferred. The probes are coupled at normal incidence to the surface of a test piece.

Experimental work with polymers (e.g., refs. [9] and [40]), metals (e.g., refs. [42] and [43]) and several composites (e.g., refs. [8], [37] [44] and [45]) showed the convenience of using such a transducer configuration. It assures that numerous wave-interactions occur in the volume of the tested material. It also presents the practical advantage of better accessibility to some usual structures as vessels, fuselages and thick-wall components.

A diagram of an AU transducer configuration and instrumentation is shown in Figure 2.4. An Ultrasonic Pulser is used to periodically excite the sending transducer. The pulse repetition rate is set by a Repetition Rate Controller. The pulse triggers the Time Base Generator to synchronize the Waveform Digitizer sweep with the receiver probe output. It is usually necessary for the receiver output to be preamplified before entering the Vertical Amplifier. The amplified signal is passed to a Waveform Digitizer that transforms the signal from analogical to digital. Both the analogical signal and the signal from the Time Base Generator are used as inputs to a Display Terminal for the visualization of the signal in time-domain. The analogical signal is eventually passed to a waveform storage medium and a waveform data analysis system.

Although the transmitting transducer injects longitudinal waves propagating in a normal direction with respect to the surface of the test specimen, it is expected that the injected pulses produce oblique reflections and shear waves. Both longitudinal and transverse components of the propagating signal interact with the microstructural and morphological features of the material that determine mechanical properties and performance; see, e.g., ref. [32].

Vary [34] observed that composite materials modulate and filter the AU signals. Signals at the receiving probe often exhibit spectra that indicate selective transmission of some guided-wave modes. The result of AU wave propagation may be a multi-modal frequency spectrum. Therefore, selection of the receiving transducer bandwidth must be done with consideration to the probable flaw-distribution and anisotropy of the material.

It is important that the emitting transducer would have a spectral bandwidth sufficient to excite all the frequencies needed to interrogate the material, while the retrieved signal heavily depends on the spectral response and sensitivity of the receiving probe. To this end, a broadband transducer is to be optimized around a central frequency for wave generation.

2.3.4. Acousto-Ultrasonics Signals

The AU hypothesis postulates a connection between stress-wave energy-loss and some mechanical properties of the tested material. It has been said (see, e.g., ref.

[32]) that usual transducer setups for AU practice give highly modulated signals which consist of several superimposed components. The simplified model of the propagation of AU signals in a flat homogeneous specimen that follows may be an aid to the understanding of this phenomenon.

Only wavelengths that are less than the plate thickness and that are reflected within the plate boundary surfaces are assumed. Let the probes be represented by a point sender and a point receiver, as it is presented in Figure 2.5. A point sender emits hemispherical waves. Let us suppose that the emitted waves are pressure waves and that they are reflected from the back surface of the plate to the receiving transducer. Then, for any nearby arbitrary point receiver, it is possible to trace a pressure-wave ray path.

Figure 2.5. shows the one-reflection path and subsequent paths for three and five reflections on the specimen boundaries. Each frequency component of the injected ultrasonic pulse may be understood as following these paths until it reaches the receiver. Hence, each path may be seen as pertaining to a peak for each waveform-component in time domain. Being the injected signal a broadband pulse, the resulting signal from such interactions may be composed of several groups of peaks or wavelets. These wavelets may overlap each other, depending on the injected frequency components and material geometry and properties.

When a pressure wave from the sender reflects on the back surface of the plate, it may be mode-converted to a transverse wave; see, e.g., ref. [3]. Transverse wave paths can also be traced as in Figure 2.5. As it has been explained for longitudinal waves, a path is travelled by each frequency component of a transverse wave as its own velocity, which may be not equal to that of the originating longitudinal wave. In addition, the angle of incidence for reflection, velocity and attenuation of each wave-component depends on the combined effect of component frequency and local material-properties. Therefore, when waves reach the receiver, they have been subjected not only to mode-conversion but also to frequency and property-dependent delays and attenuation. The interested reader is referred to [3].

This simple model aids to understand that resultant waveforms at the receiver will consist of a superposition of numerous different wavelets. Only most prominent individual reflections are distinguishable. It can be said that the received waveform will have an envelope and details that are the result of interactions with material characteristics, which in turn define material properties. As an example, Figure 2.6 shows, in time domain, an ultrasonic pulse input and the pertaining AU signal that was received at the receiver transducer after the ultrasonic wave travelled through a flat homogeneous specimen of pure polymer (Polyvinylchloride).

2.4. Conclusions

Several non-destructive examination techniques based on wave propagation have been presented. The generally called ultrasonic methods, which are based on mechanical interactions of the ultrasonic wave and the mechanical and physical properties of the test specimen, have been shown useful in the determination of the factors that affect integrity of the microstructure of materials. For each of the presented method, its suitability for a quantitative evaluation of material properties has been discussed. Applicable transducer configurations and instrument setups for QNDE data acquisition have been presented.

There has been a progressive advancement in materials research QNDE to complement more traditional testing approaches. However, almost all of this progress has been problem-oriented, applying or adapting a given NDT technique to a specific evaluation problem. There might be many advantages to the successful integration of wave propagation theory and QNDE experimentation. These advantages may include the possible explanation and consequent improvement of the reproducibility fluctuation problems, the prospect of theoretical guidance in the design of experiments and the possibility that new describing parameters are extracted from the retrieved signals.

In many instances, the QNDE approach may be used in conjunction with traditional destructive tests to reduce the cost of materials testing. Accelerated testing of new materials could benefit from non-destructive technologies. Once conventional NDE has shown a component to be free of overt defects, QNDE methods would test the material properties assumed in the design stage. Therefore, QNDE would verify material properties rather than relying solely on tabulated values based on previous tests or statistical control procedures.

The emerging technologies of thermal, electron-acoustic and electron-parametric imaging, magnetic evaluation of corrosion and rapid x-ray diffraction imaging, as well as these of non-contact transducers, may have in the near future their own impact in the field of material-property characterization. A review of the state of the art in these new technologies can be found, for instance, in the work of Green [46].

On reviewing the available literature, the Acousto-Ultrasonics Technique has shown a number of advantages. Acousto-Ultrasonics Technique requires only one-side accessibility of the test specimen. Several research works showed it may enable quantitative evaluation of a variety of impact, fatigue, stress and deterioration states in materials. It may be used not only in non-destructive examination and quality assurance of materials, but also in maintenance management of in-service components and characterization of material states.

As well as the benefits of Acousto-Ultrasonics Technique, this review has pointed out that the retrieved AU signals require careful analysis and interpretation. Quantitative analysis of these waveforms is the purpose of defining describing parameters for AU signals. Reviews of applicable describing parameters and analysis techniques follow in Chapter 3 and Chapter 4.

Chapter 3

REVIEW OF SIGNAL ANALYSIS TECHNIQUES FOR ACOUSTO-ULTRASONICS

3.1. Introduction

The ultimate purpose of the Acousto-Ultrasonics (AU) technique is to quantitatively characterize material properties through a non-destructive approach. In Acousto-Ultrasonics methodology, broadband pulses are emitted into the material specimen and allowed to interact repeatedly with the material microstructure.

The resultant AU waveform at the probe receiver consists, in general, of a superposition of numerous wavelets, having an overall envelope and details that are peculiar to the material specimen properties. In many ways, the acousto-ultrasonics signal resembles the burst-type acoustic-emission wave that arises spontaneously in a material undergoing mechanical deformation.

The AU hypothesis, mentioned earlier in Section 2.3, postulates a relation between stress-wave energy flow and strength properties of the material. Rating of the relative efficiencies of propagation of ultrasonic-wave energy through the material specimen is the purpose of several AU-signal analysis techniques. Although the AU signal is usually quite complex, this analysis may be performed by a variety of methods (see, e.g., refs [3] and [32]). One simple approach is the determination of the so-called "Stress Wave Factor" (SWF), which is introduced subsequently in the course of this chapter. The SWF is essentially a relative measure of the energy-transmission efficiency in the material.

The earliest works in the field of Quantitative NDE limited the wave analysis to the measurements of some wave propagation parameters as wave velocity and overall energy attenuation. More recent approaches resorted to more problem-oriented describing parameters for the analysis of AU data. In this way, meaningful correlations were obtained between the variations of several material properties and the variations of these parameters extracted from the acousto-ultrasonics signals, see, e.g., ref.[3].

Another trend in the analysis of AU data has been the sorting out of the waveform components that are most relevant to the particular material-state, as it is carried out by the techniques of Homomorphic Processing and Partition-Regression Method. Some of the above-said analysis techniques are reviewed in this chapter.

There may be instances, however, where it is better not to separate AU waveform components but to deal with the whole AU signal as a multivariate set of describing features. A multi-parameter technique of this type, the so-called Pattern Recognition and Classification Methodology, is presented in Chapter 4 of this thesis.

A major concern with any QNDE technique is the reproducibility of measured data. Several important factors relating to the experimental procedure, other than the material property variations, affect the received ultrasonic waveform. These factors are discussed in the course of this chapter.

3.2. Acousto Ultrasonics Wave-Propagation Measurements

A simple energy-measurement of the received AU-wave may be carried out by quantities such as wave velocity and wave attenuation. Although the use of only velocity and/or attenuation measurements implies that other features pertaining to the AU signal description are ignored, such a measurement may be enough for its correlation with some material properties, e.g., tensile strength [8].

To find the wave velocity by the so-called time-of-flight, the time for the signal to travel along a path of known length is measured (see Section 2.2.1.). The other basic approach to quantitative material characterization involves measurement of the energy losses of the ultrasonic waves by wave attenuation. As was mentioned earlier in Section 2.2., ultrasonic wave attenuation is frequency-dependent. Therefore, it is usually measured as relative to the frequency components of the AU waveform.

The procedures involved in wave-attenuation measurement are not simple to apply when wave-absorption and/or wave-scatterring mechanisms, which were mentioned earlier in Section 2.2.1, are present. Attenuation measurements on the same material may vary by an order of magnitude; see, e.g., ref. [39]. In addition, when testing high attenuation materials it is often difficult to recover the set of undistorted echoes of the input ultrasonic wave that is needed for either velocity or attenuation measurements.

3.3. Acousto-Ultrasonics Waveform Parameters

A major concern of the analysis of AU-signals is to isolate and quantify the information from the retrieved AU-signals in the most useful format. This may be accomplished by calculating a quantity called the "Stress Wave Factor" (SWF).

SWF can be taken as denoting a general measure of the efficiency of the propagation of the ultrasonic-wave. Stress Wave Factors are used to compare variations of the ultrasonic wave energy transmitted through the material microstructure pertaining to specimens of the same material, providing the same procedures of AU data acquisition and of processing of this data are applied.

Lower values of SWF are thought to correspond to material microstructure regions where high attenuation of the ultrasonic waves takes place. Interpretation of these lower values of SWF by the AU hypothesis, presented earlier in Section 2.3.2, indicates that the material specimen may present regions where strain energy is likely to be dissipated. This energy dissipation may be a consequence of localized growth of cracks and fractures, as discussed previously in Section 2.2.7.

In any particular case, the definition of an appropriate SWF depends on the test specimen (i.e., tested material and specimen geometry) and the type of material property to be measured. The following sections present some definitions of the Stress Wave Factor that have been effectively used by various researchers in the quantitative AU testing of engineering materials.

When combined with the above mentioned Stress Wave Factor, measurements of the ultrasonic wave velocity using conventional time-of-flight methods may produce better correlations than SWF alone. In this way, conventional ultrasonic measurements may be useful to reinforce or corroborate more elaborated AU measurements; see, for instance, ref. [39].

3.3.1 Peak-Voltage Stress Wave Factor

For some simple AU waveforms, the peak voltage of the retrieved signal changes inversely with the wave-energy attenuation and it may be an effective basis for the definition of a Stress Wave Factor. Using either analog or digital peak-detection, the so-called Peak Voltage SWF may be defined as follows

$$SWF = E_V \tag{3.1}$$

where E_v is the maximum voltage oscillation.

When using the definition (3.1) above of the SWF, it is assumed that the maximum voltage-swing corresponds to variations of the tested material property.

After the maximum amplitude observed in a typical AU waveform, following oscillations usually diminish, being the result of more wave attenuation along longer paths. Depending on the test specimen and the tested material property, however, not the maximum voltage of the AU waveform, but some of its smaller oscillations may be more representative; see, e.g., ref. [3]. In this case, an appropriate alternative may be the measurement of signal rise or signal decay time, as is done in Acoustic Emission practice; see, e.g., ref. [23].

3.3.2. Ringdown Stress Wave Factor

AU signals frequently resemble the typical waveforms that result from acoustic-emission bursts; see, e.g., ref. [33]. Accordingly, the SWF may be characterized by a "ringdown count". Using Acoustic-Emission methodology, the so-called Ringdown SWF is defined as follows

$$SWF = R_p \; T_R \; c \qquad (3.2)$$

where R_p is the repetition rate of the ultrasonic pulse,

T_R, usually called totalizer reset time, is the interval of time for which the measurement is carried out and after which the measurement system is reset, and

c is the digital count of oscillations per waveform.

A threshold-voltage setting is the basis for counting the number of ringdown oscillations per waveform. The repetition rate R_p is set so that the received signal rings down below the threshold voltage before a new signal starts. The reset time T_R gives a predetermined number of signals into the total count display. Defined in this way, the Ringdown SWF measures the signal strength relative to this threshold, see, e.g., ref. [33].

Figure 3.1 shows a diagram of a typical acousto-ultrasonics measurement setup for Ringdown SWF. The pulse repetition rate R_p is held constant by the Rate Repetition Controller while a Reset Timer is set to a predetermined interval T_R. The Rate Repetition Controller triggers the Ultrasonic Pulser for the emission of a pulse. The received AU signal is passed to an Amplifier and Gain Control, which in turn feeds the amplified signal to a Counter Threshold Control. The latter gives the signal for digital display and to a Oscillation Counter, which counts the number, c, of oscillations that exceed a voltage threshold just above the noise level. The signal from the Oscillation Counter is the Stress Wave Factor as defined in Equation (3.2). It is displayed in the desired form by the Digital Readout.

Since the Ringdown SWF relies on the assumption that the AU waveform has a monotonic decay envelope whose shape is not dependent on the relative distance between probes, it may be inappropriate in some cases; see, for instance, ref. [3]. However, the early success on producing good correlations of the variations of this SWF with the variations of ultimate and interlaminar strength in fibre-reinforced composite systems (see, e.g., references [36] and [37]) has made it the definition against which newly introduced similar parameters are compared.

By the above described method, Ringdown SWF can be used to rank a series of material specimens according to its ability of effectively transmitting ultrasonic-wave energy. Higher values of Ringdown SWF correspond to longer ringdowns, which, in turn, may result from more efficient energy transmission through the material specimen. However, wave oscillations toward the end of the retrieved AU signal may be due to the characteristics of the transducer rather than to those of the material. In addition, some oscillations may be due to reflections from regions just outside the material volume between the transducers. These unsiderable effects may be minimized by threshold increase or truncation of the ringdown counting zone; see, e.g., ref. [3].

3.3.3. Acousto-Ultrasonics Parameter (Weighted Ringdown SWF)

An alternative to the previously described Ringdown SWF takes the amplitude of each ringdown oscillation into account. This modified form of the Ringdown SWF was originally proposed by Williams and Lampert [8] for the evaluation of residual tensile strength of unidirectional graphite-fiber epoxy composites after subjecting the material specimen to repeated drop-weight impact. It was subsequently adopted by Tanary [42] and Tanary et al. [43] for the verification of adhesive shear strength in bonded joints and called the Acousto-Ultrasonics Parameter (AUP).

The formulation for the AUP can be defined in terms of a set of threshold voltages, V_i, which increase by some fixed voltage increment from the noise level to the voltage amplitude immediately above the maximum voltage peak. With reference to Figure 3.2, the AUP is formulated as follows

$$AUP = \sum_{i=1}^{p} \left[V_i \left(c_i - c_{i+1} \right) \right] \qquad (3.3)$$

where V_i is the voltage at the ith level above the threshold,

c_i is the number of counts at the ith level, and

V_p is the peak amplitude of the waveform

The procedure of calculation of the AUP starts by setting an initial threshold V_1 just above the noise level. Then, the total number of counts above V_1 is determined. The threshold is increased by a fixed interval until it becomes equal to or greater than the peak amplitude of the waveform. At each step, the difference between the number of counts for this level and the following is multiplied by the threshold amplitude.

Measurements of the AUP require no more than a suitable signal display to perform the weighted count. Although the Acousto-Ultrasonics Parameter is of simpler implementation than the previously introduced Ringdown SWF, in Section 3.3.2, the former provides a measure that may be more sensitive to some material properties.

3.3.4. Energy Integral Stress Wave Factor

A calculation of the magnitude of relative energy in the received acousto-ultrasonics signal may be taken as a parameter for rating the efficiency of ultrasonic wave transmission in the material. This can be expressed by the so-called Energy Integral Stress Wave Factor as follows; see, e.g., ref. [31]

$$SWF = \frac{1}{T} \int_{t_1}^{t_2} V^2 dt \qquad (3.4)$$

where T is a time interval (from t_1 to t_2), and

V is the time-varying waveform voltage.

The above-presented definition of Energy Integral SWF in Equation (3.4) is based on the mean square of the waveform-voltage. An alternative definition in terms of the mean square of the frequency domain spectrum is the following; see, e.g., ref. [31]

$$SWF = \frac{1}{F} \int_{f_1}^{f_2} s_f^2 \, df \qquad (3.5)$$

where F is a frequency interval (from f_1 to f_2), and

s_f is the frequency-varying waveform voltage.

Unlike SWF definitions in terms of ringdown count, there is no need to set a threshold voltage to calculate Energy Integral SWF. However, it is usually appropriate to specify and bound the size and location of the time or frequency domains that most closely associate with the variations of the tested material properties, see, e.g., ref. [32].

3.3.5. Homomorphic Signal Processing

The problem of sorting out AU wave components that are most relevant to the tested material property may be answered by the so-called Homomorphic Signal Processing Technique; see, e.g., references [32, 33]. This method deconvolutes the overlapping individual wavelets that constitute an AU waveform. By means of special filters, it selects and isolates some important components of the wave. Component features such as distinct peaks and/or peak positions can be then correlated with a material property variation.

Homomorphic Signal Processing may be necessary for waveforms whose Fourier transforms overlap. The so-called homomorphic filters provide the means to separate such waveform components. These components may be particularly useful in identifying significant AU wave modes and their paths; see, e.g., ref. [32].

Frequency filtering can be used to improve some correlations of the SWF values with the values of the tested material property. This procedure may be performed by taking Fourier transforms of the waveform and digitally zeroing out all but a narrow frequency band. This reduced spectrum is then inverse transformed to a reduced waveform of narrower frequency range. After a range partition gives good correlation with the tested material-property, a Weighted Ringdown SWF is calculated from the pertaining reduced waveform in the time domain. When evaluating AU waveforms that consist of superimposed multiple-echo signals, this method may lead to an improved value of the Stress Wave Factor. This method may be seen as a hybrid one between Homomorphic Signal Processing and the so-called Partition-Regression technique. The latter technique is referred-to below.

3.3.6. Partition-Regression Method

This technique of separating the most relevant components of AU waves is based on partitioning the obtained AU signal and its spectra, followed by statistical regression analysis. The basic assumption of the Partition-Regression Method is that relevant signal components and their frequency bands can be separated with simple linear filters; see, for instance, ref. [32]. In this procedure, both time and frequency domain descriptions of the waveform are divided into several equal segments. The SWF for each segment is then correlated in conjunction with the values of the pertaining material property to find corresponding time and frequency segments that best correlate with this property. The procedure is iterated until the correlation between the material property of interest and the SWF results optimized (see, e.g., reference [33]).

3.4. Stress Wave Factor Normalization

The SWF is a relative quantity that depends on the test conditions and can be either dimensionless or dimensional. When using the SWF definitions presented in this chapter, it is useful to normalize the measured values of the different dimensional quantities. In this way, normalization compares relative changes in SWF as related to pertaining variations of the material property. Further, it may be practical to normalize against the maximum value of a particular variable for a given material or a transducer configuration; see, e.g., ref. [32].

Quantitative Non-destructive Evaluation methods based on wave propagation significantly depend on signal interpretation and correlations to assess material quality and properties. Therefore, a calibration of the AU experiment should be set when nondestructive testing is performed. Without this calibration, even sophisticated AU signal correlation procedures may give unsatisfactory results. In this context, Vary [39] suggested that a set of experimental parameters must be chosen to calibrate a given material, experimental conditions and instrumentation settings. He showed that this procedure, when carefully done, gave very close correlation between the lowest value of SWF along a specimen length and the location of final fracture under tension in fibre-reinforced composite materials.

Standards of AU instrumentation calibration may benefit from multiparametric signal analysis and classification based on adaptive learning methods (see, e.g., ref. [32]). To this purpose, carefully devised learning sets comprise test specimens pertaining to controlled levels of material degradation. These learning sets form a standard database for a material property, providing they represent a realistic range of material states. A multivariate analysis method of this type, based on the Pattern Recognition and Classification approach, is presented in the following Chapter 4.

3.5. Acousto-Ultrasonics Data Acquisition

A major concern with any QNDE technique is the reproducibility of measured data. Regardless of AU data analysis methodology, AU technique is comparative. Its success depends on both adequate repeatability and significant sensitivity to the variations that the material property states may produce on the retrieved AU-signal. Hence, the obtained describing parameters must be reproducible.

Several important factors relating to the experimental procedure affect the received ultrasonic waveform other than the effects pertaining to material property variations. They may be grouped as 'external' to the system and 'internal' to it (i.e., instrument settings). These parameters are discussed below.

3.5.1. External factors affecting AU Data Acquisition

The change in distance between the sending and receiving transducers affects data acquisition to a great extent (see, for instance, references [40, 45]), as it corresponds to the amount of microstructure through which the ultrasonic wave travels.

In this thesis, values of the Acousto-Ultrasonics Parameter (AUP), introduced earlier in Section 3.3.3, were obtained for different distances between transducers. The used transducer setup is presented in Figure 3.3. A rectangular cross-section pad of high-attenuating rubber foam is placed between the specimen back-surface and the fixing clamps. The rubber pad prevents both the "noise echoes" of ultrasonic waves from specimen-clamp interface and the localized clamp pressure due to direct contact of the clams on the specimen. The preliminary experiments to design this transducer setup showed that both above-said phenomena affected the repeatability of the AU measurements.

Figure 3.4 shows measured values of AUP for rectangular cross-section Polyvinylchloride specimens of constant thickness when separation between transducers is varied, while all other parameters concerning emitted signal, specimen geometry and transducer fixation are held constant. The measured values of AUP are found constant for distance between transducers less than or equal to 0.75 inches. For larger values of distance between transducer, the obtained AUP values consistently diminish.

The pressure applied on the transducers is one of the prime factors affecting the received waveform. Although this fact was quoted in previous research (see, e.g., ref. [40]), quantitative information relating the applied pressure and the measured AU parameters remains scarce.

Russell-Floyd and Williams [45] carried out research work on the variations of the Ringdown Stress Wave Factor, introduced earlier in Section 3.3.2, when emitter and receiver transducer pressure is varied, as applied by laboratory-weights, on carbon-fibre-reinforced composite laminates. Results of those experiments are shown in Figures 3.5 and 3.6.

Figure 3.5 shows that the Ringdown SWF rises rapidly when the pressure applied on the emitter transducer varies from 0 to about 6,000 Pa and stabilizes for pressure values greater than 10,000 Pa. For the receiver transducer, the SWF values increases for the range of pressure of 0 to about 6,000 Pa and rapidly stabilizes for greater values of pressure.

Figure 3.6 displays the coefficient of variation of SWF, as the ratio of the standard deviation of the measured SWF values to the mean of these values, versus the pressure applied on the emitter and receiver transducers. Figure 3.6 shows that after a certain value of applied pressure is reached, further increases of contact pressure do not significantly affect the obtained SWF values; see, e.g., ref. [45].

The above presented results show that constant and repeatable forces applied to the transducers are of main importance. In order to apply constant pressure, Tanary [42] and Tanary et al. [43] introduced a 'constant force clamps' configuration as presented in Figure 3.7, and later used by Iyer [40]. In the case of relatively narrow-section specimens, with good accessibility from at least one side, this configuration assures constant clamping forces for series of AU tests in same-thickness specimens. In the experimental work carried out for this thesis, a transducer positioning setup that makes use of these constant force clamps is adopted, as presented earlier in Figure 3.3. Given all other factors to be constant, the transducer setup of Figure 3.3 gave adequate repeatability of the AU measurements. The results from three series of ten AUP readings, where each series pertains to one Polyvinylchloride specimen, are presented in the following Table 3.1.

Table 3.1. Repeatability of Acousto-Ultrasonics Parameter measurements pertaining to three polyvnylchloride specimens for the transducer setup of Figure 3.4. Threshold value: 32 mVolts. Input frequency: 750 KHz.

	Specimen #1	Specimen #2	Specimen #3
Number of readings	10	10	10
Mean [mVolts]	830.4	795.2	819.2
Standard Deviation [mVolts]	11.804	15.179	12.618

A procedure to obtain adequate AU signal repeatability in the experimental work of this thesis is described in Chapter 6.

The type of couplant medium used to create continuity between the transducer and the specimen is also an external factor affecting the AU waveform. Extensive data on the comparative influence of most commonly used coupling media on both repeatability and ability of wave-energy transmission was available in the reviewed literature; see, for instance, refs. [40, 45]. The results of Tanary [42] on this issue were used as basis for the selection of an adequate couplant in this thesis. He investigated the influence of different couplants, namely, water, motor oil, vacuum grease, AET SC-6™ [1] and Ultragel II™ [2], in the transmission of ultrasonic-energy as measured by AUP. Ultragel II™ showed the highest values of AUP of the experi-

---

[1] AET SC-6™ is the trademark of Hartford Steam Boiler Inspection Technologies,Inc.

[2] Ultragel II™ is the trademark of ECHO ULTRASOUND, Inc.

mented couplants, as well as the earliest stabilization and best reproducibility of AUP values.

3.5.2. Internal Factors affecting AU Data Acquisition

AU Data Acquisition is also affected by a number of factors that are dependent on the systems of ultrasonic pulse emission and AU data acquisition themselves. Since these factors are variables that can be set in the instrumentation setup, identities between these variables and the instrument settings are natural. In the experimental work of this thesis, instrument settings are controlled by an appropriate software setup. The hardware and software setups used are presented in Chapter 6.

The effects of several instrument settings were investigated for the transducer configuration used, which is shown in Figure 3.3. About the investigated ranges of variation of analysed instrument settings, most of them showed no significant influence on the obtained AU signal when external factors, which were discussed earlier in Section 3.5.1, are held constant for the investigated materials.

Only the frequency of the pulse input by the emitter transducer showed a significant influence on the measured AUP. Figure 3.8 displays the measured values of AUP when input frequency is varied. To this, the emitter and receiver transducer were held at their positions on rectangular cross-section Polyvinylchloride specimens, as previously presented in Figure 3.3, while the central frequency of the input pulse was varied by discrete values in the range of 0.625 MHz to 2.5 MHz. Central frequency of the emitter transducer used was 0.750 MHz. Figure 3.8 shows that the values of AUP significantly diminish as the emitter frequency increases from the transducer central frequency. Therefore, in the experimental work of this thesis the frequency of the input signal was chosen at 750 KHZ, provided that this value was compatible with the bandwidth of the receiver transducer.

Optimization of instruments settings was aimed at obtaining a good combination of the above said input frequency and amplitude gain. Given the chosen transducer and instrumentation setups, the amplitude gain was set for a sufficiently high ratio of signal to noise in order to obtain good signal discrimination even for the most unfavourable case, i.e., for the tested material state that produced the highest attenuation of the transmitted ultrasonic wave. By the same gain, the maximum signal amplitude was held below the maximum reading level of the instrumentation setup.

By setting a sampling rate of 3.125 MHz for the retrieving of the AU signal, the data acquisition system captured a significant number of digitalized records of each AU signal without exceeding its memory capacity. A detailed description of this AU data acquisition system follows in Chapter 6.

Another factor that could affect AU data acquisition is concerned with resonance frequencies. This is the case when natural vibration frequencies of the test specimen coincide with the frequency of the ultrasonic pulse imposed by the emitter transducer. In this way, resonant frequencies due to natural vibration modes can dominate the spectral content. Vary [31] early warned that these resonant phenomena may influence the obtained frequency spectrum of the acousto-ultrasonics waveform.

The present review about the influence of external and internal factors on the AU measurements may be summarized in the fact that the sensitivity of the AU data acquisition to a setting depends on the combination of equipment, transducer setup and material specimen to be tested. It seems that a rational approach to establish a suitable instrument setting is a customized trial under the guide of previous research experiments. To this purpose, some preliminary guidelines to the present thesis are the works of Iyer [40] and Tanary [42] concerning the changes of Acousto-Ultrasonics Parameter for several hardware settings.

3.6. Conclusions

Most Acousto-Ultrasonics analysis methods used have been presented. Their advantages and suitable fields of application have been discussed. It has been shown that parameters grouped in the broad meaning of SWF constitute an indirect but effective mean to quantify interactions of the ultrasonic wave with the microstructure factors that decide material properties. External and internal factors that may affect the AU data acquisition procedure have been discussed. Previous research works that apply to the experimental work of this thesis have been reviewed.

Stress Wave Factors are not defined in terms of the physical parameters directly associated with material properties. However, correlations of the variations of these Stress Wave Factors with the variations of the tested material property have been providing useful methods of property evaluation. It can be said that AU evaluation by the above-presented analysis techniques offers a complementary methodology of material-performance measurement. It is true that each of the introduced Stress Wave Factors may give a different numerical result when evaluating the same AU signal. However, each SWF will highlight a particular aspect of the AU waveform and may give information about different properties of the tested material.

There are several material properties that can affect a correspondingly large number of parameters of the description of the AU signal. This suggests carrying out the analysis of AU waveforms by multivariate extraction and classification. A powerful technique to perform this evaluation approach, namely, the Pattern Recognition and Classification approach, is reviewed in the following Chapter 4.

Chapter 4

REVIEW OF PATTERN RECOGNITION AND CLASSIFICATION APPROACH

4.1. Introduction

If an ultrasonic pulse is emitted into a solid, the state of the material determines its propagation. As mentioned earlier in Chapter 2, the interactions of the emitted ultrasonic wave with the material microstructure usually result in quite complicated AU waveforms. In addition, a large amount of data can be extracted from a single AU signal. Therefore, assessment of the material state from such signals may be difficult.

The analysis of AU signal can be made by multivariate extraction and classification. The Pattern Recognition and Classification methodology offers a suitable approach for this multivariate analysis of AU signals.

Generally speaking, a pattern is the description of an object. In Pattern Recognition practice, the discrimination of the available data is usually performed by means of describing attributes of the objects to be recognized. Several examples where the PR approach constitutes an efficient solving method were presented in the work of Tou and Gonzalez [47].

In developing theory and techniques to perform a given recognition task, Pattern Recognition and Classification may be defined as the categorization of input data into identifiable classes via the extraction of significant features or attributes from a background of relevant data.

As it is shown in the following sections of the present chapter, there are several mathematical tools that can be used to solve the problems of performing Pattern Recognition and Classification analysis. The choice of some of these tools to analyse a particular type of data defines a procedure. This procedure can be referred to as the design of a PR System. A review of the Pattern Recognition and Classification techniques that apply to such design is presented in the following section.

4.2 Fundamentals for the Design of Pattern Recognition Systems

To analyse the task that is expected from a Pattern Recognition System, it is convenient to understand the pattern recognition problem in three stages or spaces; namely,

- The Pattern Space,
- The Feature Space, and
- The Classification Space.

The physical world is sensed by some transducers that input their data into the Pattern Space. Transducers are usually defined by functional rather than pattern recognition specifications. For instance, the usual AU transducer configurations capture an analogical description of each AU signal from which a quite large set of scalar values can be extracted. This collection of sets of scalar values pertaining to the retrieved AU signals forms the Pattern Space.

It is desirable to reduce the dimensionality of the Pattern Space while maintaining the discriminatory power between different patterns. The Feature Space is then obtained from the Pattern Space by reducing the number of describing parameters. Suitable procedures to perform this reduction are reviewed in the following sections.

The ultimate purpose of a Pattern Recognition and Classification system is the identification of a given pattern as belonging to one of the classes under consideration. The Classification Space is the "decision space" in which one of the defined classes is selected.

Operationally speaking, the pattern recognition problem can be described as a transformation from the Pattern Space P_S, to the Feature Space F_S, and finally to the Classification Space C_S. This transformation may be expressed as

$$P_S \rightarrow F_S \rightarrow C_S \qquad (4.1)$$

Such a transformation is likely nonlinear and noninvertible, and its only objective is to maintain class discrimination throughout; see, for instance, ref. [48]. Therefore, the design of a Pattern Recognition System is the building of a procedure, or eventually of a series of procedures, to perform this transformation. It involves overcoming successive problems.

The first problem is concerned with the representation of the input data that have been retrieved from the objects to be recognized. Mathematically, a pattern is defined as an ordered array, generally called a pattern vector, consisting of elements that may just be numbers. In this case, each element is the value of a feature to describe the pattern. Feature values are the quantities that can be measured from the retrieved data.

When applying PR methodology to analyse Acousto-Ultrasonics signals, these signals contain the feature values for the process of pattern definition. Whatever the representation of the AU signal is, each measurable value of it can be a characteristic feature value for the description of the pattern.

In the case of an Acousto-Ultrasonics signal in time domain, the pattern features are values that are obtained from the measured voltage-amplitudes of the AU-signal. Examples of these describing feature values are, for instance, the voltage-amplitudes of the characteristic peaks that are observed in the AU signal. A pattern vector for the description of an Acousto-Ultrasonics waveform may be denoted by a column vector, such as

$$\alpha = \begin{bmatrix} \alpha_1 \\ \alpha_2 \\ \cdot \\ \cdot \\ \cdot \\ \alpha_n \end{bmatrix}. \qquad (4.2)$$

Where n is the number of features which have been measured from the time-domain data. Although these describing features have been proposed as taken from the time-domain description of the AU signal, there are no constraints for extracting features as functions of frequency, or of phase, or of any other variable of waveform description.

It is easy to realize that a quite large number of describing features can be extracted from an Acousto-Ultrasonics waveform. The most usual domains of waveform description from which to extract these describing features are presented in Section 4.6.1. Nevertheless, each of these features may carry information to differentiate this pattern from other patterns under consideration. Such high dimensionality makes Pattern Recognition problems very difficult.

The second problem in Pattern Recognition methodology is the one of deciding which features should be selected from the input pattern vector to proceed with in the

PR solution. It concerns the extraction of discriminating features and the reduction of pattern vector dimensionality. This is often referred to as the preprocessing and feature selection problem.

A pattern class is a group of patterns with common feature values. Features of a pattern class having common values for all patterns belonging to the class are called intraset features. Features that present different values between pattern classes are referred to as interset features. Feature values that are common to all pattern classes carry no discriminatory information. Therefore, intraset features which are not interset features of the pattern classes under consideration can be ignored; see, e.g., ref. [47].

The process of 'feature selection' means a reduction from the initial 'high-dimensional' space to a lower dimension space. It is ideally performed without losing information pertaining to the discrimination of any pattern class from all the others under consideration.

For mathematical presentation, let 'x' be defined as the feature vector, which comprises the values of the 'discriminatory features' extracted from the primitive measurement vector. This vector x is a subset of the vector α. When the feature values are real numbers, it is often useful to represent a pattern vector as a point in an Euclidean space.

For simplicity, let the pattern x be characterized by two common feature values. Each pattern vector may be represented as a point in a two-dimension space. These pattern vectors are, therefore, of the form

$$x = \begin{bmatrix} x_1 \\ x_2 \end{bmatrix} \qquad (4.3)$$

where x_1 and x_2 , respectively, are the values of feature 1 and feature 2 for a pattern vector x. In this example, the collection of all feature vectors, represented in the two dimension space for the feature values 1 and 2, is the Feature Space in the sense that was mentioned earlier in this section.

The third problem in the design of PR systems is the recognition and classification of given patterns not used for the design. It is usually solved by the determination of decision procedures. When classification of a given pattern is further performed, these procedures are used to decide the belonging of the pattern to one of the pattern classes under consideration.

The recognition and classification problem can be understood as that of generating decision boundaries to separate the pattern classes. When feature values are real numbers and pattern vectors are analysed in n-Euclidean space, these decision boundaries may be understood as n-dimension surfaces or "decision functions".

Decision functions are based on the pattern vectors used for the design. These decision functions can be generated in a variety of ways and some of them are reviewed subsequently. When a priori complete information is available about the patterns to be recognized, the decision functions may be determined with precision. When there is little a priori knowledge, reasonable guesses are possible for the forms of the decision functions. Arbitrary decision functions are initially assumed and they are made to approach satisfactory forms through learning and training procedures; see, e.g., ref [48].

The set of classes to design the Pattern Recognition system may be predefined during the procedure of data acquisition. The more general case, where a definition of classes is needed, poses an additional problem. There are three basic concepts that may answer the problem of pattern class definition.

<u>The first concept</u> is the so-called "membership-concept". It characterizes classes by the simple storage of individual patterns in a way that each of them constitutes a "one-member" class. Therefore, the recognition scheme that results in this case is a procedure of template matching with the stored patterns one by one.

The second concept is the "common-property concept". Its basic assumption is that patterns belonging to the same class possess certain common attributes. The main problem in this approach is to extract enough common properties from a limited set of sample patterns to determine a meaningful set of classes.

Finally, the third concept is the so-called "clustering concept". It is based in the relative geometrical arrangement of pattern vectors whose features are real numbers represented in the n-Euclidean space. If the classes are characterized by clusters that are enough apart to be distinguishable, cluster-seeking techniques may give appropriate class division for the design of a PR system; see, for instance, references [47], [49], [50] and [51]. Clustering properties in a given pattern space are also related with the application of some classification techniques, e.g., minimum-distance techniques. Some of these classification techniques are reviewed in Section 4.4.

4.3 Pattern Preprocessing and Feature Selection of AU Signals

Pattern preprocessing and feature selection methodology address the problems of the selection of discriminating features from the available patterns as well as that of the reduction of pattern vector dimensionality.

When designing PR systems for AU signals, feature selection may be guided by the effectiveness of the classification, which is usually expressed in terms of the percentage of correctly classified testing signals. This approach is labeled "performance-dependent feature selection" or just simply "performance feature-selection". Alternatively, feature selection may be accomplished independently of the classification scheme performance. In this case, optimum feature selection is dictated by a so-called criterion function. Such an approach is labeled "absolute feature selection". In the latter approach, to compare the different quantities that are selected as discriminating features, the feature values have to be normalized.

The so-called method of zero-mean unit-variance mapping [40, 52] is used in this thesis to normalize all the adopted features. According to this method, a normalized feature ξ_j is obtained from the unnormalized feature value x_j of a pattern vector x as follows

$$\xi_j = \frac{x_j - \mu}{s} \qquad (4.4)$$

where μ is the mean of the values of the j-feature calculated for all the pattern vectors;

s is the standard deviation of the j-feature calculated for all the pattern vectors.

The determination of a complete set of discriminating features is in practice very difficult, if possible. Some satisfactory selection of discriminating features can be carried out through distance-based algorithms. They are based on concepts of generalized distance between the values of a feature for different patterns. A useful distance definition, which is adopted in this thesis, is the concept of 'Fisher Distance'; see, e.g., refs. [53, 54].

A Fisher Distance, also called "Fisher Discriminatory Ratio", is a statistical distance between two sets of scalar numbers. It represents a distance between the averages of a feature for two sets. The Fisher distance F_{j12} between the values of feature j for two classes ω_1 and ω_2 is defined by

$$F_{j12} = \frac{[\mu(j_1) - \mu(j_2)]^2}{[s(j_1)]^2 - [s(j_2)]^2} \qquad (4.5)$$

where $j_1 = \{j_{11}, j_{12}, \ldots, j_{1r}\}$ is a set of the values of feature j for the r pattern vectors in class ω_1 ;

$j_2 = \{j_{21}, j_{22}, \ldots, j_{2q}\}$ is a set of the values of feature j for the q pattern vectors in class ω_2 ;

$\mu(j_1)$ and $\mu(j_2)$ respectively are the arithmetic means of j_1 and j_2; and

$s(j_1)$ and $s(j_2)$ respectively are the standard deviations of j_1 and j_2.

Each set is extracted from all patterns belonging to a class and the considered two sets comprise the values of the same individual feature for the two classes under consideration.

As the two classes become statistically separated, its Fisher distance for a given feature increases. Therefore, this parameter indicates the discriminating ability between the classes for the considered feature. When more than two classes occur, a summation of Fisher distances is carried out for all the possible combinations pertaining to the given classes, taken two at a time. As an example, the Fisher Distance F_{j123} for three classes ω_1 , ω_2 and ω_3 is expressed (see, e.g., ref. [54]) as

$$F_{j123} = F_{j12} + F_{j23} + F_{j13} \tag{4.6}$$

The Fisher Discrimination Ratio may be used for algorithms to automatically select features in a descending order from greater separability to lower separability.

4.4 Pattern Classification by Distance Functions

As mentioned in Section 4.2, the determination of a complete set of discriminatory features is seldom achieved in practice. It is usual to have a limited subset of discriminating features, which are selected according to their capacity of separating the classes under consideration. The design of the pertaining PR system is based, therefore, in the values of these features for the available patterns. Further, the classification of a given pattern implies a decision on its belonging to one of the classes under consideration. This decision is usually taken by means of the so-called "decision functions".

One of the simplest and most intuitive approaches to pattern classification by decision functions is based on the proximity of the patterns as defined by a distance functions. Given the simplicity of practical implementation of such proximity concept, the designed classifiers may constitute a very effective approach to the classification problem.

4.4.1. Linear Discriminant Pattern Classifier

Consider M pattern classes $\omega_1, \omega_2, \ldots, \omega_M$ and assume that these classes are respectively representable by M prototype patterns $z_1, z_2, \ldots, z_M$. The distance D_i between an arbitrary pattern vector x and the z_i prototype is given by (see, e.g., reference [47])

$$D_i = \| x - z_i \| = \left[(x - z_i)' (x - z_i) \right]^{\frac{1}{2}} \qquad (4.7)$$

where the superscript prime (') stands for the transpose of a vector, and

$$x = \begin{bmatrix} x_1 \\ x_2 \\ \cdot \\ \cdot \\ \cdot \\ x_n \end{bmatrix} \qquad (4.8) \quad ; \qquad z_i = \begin{bmatrix} z_{i1} \\ z_{i2} \\ \cdot \\ \cdot \\ \cdot \\ z_{in} \end{bmatrix} \qquad (4.9)$$

are column pattern-vectors of the values of the patterns x and z_i for the n features under consideration.

A classifier based on the distance concept computes the distance from a pattern x to the prototype of each class, and assigns the pattern x to the class whose prototype is the closest to x. It means x is assigned to the class ω_i if $D_i \leq D_k$; for k = 1, 2, ..., M ; $k \neq i$. Based on this concept, Equation (4.7) can be developed to obtain the following rule (see, e.g., Section A.1, in Appendix A of this thesis)

$$d_i(x) = w_{ij}\, x + w_{i,\, n+1} \quad , \qquad \begin{array}{l} for\ i = 1,\ 2,\ \ldots,\ M \\ for\ j = 1,\ 2,\ \ldots,\ n \end{array} \qquad (4.10)$$

where d_i (x) represents a set of linear decision fuctions, each associated with the prototype pattern,

w_{ij} is a matrix, each row of which is the vector $z_i = (z_{i1}, z_{i2}, \ldots, z_{in})$ formed by the n-feature values of the prototype pattern of a class. It is called the "weight vector" associated with the i-th decision function for class ω_i , and

$w_{i,n+1}$ is defined below

$$w_{i,n+1} = \begin{bmatrix} -\frac{1}{2} z_1' z_1 \\ -\frac{1}{2} z_2' z_2 \\ \cdot \\ \cdot \\ \cdot \\ -\frac{1}{2} z_M' z_M \end{bmatrix} \quad ; \qquad i = 1, 2, \ldots, M \qquad (4.11)$$

The complete development of the decision function (4.10) above is included in Section A.1, in Appendix A of this thesis.

In the particular case of two pattern classes, this linear decision function is easily visualized. To this, Figure 4.1 presents two classes ω_1 and ω_2 in a two-dimension feature space, where the equation of the decision function is the following

$$d(x) = w_1 x_1 + w_2 x_2 + w_3 = 0 \qquad (4.12)$$

Equation (4.12) above is represented as a separating line, of which x_1 and x_2 are the feature coordinate variables. The values w_1, w_2 and w_3 are the weight-vector parameters defined earlier by equations (4.10) and (4.11), which depend on the prototype patterns. This decision function is the perpendicular bisector of the line segment joining the two points that represent the prototypes. In the n-dimension case, the linear decision function will be a perpendicular bisector hyperplane.

Figure 4.1. shows the decision line separating the feature space in two zones. Any pattern x lying in the zone that includes ω_1 will be identified as belonging to this class, because its feature values yield a positive quantity when substituted into d(x). Any pattern y lying in the zone of ω_2 will yield a negative quantity and will be identified as belonging to class ω_2 .

When the classification problem involves more than two classes, their relative positions in the feature space give origin to three cases. In the first case, each class is separable from all the others by a single decision surface. This means that there are M decision functions with the following property (see, e.g., ref. [47])

$$d_i\ (x) = w_i\, x \left\{ \begin{array}{ll} > 0 & if\ x \in \omega_i \\ < 0 & otherwise \end{array} \right\} \quad ;\ for\ i = 1,2,..,M \qquad (4.13)$$

A simple example of this case in a two-dimension feature-space is shown in Figure 4.2. Boundaries between classes are given by the values of x for which $d_i = 0$. Although any class ω_i may cluster in a relatively small area, the actual decision region where a pattern will be assigned to this class is infinite in extent. Decision regions share some areas where d_i is greater than zero for more than one class and no decision can be taken using this scheme. Moreover, there is a remaining area where d_i yields negative values for all values of i, and no decision can be reached either.

<u>The second case</u> appears when each pattern class is separable from each other by a distinct decision surface, which may be composed by several single decision functions of the type of equation (4.10). Classes showing this relation are called pairwise separable. In this case, there are M (M-1) / 2 decision surfaces for the M classes that take the following form (see, e.g., ref.[47])

$$d_{k\,l}(x) \;=\; -\,d_{l\,k}(x) \;>\; 0 \quad ; \quad for \begin{cases} k = 1,\, 2,\, \ldots,\, M \\ l = 1,\, 2,\, \ldots,\, M \\ \quad k \neq l \end{cases} \qquad (4.14)$$

Figure 4.3. illustrates three pattern classes separable under these conditions in a two-dimension feature space. No class is separable from the others by a single decision surface. Each boundary separates just two classes and pass through the third one. Any decision for the classification of a pattern is taken based on positive values of d_{kl} for the two possible combinations of different k and l in above Equation (4.14).

It is not uncommon to find problems involving a combination of the two above-presented cases. These situations require fewer than M(M-1)/2 decision functions. The third case is the special situation of pairwise-separable classes when there are M decision functions with the property that, if x belongs to class ω_i, then the following decision functions suffice (see, e.g., ref. [47])

$$d_i(x) > d_k(x) \quad ; \quad for \begin{cases} i = 1, 2, \ldots, M \\ k = 1, 2, \ldots, M \\ i \neq k \end{cases} \tag{4.15}$$

which may be alternatively expressed by any of the following; see Equation (4.13)

$$d_{i\,k}(x) = d_i(x) - d_k(x) > 0 \tag{4.16}$$

$$d_{i\,k}(x) = [\, w_i - w_k \,]' \, x > 0 \tag{4.17}$$

$$for \begin{cases} i = 1, 2, \ldots, M \\ k = 1, 2, \ldots, M \\ i \neq k \end{cases}$$

Figure 4.4. displays this third case.

If pattern classes are classifiable into any of the above-discussed cases of linear decision functions, these classes are called linearly separable. As an example of the above-presented analysis, let us assume that each class contains only two prototype patterns, which are described by two feature values. These prototype patterns are

$$x^1 = (x_1^1 , x_2^1) \qquad ; \qquad x^2 = (x_1^2 , x_2^2) \tag{4.18}$$

where superscripts 1 and 2 respectively stand for classes ω_1 and ω_2 . The problem reduces to find a weight vector $w_i = (w_1, w_2, w_3)$ so that the following decision functions are satisfied

$$\begin{aligned} d_1 (x^1) &= w_j \, x^1{}_j + w_3 > 0 \\ d_2 (x^2) &= w_j \, x^2{}_j + w_3 > 0 \\ &\text{for } j = 1, 2 \end{aligned} \tag{4.19}$$

Where each of the above inequalities is determined by only one of the two prototype pattern vectors.

In the general case, the weight vector w_i is the solution of a set of linear inequalities determined by all patterns in the M classes. A classifier based on these linear decision functions is usually called a "Linear Discriminant Classifier", regardless of the used distance definition and/or of the criteria for the selection of the prototype patterns representing the classes.

4.4.2. Minimum-Distance Pattern Classifier

As shown earlier in Section 4.4.1, an obvious way of establishing a classification criterion for pattern vectors is by determining their Euclidean distance to every class under consideration. However, there is a variety of ways to establish measures of similarity as generalized distances between patterns; see, e.g., ref. [47].

Even if the Euclidean-distance definition is taken as the measure of proximity, different pattern prototypes may be selected, based on different criteria for the defining of such prototypes. Hence, this selection may give different linear minimum-distance classifiers.

If the average of each feature for the patterns in each class is taken as the corresponding value of this feature in the class prototype, the general frame of the foregoing Section 4.4.1 applies. By considering this average-concept into equation (4.10), the following decision functions are obtained in the form of distances to class ω_i (see, e.g, ref. [47])

$$d_i\,(\,x\,) = w_{i\,j}\,x + w_{i,n+1} \qquad (4.20)$$

$$\text{for} \quad i = 1, 2, \ldots, M$$

$$j = 1, 2, \ldots, n$$

where each row of w_{ij} is the vector $z_i = (z_{i1}, z_{i2}, \ldots, z_{in})$ as defined earlier by Equation

(4.9). Each component of z_i is the average of the values for the pertaining feature in all patterns of class ω_i ; i.e., z_i is the average feature-prototype as proposed above. Each component of $w_{i,n+1}$, as previously defined in Equation (4.11), is a constant for the pertaining class, since it depends on the class-prototype pattern.

This linear classifier is customarily called a "Minimum Distance Classifier". By using this classifier, a pattern vector is classified as belonging to the class that has the "nearest average prototype" to the pattern. An important characteristic of this classifier is that each class has the same "a priori" probability of being chosen, regardless of its size and spread. Its rather simple representation of the classes leads to relatively fast but not robust algorithms of classification; see, e.g., ref. [47].

4.4.3 Nearest Neighbour Pattern Classification

Criteria of classification are not necessarily based on the proximity to the class-prototype pattern. Another way of establishing a classification criterion is by determining the nearest neighbour (NN) to the pattern of unknown classification. The pattern is then identified as belonging to the class of its nearest neighbour.

This classification scheme for a pattern x between M classes, usually called the 1-NN rule, can be defined by saying that $s_i \in \{ s_1, s_2, .., s_P \}$ is a nearest neighbour to the given pattern vector x if

$$D (s_i , x) = \min [D (s_l , x)] \quad ; \quad for\ l = 1, 2, \ldots, P \qquad (4.21)$$

where D is any generalized distance definition;

s_i belongs to a set of P sample patterns $\{ s_1, s_2, .., s_P \}$, the classification of each of them into one of the M classes under consideration is known, and P is the number of chosen patterns from the M classes; it may even be the whole set of patterns for all classes.

This one-nearest neighbour classification is displayed in Figure 4.5. for two classes in a two-dimension feature space. It shows that x is classified into class ω_1 on the basis that the closest pattern to x belongs to this class. Figure 4.5. also shows that very complicated decision boundaries may be built just by applying the Euclidean-distance definition to the nearest-neighbour concept.

4.4.3 K-Nearest Neighbour Pattern Classifier

If K nearest-neighbours are considered when deciding a classification, and the pattern vector x is classified as belonging to the class that shows the majority of nearest-neighbours, the adopted scheme is called a K-Nearest Neighbour (K-NN rule), and the classifier is labeled a K-Nearest Neighbour Classifier.

Let us suppose that, instead of being representable by a single prototype pattern, each class is characterized by several prototypes. Each pattern of ω_i tends to cluster about one of the P_i prototypes for class ω_i . Therefore, it may be interesting to consider the distances to every P_i cluster-prototype pattern for each class ω_i . In this case, the total number P to consider for the M classes is

$$P = P_1 + P_2 + \ldots + P_M = \sum_{i=1}^{M} P_i \qquad (4.22)$$

where each of P_1, P_2, ..., P_i, ..., P_M is the respective number of considered cluster-prototype patterns of one of the M classes under consideration.

An example of a K-NN classification in a two-dimension feature space is shown in Figure 4.6. In this example, the number of clusters and pertaining prototypes is two for each of the considered classes. The number of K nearest neighbours is three, that, being odd, assures a majority of classifications in one of the two classes. Pattern x is classified in class ω_1 by this three-nearest neighbour classification.

Although this classification scheme has been based on average-prototype patterns for each class, there are no constraints to choose an arbitrary rule for the determination of the P_i patterns for every class ω_i . This possibility of using euristic rules is a characteristic of nearest-neighbour classifications. They let the classes have more complex shapes than those separable by linear decision functions. This justifies their alternative name of piecewise linear discriminant classifications; see, e.g., reference [47]. The extreme case results when all patterns from the M classes are taken as the P prototypes and $K=P$ nearest neighbours are considered. Practical considerations, however, limit both the variables P and K when computer-applied algorithms are used.

4.5 Pattern Classification by Likelihood Functions.

Pattern Recognition algorithms are often classified as parametric and nonparametric. A parametric approach to pattern classification defines discriminant functions by explicit functions of probability of occurrence, also called Likelihood Functions, of both classes and values of the feature under consideration; see e.g., ref. [48].

Nonparametric methods, despite this label, often use parameterized discriminant functions (e.g., the coefficients of the linear discriminant functions mentioned earlier in Section 4.4.1). The intended implication of this term is that nonconventional, and often nonexplicit, forms of probability distributions are assumed; see, e.g., ref. [48]. In, for instance, the previously presented schemes of classifications based on distance concepts, explicit statistical framework is absent. Thus, they can be labeled as nonparametric classifications.

Parametric approaches to the design of pattern recognition systems consider the statistical properties of pattern data to define the classification procedures. By means of a statistical parameter framework, it is possible to derive a classification that is optimal in the sense that its use yields the lowest probability of committing classification errors, see, e.g., ref [48].

4.5.1 Bayes Classification for minimum risk

Statistical Decision Theory gives the optimal decision rule to minimize a mathematically defined risk. To this purpose, it defines a set of decision functions $d_i(x_j)$, the value of which give the best choice of class to which one assigns the value x_j of the j feature in the pattern x. A risk function of taking this decision of choosing the class indicated by the n features of x, being the correct choose ω_i , has to be defined for each particular classification problem. Also, multivariate (i.e., n-dimensional) probability density functions $p(x \mid \omega_i)$ of the feature vector x in the class ω_i are known or assumed in advance (see, e.g., ref. [47]). The complete development of a general expression of the so-called Bayes' Rule of minimum risk of misclassification is included in the Section A.2, Appendix A, of this thesis.

In the particular case of the so-called "Symmetric Loss Function" (see, e.g., Section A.2, in Appendix A, of this thesis), the Bayes' Decision Rule becomes a set of decision functions of the form

$$d_i(x) = p(x \mid \omega_i)\, p(\omega_i) \leq p(x \mid \omega_k)\, p(\omega_k) \qquad \begin{matrix} i = 1, 2, \ldots, M \\ k = 1, 2, \ldots, M \\ i \neq k \end{matrix} \tag{4.23}$$

where M is the number of classes under consideration,

$p(x \mid \omega_i)$ is the multivariate probability density functions of the feature vector x in the class ω_i, and

$p(\omega_i)$ is the a priori probability of occurrence of the class ω_i.

A classifier carrying out the Bayes' Decision Rule for classification is called a "Bayesian Classifier". When the classes do not clearly cluster around prototype patterns for the considered describing features, Bayesian Classifiers show a number of advantages over the classifiers based on non-parametric concepts. Since for Bayesian Classifiers the feature values are independent from each other, more complex shape classes can be successfully treated. However, they are not as fast as the previously presented classifiers based on distance functions. In this context, the reader is referred to references [47], [48], [49], [54] and [55].

4.5.2. Bayesian Classifier for normally distributed patterns

The multivariate normal density function represents an appropriate model for most pattern recognition applications. If it assumed that the probability density functions $p(\omega_i \,|\, x_j)$, as they were introduced in the foregoing Section 4.5.1, are multivariate normal and the so-called covariance matrix is the identity matrix (see, e.g., Section A.3, in Appendix A of this thesis), the Bayes' Decision Rule of classification for normally distributed patterns can be expressed as follows

$$\log d_i(x) = \log p(\omega_i) - x' \mu_i - \frac{1}{2} \mu_i' \mu_i$$

$$i = 1, 2, \ldots, M \qquad (4.24)$$

where the superscript prime (′) stands for the transpose of a vector,

$p(\omega_i)$ is the a priori probability of occurrence of the class ω_i ,

$x = (x_i , x_2 , \ldots , x_n)$ is a pattern vector, M si the number of classes under consideration, and

μ_i is the multivariate mean vector for each class density.

The complete development of the expression (4.24) above is included in the Appendix A of this thesis.

If the multivariate mean vector μ_i is understood as the "prototype pattern vector" of class ω_i, as previously introduced in Section 4.4.1, the above expression (4.24) represents the decision function of a minimum-distance classifier; see Equation (4.10). As in that case, Equation (4.24) above is linear in the variables x and μ_i, describing a hyperplane in the n-feature space. The above discussion suggests that linear and quadratic decision functions are theoretically optimal, provided that normality of the distributions is an acceptable hypothesis.

4.6. Pattern Recognition System Design for Acousto-Ultrasonics Signals

In the previously presented sections of this chapter, all necessary information to describe the pattern classes through parametric and non parametric descriptions of the pattern vectors has been assumed to be completely known. However, when AU signals are the subjects of PR classification, we merely have some vague idea about the underlying statistical distributions.

The required statistical information for the previously presented schemes of pattern classification is seldom available from the limited-size samples of AU signals representing the classes under consideration. Therefore, either "learning" or "estimation" processes are needed to obtain the required information from the available samples.

When a priori knowledge is supplied about the belonging of each of these AU signals to a certain class, the problem is labeled as "supervised learning". This may be the case of AU experimental work presented in following chapters of this thesis, where each AU-signal is known to represent one of the different predefined material-states. In some cases, however, it is unknown to which class the AU signals belong. An estimation of the required parameters to define a suitable classification scheme is still possible through an "unsupervised learning" procedure; see, for instance, refs. [56, 57].

In the Pattern Recognition and Classification practice, decision rules are based on limited-size samples of the classes under consideration. In general, arbitrary decision functions are initially assumed. Through a sequence of iterative training steps, these decision functions are made to approach satisfactory forms; see, e.g. ref. [48].

Several deterministic and statistical algorithms to perform such a training process are available in the literature (e.g., Devijver [56]). The problem of learning and estimation in parametric decision functions is discussed, for instance, by Chen [58]. A detailed description of classic trainable classifiers by deterministic and statistical approaches is presented by Tou and Gonzalez [47].

4.6.1. AU-Signal Transformations and Feature Extraction

For the experimental work of this thesis, the softwares ARIUS-AU™ [1] (Automated Real Time Intelligent Ultrasonic System) and ICEPAK™ [2] (Intelligent Classifier Engineering Package) are adopted. The former is used for the acquisition of the AU signals, while the latter is used to carry out the analysis of retrieved AU waveforms by the Pattern Recognition and Classification approach. The AU data is input to the Pattern Recognition software as digitalized records of the analogical time-varying voltage AU signals which have been previously retrieved by the Data Acquisition software.

The Pattern Recognition software extracts values of describing features from the digitalized AU signals and some transformations of them. In particular, the features extracted from the description in time domain of the AU signal are called time-domain features. The software used isolates 36 time-domain features.

---

[1] ARIUS-AU™ is the trademark of Tektrend International Inc., Montreal.

[2] ICEPAK™ is the trademark of Tektrend International Inc., Montreal.

Four mathematical operations, which are called transformations, are performed on the time-domain description of the AU signal. A Fast Fourier Transform translates the time-domain signal into frequency domain, also called power domain, where the power of the signal at each frequency is shown. The adopted software extracts 18 feature values from this power-domain signal (see, e.g, ref. [59]). The use of this domain improves classification when phenomena occur only at some specific frequency or within a particular range of frequencies.

The Fourier Transform also produces a value of phase for each particular frequency in the spectrum of the signal. From this so-called phase domain, the software extracts 18 feature values. Phase-domain features may be employed to estimate the ratio of stored energy to dissipated energy; see, e.g., ref. [59].

In many AU applications, a signal is composed of many overlapping wavelets which are caused by echoes in the medium of propagation; see Section 3.2. A transformation called Cepstral Transform can determine the envelope shape of a wavelet and its echoes, the number of present echoes, their amplitudes and times of occurrence (see, e.g., ref. [59]). The software extracts 18 features from this cepstral domain.

A time signal may sometimes appear to repeat. Repetition may not be exact, but it gives an impression that the pattern in the signal is cyclic or periodic. The time domain signal may be compared with itself at various positions and the degree of similarity be plotted to form an autocorrelation function; see, e.g., ref. [59]. The software extracts 18 features from this autocorrelation domain.

The adopted software provides 108 features from five domains of description of the AU signals; namely, time, frequency, phase, cepstral and autocorrelation domains. The most important of these features are presented in Chapters 7 and 8 for the carried out experimental work of PR identification of AU signals applied to the characterization of impact states in polymeric base materials.

In AU-signal classification practice, however, use of the full feature set is not necessarily the most powerful in discriminating between the signal-classes of interest. A reduction of dimensionality of the extracted set of 108 features is needed. This procedure of "Feature Selection" is discussed in the following subsection.

4.6.2. AU-Signal Feature Selection

In AU practice, relatively small samples of AU-signals are available for the design of the PR system. When this design based in limited-size samples is performed, increasing the number of features used first increases the classifier ability of correct recognition until this recognition performance reaches certain peak value of correct pattern identification. Beyond this peak value for a certain number of chosen features, further increase in the feature-set dimensionality may actually decrease the recognition performance; see, e.g., ref. [58].

This feature selection problem is of significant combinatorial complexity with the consequence that no sequential algorithm can be guaranteed to produce the optimal feature set. A practical approach to the extraction of discriminating features may be a user-guided evaluation of the available features in order to select a small subset of good discriminating features; see, for instance, references [60] and [61].

The adopted software provides systematic tools to analyse features with respect to their discriminating ability between the classes under consideration. The 108 features are automatically ranked according to the Fisher Discrimination Ratio. The Probability Density Function Capability of this software plots the sample-based distribution of the probability of ocurrence of each feature for each of the classes under consideration. The observed degree of separation of these distribution, i.e., of non-overlapping between distributions, for the classes gives a practical appraisal of the discriminatory ability of each feature .

The Feature-to-Feature Projection Option of the adopted software plots the pattern distribution, for normalized feature values, of the available AU signals in each class according to any two selected features. This feature-to-feature two-dimensional projection shows a mapping of the pattern-class distributions. This analysis tool shows if different combinations of features are able to separate the considered classes. Separation of the samples into distinct clusters indicates good discrimination ability for the corresponding features. Use of these options in the experimental work of this thesis is presented in Chapters 7 and 8.

4.7. Conclusions

In this chapter, fundamentals of the design of Pattern Recognition Systems have been discussed. Basic formulations of decision functions have been presented. Principles of the practical approach and the adopted software environment to perform the experimental work of this thesis have been introduced. It has been shown that pattern classifiers, designed either in an explicit statistical framework or by a nonparametric formulation, make use of the so-called Decision Theory approach to Pattern Recognition and Classification.

It has been shown that the Pattern Recognition and Classification approach is appropriate for the identification of AU signals. An AU signal may be identified by this approach as belonging to one of some predefined classes, where each class pertains to one of the considered levels of a property in the tested material.

A pattern classifier can be viewed as a special type of information-processing system. To achieve high performance, i.e., high percentage of correctly classified patterns, the classifier system must be designed on the basis of relevant and reliable information. In the practice of AU-signal pattern recognition, however, the number of AU signals available for the PR system design is limited. Therefore, it is necessary to give the PR system the capability of either learning or estimating the unknown information from the available data.

The selection of an initial set of discriminating features draws to a large extent upon the designer's knowledge about the problem. The most practical approach to the selection of discriminating features seems to be a user-guided evaluation of available features based on classifier performances. A practical approach to the problem of selecting an optimal set of features when performing Pattern Recognition and Classification of AU signals is presented in Chapter 7.

Chapter 5

REVIEW OF IMPACT-PROPERTY TESTING TECHNIQUES FOR POLYMERIC BASE MATERIALS

5.1. Introduction

Practically all branches of engineering are concerned with materials, the properties of which are determined by tests. Understanding of the adequate techniques for the testing and specification of materials, as well as of the limitations of the applied methods, is required every time a material property is referred to.

Mechanical-test techniques not only include the procedure of the test itself, but also deal with sampling methodology and appraisal of test results. A test-technique results from considerations about the tested material and the measured material property. The starting point for the design of mechanical tests is the response functions of the tested material. Virtually all mechanical properties of engineering materials are known to depend on these response functions. When dealing with mechanical testing of, for instance, polymeric base materials, its viscoelastic response, which links time-dependent stress and strain (see, e.g., ref. [22]), may be used as starting point for the design of mechanical tests on these materials; see, e.g., ref [62].

Since mechanical properties of a tested polymeric base material are interrelated, a mutual support between different mechanical tests is always possible. In this, Turner [62] recommends that mechanical testing of polymeric material should involve two tests, one associated with stiffness and the other associated with strength, because the material-structure features that heighten the former property would simultaneously reduce the latter.

When a dynamic loading is applied to a material (e.g., from the impact of a moving mass), kinetic energy from the striking body is transferred to the tested specimen in the form of mechanical work. Resulting stresses are related to energy transfer and energy absorption and dissipation, see, e.g., ref. [62]. Therefore, energy naturally arises as an adequate magnitude to be measured when impact tests are performed. Energy-measurements are customarily used to assess the capacity of a material to resist impact and to relate an impact-loading to the resulting damage.

The present chapter reviews some conventional impact-test techniques originally designed for pure polymers. These techniques may be also applicable to polymeric base materials as the so-called polymeric-matrix composite systems. A discussion of the standard tests that are in use to quantify repeated-impact damage of polymeric materials is included. Finally, a statistical technique pertaining to the procedures of testing, sampling and appraisal of results in the carried out experimental work of this thesis is presented.

5.2. Impact Testing of Polymeric Materials

If the impacted material is able to absorb the total applied energy through elastic deformation and then dissipate this energy by any type of elastic damping, the magnitude to be measured may be the "elastic-energy capacity". The latter is usually referred to as the "resilience" of the material. Data derived from a quasi-static loading test of a material may be adequate for the assessment of its resilience; see, for instance, ref. [63].

When any mechanism other than elastic-energy absorption or dissipation arises as response to an impact, a permanent change of the material results. It implies a reduction of the impact-properties that may be revealed by some visible damage in the impacted material. In most tests, to determine the energy-absorption characteristics of a material, the energy of a blow is used to cause rupture of the test piece. The property of the material related to the work required to cause impact-rupture is often termed "impact toughness". However, this impact resistance of the material is more usually quoted as its "impact strength". The latter is defined as the ratio of the energy used to cause rupture to the cross-section area of test specimen where fracture occurs.

If impact-resistance of a polymeric base material is required, the above mentioned testing of impact strength, performed up to a complete rupture of the specimen, may be useful. However, impact resistance that corresponds to less damage than a complete fracture of the polymeric specimen may be of practical importance. In this case, some testing techniques that do not produce the complete rupture of the specimen are applicable. Standard impact tests that apply to both above mentioned approaches to the impact testing are reviewed in the following sections.

5.2.1 Standard Impact Tests for Polymeric Materials

The expected mechanical performance and acceptability of polymer and polymeric base material components, often depend on their performance in standard impact-tests. Simplicity of carrying out impact-tests accounts for their popularity in material development, quality control and product design. However, analysis of impact-test results is not as straightforward as it is for other standard mechanical tests.

Turner [62] classifies impact-tests into the following three categories:

(a) flexed-beam impact
(b) high-speed tensile impact
(c) flexed-plate impact.

The mentioned three categories comprise a variety of impact testing techniques, which specify diverse specimen geometries, sampling techniques and intended level of final damage and give different parameters for the measurement of the impact-strength. When it is necessary to refer to standard tests for polymeric materials, the above-presented categories can be respectively narrowed to three groups of tests:

(a) Izod and Charpy

(b) Standard Tensile Impact

(c) Standard Falling-Weight Impact.

These impact tests are derived from material-research approaches and they are designed to quantify a particular impact-property of a material. Hence, each one is, to some extent, aimed to a limited aspect of the impact-performance spectrum. In addition, the intrinsic dynamic nature of impact testing allows that interactions between impacting mass and impacted specimen affect the measured parameters, e.g., dynamic characteristics of the testing machine couple with those of the tested specimen. In this, Wolstenholme et al. [64] showed that the same mechanical properties that determine stress-strain response of polymers are responsible for these interactions. In general, results from different tests cannot be related.

Experimental and theoretical analysis of the dynamics of impact tests were early presented by Venzi [65] and Ireland [66]. These authors showed that interpretations of impact-tests in terms of structural dynamics response of the whole test-layout are more appropriate than those based on the dynamics of the test specimen as an isolate impacted target. Williams [67] compared some theoretical modelling with experimental data of the dynamics of impact tests in polymeric materials. A review of analytical approaches to the modelling of impact-tests is found in the work of Reed [68].

5.2.1.1 Standard Izod and Charpy Tests for Polymeric Materials

The Izod and Charpy tests for polymers are specified in ASTM D256; see, e.g., ref. [69]. Both are flexed-beam impact tests in which the blow of a swinging pendulum is used to break a notched specimen. Strict dimensions are specified for the machining of the test specimen.

In the above-referred Izod and Charpy tests, the pendulum is released from a fixed height, striking the specimen at the bottom of the swing and then continuing to a measured maximum height at the end of the first-half oscillation. The measured impact parameter is the energy absorbed from the pendulum during the first-half oscillation. Impact strength is defined either as the energy per unit cross-section area under the notch or as the energy per unit width of the notch. The latter, however, is not very informative unless the specimen thickness is specified, in which case it is just a variant of the former measure.

Charpy and Izod tests differ in specimen sizes, in notch shape and size, in the manner the specimen is held, and in the way it receives the pendulum blow. Standards state exact dimensions for the specimens, but give only broad specifications for the test-machines. This leads to the situation where different values of impact strength are obtained for the same material from Izod or Charpy tests and even from the same type of test when different machines are used.

The ideal Izod and Charpy tests would be those in which all the energy of the blow were used only in the breaking of the test specimen. However, these ideal tests are never reached in practice. Some energy is always lost through the test layout, in addition to that absorbed by the specimen as kinetic energy. Both Charpy and Izod tests measure the blow-energy in an all-inclusive term by assuming it as being the energy-to-fracture. Ireland [66] proposed that the measured energy U actually involves five terms as follows

$$U = U_A + U_{SD} + U_B + U_{MV} + U_M \qquad (5.1)$$

where U_A is the energy to accelerate the specimen from rest;

U_{SD} is the energy to bend the specimen;

U_B is the energy consumed by Brinnell deformation under the nose of the hammer;

U_{MV} is the energy absorbed by the machine through vibration after initial contact; and

U_M is the energy stored by the machine.

Besides the standards, different methods of performing and analysing the Charpy and Izod tests were proposed. A complete discussion on some of these methods and their significance are presented by Reed [68].

5.2.1.2 Standard Tensile Impact Tests for Polymeric Materials

When materials are too flexible or too thin to be tested as flexed-beam specimens, Tensile-Impact Tests are recommended. The impact is applied as a tensile loading by clamping one end of the specimen to a swinging pendulum, while the other is gripped by a crosshead. When the pendulum swings down, the crosshead is arrested by stop brackets, tensing the specimen to fracture.

A Standard Tensile Impact Test is established by ASTM D1822; see, e.g., ref. [70]. It can be performed in slightly modified Izod or Charpy testing machines. In this test, impact strength is quoted as the ratio of the energy of the impact-blow to the cross-sectional area of test specimen where fracture occurs.

An immediate advantage of this kind of test should be that the strain-rate over the entire specimen seems to be approximately constant during deformation. However, stress redistribution during impact gives stress-waves within the specimen. They actually result in significant values of local strain-rates. In a series of tests, this phenomenon may account for large deviations from the constant tensile-stress value, see, e.g, ref. [69]. In addition, the measured energy to break the specimen is just as dependent on geometry as it is in other impact tests.

5.2.1.3 Standard Falling-Weight Impact Tests for Polymeric Materials

Impact testing of polymer sheets or films is difficult when using notched-bar tests. Supply and use of polymers by small-thickness shapes require testing by alternative methods. In the case of Falling-Weight Impact Tests, the specimen can be a received commercial form or even a finished component.

Standard Falling-Weight Impact Tests are performed by dropping a mass onto the test specimen, computing impact-energy as the product of falling weight by drop height. The obtained level of damage is then classified as a fail or a pass of the specimen, as per some criteria that is presented in this section. Although the threshold of specified damage for a specimen to be classified as failed may be well below that of a complete rupture, it may render a polymer piece not useful for its intended service. Therefore, Falling-Weight Impact Tests are appropriate to assess the impact strength of the material specimen to withstand impact-energy inputs which may not result on the complete fracture of the specimen. In this respect, it may be said that the Falling-Weight Impact Test is more sensitive than Charpy, Izod, and Tensile Impact tests.

In the Falling-Weight Impact Test, the nature of the resulting stress distribution is essentially tridimensional and strongly dependent on size and geometry of the specimen. Impact strength is quoted as an impact-energy value, the calculation of which, based on the test result, is presented in the course of this chapter. Such an impact-strength parameter does not account for specimen dimensions and is useful only for comparison between same size and shape specimen tests. Although this appears as a disadvantage with respect to flexed-beam tests, it is not as such when specimens of different thickness have to be tested. Different thickness specimens may absorb very different values of energy by elastic deformation. Falling-Weight Impact Tests performed on different thickness specimens reflect these differences, while flexed-beam tests, performed on same-size machined specimens, do not.

An important advantage of Falling-Weight Impact Tests is that they may provide a spectrum of the probability of damage over a range of impact-energy values, as is explained in the followings sections of this Chapter. Its disadvantageous counterpart is the large number of tests required to estimate this spectrum. However, material sensitivity to low-energy repeated impact may well justify the choice of such a testing method, as is discussed below.

It was previously said that the ideal test, where all the measured energy is absorbed by the specimen, is never performed. Even if the ideal test were reached, the best that mechanical testing of a sample of specimens could provide would be a sample-based mean of the value of a property. This estimate of the mean should be taken with the statistical errors that derive from a limited-size sampling procedure. Significance of dealing with such statistical estimates in the case of Falling Weight Impact Test is discussed in the following sections of this chapter.

If the impact-properties of a tested polymer are assumed sensitive to low-energy repeated impact, an initial assumption of the experimental work of this thesis, an additional difficulty arises. That is, once a specimen has been tested for a certain level of falling-weight energy, i.e., for a certain weight falling from a certain height, the measured property is altered and it should never be tested again on the same specimen. Moreover, even if the specified level of damage is not reached after the single impact, the tested specimen is still part of the tested sample from the statistical point of view. Statistical considerations are then essential if repeated-impact sensitive materials have to be tested. In statistical terminology, this type of testing is called a "True Sensitivity Experiment", whose characteristics are discussed in following sections.

The American Society for Testing and Materials (ASTM) established some Standard Falling-Weight Impact Tests to assess impact-resistance of polymers. Those of interest to the carried out experimental work in this thesis are the following:

- ASTM D3029 - 'Standard Test Methods for Impact Resistance of Rigid Plastic Sheeting or Parts by Means of a Tup (Falling Weight)'; see, e.g., ref. [71].

- ASTM D2444 - 'Standard Test Method for Impact Resistance of Thermoplastics Pipe and Fittings by Means of a Tup (Falling Weight)'; see, e.g., ref. [72].

Both above-said test methods are used to obtain estimates of the so-called Mean Failure Energy of the tested sample. Mean Failure Energy is defined as the mean of the distribution of "impact failure energy" in the sample or, alternatively, the product of the falling weight by the drop height that will cause 50% of the sample of tested specimens to fail.

Since the tested polymer can be repeated-impact sensitive, ASTM standards also established the so-called Up-and-Down (also named Bruceton Staircase-Method) for the corresponding statistical procedures; see, e.g., refs. [71] and [72]. This method determines both a set of levels of energy to test a sample of material specimens and a procedure to obtain an estimate of the Mean Failure Energy of the tested sample from the test results. Statistical significance of this estimate is discussed in Section 5.3.3.

Also, ASTM D3029 defines what types of observed damage are considered fails after the falling weight impact on the test specimen as follows:

(i) crack or cracks on one surface only,

(ii) cracks that penetrate the entire thickness,

(iii) a brittle shatter, or

(iv) ductile failure (penetration).

The standard Falling-Weight Impact Test procedure proposes either dropping of different weights from a fixed height or of a constant weight from varying heights. In this, Hagan et al. [73] showed that the Mean Failure Energy for polymeric material specimens was not influenced by the variation of impact velocity resulting from different drop heights, if the range of height used is held between 0.30 and 1.5 metres. This suggests that a constant-weight method will give an equivalent result to that given by a constant-height technique in this range.

As it is presented in following sections, the Falling-Weight Impact Test carried out by the Up-and Down Method always gives an estimate of the Mean Failure Energy for a tested sample of specimens. Errors of this estimate come out not only from testing equipment and measurements, but also from the statistical procedure itself. Therefore, the choice of a sample of tested specimens and the expected accuracy of the obtained results should always be based on the statistical rationale.

5.2.1.4 Instrumented Impact Testing

The discussion of standard tests in previous Sections 5.2.1 to 5.2.1.3 have presented some of the complexities of both setting impact tests and analysing their results. Practical simplicity of choosing impact energy as the measure parameter to impact-resistance was shown. For the purposes of materials research, several techniques to record other impact parameters have been developed. These techniques to record impact parameters other than impact energy, when performing conventional impact tests, characterize the so-called instrumented impact testing.

There are several methods of instrumentation, each introduced for the purpose of testing a particular impact characteristic of a material. These methods allow recording of parameters such as impact velocity, deceleration and loading-deformation characteristics of the impacting mass. However, equivalences between different tests and even between different machines for the same type of test are not yet possible and difficulties in result interpretation persist.

ASTM compilations of several approaches to the instrumentation equipment and analysis techniques for the instrumented impact testing can be found in references [74-77]. A critical review of some researchers' attempts to a rationalization of the instrumented impact testing is presented in the work of Reed [68].

5.3. True Sensitivity Experiments

Experimental research often deals with continuous variables that cannot be directly measured in practice. This is the case of the so-called True Sensitivity Experiments (TSE). TSE are performed when it is not possible to do more than one observation on a given specimen. Once a trial has been performed, the specimen is altered and a second test will not result on a bona fide measure of the variable. Data obtained from TSE is often called sensitivity data, all-or-none data, or quantal-response data.

If a TSE has only two possible results, usually called pass and fail, for each particular variable level, it is assumed that there is a critical level of the variable associated with each specimen. The Critical Level of the Variable (CLV) is defined as the threshold at or above which the specimen will fail, and below which it will pass. Although the previous definition holds in the present thesis, it may happen, depending on the nature of both test and tested variable, that the fails occur below the CLV and the passes above it.

A population of specimens is thus characterized by a continuous variable, the Critical Variable-Level of the Population (CVLP), associated with the pertaining probabilities of failure for the specimens of the population at each level of the variable,see, e.g., ref [78]. Since neither the value of the CLV of the specimen nor the

CVLP can be directly measured, results from a set of performed trials must be statistically analysed to estimate these critical variable levels.

Experimental testing procedures to estimate the CVLP must start by some arbitrary selection of a Test-Level of the Variable (TLV). Although the selection of an initial TLV ultimately results from a non-formalized process and it relies on the researcher's experience, it should be based on any available information about the tested population.

The testing of any single specimen will determine only if the critical level of the variable for this specimen is less than or greater than the selected TLV. Once a first trial has been performed, following values of the TLV can be based on previous trial results from the same sample. Among the statistical methods to determine the following value of TLV, there are two that are widely used:

(a) The Probit Method

(b) The Up-and-Down or Step (or Bruceton Staircase) Method.

The two above-mentioned methods are introduced in following sections of this chapter.

A modified Up-and-Down Method for small number of specimens is chosen in this thesis to calculate estimates of the so-called Mean Failure Energy of a sample of polymer specimens. This method is discussed in Section 5.3.3.

5.3.1 The Probit Method

In the Probit Method, a predetermined number of specimens are tested at each of several levels of the tested variable. It follows the determination of a curve, called the probit curve, of the percentage of failure versus the tested variable; see, for instance, ref. [78]. Although simple, its disadvantage is the high number of specimens to be used for the determination of this curve.

The estimate of the critical level of the variable for a probability of failure of any percentage of the population may be determined by interpolation over the probit curve. However, when there is a rapid change of CLV in the 10% to 90% range of failure, as it is often found when testing the impact failure energy of polymers, the Probit Method is not recommended. In this case, the Up-and-Down Method should be adopted. A comparison of the Probit Method against the Up-and-Down Method in the case of small samples is presented in the work of Brownlee et al.[79].

5.3.2 The Up-and-Down Method

The Up-and-Down Method (UDM) is a procedure to both obtain and analyse statistical sensitivity data for the assessment of the critical-value of a tested variable. As it was previously said, the UDM needs the choice of an initial Test Level of the

Variable (TLV). Also, a initial Variable-Level Interval (VLI) must also be decided in advance. After the first specimen has been tested, the following level of testing results from the succession obtained by either adding or subtracting the VLI from the previous TLV, according to the procedure described below.

The UDM procedure is run under the simple rule that if the result for the previous level has been a fail, the following TLV will be obtained by subtracting the VLI to the previous TLV, while if the previous result has been a pass, the following TLV will be obtained by adding the VLI. As a result of this rule, each specimen will be tested at a level immediately below or immediately above the level of the previous trial.

The primary advantage of the UDM is that it concentrates the succession of trials near the mean of the tested variable for the sample. Its inherent disadvantage is that the specimens must be tested sequentially.

Although statistical analysis of data obtained by the UDM is always possible, the simplicity of its application and the expected error of the resulting estimate of the CLV depend on the choice of the initial TLV and VLI, see, e.g., ref. [78]. It is intuitive that the better the determination of the initial TLV, the fewer the number of trials to be performed until the Critical Level of the Variable of the sample is trespassed and the testing concentrates around the mean.

A more restrictive condition limits the determination of a VLI for the UDM statistical analysis to be simple. The chosen initial VLI should be less than twice the standard deviation of the tested variable in the tested sample. However, a rough estimate of this distribution-parameter for the tested sample is usually appropriate for the choosing of the initial TLV and VLI; see, e.g., refs. [71] and [79]. A detailed discussion of the Up-and-Down Method in true sensitivity experiments was presented by Dixon and Massey [78].

5.3.3. Modified Up-and-Down Method for Small Samples

When the initial TLV is not too far from the mean, satisfactory estimates of the values of mean and standard deviation of a tested sample can be obtained from statistical analysis of UDM data for as few as 10 to 15 specimens. Nevertheless, even shorter series can render good estimates; this possibility was first proposed in the work of Brownlee et al. [79].

If very short series with a predeterminated number of trials are used, not only the estimate of the mean, but also the expected error of this mean depends on the initial TLV, see, e.g., ref. [78]. However, if the number of predetermined trials is allowed to vary slightly, the estimate of the mean becomes less dependent on the initial TLV. This alternative approach of UDM for small-size samples is following presented.

When performing tests under the UDM, the researcher is usually interested in the critical level of the variable that corresponds to a particular value of the probability of fail of the specimens of the tested sample when this critical level is used. This is the case of standard Falling-Weight Impact Tests for the impact-strength of polymeric materials, which are aimed to give an estimate of the so-called Mean Failure Energy for the probability of fail of the 50% of the specimens of the tested sample. The scheme of UDM previously presented in Section 5.3.2. may be appropriate to the latter purpose. However, it does not make full use of the initial series of trials and of the occurrence of unequal number of passes and fails.

A modified UDM and the statistical analysis of the pertaining data to obtain an estimate of the variable value P_{50} for the probability of fail of 50% of the tested sample are following presented. With reference to the Falling-Weight Impact Test procedure, this variable value P_{50} is a "critical height" value when a constant weight is dropped from varying weight, or a "critical weight" value when varying weights are dropped from a constant height.

Further, the Mean Failure Energy is calculated as the product of this critical value P_{50} by the corresponding test weight or height, whichever has been held constant during the test.

Having set an initial value of the tested variable, the testing procedure to choose the following TLV is here run by the same rule presented earlier, in Section 5.3.2., for the ordinary UDM. The total number N′ of "weight-drops", each on a different specimen of the test-series, is carried out until a predetermined nominal number N is obtained. The nominal number N of "weight-drops" is defined as the count of the number of drops from the first impact-drop that shows a change of response with respect to the previous, either from pass to fail or from fail to pass, plus one. It is intuitive that the nominal N includes only the count of tests since they reach the "near-to-the-mean" and concentrate around it.

The estimate of P_{50} depends on the choice of the initial TLV and VLI. It can be proved that by continuing the series of drops until a predetermined nominal number N is reached, P_{50} becomes less dependent on the initial TLV; see, for instance, ref. [78].

The estimate of P_{50} is obtained from the last value of the test-series plus a function of both the VLI and the outcome of responses. This is computed as follows

$$P_{50} = h_N + k\ d \qquad (5.2)$$

where h_N is the series last-drop value of the test;

k is a function of the expected error of P_{50} and the outcome of responses, as displayed in Table B.1, in Appendix B, and

d is the Variable-Level Interval (VLI).

Before starting a test, a rough estimate for the standard deviation of the distribution of the tested variable is known in advance. The expected error of P_{50} can be limited by choosing it as a percentage of the standard deviation σ from the right side of Table B.1, which is included in Appendix B. This percentage defines the required nominal number N of drops for the test series. After the sample is tested, the obtained outcome of responses for the required "nominal number N" corresponds to a value of k. Tables B.3 to B.12, in Appendix B, also present the outcomes of the several Falling Weight Impact Tests that are carried out in the experimental work of this thesis, according to the above presented design of the Up-and-Down Method, for a constant value of falling weight while the drop height is varied consequently. Results of these tests are extensively discussed in following sections of this thesis.

For N greater than six, P_{50} may be estimated as follows

$$P_{50} = \frac{\sum_{i=1}^{N} h_i}{N} + \frac{d}{N} (A + C) \qquad (5.3)$$

where h_i are the N test drop-values of the test,

d is the Variable-Level Interval (VLI), and

A and C are functions of both the number of passes n_O and the number of fails n_x , for the nominal N trials, and of the outcome of responses, as displayed in Table B.2, in Appendix B.

Although the above-presented UDM assumes the chosen VLI is equal to the standard deviation of the distribution of the variable for the sample, estimates with $N \geq 3$ prove to have expected errors that depend very little on the actual value of P_{50}; see, e.g., ref. [78]. In practice, choosing the VLI within the range of about 0.5 to 2 times the value of the standard deviation of the distribution of P_{50} assures appropriate independence of the error of P_{50} from the standard deviation value.

A necessary hypothesis of the UDM is that the statistical distribution of critical variable levels of the population, or a known transformation of them, should be given by a normal distribution; see, e.g., ref. [78]. This is an important assumption when estimating either small or large percentage-probabilities of fail. When estimating P_{50}, however, it is enough to assume normality of the distribution in a range of plus to minus one standard deviation around the mean. The latter assumption has been largely confirmed for the usual range of falling weight impact testing of ordinary polymeric materials and constitutes one of the basis for the establishing the standard Falling Weight Impact Test; see, e.g., refs. [62], [71] and [73].

5.4. Conclusions

Most important impact-test techniques for polymers and corresponding standard tests have been presented. When reviewing them, it has been shown that the impact-resistance of polymeric materials includes many different aspects. Some characteristics of the impact phenomenon carry on to the impact test itself, making results difficult to interpret. Impact resistance is not a simply definable property and its testing may be extremely sensitive to the processing conditions of the material specimen.

Falling-Weight Impact Test shows as a suitable destructive testing approach for the purposes of the experimental work of this thesis. Its flexibility to test polymeric material components regardless of their shape, makes it particularly attractive to correlate its results with the values of quantitative non-destructive measurements performed on these components. An appropriate statistical technique to this purpose, the UDM for small number of samples, was discussed.

The application of the Pattern Recognition and Classification technique to the analysis of Acousto-Ultrasonics signals, presented earlier in Chapter 4, requires sets of specimens pertaining to same-levels of the tested variable, from which to establish corresponding classes. In the experimental work of this thesis, each set pertaining to one of the considered levels of impact may be further used to estimate the value of the polymeric material impact-strength by a Falling-Weight Impact Test.

As mentioned earlier in Section 5.1, a mechanical test for the appraisal of the quasi-static loading response of the polymeric material should complement this impact testing. In the experimental work of this thesis, a uniaxial tensile test for the testing of the residual tensile-strength of the polymeric material specimens may be appropriate, as it was investigated by Williams and Lampert [8] for the evaluation of impact damage of graphite-fibre/epoxy composite. Applications of both standard Falling Weight Impact and Uniaxial Tensile tests to the characterization of low-energy repeated-impact damage conditions in polymeric base materials follow in Chapters 6 and 8.

Chapter 6

EVALUATION OF REPEATED-IMPACT DAMAGE IN SOLID POLYMERS

6.1. Introduction

It is well known that several degrading conditions may affect polymer impact-properties, among such conditions are, for instance, temperature, environmental or chemical aging and mechanical stress conditions. As presented earlier, in Chapter 2, polymer degradation due to some of these conditions are successfully studied by non-destructive testing methodologies.

Low energy impact loading, when applied in a repeated manner, is considered to be a significant source of degradation of the mechanical properties of polymeric material systems. Such degradation is particularly feared when these materials are applied in load-bearing structural components because this repeated-impact damage may reduce the ability of the structural member to carry the design load and/or to withstand subsequent impacts. Therefore, it is important to be able to predict the impact-strength reduction of the material for a given low-energy repeated-impact loading.

Moreover, when in-service, polymer components are subjected to repeated-impact loading. Quantitative non-destructive examination methodologies are needed to know whether or not the impact resistance of the structural member has been affected.

Impact strength of solid polymers is often tested for the purpose of acceptability or quality control of the material supply. This is performed by means of standard tests, namely, Charpy an Izod Impact tests, that require the use of strict-dimension specimens. As mentioned earlier, in Section 5.2.1.1, polymer sensitivity to the methods of specimen machining and/or fabrication may strongly affect specimen properties. Therefore, polymer impact-properties as measured by the above mentioned impact tests may differ with respect to those of the actual in-service component. Instead, a Falling Weight Impact Test is seen to be more appropriate to evaluate low-energy repeated-impact damage in the structural components in service.

An alternative evaluation of the impact properties of a degraded polymer may be possible by its residual tensile strength characterization. However, such an evaluation may give at best an appraisal of the impact-degraded polymer response to quasi-static loading. Actual residual strength to withstand subsequent impact loading may be very different.

As a nondestructive alternative to the above mentioned methods, Quantitative Non-Destructive Examination (QNDE) techniques are considered to quantify impact-strength in polymeric materials if a reduction of this property is likely to affect in-service structural components. As presented earlier, in Chapter 2, Acousto-Ultrasonics (AU) is a QNDE technique that has been proven to be useful in the detection and quantification of degraded states of materials and the pertaining variations in mechanical properties. It has been successfully used, for instance, by Iyer [40] to test mechanical properties of solid polymers. Therefore, AU is seen as a viable non-destructive technique to quantify impact-resistance reduction in polymeric materials.

This chapter presents an application of the destructive Falling Weight Impact and Uniaxial Tensile Tests and the nondestructive AU methodology to characterize the residual impact-properties in polymeric material specimens. A pure polymer, namely, Polyvinylchloride (PVC), which has been subjected to controlled low-energy repeated-impact damage is evaluated. Controlled impact damage is obtained by repeatedly dropping a particular weight from a fixed height to each specimen, hence defining the pertaining impact-damage level for each specimen by the final number of applied impacts.

Correlations are carried out of the measured values of the mentioned two destructive tests with the levels of impact, as defined by the final number of applied repeated impacts to each specimen. The same values are then correlated with the pertaining values of the Acousto-Ultrasonics Parameter obtained by AU measurements, and the obtained destructive and nondestructive characterizations of the low-energy repeated-impact properties of the material are compared.

6.2. Material and Test Specimens

The solid polymer Polyvinylchloride (PVC) is evaluated for its residual impact properties after being subjected to controlled low-energy repeated-impact. The specimen shown in Figure 6.1 is adopted to perform the destructive Falling-Weight Test as per ASTM D3029 - Test Method G (Falling-Weight striking an Impactor; [71]) and Uniaxial Tensile Test as per ASTM D638 [80] and the non-destructive Acousto-Ultrasonics examination. The specimens are machined as specified in Figure 6.1 from a single sheet of the material. After manufacturing, every specimen is visually examined to assure that it is free of macroscopic cracks and/or imperfections.

6.3. Controlled Repeated-Impact Procedure

The purpose of this procedure is to obtain specimens of controlled repeated-impact damage levels, where the level of impact-damage on each specimen is determined by the final number of falling-weight impacts applied to it. Specimens subjected to the same level of repeated-impact constitute a sample of specimens representing this impact condition for the purpose of the subsequent destructive and nondestructive tests.

Controlled low-energy repeated-impact is performed by using the specially designed device of Figure 6.2. Each specimen is impacted by repeatedly dropping a constant weight of 0.9 Kg from a fixed height of 1.2 m, to strike the semi-spherical-end impactor of Figure 6.2, a predetermined number of times. Each falling-weight impact of the series of repeated-impacts onto each specimen corresponded to an impact-energy of 10.6 Joules at 4.85 m/s of impact velocity.

Six levels of repeated-impact damage are defined by the final number of impacts applied to each specimen, namely, 0, 5, 10, 15, 20 and 40 impacts. After this controlled repeated impact procedure, each specimen is visually examined to determine if it presents any failure.

Some specimens fail before or just as reaching the corresponding final number of impacts. The criteria of ASTM D3029 [71] is used to determine the presence of failure; see Section 5.2.1.3. Although these "failed" specimens may be suitable for the purposes of the subsequent uniaxial tensile tests and/or AU examination, the Falling Weight Impact Test cannot be performed on them. Therefore, they are not included in any subsequent test.

6.4. Acousto-Ultrasonics data acquisition

The acquisition of AU data is performed by means of the two-transducer experimental configuration shown earlier, in Figure 6.3. Constant-force clamps are used to obtain adequate contact between the specimen and the transducers. A fixed distance of 19mm is held constant between transducers for all signal readings.

Ultragel II™ [1] is placed as a coupling medium between the specimen and the transducers. Among usual ultrasonic-coupling media, Ultragel II™ is chosen because of its excellent transmission of ultrasonic wave-energy. For the carried out experimental work, it gave consistent repeatability of the AU measurements (see Section 3.5.1) and it showed adequate facility of application and removal. In addition, it is widely applied in experimental and industrial non-destructive evaluation.

The equipment used for the acquisition of AU data is shown in Figure 6.4. The pulse emitter device, simply called "pulser", is a circuit board that sends electric pulses to the piezoelectric emitter-transducer, which correspondingly emits the ultrasonic pulse. The pulser is controlled by a PC computer through a dedicated circuit board, usually called "trigger". The signal that is captured by the receiver transducer is sent to a Acoustic-Emission Testing facility. The latter converts signals from analogical to digital. The obtained digital AU signal is then passed to the "trigger",

---

[1] Ultragel II™ is the trademark of ECHO ULTRASOUND Inc.

which commands the pulser to emit the following pulse. The digital signal is finally fed to the PC mother board and stored as a data record on the PC hard-disk.

The whole process of pulse emission and signal acquisition is user-definable by means of software-controlled parameters. As mentioned earlier, in Sections 3.5.1 and 3.5.2, several important parameters relating to the experimental procedure, other than those pertaining to material property variations, affect the received ultrasonic waveform and, therefore, its repeatability. They are classified as 'external' to the instrumental system and 'internal' in the instrumental setting. The following Table 6.1 summarizes the values of the most relevant parameters that give adequate repeatability of the AU measurements for the material and specimens used in the present experimental work.

TABLE 6.1. Controlled parameters for the acquisition of AU data for Polyvinylchloride specimens pertaining to controlled low energy repeated impact states.

TYPE OF PARAMETER	CONTROLLED PARAMETER	SET VALUE
EXTERNAL	-Distance between Transducers -Couplant Medium	19 mm (0.75") Ultragel II™
INTERNAL	-Voltage Range -Gain -Wave Frequency	0 to +12 Volts 30 deciBels 750 KHz

These values are chosen according to the characteristic central-frequencies of the broadband emitter and receiving transducers. An appropriate combination of input frequency and amplitude gain is found as described earlier, in Section 3.5.2.

Several readings are carried out for each specimen until an appropriate repeatability of the signal AUP value is obtained under the same testing conditions. To this, repeatability of the retrieved AU-signal for a given specimen is considered satisfactory when the measured values of AUP are obtained with maximum discrepancies of 32 mVolts between two consecutive readings, being 32 mVolts the voltage interval for the calculation of the value AUP in this experimental work. Figure 6.5. shows a typical ultrasonic signal input and the corresponding readings for some of the investigated levels of impact damage.

6.5. Falling Weight Impact Testing

The controlled repeated-impact procedure, previously described in Section 6.3, supplies specimens presenting discrete levels of repeated-impact, where each level is represented by a sample of specimens, as earlier defined in Section 6.3, which have been subjected to the same final number of repeated impacts. These samples of specimens are the subject of the subsequent Falling Weight Impact Test, which is presented below.

The standard Falling Weight Impact Test is conventionally performed by dropping a mass onto each of the specimens of the tested sample, from a drop height and computing the pertaining impact-energy of this single-impact as the product of the falling weight by the corresponding drop height. The Falling Weight Impact Test of a sample of specimens is carried out by applying to each specimen of the sample a single-impact of a certain impact-energy. The level of the latter is determined by the Up-and-Down Method, described earlier in Section 5.3.2.

In the Falling Weight Impact Test, discrete levels of impact energy may be obtained for either fixed weight with varying height or, alternatively, for a fixed height with varying weight. In this study, the former method is adopted. After a single-impact trial on each specimen, the observed damage is then classified as a pass or a fail of the specimen as per ASTM D3029 [71]; see Section 5.2.1.3. The outcome of this series of single impacts results in a succession of "fails" and "passes" pertaining to the range of impact-energy values used to test the sample.

A statistical procedure is, then, used to determine the Mean Failure Energy (MFE) of each tested sample of specimens from the test outcome of passes and fails. In this, the MFE of a sample is defined as the product of the falling weight by the corresponding drop height that will cause 50% of the specimens of the tested sample to fail. It is estimated as the mean of the statistical distribution of impact failure energy for the tested sample of specimens. In the experimental work of this thesis, the UDM statistical procedure for small-size samples of specimens, introduced earlier in Section 5.3.3, is adopted to obtain the estimate of Mean Failure Energy from the test outcome of each sample.

6.6. Experimental Results

6.6.1 Characterization of Polymer Repeated-Impact Properties by Falling-Weight Impact Test

A Falling-Weight Impact Test as per ASTM D3029-Method G [71] is performed for each of the samples of eight specimens pertaining to the controlled repeated-impact damage levels mentioned in Section 6.3, but for the sample of 40-impact damage level. In the latter sample, low percentage of surviving specimens with respect to the initial (no-impact) sample make the testing non representative.

The outcome of passes and fails for the testing of each sample of the material is displayed in the corresponding table of Appendix B. Each of these outcomes gives an estimate of the corresponding mean, called Mean Failure Energy, of the distribution of impact failure energy of the sample, pertaining to one of the levels of controlled repeated-impact, mentioned earlier in Section 6.3.

The estimates of the Mean Failure Energy (MFE) for the tested samples are presented in Figure 6.6 versus corresponding final number of controlled repeated impacts. The intervals of minus to plus one estimate of the standard deviation of the impact failure energy distributions are represented around the corresponding MFE values. A correlation factor of 0.98 is obtained by a straight line fitting through the data points shown in Figure 6.6 using the "least squares" method. Consequently, a characterization of the low-energy repeated-impact conditions in PVC specimens can be made by the Mean Failure Energy obtained by Falling Weight Impact Test.

6.6.2. Characterization of Polymer Repeated-Impact Properties by Acousto-Ultrasonics

Acousto-Ultrasonics Parameter values are calculated as per Equation (3.3), Section 3.3.3, from the AU readings of specimens pertaining to the defined levels of low-energy controlled repeated-impact. At each level of impact, the average value of AUP for the sample of specimens is calculated of the measured values of AUP for the specimens of this sample.

Obtained AUP value for each specimen and average AUP value for each sample are, then, normalized with respect to the maximum average of AUP for all samples under consideration as follows

$$AUP_N = \text{Normalized } AUP = \frac{AUP}{\text{Maximum average } AUP} \qquad (6.1)$$

where in Equation (6.1) above

AUP is either the measure Acousto Ultrasonics Parameter for a specimen or the calculated "average of AUP" for a sample of specimens,

AUP_N is the pertaining value of normalized AUP, and

"Maximum average AUP" is the largest observed value among the averages of AUP for all samples. It is found to represent the average of AUP values for the "no-impact" level sample considered.

In a similar manner, the MFE value for each level of impact is normalized with respect to the maximum MFE value for all samples as follows

$$MFE_N = \text{Normalized } MFE = \frac{MFE}{\text{Maximum } MFE} \qquad (6.2)$$

where in the Equation (6.2) above

MFE is the value of Mean Failure Energy for a level of impact,

MFE_N is the pertaining value of normalized Mean Failure Energy, and

"Maximum MFE" is the largest observed value of MFE of the calculated MFE values for all samples of specimens. It corresponds to the MFE value for the "no-impact" level sample considered.

Figure 6.7 presents the normalized AUP values versus normalized Mean Failure Energy values for the tested samples. A correlation factor of 0.98 is obtained by a straight line fitting through the data points of Figure 6.7, whereby the "least squares" method is used. This linear relation is expressed as follows

$$MFE_N = 1.96\ AUP_N - 0.920 \qquad (6.3)$$

where in the above Equation (6.3), AUP_N and MFE_N are as previously defined by equations (6.1) and (6.2), respectively. Therefore, an estimation can be made of the residual MFE of PVC specimens presenting a degraded condition due to low-energy repeated-impact by using above Equation (6.3), provided that the specimen geometry and Acousto-Ultrasonics methodology are the same with those used to establish the equation.

The above-presented results show the viability of a nondestructive characterization of the low-energy repeated-impact conditions in PVC specimens by using the Acousto-Ultrasonics approach.

6.6.3. Characterization of Polymer Repeated-Impact Damage by Uniaxial Tensile Testing

Uniaxial tensile tests, as per ASTM D638 [80], are performed on specimens presenting the different levels of repeated-impact damage previously mentioned in Section 6.3. Tensile Tests are carried out in a Universal Testing Machine. The specimen is loaded at a continuous cross-head speed until failure. Values of Ultimate Tensile Strength (UTS) are calculated as the ratio of the maximum recorded load to the initial cross-sectional area of the specimen.

Figure 6.8 presents values of UTS versus corresponding levels of controlled repeated impact, as measured by the final number of controlled repeated impacts on the tested specimens. A correlation factor of 0.94 is obtained by a straight line fitting through the data points of Figure 6.8 using the "least squares" method. Consequently, a characterization of the low-energy repeated-impact conditions in PVC specimens may be made by residual tensile strength obtained from a uniaxial tensile test.

6.6.4. Correlation of Uniaxial Tensile Test Results and Acousto-Ultrasonics Data

The values of AUP were calculated from the AU readings taken from the specimens presenting the considered levels of controlled repeated-impact damage mentioned in

Section 6.3. These AUP values were normalized as per Equation (6.1). Also, at each level of impact, the average value of UTS for the pertaining sample of specimens is calculated of the measured values of UTS for the specimens of the sample. Obtained UTS value for each specimen and average UTS value for each sample are normalized as follows

$$UTS_N = Normalized\ UTS = \frac{UTS}{Maximum\ average\ UTS} \qquad (6.4)$$

where in the Equation (6.4) above

UTS is either the measure Ultimate Tensile Strength for a specimen or the calculated "average of UTS" for a sample of specimens,

UTS_N is the pertaining value of normalized UTS, and

the "Maximum average UTS" is the largest observed value among the averages of UTS for all samples. It is the average of UTS values for the "no-impact" level sample considered.

Figure 6.9 presents the values of normalized AUP for the tested specimens and of normalized average AUP versus corresponding normalized UTS values for the different levels of impact considered. A correlation factor of 0.89 is obtained by a straight line fitting through the data points of Figure 6.9 using the "least squares" method. This linear relation is expressed as follows

$$UTS_N \quad = \quad 0.296 \;\; AUP_N \; + \; 0.719 \qquad\qquad (6.5)$$

where in the Equation (6.5) above, AUP_N and UTS_N are as previously defined by equations (6.1) and (6.4), respectively. Therefore, an estimation can be made of the residual UTS of PVC specimens presenting a degraded condition due to low-energy repeated-impact by using Equation (6.5), provided that the specimen geometry and Acousto-Ultrasonics methodology are the same with those used to establish the equation.

The above presented results show the viability of a characterization of the residual tensile strength of PVC specimens presenting low-energy repeated-impact conditions by Acousto-Ultrasonics measurements.

6.7. Discussion of the obtained characterizations

Characterizations of low-energy repeated-impact damage in PVC specimens have been made by destructive Falling-Weight Impact and Uniaxial Tensile Tests, as well as by nondestructive AU technique. Both Ultimate Tensile Strength and Mean Failure

Failure Energy are mechanical properties that can be used to assess different aspects of the structural worthiness of polymers.. It has been shown that the nondestructive AU methodology is able to relate both the MFE and UTS with the so-called Acousto-Ultrasonics Parameter for samples of PVC specimens presenting discrete levels of low-energy repeated-impact damage. Also, the expressions (6.3) and (6.5) were obtained for such relations, showing the viability of estimating the values of both MFE and UTS by nondestructive AU measurements on PVC specimens presenting a repeated-impact damage condition.

It is of interest to evaluate how the measured AUP values are able to relate the MFE with the UTS values for samples of specimens presenting the same level of low-energy repeated-impact damage. For this purpose, two relations between the MFE and UTS are obtained and compared. The <u>first relation</u> is determined by relating the previously obtained straight-line relations between the normalized AUP and both the normalized MFE and normalized UTS, which are shown in Figures 6.7 and 6.9, respectively. The obtained relation is

$$UTS_N = 0.151\ MFE_N + 0.858 \qquad (6.6)$$

where MFE_N and UTS_N are as previously defined by equations (6.2) and (6.4), respectively.

The second relation is determined by relating the previously obtained straight-line relations between the number of repeated impacts of the considered levels of impact and both MFE and UTS, which are shown in Figures 6.6 and 6.8, respectively. After normalizing as per Equations (6.2) and (6.4), the obtained relation is

$$UTS_N = 0.147 \; MFE_N + 0.853 \tag{6.7}$$

where MFE_N and UTS_N were previously defined by equations (6.2) and (6.4), respectively.

Expressions (6.6) and (6.7) are represented in Figure 6.10. for the range of the carried out experimental work. As it can be seen in Figure 6.10, the results of these expressions (6.6) and (6.7) are quite close, with a maximum variation of 1% in the considered experimental range. Therefore, Figure 6.10 confirms that the Acousto-Ultrasonics technique is a viable method for the quantitative non-destructive characterization of low-energy repeated-impact damage in PVC specimens.

6.8. Conclusions

A characterization of the residual impact strength of solid Polyvinylchloride specimens was carried out by both the destructive Falling-Weight Impact Test and the nondestructive Acousto-Ultrasonics evaluation method. A straight line relation was found between the Mean Failure Energy and the pertaining number of low-energy repeated impacts for the considered levels of impact. The possibility was shown of characterizing the residual impact strength in the material specimens pertaining to low-energy repeated-impact states by the Falling-Weight Impact Test and statistical estimates of the Mean Failure Energy.

A quantitative non-destructive evaluation of repeated impact damage in the material was also carried out using Acousto-Ultrasonics methodology. A characterization based on the Acousto-Ultrasonics Parameter (AUP) was used. A straight line relation was found between the average AUP values and the residual Mean Failure Energy of the PVC specimens for the considered levels of impact. The results indicate that a quantitative non-destructive characterization of the impact-damage state of Polyvinylchloride specimens can be made by Acousto-Ultrasonics approach. By this characterization, a prediction of the residual impact strength of a PVC specimen, as measured by the Mean Failure Energy, can be made by AU measurements.

Application of such characterization of repeated-impact conditions in other polymers may be possible, given that the Acousto-Ultrasonics system is calibrated for the material and geometry variations. The review of the available literature, presented earlier in Chapter 2, show no previous research work was carried out by using statistical estimates of the Mean Failure Energy or its correlation with AU measurements to characterize repeated-impact damage conditions in engineering materials.

Finally, a characterization of the residual tensile strength in PVC specimens subjected to low-energy repeated-impacts was carried out by the Ultimate Tensile Strength measured from a uniaxial tensile test. Also, a characterization of residual tensile strength based on the Acousto-Ultrasonics Parameter (AUP) was used. A straight line relation was found between the average AUP values and the average UTS values for the samples.

The results indicate that a quantitative non-destructive characterization of the residual tensile strength of Polyvinylchloride specimens presenting impact-damage states can be made by Acousto-Ultrasonics measurements. Significant scattering was observed for the UTS values. This indicates larger-size samples, as those used for Falling-Weight Impact Tests, may be required for such an alternative evaluation. With the above said limitations, a prediction of the UTS of PVC specimens pertaining to repeated impact damage conditions may be made by Acousto Ultrasonics measurements.

The impact-damage characterization approaches that are dealt with in this chapter are also of particular interest in the evaluation of the residual impact strength in polymeric base composite systems, whose low resistance to impact prevents its use in critical lightweight structures. A study on the applicability of these approaches to polymeric-matrix composites is presented in Chapter 8.

Chapter 7

PATTERN RECOGNITION APPROACH TO THE EVALUATION OF REPEATED IMPACT DAMAGE IN SOLID POLYMERS

7.1. Introduction

If an ultrasonic signal is emitted into a solid, its mechanical worthiness influences the characteristic propagation of the ultrasonic wave. Interactions of the ultrasonic-waves with the factors that affect material properties usually result in quite complicated waveforms, which may be difficult to analyse. Chapter 6 presented a single-parameter analysis of the Acousto-Ultrasonics signals pertaining to low-energy repeated-impact states in a solid polymer; namely, Polyvinylchloride (PVC). Alternatively, characterizations of material deterioration states can be made by multivariate extraction and classification of these Acousto-Ultrasonics waveforms. This chapter presents an application of Pattern Recognition and Classification techniques to the identification of residual impact properties in PVC specimens presenting low-energy repeated-impact damage.

The retrieved AU signals from PVC specimens pertaining to different low-energy repeated impact states are stored in the form of digitalized records. These AU signals are grouped as distinct classes, each pertaining to a known level of repeated-impact damage. Describing features of these AU signals are used to build "Pattern Recognition (PR) Classifiers". These PR Classifiers are used to identify damage states in PVC specimens by classifying pertaining AU signals as belonging to one of the classes.

On using Pattern Recognition methodology, some aspects of the design of AU-signal classifiers from limited-size samples were found largely dependent on user-intuition. For the purpose of classifier design in this chapter, a procedure is proposed to select an appropriate set of describing features. A combination of "absolute feature selection" and "performance feature selection" is designed.

7.2. Experimental Pattern Recognition and Classification of AU-Signals

In the Pattern Recognition and Classification approach to the analysis of Acousto-Ultrasonics data, classification of AU-signals is performed by means of a computer-based Pattern Recognition System. This system, labelled "Pattern Recognition Classifier", is designed on the basis of retrieved AU signals pertaining to known material states.

AU-waveforms are identified as belonging to a class, where each class represents one of the different predefined states of the tested material-property. To this purpose, each AU-waveform is mathematically treated as a multiparametric description, which is called a "pattern vector" (see Section 4.2). Each component of such a vector is the value of a parameter, also called "feature", for the describing of the AU signal.

In PR methodology, the classification of unknown patterns is based on the so-called decision functions; see Section 4.5. In AU practice, decision functions are based on the limited-size samples of AU signals. In the experimental work of this chapter, some describing features of these AU signals are selected to build the decision functions. Based on these decision functions, the following types of Pattern Recognition Classifiers are designed (see Sections 4.4 and 4.5):

(i) Empirical Bayesian,

(ii) Linear Discriminant,

(iii) K-Nearest Neighbour, and

(iv) Minimum Distance Classifiers.

These PR Classifiers are tested for their performances when identifying the damage states in PVC specimens. These performances, expressed as experimental percentages of correctly classified AU-signals, are obtained when testing the classifier identification ability by AU-signals of a priori known classification. The following types of "classifier testing" are used:

-Testing of "Training" Performances, when classifying the same AU signals used for the classifier design,

-Testing of "Evaluation" Performances, when classifying AU signals not used for the classifier design, but obtained from the same PVC specimens used in the design, and

-Testing of "Classification" Performances, when classifying AU signals pertaining to PVC specimens not used for the classifier design.

7.3. Experimental Feature Extraction and Normalization

Digitalized records of AU signals from the interactions of ultrasonic pulses with the microstructure of Polyvinylchloride (PVC) specimens were retrieved according to the procedure described earlier, in Section 6.4. These PVC specimens pertain to discrete levels of controlled low-energy repeated-impact damage, as previously mentioned, in Section 6.3. Each of these levels is characterized by the final number of impacts applied to each specimen.

Accordingly to Pattern Recognition and Classification purposes, the retrieved AU-signals were grouped in classes, each representing one of the considered impact-damage states. Three classes were grouped as follows:

- Class A : No impacts,
- Class B : Five Impacts, and
- Class C : Twenty Impacts.

Figure 7.1 presents schematics of the procedures used in this chapter to perform the partial transformation from Pattern Space to Feature Space (see Section 4.2). With reference to Figure 7.1, the retrieved AU signals pertaining to each class are divided in two sets; namely, "Classifier" and "Testing" Sets. Classifier Sets are used for building the classifiers, as well as for further testing of "Training" and "Evaluation" Performances (see Section 7.2). Testing Sets are used for testing of the "Classification" Performance.

The used software extracts 108 feature values from each digitalized record of an AU signal. These values are of diverse order of magnitude in five domains of wave-description (Time, Frequency, Phase, Cepstral and Autocorrelation domains; see Section 4.6.1). Hence, Feature Normalization is necessary to make these values comparable in a n-feature space. In this experimental work, normalization is performed by means of the Method of Zero-Mean Unit-Variance Mapping (see Section 4.4).

With reference to Equation (4.4), in Section 4.3, normalization of each feature has to be carried out with respect to a certain set of values of this feature, which in turn define the "global mean" and standard deviation values of the feature for the normalization. On carrying out this experimental work, it was revealed that, given a limited-size sample of AU signals from a limited number of PVC specimens, the normalization outcome depends on the set of AU signals that is chosen to perform this normalization. In this experimental work, this set of AU signals is defined by the choice of both "Classifier" and "Normalization" trees to normalize the Classifier and Testing sets, respectively.

Figure 7.3 shows one of the "Normalization Tree" used in this experimental work. It comprises the same three Classifier Sets used to build the Classifier, plus one of the Testing Sets of specimens. The use of this Normalization Tree assures that the features pertaining to the testing AU signals are normalized with respect to the same set of AU signals used to built the classifier.

With reference to Figure 7.1, the Classifier and Testing Sets are subjected, when it applies, to Feature-value Splitting. This procedure is to obtain two files of feature values representing the same AU signals for the further "Training" and "Evaluation" testing of the classifiers. Half of the normalized feature values are stored in a so-called "training feature file", while the other half are stored in a so-called "evaluation feature file".

With reference to Figure 7.1, features values from Testing Sets are not usually split. Instead, they give "classifier feature files", each for one of the classes under consideration. The obtained set of feature-files is the feature-value database for the following procedures of building and testing of the designed classifiers.

7.4. Feature Selection and Classifier Building

Figure 7.4 presents schematics of the procedures used in this study for building and testing of classifiers by features files. They correspond to the partial transformation from the Feature Space to the Classification Space (see Section 4.2.)

With the use of a significantly large number of features for the describing the AU signals, the problem of selecting an optimal set of best discriminating features may be extremely complex. The literature review of Chapter 4 revealed that the feature-selection problem was not solved by any general algorithm, but rather afforded by user-guided evaluation on the basis of some loose guidelines; see Section 4.6.2.

The determination of a complete set of best discriminating features is seldom achieved in practice. Meantime, increasing gradually the number of used features would increase the classifier ability of correct recognition until a peak of this recognition performance is reached. Beyond such peak, further increases in the number of used features may actually decrease the recognition performance.

To solve the problem of feature selection in this thesis, a procedure was designed that obtains the classifier of the highest average of the classification performances for the classes under consideration. For each particular classification problem, it is possible to establish a ranking of the feature's discriminating-ability between classes. In this chapter, the Fisher Distance, also called the Fisher Discriminatory Ratio, is used for this ranking of features; see Section 4.3. The following presented Table 7.1 gives a description of the twelve best-ranked features, based on this ranking, for this classification problem of AU-signals pertaining to PVC specimens.

Table 7.1. Ranking based on Fisher Discrimination Ratio of the twelve best discriminating features for the classification of Polyvinylchloride specimens.

FEATURE RANKING	WAVE-DESCRIPTION DOMAIN	DESCRIPTION
1	AutoCorrelation	Greatest Peak Amplitude
2	Frequency	Greatest Peak Amplitude
3	AutoCorrelation	% of Partial Power in 5th Octant
4	AutoCorrelation	% of Partial Power in 7th Octant
5	AutoCorrelation	% of Partial Power in 8th Octant
6	Time	Greatest Peak Slope
7	AutoCorrelation	Number of Peaks above signal base line
8	Frequency	Greatest Peak Position
9	AutoCorrelation	Greatest Peak Amplitude
10	Cepstral	Greatest Peak Amplitude
11	Time	Greatest Peak Amplitude
12	Phase	Second Greatest Peak Amplitude

The feature-selection procedure was designed as following described. For each type of classifier, the selection of features is guided by strictly following the above said ranking of features. Thus, no isolated features are chosen. Instead, only complete ranking-series are taken, beginning with the first ranked feature up to a certain total number. To determine the best number of chosen features, this procedure is carried out for each type of classifier by building a series of classifiers of this type. This series starts with the classifier designed with the first-ranked feature. Following classifiers of the same type are obtained by adding features from the succession indicated by the discriminating ranking of features. The "Classification Performances", mentioned earlier in Section 7.2, are then experimentally obtained for each classifier of the designed series.

The obtained Classification Performances by the above described procedure are shown in Figures 7.5 to 7.8 for the four types of used classifiers. With reference to these figures, Classification Performances are displayed for the three classes A, B and C, up to the classifier pertaining to the 22-best ranked features. They give a description of the change of classification ability by successive adding of ranked features.

In general, the best classification performances are reached at different number of discriminating features for each of the three classes. Therefore, it is not possible to fix a number of selected features that gives these maximum performances for the three classes in the same classifier. Instead, the classifier that shows the best recognition as the average of the obtained performances for the three classes under consideration as an appropriate as solution for the multiple-class problem.

With reference to Figures 7.5 to 7.8, the average of performances of the three classes A, B and C in each classifier are also displayed. Finally, for each type of classifier, the number of features that gives the highest average of performances is chosen to design the most appropriate classifier for the classification problem.

The classifiers built by the above-described procedure, are the following:

(i) Empirical Bayesian Classifier designed for the three best-ranked features.

(ii) Linear Discriminant Classifier designed for the first best-ranked feature.

(iii) K-Nearest Neighbour Classifier designed for the four best-ranked features.

(iv) Minimum Distance Classifier designed for the four best-ranked features.

7.5. Training and Evaluation Performances of Classifiers

The designed classifiers work on the basis of decision functions. In PR practice, the statistical information to determine decision functions has to be obtained from limited-size samples of AU signals. Therefore, a process of "learning" or "estimation" is used to this purpose. Since belonging of these AU-signals to predefined classes is known for the classification problem of this thesis, the process, labelled "training" in this chapter, is a so-called "unsupervised learning" (see Section 4.6).

The ability of these decision functions to discriminate between the same digitalized records used to build them can be expressed as the percentage of these AU-records that are correctly classified. Since this percentage represents the effectiveness of the training of the classifier to recognize the AU signals used for this training, it is called "Training Performance".

A classifier may also be evaluated by the percentage of correct classification when classifying AU records obtained from the same specimens used for classifier design, though not the same digitalized records used for the training. In this chapter, this percentage is called "Evaluation Performance". The used procedures for testing these Training and Evaluation performances are displayed in Figure 7.4.

7.6. Testing of Classification Performances

With reference to Figure 7.4, the performance of each classifier should be finally tested by the Testing Feature Files of classes A, B and C. "Classification" performances for each of these classes can be expressed as the percentage of AU records from the respective Testing Set which are correctly classified in the pertaining class.

Since this testing by means of Testing Sets gives the "Classification Performances" for AU signals pertaining to PVC specimens not used for the classifier building, which will be the actual classifier task in the practice, this testing was preferred over "Training" and "Evaluation" for the procedure of Feature Selection, presented earlier in Section 7.4.

7.7. Experimental Results of Pattern Recognition and Classification

7.7.1. Material and Test Specimens

Specimens of a solid polymer, namely, Polyvinylchloride, previously described in Section 6.2, are chosen for the purposes of the PR experimental work of this chapter. They were subjected to different levels of controlled low-energy repeated-impact by repeatedly dropping a constant weight from a constant height a number of times as described earlier, in Section 6.3. Three levels of repeated-impact damage are obtained by the final number of impacts applied to each specimen; see Section 7.2.

7.7.2. Experimental Training and Evaluation Performances

Results of the testing of 'Training" and "Evaluation" Performances as the average of correct classification for the three classes of repeated impact are presented in the following Table 7.2.

Table 7.2. Average of Training and Evaluation performances in % of correctly classified AU-signals for polyvinylchloride specimens.

	Empirical Bayesian Classifier	Linear Discriminant Classifier	K-Nearest Neighbour Classifier	Minimum Distance Classifier
Training	81.82%	85.23%	100%	86.36%
Evaluation	82.18%	86.21%	100%	83.33%

For the visualization of these percentages of correct classification, Figure 7.9 graphically displays these Training and Evaluation performances as the average for the three impact-classes for each of the four designed classifiers. Excellent Training and Evaluation performances are obtained for the designed classifiers.

On carrying out this experimental work, it was observed that classifiers that do not show good "Training" and "Evaluation" performances subsequently give poor

"Classification" performances. Thus, if a classifier is to be used in further identification of unknown-classification signals, excellent Training and Evaluation performances should be a minimum condition for such classifier.

Figure 7.10. presents a plotting of normalized feature values used to build the classifiers. As an example, the three training sets for classes A, B and C and the evaluation set for class A are presented in a two-feature space pertaining to the two-best-ranked features. Figure 7.10 shows that the used features are able to discriminate between the considered levels of impact, by separating the classes into distinct clusters.

Also, for each of the designed classifiers, Training and Evaluation performances are very close. This is an indication of good AU-signal repeatability for the same specimen as well as between specimens of same level of impact damage. With reference to Figure 7.10, it can be seen that the feature values for training and evaluation sets of, for instance, Class A, significantly cluster, i.e, excellent repeatability of the feature values for different AU signals is shown.

7.7.3. Experimental Classification Performances

The following Table 7.3 presents the "Classification" performances for the four designed classifiers as the percentages of correctly classified AU signals from PVC specimens not used for the classifier building. These experimental Classification performances are obtained for each class by classifier testing with the respective Testing Set. Averages of these performances are also presented in Table 7.3.

Table 7.3. Classification performances in % of correctly classified AU-signals for polyvinylchloride specimens.

	Empirical Bayesian Classifier	Linear Discriminant Classifier	K-Nearest Neighbour Classifier	Minimum Distance Classifier
Class A	100%	100%	66%	100%
Class B	100%	75%	98%	92%
Class C	75%	75%	75%	75%
Average	91.67%	83.33%	79.67%	89%

For the visualization of these experimental percentages of classification, Figure 8.6 graphically displays these Classification performances. Good performances are obtained for the four types of built classifiers. The maximum of Classification Performances are reached for the case of Empirical Bayesian Classifier. These performances give an appraisal of the classifier recognition of specimens of unknown classification, which will be the actual classifier task in the practice. Therefore, they indicate that Pattern Recognition techniques applied to classification of AU signals can be used for the quantitative non-destructive identification of damage states in PVC specimens pertaining to different levels of low-energy repeated impact.

7.7.4. Discussion of the obtained Classification Performances

With reference to Figure 7.11, better performances correspond, in general, to the identification of class A comprising undamaged specimens. On carrying out the present study, it was observed that incorrectly classified AU signals actually belonging to one class of damaged specimens, were identified as belonging to the other, rather than belonging to class A (I.e., signals incorrectly classified as class B actually pertained to class C, and vice versa). That showed the discrimination of AU signals between different levels of effective damage may be more difficult than between damaged and undamaged-specimen classes.

This may be explained by higher overlapping of probability density functions between B and C classes than the one between class A and any of the other two classes. As an example, Figures 7.12 and 7.13 present the probability density functions for the first and second ranked features, respectively, of the Classifier Tree, showing the higher overlapping between classes B and C. These experimental probability density functions show the probability of occurrence of a given feature-value in a class, obtained from the limited-size Classifier Set pertaining to the class (see Section 4.6.2). A listing of the best twelve-ranked features of this experimental work can be seen in Table 7.1, Section 7.4.

With reference to Figures 7.12 and 7.13, higher overlapping of probability density functions is observed between classes B and C than between any of them and class A. In general, this phenomenon was observed for the rest of the best-ranked features. As an example, Figure 7.14 presents a plotting of the "cluster boundaries" for the Classifier Sets compared with the feature values for the three pertaining Testing-Sets. This two-feature space plotting is given for the two best-ranked features. Figure 7.14 shows that testing AU signals for class A may be easily identified in the correct class, even if they show some scattering with respect the original Classifier-Set values used to built the classifier. On the contrary, classes B and C may present more difficult identification because of some overlapping. Therefore, more difficult discrimination between different levels of effective damage than between damaged and undamaged-specimen classes is likely explained by the overlapping of probability density functions for the used discriminating features.

A literature review revealed that Bartos [81] studied the feasibility of performing Pattern Analysis of impact-damage due to single impacts of different impact-energy on graphite-epoxy composite panels. Although using different AU procedures than those described in this chapter, he obtained Bayesian Classifier's performances which are in very good agreement with the performances obtained for this type of classifier in the experimental work of this chapter.

With the above-discussed limitations, these experimental results show the viability of identifying low-energy repeated-impact states in PVC specimens by the AU technique combined with Pattern Recognition and Classification approach.

7.8. Conclusions

A characterization of repeated-impact damage in PVC specimens due to low-energy impact was carried out by Pattern Recognition and Classification methodology. Acousto-Ultrasonics signals from the interactions of ultrasonic pulses with Polyvinylchloride specimens were processed to build Classifiers. Acousto-Ultrasonics signals were identified as belonging to a class, being each class pertaining to a repeated-impact damage level.

Good discrimination was obtained for the considered levels of low-energy repeated impact. Also, good identification of the damage states in testing AU signals not used for the classifier design, was obtained for the four considered types of PR classifiers.

The obtained results indicate that Pattern Recognition and Classification techniques applied to AU signals analysis can be used for the quantitative non-destructive identification of damage states in PVC specimens pertaining to discrete levels of low-energy repeated impact. Application of this AU analysis approach may be possible to characterize repeated-impact in other solid polymers, providing the Acousto-Ultrasonics system is calibrated and Pattern Recognition Classifier design is performed with consideration of the particular material and test specimen.

To carry out this Pattern Recognition characterization, a procedure for the selection of discriminating features was adopted. It was observed that a selection of complete series of features from a ranking based on the feature's discriminating-power leads to classifiers of good performances when identifying specimens not used for the classifier design, while feature selection procedures intuitively based on the isolation of seemingly good discriminating features may not lead to good classifier performance.

Chapter 8

EVALUATION OF REPEATED-IMPACT DAMAGE IN POLYMERIC-MATRIX COMPOSITES

8.1. Introduction

When polymeric base composite materials are applied to structural uses, their impact strength may be a serious weakness. Because polymeric base composite systems are used in aircraft structures often subjected to a variety of low-energy impact loading, it is important that impact-behaviour of these materials in such damage conditions be well known and understood. Recent emphasis on impact degradation of polymeric-matrix composites is due to their increasing use in structures that may be exposed to impact loading.

Boukhili et al. [82] identified as a major cause of damage on, for instance, aircraft composite structures the impact caused by runway debris, large hailstone, dropped tools and contact with ground servicing equipment. These causes of mechanical-property degradation may be crucial when they appear as low energy impact in a repeated manner. They are particularly feared if they can induce damage without any external indication on the visually accessible area; see, e.g., ref. [83].

The process of composite fracture under static and/or dynamic loading is known to involve a sequence of damage mechanisms. In general, it is initiated by a matrix-dominated cracking, prior to final fracture by fibre breakage; see, for instance, references [84-87]. Low-energy repeated-impact may accelerate the initiation of matrix cracking on non visually accesible surfaces of the composite structure, significantly reducing its residual mechanical properties. Since low-energy repeated impact may constitute an important degrading factor in the residual ability of a composite structure to withstand static and/or dynamic loadings, both the prediction and non-destructive testing of the composite residual mechanical strength represent a key issue.

The problems of manufacturing process control and quality assurance of polymeric base composite systems have been adequately answered by qualitative non-destructive testing techniques, which are primarily aimed to the detection, characterization and evaluation of flaws introduced in the fabrication stage; see, e.g., references [88] and [89]. Nevertheless, quantitative measurement of the effect of low-energy impact in the residual mechanical strength of polymeric-matrix composites is needed in material selection, structural design, structural integrity prediction and maintenance planning.

Chapter 6 of this thesis presented a characterization of the residual impact properties of a solid-polymer degraded due to low-energy repeated-impact by means of destructive and nondestructive techniques. Also, Chapter 7 presented an evaluation of the residual impact-resistance of the solid polymer by multivariate Pattern Recognition and Classification of AU signals. The present chapter deals with the applicability of these techniques to quantify and, then, predict the residual impact-strength in a graphite-fibre/polycarbonate-matrix composite system presenting low-energy repeated impact damage.

8.2. Material and Test Specimens

A graphite-fibre/polycarbonate-matrix composite system is evaluated for its residual impact properties after being subjected to controlled low-energy repeated-impact. The structure of the chosen composite comprises two exterior graphite-fibre woven fabric/polycarbonate layed up in a $[(0/90)_4]$ configuration enclosing a 1.58mm-core of polycarbonate. Specimens of rectangular cross-section (i.e., 25.4mm of width by 3.3mm of thickness) and 108mm of length are machined from a single sheet of the material. Every specimen is subsequently examined to assure it is free of macroscopic cracks and/or imperfections.

8.3. Controlled Repeated Impact Damage

The purpose of this procedure is to obtain specimens of controlled repeated-impact damage levels, where the level of impact-damage on each specimen is determined by the number of falling-weight impacts applied to it. Specimens subjected to the same level of repeated-impact constitute a sample of specimens representing this impact condition for the purposes of the subsequent destructive and nondestructive tests.

The specimen is clamped in the device presented earlier in Figure 6.2 and described in Section 6.3. Different levels of controlled low-energy impact damage are obtained by repeatedly dropping a constant weight (0.4 kg) from a fixed height (0.75 m) onto each specimen a predetermined number of times. Six levels of repeated-impact damage are defined by the final number of impacts applied to each specimen, namely, 0, 1, 3, 4, 6 and 10 impacts.

After controlled repeated-impact, every specimen is visually examined to determine if it presents any failure. When composite specimens are subjected to one to four impacts, no change is observed on either side of the specimens. Further, when the specimens are subjected to six and ten impacts, they present a small deformed area which is marginally distinguished on the impacted side of the specimen. Also, it is observed that after six impacts, some specimens fail by presenting a slight surface cracking on the side opposite to the impact. Although these "failed" specimens may be suitable for the purposes of uniaxial tensile testing and/or Acousto-Ultrasonics examination, the Falling Weight Impact Test cannot be performed on these "failed" specimens. Therefore, they are not included in the latter test.

8.4. Acousto-Ultrasonics Data Acquisition

Acquisition of the AU signals for the tested composite specimens is performed by means of the previously presented two-transducer configuration of Figure 6.3 and instrument setup of Figure 6.4, which were used earlier for the AU testing of PVC specimens (see Section 6.4). The set of AU controlled parameters used for the purpose of AU testing of the graphite/polycarbonate composite specimens is presented in the following Table 8.1.

TABLE 8.1 AU controlled parameters for graphite/polycarbonate composite specimens.

TYPE OF PARAMETER	CONTROLLED PARAMETER	SET VALUE
EXTERNAL	-Distance between Transducers	31.8 mm (1.25")
	-Couplant Medium	Ultragel II™ [1]
INTERNAL	-Voltage Range	0 to +12 Volts
	-Gain	26 deciBels
	-Wave Frequency	750 KHz

[1] Ultragel II™ is the trademark of ECHO ULTRASOUND Inc.

Since the bandwidth of the emitter transducer is the same with that used for the AU testing of pure polymer specimens (see Section 3.5.2), the same input wave frequency (750 KHz; see Table 6.1 in Section 6.4) is chosen here. An optimization trial is carried out to obtain a good combination of this frequency and the amplitude gain. The chosen value of the latter (26 deciBels) assures the ratio of signal to noise sufficiently high to obtain good signal discrimination for the tested material states of the composite specimens.

For the choosing of the distance between transducers, this is fixed as the largest distance (31.8 mm) compatible with the retrieving of significant AU-signal amplitudes, while assuring adequate interaction of the ultrasonic-wave with the composite microstructure (see Section 3.5.1).

All other internal and external controlled AU parameters are held at the same values with those chosen for the AU testing of pure polymer specimens (see Table 6.1 in Section 6.4). Several readings are carried out for each specimen until appropriate repeatability of the signal AUP value is obtained. Signal reading is repeated by the procedure described earlier, in Section 6.4, for the AU data acquisition from pure polymer specimens.

8.5 Experimental Results

8.5.1 Characterization of Composite Repeated-Impact Properties by Falling-Weight Impact Test

A Falling-Weight Impact Test, as per ASTM D3029-Method G [71], is performed for each sample of eight specimens pertaining to each of the controlled repeated-impact damage levels mentioned in Section 8.3, but for the sample of ten-impact damage level. In the latter sample, low percentage of surviving specimens with respect to the initial (no-impact) sample, make this testing non representative. Differences of this destructive test with respect to the previously performed controlled repeated-impact procedure (see Section 8.3) were explained earlier in Section 6.5.

Statistical analysis of the outcome of passes and fails from the testing of each sample of specimens is carried out by the earlier described Up-and-Down Method (see Sections 5.3.2 and 5.3.3). It gives estimates of the mean, called Mean Failure Energy, of the distribution of impact failure energy pertaining to each level of impact. The outcome of passes and fails and the calculated value of this estimate for each tested sample is displayed in the pertaining table of Appendix B.

The estimates of the Mean Failure Energy (MFE) for the tested samples are presented in Figure 8.1 versus pertaining levels of repeated impact, as measured by the final number of repeated impacts. The intervals of minus to plus one estimate of the standard deviation of the impact failure energy distributions are represented in Figure 8.1 around MFE values. A correlation factor of 0.98 is obtained by a straight line fitting through the data points of Figure 8.1 using the "least squares" method.

8.5.2. Characterization of Composite Repeated Impact Properties by Acousto-Ultrasonics

Acousto-Ultrasonics Parameter (AUP) values are calculated from the AU readings in specimens pertaining to known levels of controlled low-energy repeated-impact. At each level of impact, the average value of AUP for the sample of specimens is calculated of the measured values of AUP for the specimens of this sample. All obtained AUP values are, then, normalized as per Equation (6.1), Section 6.6.2. Also, the MFE value for each level of impact is normalized with respect to the maximum MFE for all samples as per Equation (6.2), Section 6.6.2.

Figure 8.2 presents the normalized AUP values versus normalized Mean Failure Energy values for the tested samples. A correlation factor of 0.94 is obtained by a straight line fitting through the data points of average AUP and pertaining MFE values in Figure 8.2 using the "least squares" method. This linear relation is expressed as follows

$$MFE_N = 0.655\ AUP_N - 0.323 \qquad (8.1)$$

where in the above Equation (8.1), AUP_N and MFE_N are as previously defined by equations (6.1) and (6.2), in Section 6.6.2, respectively. Therefore, an estimation can be made of the residual MFE of specimens of the tested composite presenting a degraded condition due to low-energy repeated-impact by using above Equation (8.1), provided that the specimen geometry and Acousto-Ultrasonics methodology are the same with those used to establish the equation.

The above-presented results show the viability of a nondestructive characterization of the low-energy repeated-impact conditions in the Graphite-fibre/Polycarbonate matrix composite specimens by AU methodology.

8.5.3. Characterization of Composite Repeated-Impact Damage by Uniaxial Tensile Test

Uniaxial tensile tests, as per ASTM D638 [80], are performed on composite specimens presenting the levels of repeated-impact damage previously defined in

Section 8.3. Tensile tests were performed in a Universal Testing Machine. Values of Ultimate Tensile Strength (UTS) are calculated as the ratio of the maximum recorded load to the initial cross-sectional area of the specimen.

The results from these tests are presented in Figure 8.3. It presents values of UTS for each tested specimen and average UTS for the samples of each level of impact versus pertaining number of repeated impacts. With reference to Figure 8.3, no significant difference is observed of values of tensile strength, as measured by average UTS of the impacted samples, with respect to the average UTS of the non-impact sample. Therefore, the average of UTS values of the samples of the tested composite are not affected by the different levels of impact-damage in the experimented range of controlled low-energy repeated impact.

8.5.4. Discussion of the obtained characterizations of Polymer-Matrix Composite

A characterization of the residual impact strength of the graphite/polycarbonate composite specimens presenting a degraded condition due to low-energy repeated impact was carried out by Falling-Weight Impact Test. A relation was found of the residual impact-strength of the specimens as measured by the so-called Mean Failure Energy (MFE) of the samples with the number of low-energy repeated-impacts. Also, a characterization of the residual impact strength of composite samples was made by establishing a correlation between the MFE and the Acousto-Ultrasonics Parameter values calculated from AU signals.

In the considered range of impact damage, the tensile strength of the composite specimens, as measured by average UTS of the samples, was not affected by the different number of applied low-energy repeated-impacts. A likely explanation of this behaviour may be based on the consideration of the typical failure mechanism of polymer-based composites. In this, Cristescu et al. [85] and Sierakowski et al. [86] showed that the breaking of polymeric-matrix composite is typically initiated by a matrix-dominated cracking, prior to delamination and final fracture by fibre breakage. Thus, the Ultimate Tensile Strength of the composite specimens may be judged to be more related to the breaking-resistance of the fibre, than to the resistance of the polymeric matrix. The former is unlikely to be affected by the controlled low-energy impact that was applied onto the composite specimens in the range of the carried out experimental work. To corroborate this hypothesis, experimental work was carried out as presented below.

As mentioned earlier in Section 8.3, some specimens presented failure in the form of slight surface cracking after the controlled repeated-impact and they were considered as "failed" for the subsequent procedure of Falling Weight Impact Test. It is of interest to determine if those "failed" specimens show diminished tensile strength, as measured by UTS, with respect to the "surviving" specimens previously

Figure 8.3. To this, uniaxial tensile tests, as per ASTM D638 [80], are performed for two samples of "failed" composite specimens pertaining to the levels of six and ten low-energy repeated impacts.

The obtained values of UTS from these tests are presented in Figure 8.4. Also, averages of the UTS values are presented for these samples of "failed" specimens and for the samples of "surviving" specimens for the considered levels of impact. With reference to Figure 8.4, the measured values of UTS for these failed composite specimens are clearly lower than those of the surviving specimens, for similar levels of impact damage.

The results presented in Figure 8.4 indicate that low-energy repeated impact damage, which was in turn revealed by reduction of the Mean Failure Energy of the samples of surviving specimens, does not influence the Ultimate Tensile Strength of the composite if no matrix failure results from this repeated-impact. Meantime, when a initial matrix cracking is present, as it is the case of "failed" specimens displayed in Figure 8.4, the composite specimens show lower values of Ultimate Tensile Strength.

There are two likely explanations of the latter phenomenon: The <u>first explanation</u> was proposed by Crossman and Wang [84] when they investigated the tensile strength to initiate transverse-cracking in graphite/epoxy composite laminate. They showed that matrix-cracking dominated damage can be detrimental to the structural resistance of polymer-matrix composites, because it results in a redistribution of stresses that can influence the onset of final fibre-fracture. The second explanation is that the presence of a polymeric-matrix cracking as a result of, for instance, repeated-impact damage, also indicates an initial damage of the reinforcing graphite-fibre, which may lead to the observed lower values of UTS (see, e.g., ref. [85]).

8.6. Pattern Recognition and Classification Analysis of Composite Repeated-Impact Damage.

8.6.1. Classifier Design

AU signals from the interactions of ultrasonic pulses with the microstructure of composite specimens are retrieved according to the procedure previously described in Sections 8.4. These composite specimens pertain to the discrete levels of low-energy repeated-impact damage, mentioned earlier in Section 8.3.

According to PR purposes, the retrieved AU-signal are grouped in classes, each representing one of the considered impact-damage states. Three classes are grouped as follows:

- Class D : No impacts,
- Class E : Three impacts, and
- Class F : Ten impacts.

In this chapter, the used procedures to perform the Feature Extraction, Normalization and Selection, and Classifier Building and Testing are similar to the respective procedures described earlier, in Chapter 7, for the Pattern Recognition and Classification Analysis of PVC specimens. Accordingly, the Feature Extraction and Normalization procedures are based on Classifier and Testing Sets, and on the pertaining "Classifier Trees" and "Normalization Trees" of the types described in Section 7.3, and respectively presented in Figures 7.2 and 7.3.

Also, the feature-selection procedure earlier described in Section 7.4 is adopted. Based on this procedure, the designed classifiers are the following:

(i) Empirical Bayesian Classifier designed for the four best-ranked features.

(ii) Linear Discriminant Classifier designed for the four best-ranked features.

(iii) K-Nearest Neighbour Classifier designed for the three best-ranked features.

(iv) Minimum Distance Classifier designed for the two best-ranked features.

A listing of the twelve best-ranked features for the purpose of discrimination of the mentioned three repeated-impact states is presented in the following Table 8.2.

Table 8.2. Ranking based on Fisher Discrimination Ratio and description of the twelve best-discriminating features for graphite/polycarbonate composite specimens.

FEATURE RANKING	WAVE-DESCRIPTION DOMAIN	DESCRIPTION
1	Time	% of Partial Power in 4th Octant
2	Time	Inter-peak distance from 1st to 2nd greatest
3	Time	Inter-peak distance from 2nd to 3rd greatest
4	Phase	% of Partial Power in 3rd Octant
5	Time	Second Greatest Peak Amplitude
6	Time	Greatest Peak Rise Slope
7	Time	Greatest Peak Amplitude
8	Frequency	Second Greatest Peak Position
9	Time	Second Greatest Peak Position
10	Frequency	Inter-peak distance from 1st to 3rd greatest
11	Frequency	Number of Peaks above signal base line
12	Phase	% of Partial Power in 2nd Octant

8.6.2 Performances of Classifiers for Training, Evaluation and Testing of Classification

The four designed PR Classifiers are tested for their performances when identifying damage states in composite specimens. These performances, expressed as experimental percentages of correctly classified AU-signals, are obtained when testing the classifier identification ability by AU-signals of a priori known classification. The following types of "classifier testing" are used:

-Testing of "Training" Performances, when classifying the same AU signals used for the classifier design,

-Testing of "Evaluation" Performances, when classifying AU signals not used for the classifier design, but obtained from the same composite specimens used in the design, and

-Testing of "Classification" Performances, when classifying AU signals pertaining to composite specimens not used for the classifier design.

Results of the testing of "Training" and "Evaluation" Performances for graphite/polycarbonate specimens are presented in the following Table 8.3.

Table 8.3. Average of Training and Evaluation performances in % of correctly classified AU-signals pertaining to graphite/polycarbonate composite specimens.

	Empirical Bayesian Classifier	Linear Discriminant Classifier	K-Nearest Neighbour Classifier	Minimum Distance Classifier
Training	86.33%	95%	100%	96.67%
Evaluation	89.67%	100%	100%	98.33%

For the visualization of these percentages of correct classification, Figure 8.5 graphically displays these Training and Evaluation performances as the average for in the three impact-classes for each of the four designed classifiers. Excellent Training and Evaluation performances are obtained for the design classifiers. On carrying out this experimental work, it was observed that classifiers that do not show good Training and Evaluation performances subsequently give poor Classification performances when further used for the identification of composite specimens not used for classifier building, which will be the actual classifier task in the practice; see Section 7.6.

Also, for each of the designed classifiers, Training and Evaluation performances are very close. As previously discussed when performing PR Classification of PVC specimens, in Chapter 7, this is an indication of good AU-signal repeatability for the same specimen as well as between specimens of the same level of impact damage.

The following Table 8.4 presents the "Classification" performances for the four designed classifiers of composite specimens as the percentages of correctly classified AU signals from composite specimens not used for the classifier building.

Table 8.4. Classification performances in % of correctly classified AU-signals for graphite/polycarbonate composite specimens.

	Empirical Bayesian Classifier	Linear Discriminant Classifier	K-Nearest Neighbour Classifier	Minimum Distance Classifier
Class D	90.67%	98.67%	100%	100%
Class E	100%	95%	81%	76%
Class F	85%	80%	96%	85%
Average	91.89%	91.22%	92.33%	87%

For the visualization of these experimental percentages of classification, Figure 8.6 graphically displays these Classification performances. With reference to Figure 8.6, better performances correspond, in general, to the identification of class D comprising undamaged specimens. On carrying out the present study, it was observed that incorrectly classified AU signals actually belonging to one class of damaged specimens, were identified as belonging to the other, rather than belonging to class

D (I.e., signals incorrectly classified as class E actually corresponded to class F, and vice versa). That phenomenon, also observed when previously performing PR Classification of impact states in PVC specimens, showed that the discrimination of AU signals between different levels of effective damage in composite specimens may be more difficult than between the levels pertaining to damaged and undamaged composite specimen.

Figures 8.7 and 8.8 display the normalized feature values for the first and the second ranked features and for the second and the third ranked features, respectively, in the Classifier Sets. They present the clusters of values for the used features, where each cluster represents one of the considered impact classes.

With reference to Figures 8.7 and 8.8, it can be observed that the used features are able to discriminate the different levels of impact damage. Figures 8.7 and 8.8 also show that the clusters representing classes E and F of effective impact damage are closer than any of them is to Class D of undamaged specimens. This phenomenon may explain the better classification performances for Class D.

The above presented results indicate the viability of characterizing low-energy repeated-impact states in the tested composite specimens by the AU technique in conjunction with Pattern Recognition and Classification approach.

8.7. Conclusions

The applicability has been assessed of some characterizations of residual impact strength in a Graphite-fibre/Polycarbonate matrix composite system subjected to low-energy repeated-impact. Both destructive and non-destructive methodologies has been used. A characterization of residual impact strength has been carried out by Falling-Weight Impact Test. A straight line relation was found between the Mean Failure Energy and the final number of low-energy repeated impacts for the considered levels of impact damage. The viability was shown of characterizing the residual impact strength of the tested composite specimens pertaining to low-energy repeated-impact states by Falling-Weight Impact Test.

A quantitative non-destructive evaluation of repeated impact damage in the composite specimens has been carried out by Acousto-Ultrasonics methodology. A characterization based on the Acousto-Ultrasonics Parameter was used. A straight line relation was found between the average AUP of the samples of composite specimens and the pertaining Mean Failure Energy values of that samples. Therefore, a quantitative non-destructive characterization of the impact-damage state of the tested composite specimens can be made by Acousto-Ultrasonics approach. By this characterization, a prediction of the residual impact strength of a PVC specimen, as measured by the Mean Failure Energy, can be made by AU measurements. Application of such characterization of the repeated-impact conditions in other polymeric-matrix composites systems may be possible, given that the Acousto-Ultrasonics system is calibrated for material and geometry variations. On reviewing the available literature, no research work was found on using Mean Failure Energy or its correlation with AU measurements to characterize the repeated-impact damage conditions in polymeric-matrix composites.

A characterization has been carried out of the residual tensile strength in the composite by the Ultimate Tensile Strength of samples of specimens. When the specimens survived the controlled repeated impact without presenting visible damage, no significant change of the Ultimate Tensile Strength (UTS) values was observed, in the considered range of damage, for the different levels of repeated impact. If the specimens presented, instead, failure as an initial-cracking after similar levels of repeated impact, significant reduction of UTS values was observed. When evaluating the residual ultimate tensile resistance of the composite, associated with the final breaking of the reinforcing fibre, this characterization of the impact damage by means of Uniaxial Tensile Test may be an appropriate approach.

Finally, an AU-signal identification analysis based on Pattern Recognition and Classification has been carried out. Acousto-Ultrasonics signals were processed to build Pattern Recognition classifiers. Good discrimination between composite specimens of different levels of impact damage were obtained for the four types of designed PR classifiers. Also, good identification of testing AU-signals in the correct impact class was obtained. This indicates that the Pattern Recognition and Classification approach applied to the identification of AU signals can be used for the quantitative non-destructive identification of low-energy repeated-impact states in the tested graphite/polycarbonatecomposite material. Application of such characterization may be possible to evaluate the repeated-impact conditions in other polymeric base composite systems, provided the Acousto-Ultrasonics system is calibrated and Pattern Recognition Classifier design is performed with consideration of the tested material and test specimen configuration.

CHAPTER 9

CONCLUSIONS AND REMARKS

9.1. CONCLUSIONS

Polymeric material systems, either as pure polymer components or as part of polymeric-matrix composites have increasingly been used as load-bearing lightweight structures. Proper understanding of the behaviour of these materials under different loading conditions is, therefore, an important consideration.

Low-energy repeated-impact loading may degrade the mechanical properties of polymeric base material systems without changes on the visually accessible surfaces or without the presence of overt flaws. Prediction of the residual impact-strength of polymeric base material structures is of importance at the design stage to determine the expected resistance of the structure for a given repeated-impact loading. Also, when an in-service polymeric base material part is likely to be affected by repeated-impact, a nondestructive evaluation of its structural worthiness is essential for the purposes of maintenance planning and structural integrity prediction.

Further, development of criteria for the evaluation of particular degrading states that may affect polymeric base material systems is needed. Adequate destructive testing techniques for the assessment of, for instance, the repeated-impact damage of polymeric base materials is of main importance for the correlation of the destructive test values with the pertaining nondestructive measurements.

The experimental work of this thesis showed the viability of a characterization of the low-energy repeated impact damage in the tested materials by means of the Mean Failure Energy of samples of specimens, as obtained by Falling Weight Impact Test and the Up-and-Down Method.

In the range of low-energy repeated-impact loading of this thesis, Acousto-Ultrasonics is shown to be a suitable quantitative nondestructive evaluation technique for the assessment of the residual impact-strength of the tested polymeric base materials. When AU is used as demonstrated in this thesis, the residual ability of these materials to withstand subsequent impact loading, measured by the Mean Failure Energy, can be predicted by AU measurements. Also, a similar prediction may be viable for the residual tensile strength, measured by the Ultimate Tensile Strength, of the tested Polyvinylchloride.

Further, it has been shown that estimations of both the residual MFE and residual UTS in the Polyvinylchloride specimens, and of residual MFE in the tested graphite/polycarbonate composite specimens can be made by using experimental correlations of the tested values of these quantities with the Acousto-Ultrasonics Parameter values calculated from AU measurements.

Finally, the viability was shown of identifying low-energy repeated-impact damage conditions in the tested materials by Pattern Recognition and Classification of Acousto-Ultrasonics signals. Good discrimination of the considered levels of impact damage was observed. Good classification performances were obtained when identifying AU-signals pertaining to test specimens not used for the classifier design, which is the actual classifier task in the practice.

The obtained results indicate that applications of the characterizations of repeated-impact states carried out in this thesis by means of destructive testing, Acousto Ultrasonics technique and Pattern Recognition and Classification of AU signals are worth to be investigated for other polymeric base material systems.

9.2. REMARKS

On carrying out the research work of this thesis, it was found that the repeatability of the AU measurements can be affected by many factors pertaining to transducer configuration and instrument settings. The implementation of the AU technique used, based on a careful design of the AU data acquisition procedure, allowed the retrieving of repeatable AU signals. In this, it was found that preliminary experimental work to determine the most important factors affecting each particular AU testing problem, followed by a customized trial of suitable values of these factors, may lead to an appropriate experimental setup.

The need for customized designs of transducer and instrumentation configurations is seen as a major difficulty for the application of the AU technique in industrial fields. Research work is needed to develop, for instance, appropriate transducer and instrumentation setups to perform the AU measurements not only in the material research laboratory, but also in the industrial environment. The ultimate purpose of such research work should be the establishing of suitable criteria of calibration for different AU setups. Further, adequate normalization of results may allow the comparison between measurements taken at different instrumentation conditions. Fundamentals for the defining of such criteria can be found in the work of Horne and Duke [90].

Some aspects of the AU characterization of impact-damage conditions in polymeric base material systems remain uncertain and they should be the objectives of future research work. Among them, a major concern for the industrial use of this AU characterization is the possibility that impact damage be sensed by AU signals without actually passing through the point of impact, allowing the inspection of larger areas of in-service structural parts and, ultimately, the location of the point of impact.

Research work in this field has been recently presented by Bartos [81].

On carrying out Pattern Recognition classifier design, it was shown that a combination of "absolute feature selection", based on Fisher Discrimination Ratio, and "performance feature selection", based on classification performances, can be a suitable approach to the feature selection problem when limited-size samples of test specimens are used to represent the considered classes. Given each particular classification problem, however, further research work should be carried out to determine the validity of such a criterion for the design of the appropriate PR classifier.

REFERENCES

1. Heiman,J.S., Winfree,W.P., Raymond Parker,F., Heath,D.M. and Welch,C.S., 'Quantitative NDE Application to Composite and Metals', Non-Destructive Monitoring of Materials Properties, Holbrook,J. and Bussière,J. (editors), Material Research Society, Philadelphia, 1989, pp. 211-220.

2. Vary, A., 'New Developments and Future Trends in NDE of Composites', Proceedings of the Second Canadian International Composites Conference and Exhibition (Cancom'93, Ottawa, Canada), Wallace,W., Gauvin,R. and Hoa,S.V. (editors), Canadian Association for Composite Structures and Materials, Montreal, 1993, pp. 17-22.

3. Henneke,E.G., 'Ultrasonic Nondestructive Evaluation of Advanced Composites', Non-Destructive Testing of Fibre-Reinforced Plastic Composites, Summerscales,J. (editor), Elsevier Science Publ. Ltd, Essex, England, 1990, Vol.2, pp. 55-160.

4. Chiou,S. and Hahn,T.H., 'Ultrasonic Characterization of Sol-Gel Processing', Non-Destructive Monitoring of Materials Properties, Holbrook,J. and Bussière,J. editors, Material Research Society, Philadelphia, 1989, pp. 295-302.

5. Reynolds,W.N., Scudder,L.P., and Pressmann,H., 'The use of Ultrasonic Wave Attenuation to Monitor Polymer and Composite Quality', Polymer Testing, 6, 1986, pp. 225-336.

6. Dickstein,P. Sinclair,A.N., Segal,E. and Segal,Y. , 'Ultrasonic Characterization of Thin Adhesive Bonds', Non-Destructive Monitoring of Materials Properties, Holbrook,J. and Bussière,J. (editors), Material Research Society, Philadelphia, 1989, pp. 349-355.

7. Alers,G.A., Flynn,P.I. and Buckley,H.J., 'Ultrasonic Technique for Measuring the Strength of Adhesive Bonds', Materials Evaluation, Vol.35, No.4, April 1977, pp. 77-84.

8. Williams,J.H.Jr. and Lampert,N.R., 'Ultrasonic Evaluation of Impact-Damaged Graphite Fiber Composites', Materials Evaluation, Vol.38, No.12, December 1980, pp. 68-72.

9. Lee,O.S. and Williams,J.H.,Jr., 'Ultrasonic Wave Characterization of Polymers', Materials Evaluation, Vol.49, No.3, March 1991, pp. 351-355.

10. Lambert,A. and Bossuat,B., 'Automatization of Inspection with Rayleigh Waves on Curved and Complex Surfaces', Non-Destructive Testing, Farley,J.M. and Nichols,R.W. (editors), Pergamon Press, Exeter, England, 1988, Vol.4, pp. 2358-2367.

11. Schlawne,F. and Schneider,H., 'Surface Inspection of Tubes by Surface or Plate Waves with Electromagnetic Excitation', Non-Destructive Testing, Farley,J.M. and Nichols,R.W. (editors), Pergamon Press, Exeter, England, 1988, Vol.4, pp. 2218-2227.

12. Dumcumb,A.C. and Keighley,D.M., 'Inspection of Titanium Tubing using Ultrasonic Lamb Waves Generated by an Electromagnetic Acoustic Transducer', Non-Destructive Testing, Farley,J.M. and Nichols,R.W. (editors), Pergamon Press, Exeter, England, 1988, Vol.4, pp. 2228-2236.

13. Kline,R.A. and Hashemi,D., 'Ultrasonic Guided-Wave Monitoring of Fatigue Damage Development in Bonded Joints', Materials Evaluation, Vol.45, No.9, September 1987, pp. 1076-1082.

14. Chapman,G.B., 'A Nondestructive Method of Evaluating Adhesive Bond Strength in Fibreglass Reinforced Plastic Assemblies', Joining of Composite Materials, ASTM STP 749, Kedward,K.T. (editor), American Society for Testing and Materials, Philadelphia, Pa, 1981, pp. 32-60.

15. Pilarski,A., Rose,J.L., Balasubramanian,K. and Da-Le,J., 'Utilization of Oblique incidence in Acousto-Ultrasonics', Non-destructive Testing of Fibre-reinforced Plastics Composite, Summerscales,J. (editor), Elsevier Science Publ. Ltd, Essex, England, 1990, Vol.2, pp.79-93.

16. Boser,O., Kellawon,P. and Geyer,R., 'Rapid Non-Destructive Testing of Ceramic Multilayer Capacity by a Resonance Method', Non-Destructive Monitoring of Materials Properties, Holbrook,J. and Bussière,J. (editors), Material Research Society, Philadelphia, 1989, pp. 329-334.

17. Brown,A.F., 'Ultrasonic Spectroscopy', Ultrasonic Testing, Szilard,J. (editor), John Wiley & Sons Ltd, New York, 1982, pp. 176-216.

18. Schlengermann,U., 'Ultrasonic Testing with Broad Band Probes', Non-Destructive Testing, Farley,J.M. and Nichols,R.W. (editors), Pergamon Press, Exeter, England, 1988, Vol.4, pp. 2257-2266.

19. Krautkramer,J. and Krautkramer,H., 'Ultrasonic Testing of Materials', Springer-Verlag, New York, 1983, pp. 3-59.

20. Rose,J.L. and Meyer,P.A., 'Ultrasonic Procedure for Predicting Adhesive Bond Strength', Materials Evaluation, Vol.31, No.6, June 1973, pp. 109-114.

21. Lloyd,E.A., and Wadhawani,D.S., 'Ultrasonic Spectroscopy and Detection of Hygrothermal Degradation in Adhesive Bonds', Adhesion, Allen,K.W. (editor), Applied Science Publ. Ltd, London, 1980, pp. 159-174.

22. Flügge,W., 'Viscoelasticity', Springer-Verlag, New York, 1975, pp. 75-80.

23. Scruby,C.B., 'Acoustic Emission: Theory and Practice', Non-Destructive Testing, Farley,J.M. and Nichols,R.W. (editors), Pergamon Press, Exeter, England, 1988, Vol.4, pp. 2832-2838.

24. Matthews,J.R. and Hay,R.D., 'Acoustic Emission Evaluation', Acoustic Emission. Nondestructive Monographs and Tracts, Matthews,J.R. (editor), Gordon and Breach Science Publ., New York, 1983, Vol.2, pp. 1-14.

25. Nixon,J.A., Phillips,M.G., Moore,D.R. and Prediger,R.S., 'A Study of the Development of Impact Damage in Cross-ply Carbon Fibre/PEEK Laminates using Acoustic Emission', Composite Materials and Technology, Elsevier Applied Science Pub. Ltd, London, England, 31, 1988, pp. 1-14.

26. Hill,R., Cowking,A. and Carswell,W.S., 'An Acoustic Emission Study of Stress Corrosion Cracking in GFRP', Non-Destructive Testing, Farley,J.M. and Nichols,R.W. (editors), Pergamon Press, Exeter, England, 1988, Vol.4, pp. 2872-2880.

27. Liu,Y. and Li,X., 'A Study of Microdeformation and Creep-Fatigue Damage Using Acoustic Emission Technique', Non-Destructive Monitoring of Materials Properties, Holbrook,J. and Bussière,J. (editors), Material Research Society, Philadelphia, Pa, 1989, pp. 159-164.

28. Mihovsky,M., Lozev,M., Takov,T. and Bojinov,K., 'Problems of the Acoustic Emission Testing in the Chemical Machine Building Industry', Non-Destructive Testing, Farley,J.M. and Nichols,R.W. (editors), Pergamon Press, Exeter, England, 1988, Vol.4, pp. 2935-2942.

29. Cherfaoui,M. and Roget,J., 'Acoustic Emission (AE) Associated with Fatigue Damage: Application of Data Analysis Technique', Non-Destructive Testing, Farley,J.M. and Nichols,R.W. (editors), Pergamon Press, Exeter, England, 1988, Vol.4, pp. 2849-2856.

30. Maslouhi,A, Kioua,H. and Roy,C., 'Application of Artificial Neural Networks to the Classification of Acoustic Emission Signals Captured during CRFP Fatigue Loading', Proceedings of the Second Canadian International Composites Conference and Exhibition (Cancom'93, Ottawa, Canada), Wallace,W., Gauvin,R. and Hoa,S.V. (editors), Canadian Association for Composite Structures and Materials, Montreal, 1993, pp. 467-478.

31. Vary,A., 'The Acousto-Ultrasonics Approach', Acousto-Ultrasonics: Theory and Applications, Duke,J.C. (editor), Plenum Press, New York, 1988, pp. 1-22.

32. Vary,A., 'The Acousto-Ultrasonics Approach, NASA Technical Memorandum 89843, April 1987.

33. Vary,A., 'Acousto-Ultrasonics', Non-destructive Testing of Fibre-Reinforced Plastic Composites, Summerscales,J. (editor), Elsevier Science Publ. Ltd, Essex, England, 1990, Vol.2, pp. 1-54.

34. Vary,A., 'Acousto-Ultrasonics - Un Update', Acoustic Emission: Current Practice and Future Directions, ASTM STP 749, Sachse,W., Roget,J. and Yamaguchi,K. (editors), American Society for Testing and Materials, Philadelphia, PA, 1991, pp. 95-104.

35. Egle,D.M. and Brown,A.E., 'A note on Pseudo-Acoustic Emission Sources', Journal of Testing and Evaluation, Vol.4, No.3, March 1976, pp. 196-199.

36. Vary,A., and Bowles,K.J., 'An Ultrasonic Technique for Nondestructive Evaluation of Fibre Composite Quality', Polymers Engineering and Science, Vol.19, No.5, April 1979, pp. 185-191.

37. Vary,A. and Lark,R.F., 'Correlation of Fibre Composite Tensile Strength with the Ultrasonic Stress Wave Factor', Journal of Testing and Evaluation, Vol.7, No.4, July 1979, pp. 185-191.

38. Culpan,E.A., Jemison,S. and Taylor,J., 'The Use of a Portable Laser System as a Simulated Source of Acoustic Emission', Non-Destructive Testing, Farley,J.M. and Nichols,R.W. (editors), Pergamon Press, Exeter, England, 1988, Vol.4, pp. 2857-2871.

39. Vary,A., 'Ultrasonic Measurement of Material Properties', Research Techniques in Nondestructive Testing, Sharpe,R.S.(editor), Academic Press, New York, 1977, Vol.IV, pp. 159-204.

40. Iyer,S.S., 'On the Characterization of the Viscoelastic Response of a Class of Materials using Acousto-Ultrasonics - A Pattern Recognition Approach', Master Thesis, 1993, University of Ottawa, Canada.

41. Iyer,S.S. and Haddad,Y.M., 'On the Characterization of the Linear Viscoelastic Response of a Class of Materials by Acousto-Ultrasonics - A Pattern Recognition Approach', Proceedings of the Second Canadian International Composites Conference and Exhibition (Cancom'93, Ottawa, Canada), Wallace,W., Gauvin,R. and Hoa,S.V. (editors), Canadian Association for Composite Structures and Materials, Montreal, 1993, pp. 479-489.

42. Tanary,S., 'Characterization of Adhesively Bonded Joints using Acousto-Ultrasonics', Master Thesis, 1988, University of Ottawa, Canada.

43. Tanary,S., Haddad,Y.M., Fahr,A. and Lee,S., 'Nondestructive Evaluation of Adhesively Bonded Joints in Graphite/Epoxi Composites using Acousto-Ultrasonics', Journal of Pressure Vessel Technology, Transactions of the ASME, Vol.114, August 1992, pp. 344-352.

44. Vary,A., 'Acousto-Ultrasonic Characterization of Fiber Reinforced Composites', Materials Evaluation, Vol.4, No.6, May 1982, pp. 650-662.

45. Russell-Floyd,R. and Phillips,M.G., 'A Critical Assesment of Acousto-Ultrasonics as a Method of Nondestructive Examination for Carbon-Fibre-Reinforced Thermoplastic Laminates', NDT International, Vol.21, No.4, 1988, pp. 247-257.

46. Green,R.E.Jr., 'Non-Destructive Evaluation for Material Characterization', Non-Destructive Monitoring of Materials Properties, Holbrook,J. and Bussière,J. (editors), Material Research Society, Philadelphia, 1989, pp. 15-25.

47. Tou,J.T. and Gonzalez,R.C., Pattern Recognition Principles, Addison Wesley, Massachussets, 1974, pp. 39-130.

48. Andrews,H.C., Introduction to Mathematical Techniques in Pattern Recognition, John Wiley & Sons Inc., Toronto, 1972, pp. 103-130.

49. Fukunaga,K., Introduction to Statistical Pattern Recognition, Academic Press Inc., New York, 1972, 10-176.

50. Diday,E. and Simon,J.C., 'Clustering Analysis', Digital Pattern Recognition, Fu, K.S., Keidel,W.D. and Wolter, H. (editors), Springer Verlag, New York, 1976, pp. 47-94.

51. Chen,C.H., Statistical Pattern Recognition, Hayden Book Company Inc., Rochelle Park, New Jersey, 1973, 1-45.

52. Huntsberger,D.V. and Billingsley,P., Elements of Statistical Inference, Allyn and Bacon,Inc., New York, 1973, 97-199.

53. Goulden,C.H., Methods of Statistical Analysis, John Wiley and Sons,Inc., New York, 1952, pp. 378-393.

54. Meisel,W.S., Computer-Oriented Approaches to Pattern Recognition, Academic Press Inc., New York, 1972, pp. 120-212.

55. Fu,K.S., 'Introduction', Digital Pattern Recognition, Fu, K.S., Keidel,W.D. and Wolter, H. (editors), Springer Verlag, New York, 1976, pp. 1-14.

56. Devijver,P.A., 'Statistical Pattern Recognition', Applications of Pattern Recognition, Fu,K.S. (editor), CRC Press Inc., Boca Raton, Florida, 1982, pp. 15-36.

57. Devijver,P.A. and Kittler,J., 'Pattern Recognition: A Statistical Approach', Prentice-Hall International Inc., Englewood Cliffs, New Jersey, 1982, pp. 11-279.

58. Chen,C.H., 'Statistical Pattern Recognition', Digital Waveform Processing and Recognition, Chen,C.H. (editor), CRC Press Inc., Boca Raton, Florida, 1982, pp. 59-74.

59. Douglas,D.F. and Rao,K.R., Fast Transforms: Algorithms, Analyses, Applications, Academic Press, Inc., New York, 1982, pp. 334-410.

60. Devijver,P.A., 'Non Parametric Estimation of Feature Evaluation Criteria', Pattern Recognition and Signal Processing, Proceedings of the NATO Advanced Study Institute of Pattern Recognition and Signal Processing, Chen,C.H. (editor), Sijthoff and Noordhoff International Publishers, Alphen aan den Rijn, The Netherlands, 1978, pp. 61-91.

61. Chen,C.H., 'A Review of Statistical Pattern Recognition', Pattern Recognition and Signal Processing, Proceedings of the NATO Advanced Study Institute of Pattern Recognition and Signal Processing, Chen,C.H. (editor), Sijthoff and Noordhoff International Publishers, Alphen aan den Rijn, The Netherlands, 1978, pp. 117-125.

62. Turner,S., 'Mechanical Testing of Plastics', Godwin,G. (editor), The Plastics and Rubber Institute, Longman Inc., New York, 1983, 139-154.

63. Davis,H.E., Troxell,G.E. and Hauck,G.F.W., 'The Testing of Engineering Materials', McGraw Hill, New York, 1982, 1-51.

64. Wolstenholme,W.E., Pregun,S.E. and Stark,C.F., 'Factors influencing Izod Impact Properties of Thermoplastics Measured with Autographic Impact Test', Journal of Applied Polymer Science, John Wiley & Sons, New York, Vol. 8, No.1, 1964, pp. 119-140.

65. Venzi,S., Priest,A.H. and May,M.J., 'Influence of Inertial Load on Instrumental Impact Test', Impact Testing of Metals, ASTM-STP 466, American Society for Testing and Materials, Philadelphia, 1973, pp. 133-145.

66. Ireland,D.R., 'Procedures and Problems Associated with Reliable Control of the Instrumented Impact Test', Instrumented Impact Testing, ASTM-STP 563, American Society for Testing and Materials, DeSisto,T.S. (editor), Philadelphia, 1974, pp. 3-29.

67. Williams,G.J., 'Fracture Mechanics of Polymers', John Wiley & Sons, New York, 1984, pp. 237-292.

68. Reed,P.E., 'Impact Performance of Plastics', Developments in Polymer Fracture, Andrews,E.H. (editor), Applied Science Publisher, London, 1980, pp. 121-153.

69. ASTM D256-90, 'Impact Resistance of Plastics and Electrical Insulating Materials', Annual Book of ASTM Standards, Vol.08.01, American Society for Testing and Materials, Philadelphia, 1990, pp. 58-69.

70. ASTM D1822-90, 'Tensile Impact Energy to Break Plastics and Electrical Insulating Materials', Annual Book of ASTM Standards, Vol.08.02, American Society for Testing and Materials, Philadelphia, 1990, pp. 183-195.

71. ASTM D3029-90, 'Standard Test Methods for Impact Resistance of Rigid Plastic', Annual Book of ASTM Standards, Vol.08.04, American Society for Testing and Materials, Philadelphia, 1990, pp. 524-535.

72. ASTM D2444-90, 'Standard Test Method for Impact Resistance of Thermoplastics Pipe and Fittings by Means of a Tup (Falling Weight)', Annual Book of ASTM Standards, Vol.08.04, American Society for Testing and Materials, Philadelphia, 1990, pp. 142-148.

73. Hagan, R.S., Schmitz,J.V. and Davis,D.A., 'Impact Testing of High Impact Thermoplastic Sheet', Technical Papers, 17th Annual Technical Conference of the Society of Plastic Engineers, Vol. VII, Jan.1961, pp. 34-52.

74. Impact Testing of Metals, ASTM-STP 466, American Society for Testing and Materials, Philadelphia, 1973, pp. 3-106.

75. Instrumented Impact Testing, ASTM-STP 563, DeSisto,T.S. (editor), American Society for Testing and Materials, Philadelphia, 1974, pp. 3-145.

76. Computer Automation of Material Testing, ASTM-STP 710, Wonsiewicz,B.C. (editor), American Society for Testing and Materials, Philadelphia, 1978, pp. 141-200.

77. Lum,P.T. and Curll,C.H., 'Variables affecting Reproducibility of the Instrumented Impact Test', Reproducibility and Accuracy of Mechanical Tests, ASTM-STP 626, Holt,J.M.(editor), American Society for Testing and Materials, Philadelphia, 1976, pp. 21-31.

78. Dixon,D.W. and Massey,F.J.,Jr., 'Introduction to Statistical Analysis', McGraw Hill Book Co., New York, 1969, pp. 377-394.

79. Brownlee,K.A., Hodgest,J.L.Jr. and Rosenblatt,M., 'The Up-and-Down Method with Small Samples', American Statistical Association Journal, Vol.48, 1953, pp. 262-277.

80. ASTM D638-91. 'Standard Test Method for Tensile Properties of Plastics', Annual Book of ASTM Standards, Vol.08.01, American Society for Testing and Materials, Philadelphia, 1990, pp. 159-167.

81. Bartos,A.L., 'Acousto-Ultrasonic Pattern Analysis of Impact-Damaged Composite Panels', Topical Conference Proceedings Book of the Second International Conference on Acousto-Ultrasonics (Atlanta, GA), Vary,A. (editor), The American Society for Nondestructive Testing, Inc., Columbus, OH, 1993, pp. 133-142.

82. Boukhili,R., Bojji,C. and Gauvin,R., 'Damage Growth Under Repeated Impact in Graphite Epoxy Plates', Proceedings of the Second Canadian International Composites Conference and Exhibition (Cancom'93, Ottawa, Canada), Wallace,W., Gauvin,R., and Hoa,S.V. (editors), Canadian Association for Composite Structures and Materials, Montreal, 1993, pp. 425-432.

83. Straznicky,P.V. and Vietinghoff,H., 'Damage Accumulation in Composite Laminates Resulting from Multiple Impacts', Proceedings of the Second Canadian International Composites Conference and Exhibition (Cancom'93, Ottawa, Canada), Wallace,W., Gauvin,R., and Hoa,S.V. (editors), Canadian Association for Composite Structures and Materials, Montreal, 1993, pp. 433-440.

84. Crossman,F.W. and Wang,A.S.D., 'The dependence of Transverse Cracking and Delamination of Ply Thickness in Graphites/Epoxy Laminates', Damage in Composite Materials, ASTM STP-775, Reifnisder,K.L. (editor), American Society for Testing and Materials, Philadelphia, 1982, pp. 118-139.

85. Cristescu,N., Malvern,L.E. and Sierakowski,R.L.,'Failure Mechanisms in Composite Plates Impacted by Blunt-Ended Penetrators', Foreign Impact Damage to Composites, ASTM STP-568, Greszczuk,L.B. (editor), American Society for Testing and Materials, Philadelphia, 1975, pp. 159-172.

86. Sierakowski,R.L., Malvern,L.E. and Ross,C.A., 'Dynamic Failure Modes in Impacted Composite Plates', Failure Modes in Composites III, Chiao,T.T. (editor), Proceedings of the 105th AIME Annual Meeting, Las Vegas, Nevada, The Metallurgical Society of AIME, New York, 1976, pp. 73-88.

87. Dharan,C.K.H. and Beardmore,P., 'The Resistance of Graphite Fiber-Reinforced Composites to Impacts', Failure Modes in Composites III, Chiao,T.T. (editor), Proceedings of the 105th AIME Annual Meeting, Las Vegas, Nevada, The Metallurgical Society of AIME, New York, 1976, pp. 89-99.

88. Konishi,D.Y. and Lo,K.H., 'Flaw Criticality of Graphite/Epoxy Structures', Damage in Composite Materials, ASTM STP-775, Reifnisder,K.L. (editor), American Society for Testing and Materials, Philadelphia, 1982, pp. 125-144.

89. Liber,T., Daniel,I.M. and Schramm,S.W.,'Ultrasonic Techniques for Inspecting Flat and Cylindrical Composite Specimens', Nondestructive Evaluation and Flaw Criticality for Composite Materials, ASTM STP-696, Pipes,R.B. (editor), American Society for Testing and Materials, Philadelphia, 1979, pp. 5-25.

90. Horne, M.R. and Duke,J.C.Jr., "Methods for Implementation of the AU Method/Approach', Topical Conference Proceedings Book of the Second International Conference on Acousto-Ultrasonics (Atlanta, GA), Vary,A. (editor), The American Society for Nondestructive Testing, Inc., Columbus, OH, 1993, pp. 13-20.

APPENDIX A

DECISION RULES FOR PATTERN CLASSIFICATION

A.1. Linear Discriminant Decision Rule

Consider M pattern classes ω_1 , ω_2 , ... , ω_M and assume that these classes are respectively representable by prototype patterns z_1 , z_2 , ... , z_M . The Euclidean distance D_i between an arbitrary pattern vector x and the z_i prototype is given by

$$D_i = \| x - z_i \| = \left[(x - z_i)' (x - z_i) \right]^{\frac{1}{2}} \qquad (A.1)$$

where the superscript prime (′) stands for the transpose of a vector, and

$$x = \begin{bmatrix} x_1 \\ x_2 \\ \cdot \\ \cdot \\ \cdot \\ x_n \end{bmatrix} \qquad (A.2) \qquad ; \qquad z_i = \begin{bmatrix} z_{i1} \\ z_{i2} \\ \cdot \\ \cdot \\ \cdot \\ z_{in} \end{bmatrix} \qquad (A.3)$$

are column pattern-vectors of the values of the patterns x and z_i , respectively, for the n features under consideration.

By developing the Equation (A.1) above, the following alternatively expresions of the Euclidean distance are obtained

$$D_i^2 = x' x - 2 x' z_i + z_i' z_i \qquad (A.4)$$

$$D_i^2 = x' x - 2 \left(x' z_i - \frac{z_i' z_i}{2} \right) \qquad (A.5)$$

where x' and z_i' in equations (A.4) and (A.5) respectively are the transposes of vectors x and z_i .

A minimum distance classifier computes the distance from a pattern x to the prototype of each class, and assigns the pattern to the class to which it is closer. It means x is assigned to the class ω_i if $D_i \leq D_k$; for k=1, 2, ..., M ; $k \neq i$.

The term x'x in above equation (A.5) is independent of i and it can be dropped. Therefore, the condition of the minimum of D_i is equivalent to that of the maximum of $(x' z_i - z_i' z_i) / 2$ in Equation (A.5), defining the following linear minimum-distance decision function

$$d_i(x) = \left(x' z_i - \frac{z_i' z_i}{2} \right) \quad ; \qquad for\ i = 1, 2, \ldots, M \qquad (A.6)$$

from which a pattern x is assigned to the class ω_i among the M classes under consideration if :

$$d_i\ (x)\ \geq\ d_k\ (x) \qquad ;\ \ for\ k = 1,\ 2,\ \ldots\ ,\ M\ ;\quad k \neq i \qquad (A.7)$$

By considering the M prototype patterns for the classes under consideration in the decision function (A.6) above, the following <u>general expression of the linear discriminant rule</u> is obtained

$$d_i(x) = w_{i\,j}\ x + w_{i,\ n+1}\ , \qquad for\ i = 1,\ 2,\ \ldots,\ M$$
$$for\ j = 1,\ 2,\ \ldots,\ n \qquad (A.8)$$

where $d_i\ (x)$ represents a set of linear decision fuctions, each associated with the prototype pattern of the pertaining class,

w_{ij} is a matrix, each row of which is the vector $z_i = (z_{i1},\ z_{i2},\ \ldots,\ z_{in}\ )$ formed by the n-feature values of the prototype pattern of a class; z_i is called the weight vector associated with the i-th decision function for the class ω_i , and

$w_{i\,,\,n+1}$ is defined below

$$w_{i\,,\,n+1} = \begin{bmatrix} -\frac{1}{2}\, z_1'\, z_1 \\ -\frac{1}{2}\, z_2'\, z_2 \\ \cdot \\ \cdot \\ \cdot \\ -\frac{1}{2}\, z_M'\, z_M \end{bmatrix}$$

$$(\, i = 1,\, 2,\, \ldots,\, M\,) \qquad (A.9)$$

A.2. Bayes' Decision Rule of Classification for minimum risk

The risk function $r[(d(x_j)\,,\,\omega_i)]$ of taking the decision $d_i\,(x_j)$ of choosing the class indicated by the n features of x_j, being the correct choose the class ω_i , is expressed as

$$r\;[d(x_j)\,,\;\omega_i\;] \;=\; \int_{X_n} \left\{ L\;[\;d(x_j)\,,\;\omega_i\;] \right\}\; p(\;x \;|\; \omega_i\;)\;\; dx \qquad (A.10)$$

where $p(x \mid \omega_i)$ is the multivariate (n-dimensional) probability density function of the feature vector x in the class ω_i ,

$L[\;\omega_i\;,\; d(x_j)\;]$ is the loss associated with choosing the class indicated by x_j when the correct choice is ω_i , and the integration of equation (A.10) extends over the n features of vector x.

For the following set of a priori probabilities of occurrence of the M classes under consideration

$$\{ p(\omega_1) , p(\omega_2) , \dots , p(\omega_M) \} \qquad \text{(A.11)}$$

the average loss R of taking a decision $d(x_j)$ for the M classes is given by a summation over the M classes of the products of the probability of each class by the pertaining risk of choosing this class as it follows

$$R = \sum_{i=1}^{M} p(\omega_i) \quad r\,[d(x_j) , \omega_i] \quad dx \qquad (A.12)$$

By considering the Equation (A.10) into Equation (A.12) above, the latter becomes

$$R = \sum_{i=1}^{M} p(\omega_i) \int_{X_n} L\,[\,d(x_j) , \omega_i\,]\; p(x|\omega_i)\; dx \qquad (A.13)$$

Equation (A.13) above can be alternatively expressed as (see, e.g., ref. [47])

$$R = \int_{X_n} \sum_{i=1}^{M} \{ L [d (x_j), \omega_i] \} p (\omega_i , x_j) \, dx \qquad (A.14)$$

where $p (\omega_i , x_j) = p (\omega_i) \; p(x \mid \omega_i)$ is the joint probability density of feature x_j occurring and being represented by the values of the j feature in class ω_i . The integral in Equation (A.14) above is over the entire n-feature space X_n .

In Equation (A.14) above, the expected value of loss R, of assigning a pattern of unknown classification to a pattern class, based on the values of its n features, is an average over the M classes and over the n features of the feature space X_n . It is implicit that each feature is taken independently. The loss function L is defined arbitrarily. Some examples of typical loss functions are subsequently presented.

Minimizing the product of the loss function L by the joint probability means minimizing the expected value of loss R. For any given x_j, the summation over the M classes under consideration of the following function $F (\omega_i)$ must be minimized.

$$F (\omega_i) = \sum_{i=1}^{M} \left\{ L [d (x_j) , \omega_i] \right\} p (\omega_i , x_j) \qquad (A.15)$$

The optimum decision function that minimizes the above expression (A.15) is called the Bayes' Rule for minimum risk of misclassification. It is sufficient to consider each feature x_j separately and to minimize the expressions of the form (see, e.g., ref. [54])

$$\left\{ L \left[d \left(x_j \right) , \omega_i \right] \right\} p \left(\omega_i , x_j \right) \qquad (A.16)$$

for all j = 1, 2, ... , n features and i = 1, 2, ..., M classes.

The minimization of the expressions of the form of the expression (A.16) above, means that $d^*(x_j)$ is an optimum decision function if

$$\sum_{i=1}^{M} L\left[d^* (x_j) , \omega_i \right] p(\omega_i , x_j) \leq$$

$$\leq \sum_{i=1}^{M} L\left[d(x_j) , \omega_i \right] p(\omega_i , x_j) \qquad (A.17)$$

The expression (A.17) above may be taken as a <u>general expression of the Bayes' Rule for minimum risk of misclassification</u> for a given loss function. (see references [47], [48], [54] and [55]).

A specific loss function that leads to some simple expressions for decision functions is the "Symmetric Loss Function". It is defined as; see, e.g., ref. [48]

$$L[d(x_k), \omega_i] = 1 - \delta_{ik} = \begin{cases} 0, & if\ i = k \\ 1, & if\ i \neq k \end{cases} \qquad (A.18)$$

where δ_{ik} is the Kronecker delta function.

This loss function penalizes all misclassifications with a maximum value of one, while any right guess is given a nil value.

A more sophisticated loss function that weights the importance of correctly guessing one class is the following; see, e.g., ref. [48]

$$L[d(x_k), \omega_i] = \begin{cases} -h_i & if\ i = k \\ 0 & if\ i \neq k \end{cases} \qquad (A.19)$$

The loss function (A.19) above assigns an arbitrary negative loss $-h_i$ (i.e., a positive gain) to a correct decision and no loss to an erroneous decision. It can be expressed as a diagonal matrix and it be called "Diagonal Loss Function".

For the previously introduced two loss functions of expressions (A.18) and (A.19) above, each term in the summation of expression (A.13) may be considered independent of the values of L if the pertaining probability functions are monotonic; see, e.g., ref. [48]. Therefore, the Bayes' decision function of Equation (A.17), when the Diagonal Loss Function is taken, is expressed as follows

$$d^* (x_j) = d_i (x_j)$$

$$i.e., \quad x \in \omega_i \quad if \qquad (A.20)$$

$$h_i \; p (\omega_i , x_j) \geq h_k \; p (\omega_k , x_j) \quad for \begin{cases} k = 1,2,\ldots,M \\ k \neq i \end{cases}$$

where M is the number of classes

The so-called Likelihood Ratio λ between any two classes ω_k , ω_i for the classification by j feature of vector x is defined as (see, e.g., ref. [48])

$$\lambda = \frac{p (\omega_i , x_j)}{p (\omega_k , x_j)} \qquad (A.21)$$

By applying the definition (A.21) above into the Bayes' Decision Function (A.20), the latter reduces to

$$d^{*}(x_j) = d_i(x_j)$$

$$i.e., \quad x \in \omega_i \quad if \qquad (A.22)$$

$$h_i \geq \frac{h_k}{\lambda} \qquad ; for \begin{cases} k = 1, 2, \ldots, M \\ k \neq i \end{cases}$$

Therefore, in the case of Diagonal Loss Function, the Equation (A.22) above expresses the condition for taking the optimum decision when classifying the vector x in the class ω_i based on the feature-value j .

In the case of the Symmetric Loss Function, defined earlier by Equation (A.18), a more explicit Bayes' Decision Function can be expressed by applying the following expression; see, e.g., ref. [48]

$$p(\omega_i, x_j) = p(\omega_i)\ p(x \mid \omega_i) \qquad (A.23)$$

When applying the definition (A.23) above to the Equation (A.15), the latter becomes the following

$$F(\omega_i) = \sum_{i=1}^{M} \left\{ L\,[d(x_j),\ \omega_i] \right\} p(x|\omega_i)\ p(\omega_i) \qquad (A.24)$$

If the definition (A.18) of Symmetric Loss Function is then included in the Equation (A.24) above, the following expressions are obtained

$$\begin{aligned} F(\omega_i) &= \sum_{i=1}^{M} (1-\delta_{ij})\ p(x\,|\,\omega_i)\ p(\omega_i) \\ &= \left\{ \sum_{i=1}^{M} p(x\,|\,\omega_i)\ p(\omega_i) \right\} - \\ &\quad - p(x\,|\,\omega_i)\ p(\omega_i) \end{aligned} \qquad (A.25)$$

The optimum decision of choosing the class ω_i for the classification of vector x is given by the condition of a minimum of the expression (A.25) above for this class. Therefore, the Bayes' Decision Function becomes

$$\begin{aligned} &\sum_{i=1}^{M} p(x|\omega_i)\ p(\omega_i) - p(x|\omega_i)\ p(\omega_i) \\ &\qquad \le \sum_{k=1}^{M} p(x|\omega_k)\ p(\omega_k) - p(x|\omega_k)\ p(\omega_k) \end{aligned} \qquad (A.26)$$

Also, in the above expression (A.26) above, the terms of the forms

$$\sum_{i=1}^{M} p(\ x|\omega_i\ )\ p(\ \omega_i\ )$$

$$\sum_{i=1}^{M} p(\ x|\omega_k\ )\ p(\ \omega_k\ ) \qquad (A.27)$$

are summations that are carried over the M classes. Therefore, they are constant for a given set of classes and they may be dropped. The Bayes' Decision Rule becomes a set of decision functions of the form

$$d_i\ (x) = p\ (\ x\ |\ \omega_i\ )\ p\ (\ \omega_i\ ) \quad \le \quad p\ (\ x\ |\ \omega_k\ )\ p\ (\ \omega_k\ )$$
$$i = 1,\ 2, \ldots,\ M$$
$$k = 1,\ 2, \ldots,\ M \qquad (A.28)$$
$$i \neq k$$

Finally, by applying the expression (A.23), the decision rule (A.28) above can be alternatively expressed as

$$d_i\ (\ x\ ) = p\ (\ \omega_i\ ,\ x_j\ ) \quad \le \quad p\ (\ \omega_k\ ,\ x_j\ )$$
$$i = 1,\ 2,\ \ldots,\ M$$
$$k = 1,\ 2,\ \ldots,\ M$$
$$i \neq k \qquad (A.29)$$

A classifier carrying out the Bayes' Decision Rule for classification is called a "Bayesian Classifier".

A.3. Bayes' Decision Rule for normally distributed patterns

The multivariate normal density function represents an appropriate model for most pattern recognition applications. If it assumed that probability density functions $p(\omega_i | x_j)$, introduced in Equation (A.10), Section A.2, are multivariate normal, the Bayes' decision rule may be expressed by some analytically tractable decision functions. The multivariate normal probability density functions for M given classes are of the following form (see, e.g., ref. [47])

$$p(x | \omega_i) = \frac{1}{(2\pi)^{\frac{n}{2}} | C_i |^{\frac{1}{2}}} \exp\left[-\frac{1}{2} (x - \mu_i)' \, C_i^{-1} \, (x - \mu_i) \right]$$

$$(i = 1, 2, \ldots, M) \qquad (A.30)$$

where the superscript prime (') stands for the transpose of a vector,

$x = (x_i , x_2 , \ldots , x_n)$ is a pattern vector,

n is the number of features of each pattern vector,

μ_i is the multivariate mean vector for each class density,

$\mathbf{C}_i$ is the covariance matrix of class ω_i (see Equation (A.31) below), and

$| \mathbf{C}_i |$ is the determinant of the covariance matrix.

The multivariate mean vector μ_i of class density ω_i can be calculated as follows; see, e.g., ref. [47]

$$\mu_i = E_i\left\{ x \right\} = \int_{X_n} x\, p\,(\, x\,)\; dx \qquad (A.31)$$

where $x = (\, x_i\,, x_2\,, \ldots\,, x_n\,)$ is a pattern vector of class ω_i ,

$E_i\{\, x\,\}$ is the so-called expectation operator over the patterns of class ω_i,

and the integration of Equation (A.31) extends over the n features of vector x .

The covariance matrix $\mathbf{C}_i$ of class ω_i is defined as the following

$$\boldsymbol{C_i} = E_i\left\{ (\, x - \mu_i\,)\;\; (\, x - \mu_i\,)' \right\} \qquad (A.32)$$

where $(\, x - \mu_i\,)'$ stands for the transpose of $(\, x - \mu_i\,)$.

The covariance matrix define by Equation (A.32) above is symmetric and positive semidefinite; see, e.g., ref. [47]. The diagonal element c_{kk} of such matrix is the variance of the k-th element of the pattern vectors. Its off-diagonal element c_{kl} is the covariance of x_k and x_l . If the pattern features k and l are statistically independent, then $c_{kl} = 0$

Taking logarithms of the Bayesian Decision Rule d_i (x) of Equation (A.28), in Section A.2, for Symmetric Loss Function does not change the discriminatory characteristics of this rule, because the logarithm function is a monotonically increasing function of d_i (x). Therefore, taking the value of log d_i (x) as decision function , the Bayes' Decision Rule for M classes is expressed as; see, e.g., ref. [47]

$$\log d_i(x) = \log p(x|\omega_i) + \log p(\omega_i) \quad \le \quad \log d_k(x) = \log p(x|\omega_k) + \log p(\omega_k)$$

$$i = 1, 2, \ldots, M$$
$$k = 1, 2, \ldots, M \qquad (A.33)$$

Where ω_i is the optimum choice of class in wich to classify the vector x among the M classes under consideration.

By applying the expression of the multivariate normal probability density for M classes of Equation (A.30) into the Equation (A.33) above, the following expression is obtained

$$\log d_i(x) = \log p(\omega_i) - \frac{n}{2} \log 2\pi - \frac{1}{2} \log|\boldsymbol{C}_i| - \\ - \frac{1}{2} \left[(x - \mu_i)' \, \boldsymbol{C}_i^{-1} \, (x - \mu_i) \right] \quad \le \quad \log d_k(x)$$

$$i = 1, 2, \ldots, M \qquad (A.34)$$
$$k = 1, 2, \ldots, M$$

Elimination of terms that do not depend on i in Equation (A.34) gives the Bayes' Decision Function for normal patterns as follows

$$\log d_i\,(x) = \log p\,(\omega_i) - \frac{1}{2}\log|C_i| - \\ - \frac{1}{2}\left[(x-\mu_i)'\, C_i^{-1}\,(x-\mu_i)\right] \leq \log d_k(x)$$

$$i = 1, 2, \ldots, M \qquad (A.35)$$
$$k = 1, 2, \ldots, M$$

Where the optimum choice of class in which to classify the vector x is ω_i if it gives the minimum of the expression (A.35) above for all M classes under consideration. Expression (A.35) represents a set of equations where no terms higher than second degree in the components of x appear.

In the particular case of having the same covariance matrices for the M classes under consideration, the value of the determinant of these covariance matrix can be dropped in the Equation (A.35) above, giving the following set of linear decision functions (see, e.g., ref. [47])

$$\log d_i(x) = \log p\,(\omega_i) - x'\, C_i^{-1}\,\mu_i - \frac{1}{2}\,\mu_i'\, C_i^{-1}\,\mu_i$$

$$i = 1, 2, \ldots, M \qquad (A.36)$$

Another particular case is obtained when the variances and the covariances for all the classes respectively take value one and zero; i.e, when the covariance matrix is the identity matrix. Thus, the decision function (A.36) becomes the following expression

$$\log d_i (x) = \log p (\omega_i) - x' \mu_i - \frac{1}{2} \mu_i' \mu_i$$

$$i = 1 , 2 , \ldots , M \qquad (A.37)$$

If the multivariate mean vector μ_i is understood as the "prototype pattern vector" of class ω_i , the expression (A.37) represents the decision function of a minimum-distance classifier.

APPENDIX B

FALLING WEIGHT IMPACT TEST RESULTS AND ESTIMATES OF MEAN FAILURE ENERGY FOR THE TESTED SAMPLES

Table B.1. Values of the coefficient k to estimate P_{50} from an Up-and-Down sequence of trials of nominal number N.

An × indicates a fail, while an O indicates a pass. If the table is entered from the foot, the sign of k has to be reversed. (From Dixon,D.W. and Massey, F.J.,Jr [78]).

Sample size N	*Second part of series*	k for test series whose first part is O	OO	OOO	OOOO		Error of P_{50}
2	×	−.500	−.388	−.378	−.377	O	.88σ
3	× O	.842	.890	.894	.894	O ×	.76σ
	× ×	−.178	.000	.026	028	O O	
4	× O O	.299	.314	.315	.315	O × ×	.67σ
	× O ×	−.500	−.439	−.432	−.432	O × O	
	× × O	1.000	1.122	1.139	1.140	O O ×	
	× × ×	.194	.449	.500	.506	O O O	
5	× O O O	−.157	−.154	−.154	−.154	O × × ×	.61σ
	× O O ×	−.878	−.861	−.860	−.860	O × × O	
	× O × O	.701	.737	.741	.741	O × O ×	
	× O × ×	.084	.169	.181	.182	O × O O	
	× × O O	.305	.372	.380	.381	O O × ×	
	× × O ×	−.305	−.169	−.144	−.142	O O × O	
	× × × O	1.288	1.500	1.544	1.549	O O O ×	
	× × × ×	.555	.897	.985	1.000^{+1}	O O O O	
6	× O O O O	−.547	−.547	−.547	−.547	O × × × ×	.56σ
	× O O O ×	−1.250	−1.247	−1.246	−1.246	O × × × O	
	× O O × O	.372	.380	.381	.381	O × × O ×	
	× O O × ×	−.169	−.144	−.142	−.142	O × × O O	
	× O × O O	.022	.039	.040	.040	O × O × ×	
	× O × O ×	−.500	−.458	−.453	−.453	O × O × O	
	× O × × O	1.169	1.237	1.247	1.248	O × O O ×	
	× O × × ×	.611	.732	.756	.758	O × O O O	
	× × O O O	−.296	−.266	−.263	−.263	O O × × ×	
	× × O O ×	−.831	−.763	−.753	−.752	O O × × O	
	× × O × O	.831	.935	.952	.954	O O × O ×	
	× × O × ×	.296	.463	.500	$.504^{+1}$	O O × O O	
	× × × O O	.500	.648	.678	.681	O O O × ×	
	× × × O ×	−.043	.187	.244	$.252^{+1}$	O O O × O	
	× × × × O	1.603	1.917	2.000	2.014^{+1}	O O O O ×	
	× × × × ×	.893	1.329	1.465	1.496^{+1}	O O O O O	
		×	× ×	× × ×	× × × ×	*Second part of series*	
		−k for series whose first part is					

Table B.2. Values of the coefficients A and C to estimate P_{50} from an Up-and-Down sequence of trials of nominal number N, for N > 6.

n_O is the number of passes and n_x is the number of fails in the final N trials. If the table is entered from the foot, signs of both A and C have to be reversed. (From Dixon,D.W. and Massey, F.J.,Jr [78]).

		C for test series whose first part is			
$n_O - n_X$	A	OO	OOO	OOOO	OOOOO
5	10.8	0	0	0	0
4	7.72	0	0	0	0
3	5.22	.03	.03	.03	.03
2	3.20	.10	.10	.10	.10
1	1.53	.16	.17	.17	.17
0	0	.44	.48	.48	.48
−1	−1.55	.55	.65	.65	.65
−2	−3.30	1.14	1.36	1.38	1.38
−3	−5.22	1.77	2.16	2.22	2.22
−4	−7.55	2.48	3.36	3.52	3.56
−5	−10.3	3.5	4.8	5.2	5.3
$n_X - n_O$	$-A$	XX	XXX	XXXX	XXXXX
		$-C$ for test series whose first part is			

Table B.3. Results of Falling-Weight Impact Test for the sample of polyvinylchloride specimens of non-impact damage level.

Specimen Number	CONTROLLED REPEATED IMPACT			FALLING WEIGHT TEST IMPACT		
	Weight [Kg]	Height [m]	Number of Impacts	Weight [Kg]	Height [m]	Result P=Pass F=Fail
1	None	None	None	4.5	1.6	F
2	None	None	None	4.5	1.5	F
3	None	None	None	4.5	1.4	F
4	None	None	None	4.5	1.3	P
5	None	None	None	4.5	1.4	F
6	None	None	None	4.5	1.3	F
7	None	None	None	4.5	1.2	P
8	None	None	None	4.5	1.3	F
				P_{50} =	1.262 m	
				MFE =	5.68 Kgm =	55.7 Joules

P_{50} : height value for a probability of fail of 50% of the sample.

MFE = Mean Failure Energy.

Table B.4. Results of Falling-Weight Impact Test for the sample of polyvinylchloride specimens of five-impact damage level.

Specimen Number	CONTROLLED REPEATED IMPACT			FALLING WEIGHT TEST IMPACT		
	Weight [Kg]	Height [m]	Number of Impacts	Weight [Kg]	Height [m]	Result P = Pass F = Fail
9	0.9	1.2	5	4.5	1.1	P
10	0.9	1.2	5	4.5	1.2	P
11	0.9	1.2	5	4.5	1.3	P
12	0.9	1.2	5	4.5	1.4	F
13	0.9	1.2	5	4.5	1.3	F
14	0.9	1.2	5	4.5	1.2	F
15	0.9	1.2	5	4.5	1.1	F
16	0.9	1.2	5	4.5	1.0	F
				P_{60} =	1.147 m	
				MFE =	5.16 Kgm =	50.6 Joules

P_{50} : height value for a probability of fail of 50% of the sample.

MFE = Mean Failure Energy.

Table B.5. Results of Falling-Weight Impact Test for the sample of polyvinylchloride specimens of ten-impact damage level.

Specimen Number	CONTROLLED REPEATED IMPACT			FALLING WEIGHT TEST IMPACT		
	Weight [Kg]	Height [m]	Number of Impacts	Weight [Kg]	Height [m]	Result P = Pass F = Fail
17	0.9	1.2	10	4.5	1.2	F
18	0.9	1.2	10	4.5	1.1	F
19	0.9	1.2	10	4.5	1.0	F
20	0.9	1.2	10	4.5	0.9	P
21	0.9	1.2	10	4.5	1.0	P
22	0.9	1.2	10	4.5	1.1	F
23	0.9	1.2	10	4.5	1.0	F
24	0.9	1.2	10	4.5	0.9	P
				P_{60} =	0.975 m	
				MFE =	4.39 Kgm =	43.1 Joules

P_{50} : height value for a probability of fail of 50% of the sample.

MFE = Mean Failure Energy.

Table B.6. Results of Falling-Weight Impact Test for the sample of polyvinylchloride specimens of fifteen-impact damage level.

Specimen Number	CONTROLLED REPEATED IMPACT			FALLING WEIGHT TEST IMPACT		
	Weight [Kg]	Height [m]	Number of Impacts	Weight [Kg]	Height [m]	Result P=Pass F=Fail
25	0.9	1.2	15	4.5	1.2	F
26	0.9	1.2	15	4.5	1.1	F
27	0.9	1.2	15	4.5	1.0	F
28	0.9	1.2	15	4.5	0.9	P
29	0.9	1.2	15	4.5	1.0	F
30	0.9	1.2	15	4.5	0.9	F
31	0.9	1.2	15	4.5	0.8	P
32	0.9	1.2	15	4.5	0.9	F
				P_{50} =	0.862 m	
				MFE =	3.88 Kgm =	38.1 Joules

P_{50} : height value for a probability of fail of 50% of the sample.

MFE = Mean Failure Energy.

Table B.7. Results of Falling-Weight Impact Test for the sample of polyvinylchloride specimens of twenty-impact damage level.

Specimen Number	CONTROLLED REPEATED IMPACT			FALLING WEIGHT TEST IMPACT		
	Weight [Kg]	Height [m]	Number of Impacts	Weight [Kg]	Height [m]	Result P = Pass F = Fail
33	0.9	1.2	20	4.5	1.0	F
34	0.9	1.2	20	4.5	0.9	F
35	0.9	1.2	20	4.5	0.8	F
36	0.9	1.2	20	4.5	0.7	P
37	0.9	1.2	20	4.5	0.8	F
38	0.9	1.2	20	4.5	0.7	P
39	0.9	1.2	20	4.5	0.8	P
40	0.9	1.2	20	4.5	0.9	P
				P_{50} =	0.824 m	
				MFE =	3.71 Kgm =	36.4 Joules

P_{50} : height value for a probability of fail of 50% of the sample.

MFE = Mean Failure Energy.

Table B.8. Results of Falling-Weight Impact Test for the sample of graphite/polycarbonate composite specimens of non-impact damage level.

Specimen Number	CONTROLLED REPEATED IMPACT			FALLING WEIGHT IMPACT TEST		
	Weight [Kg]	Height [m]	Number of Impacts	Weight [Kg]	Height [m]	Result P=Pass F=Fail
1	None	None	None	0.9	0.65	F
2	None	None	None	0.9	0.60	F
3	None	None	None	0.9	0.55	F
4	None	None	None	0.9	0.50	P
5	None	None	None	0.9	0.55	F
6	None	None	None	0.9	0.50	P
7	None	None	None	0.9	0.55	F
8	None	None	None	0.9	0.50	F
				P_{50} = 0.498 m		
				MFE = 0.448 Kgm = 4.40 Joules		

P_{50} : height value for a probability of fail of 50% of the sample.

MFE = Mean Failure Energy.

Table B.9. Results of Falling-Weight Impact Test for the sample of graphite/polycarbonate composite specimens of one-impact damage level.

Specimen Number	CONTROLLED REPEATED IMPACT			FALLING WEIGHT TEST IMPACT		
	Weight [Kg]	Height [m]	Number of Impacts	Weight [Kg]	Height [m]	Result P=Pass F=Fail
9	0.4	0.75	1	0.9	0.55	F
10	0.4	0.75	1	0.9	0.50	F
11	0.4	0.75	1	0.9	0.45	F
12	0.4	0.75	1	0.9	0.40	P
13	0.4	0.75	1	0.9	0.45	P
14	0.4	0.75	1	0.9	0.50	P
15	0.4	0.75	1	0.9	0.55	F
16	0.4	0.75	1	0.9	0.50	P

P_{50} = 0.488 m

MFE = 0.439 Kgm = 4.31 Joules

P_{50} : height value for a probability of fail of 50% of the sample.

MFE = Mean Failure Energy.

Table B.10. Results of Falling-Weight Impact Test for the sample of graphite/polycarbonate composite specimens of three-impact damage level.

Specimen Number	CONTROLLED REPEATED IMPACT			FALLING WEIGHT IMPACT TEST		
	Weight [Kg]	Height [m]	Number of Impacts	Weight [Kg]	Height [m]	Result P=Pass F=Fail
17	0.4	0.75	3	0.9	0.60	F
18	0.4	0.75	3	0.9	0.55	F
19	0.4	0.75	3	0.9	0.50	F
20	0.4	0.75	3	0.9	0.45	P
21	0.4	0.75	3	0.9	0.50	F
22	0.4	0.75	3	0.9	0.45	P
23	0.4	0.75	3	0.9	0.50	F
24	0.4	0.75	3	0.9	0.45	F
				P_{50} = 0.448 m		
				MFE = 0.403 Kgm = 3.95 Joules		

P_{50} : height value for a probability of fail of 50% of the sample.

MFE = Mean Failure Energy.

Table B.11. Results of Falling-Weight Impact Test for the sample of graphite/polycarbonate composite specimens of four-impact damage level.

Specimen Number	CONTROLLED REPEATED IMPACT			FALLING WEIGHT TEST IMPACT		
	Weight [Kg]	Height [m]	Number of Impacts	Weight [Kg]	Height [m]	Result P=Pass F=Fail
25	0.4	0.75	4	0.9	0.55	F
26	0.4	0.75	4	0.9	0.50	F
27	0.4	0.75	4	0.9	0.45	F
28	0.4	0.75	4	0.9	0.40	P
29	0.4	0.75	4	0.9	0.45	F
30	0.4	0.75	4	0.9	0.40	P
31	0.4	0.75	4	0.9	0.45	F
32	0.4	0.75	4	0.9	0.40	P
				P_{50} = 0.423 m		
				MFE = 0.381 Kgm = 3.74 Joules		

P_{50} : height value for a probability of fail of 50% of the sample.

MFE = Mean Failure Energy.

Table B.12. Results of Falling-Weight Impact Test for the sample of graphite/polycarbonate composite specimens of six-impact damage level.

Specimen Number	CONTROLLED REPEATED IMPACT			FALLING WEIGHT TEST	IMPACT	
	Weight [Kg]	Height [m]	Number of Impacts	Weight [Kg]	Height [m]	Result P = Pass F = Fail
33	0.4	0.75	6	0.9	0.55	F
34	0.4	0.75	6	0.9	0.50	F
35	0.4	0.75	6	0.9	0.45	F
36	0.4	0.75	6	0.9	0.40	P
37	0.4	0.75	6	0.9	0.45	F
38	0.4	0.75	6	0.9	0.40	F
39	0.4	0.75	6	0.9	0.35	P
40	0.4	0.75	6	0.9	0.40	F

P_{50} = 0.381 m

MFE = 0.343 Kgm = 3.36 Joules

P_{50} : height value for a probability of fail of 50% of the sample.

MFE = Mean Failure Energy.

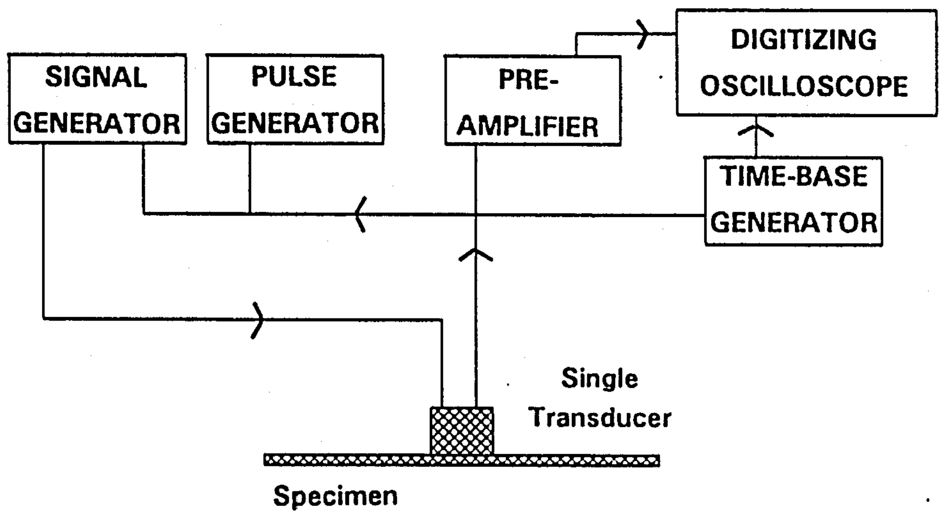

Figure 2.1. Instrumentation setup for NDE Pulse Echo technique.

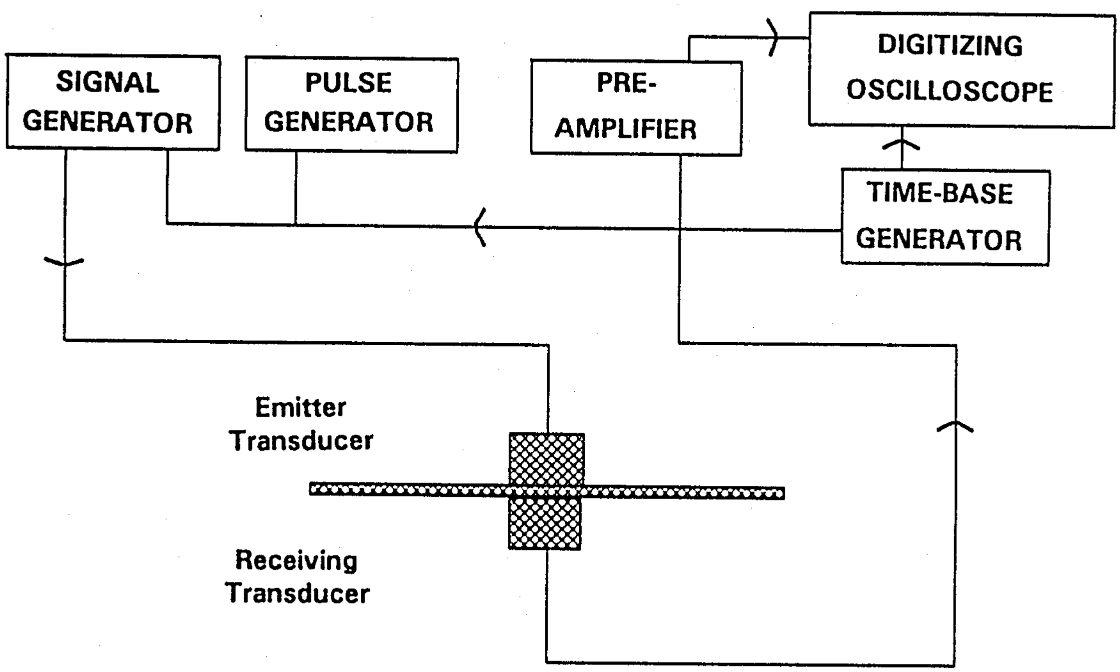

Figure 2.2. Instrumentation setup for NDE Trough Transmission technique.

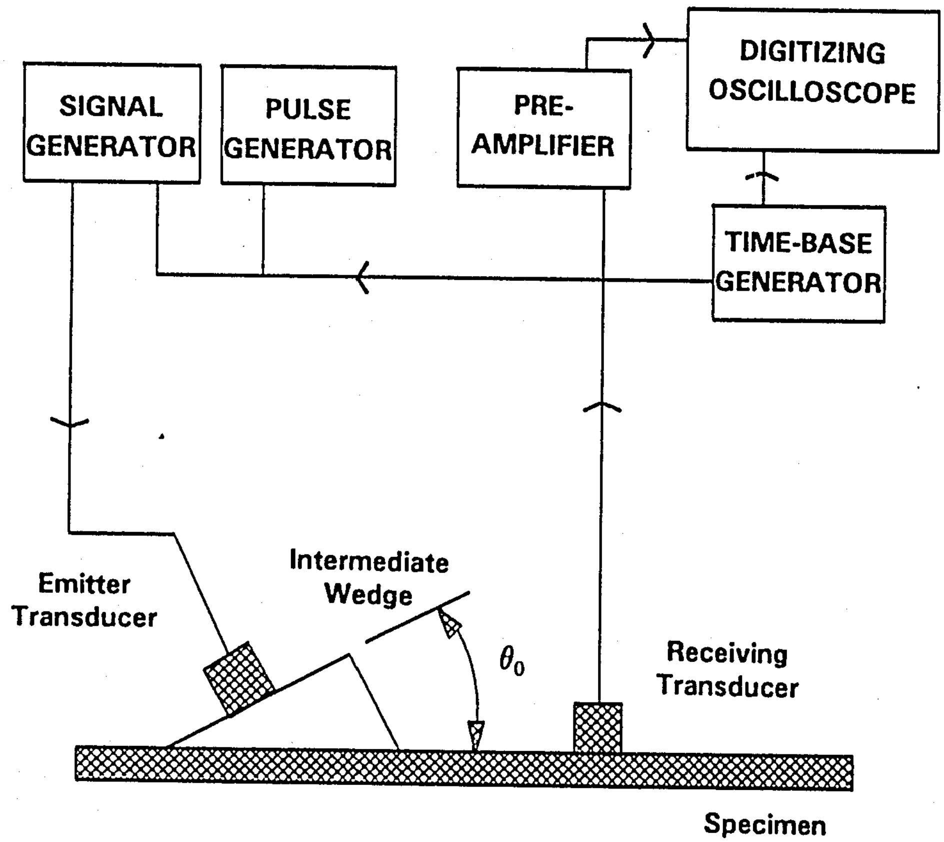

Figure 2.3. Instrumentation setup for NDE Surface and Lamb Wave technique.

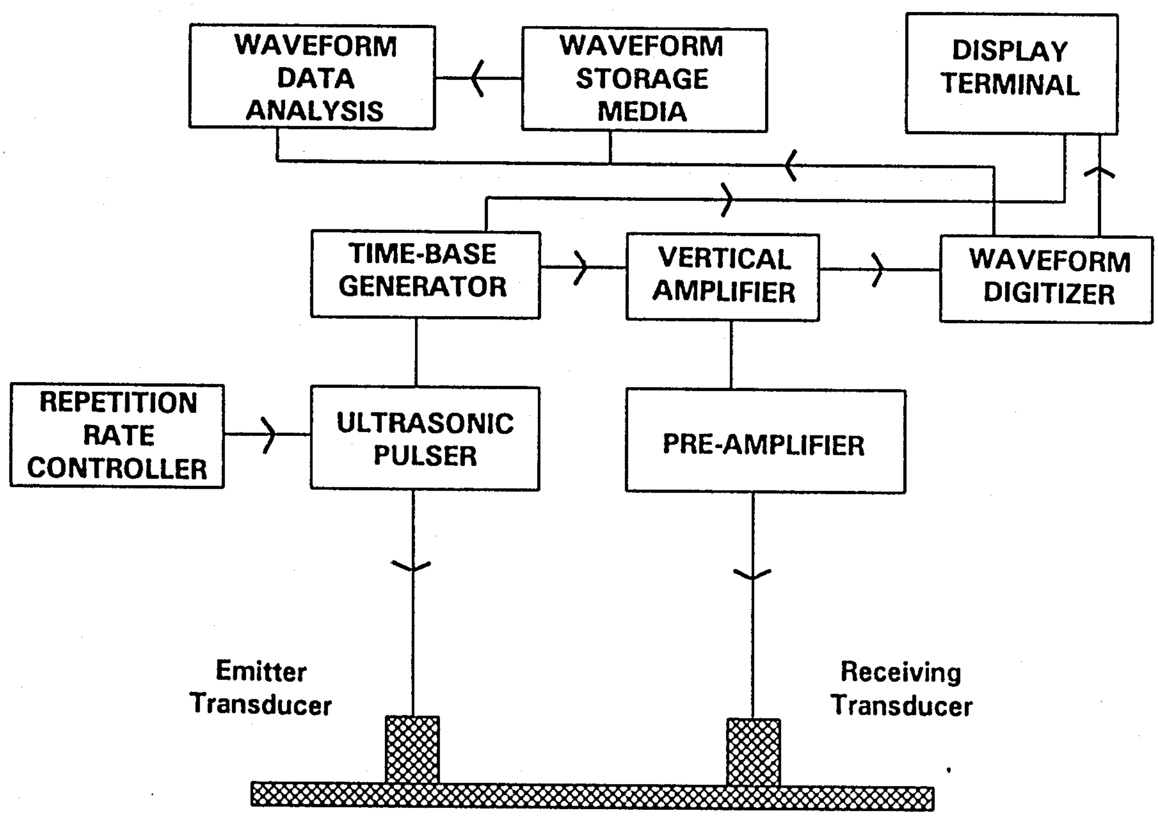

Figure 2.4. Instrumentation setup for NDE Acousto-Ultrasonics technique.

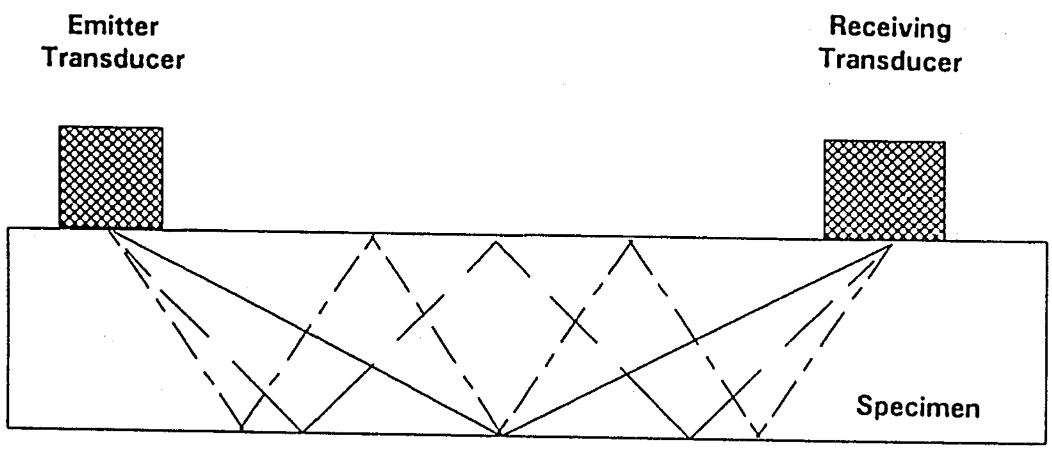

Figure 2.5. Diagram of some reflections paths of ultrasonic waves in a flat homogeneous solid (from Vary,A., ref. [33]).

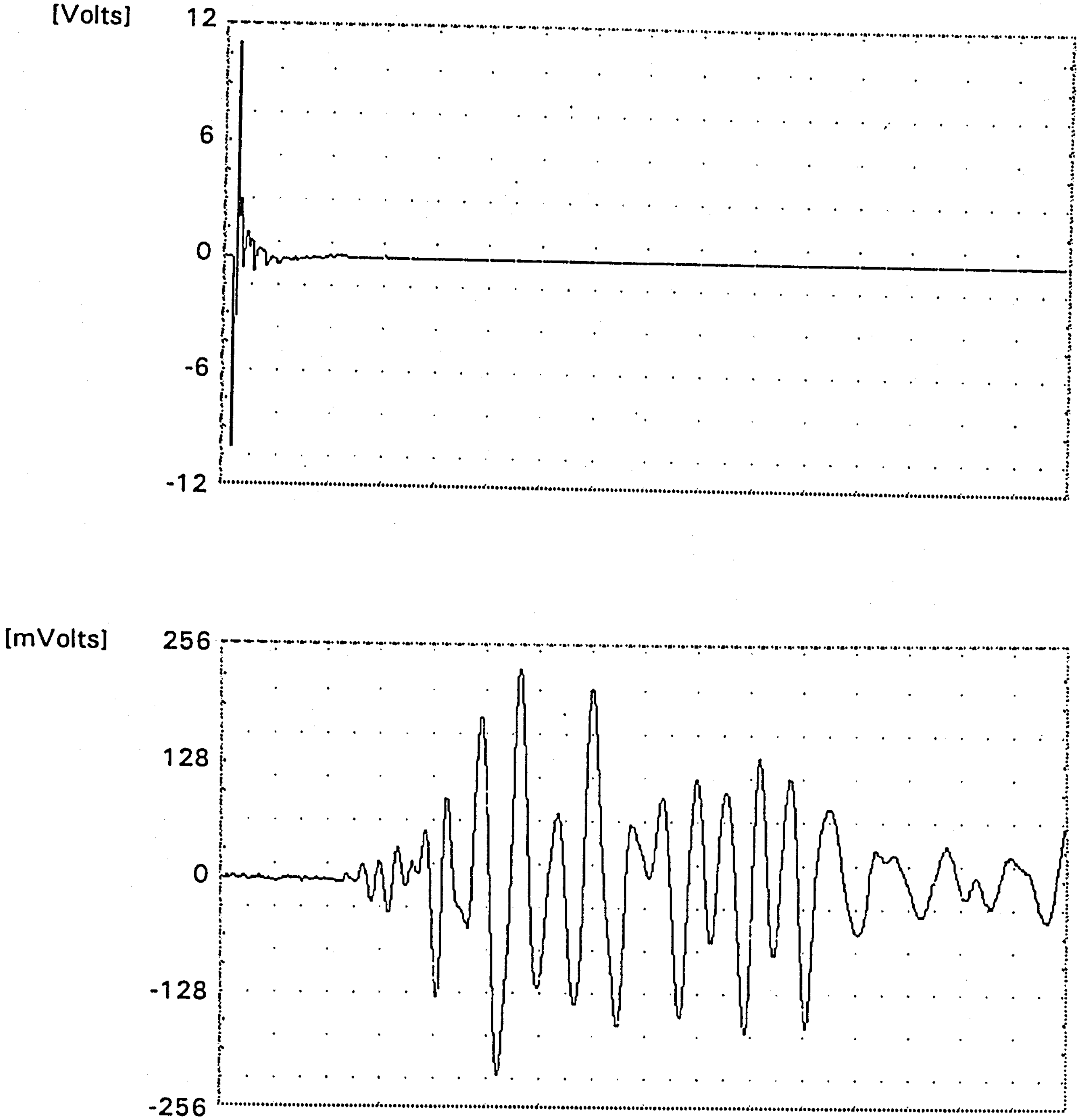

Figure 2.6. Ultrasonic pulse input and retrieved Acousto-Ultrasonics signal for a flat polyvinylchloride Specimen. Input frequency: 750 KHz. Distance between transducers: 3/4".

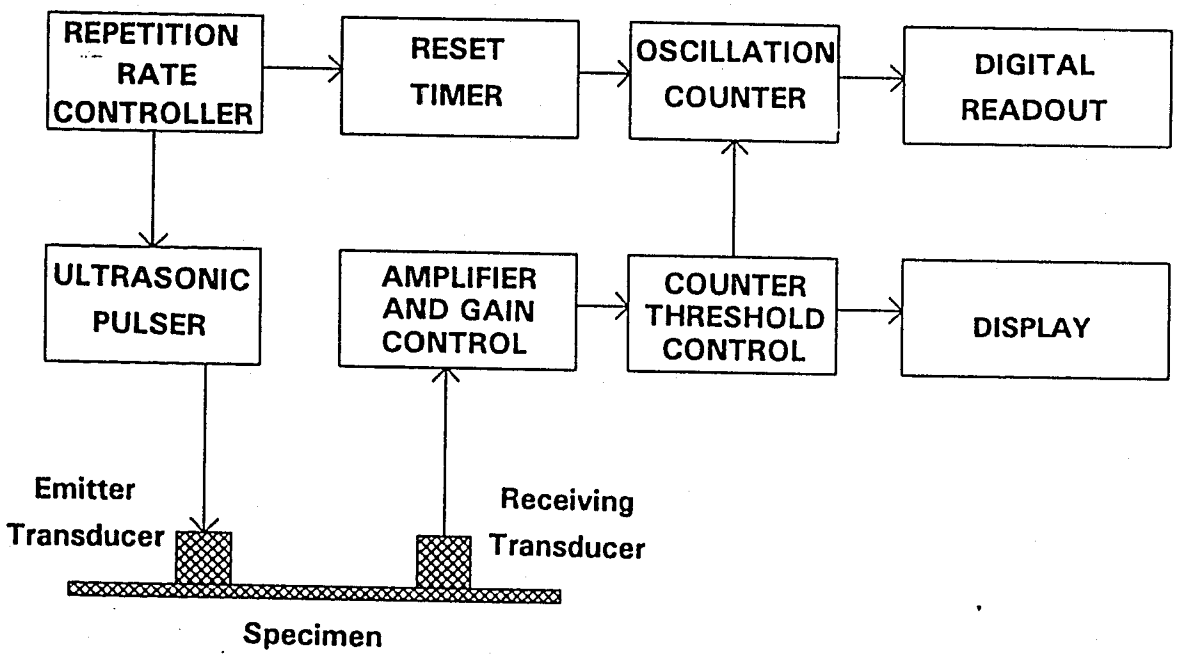

Figure 3.1. Instrumentation setup for the measurement of Ringdown Stress Wave Factor (From Henneke,E.G, [3]).

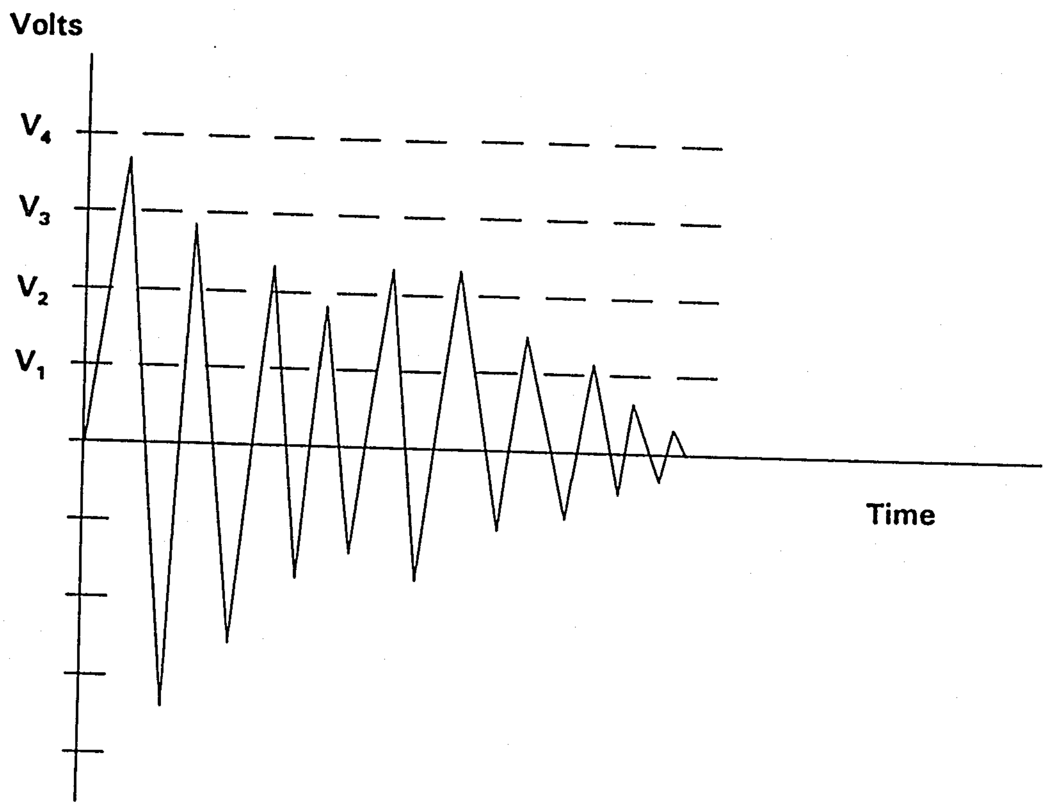

Figure 3.2. Schematics for the calculation of the Acousto-Ultrasonics Parameter.

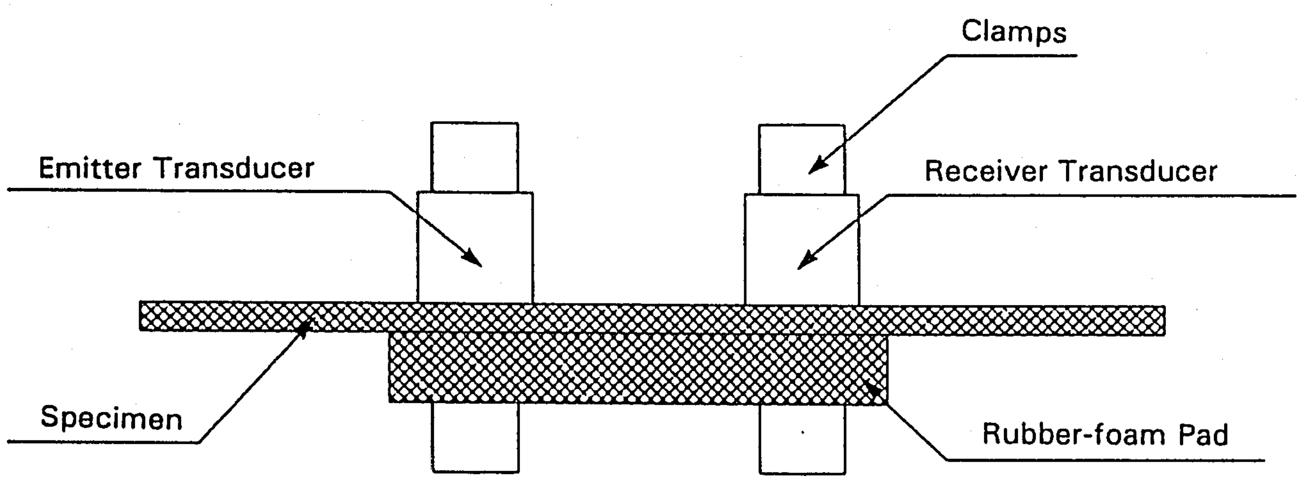

Figure 3.3. Transducer setup for the experimental evaluation of the factors affecting Acousto-Ultrasonics data acquisition.

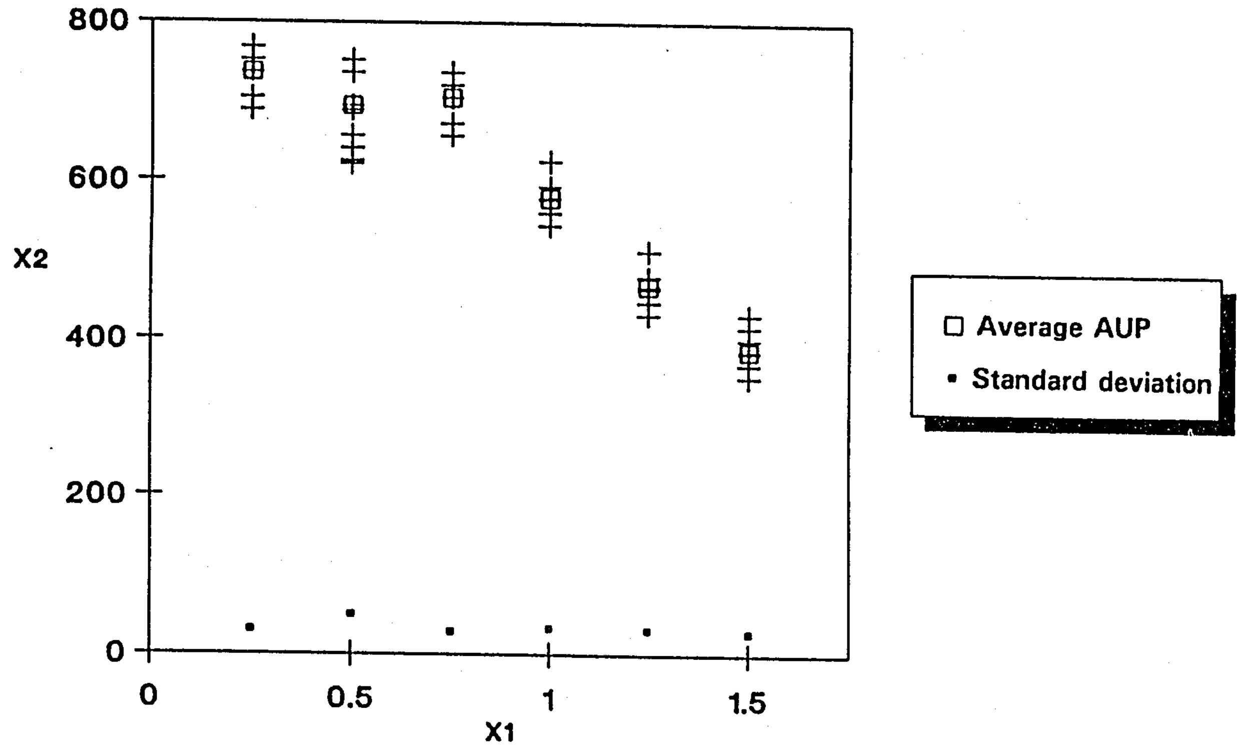

X1 : Distance between transducers in inches.
X2 : Acousto-Ultrasonics Parameter (AUP) in mVolts.

Figure 3.4. Sensitivity of AU measurements to Distance between transducers. Acousto Ultrasonics Parameter versus Distance between emitter and receiver transducers for polyvinylchloride specimens.

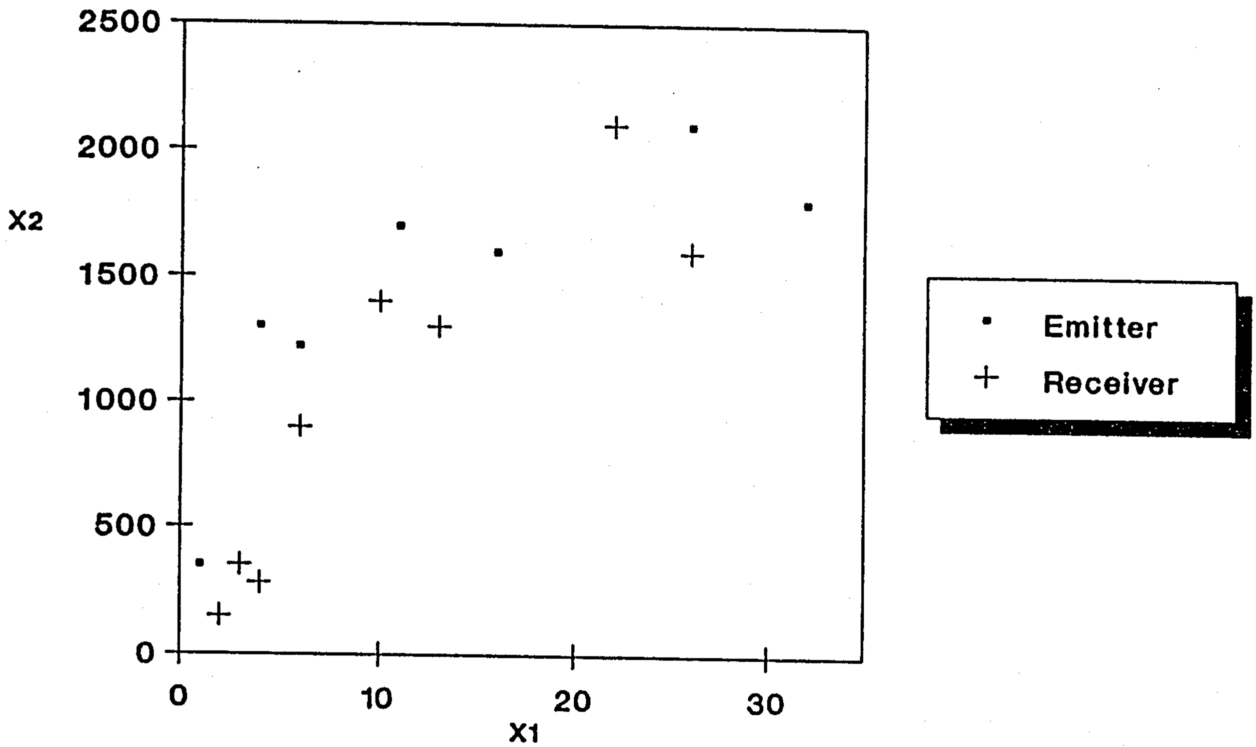

X1 : Contact-pressure applied to transducers in KPa.

X2 : Ringdown Stress Wave Factor (SWF) in mVolts.

Figure 3.5. Sensitivity of AU measurements to the contact-pressure applied to transducers. Ringdown Stress Wave Factor versus contact pressure applied to emitter and receiver transducers. (From Russell-Floyd,R. and Phillips,M.G., [45]).

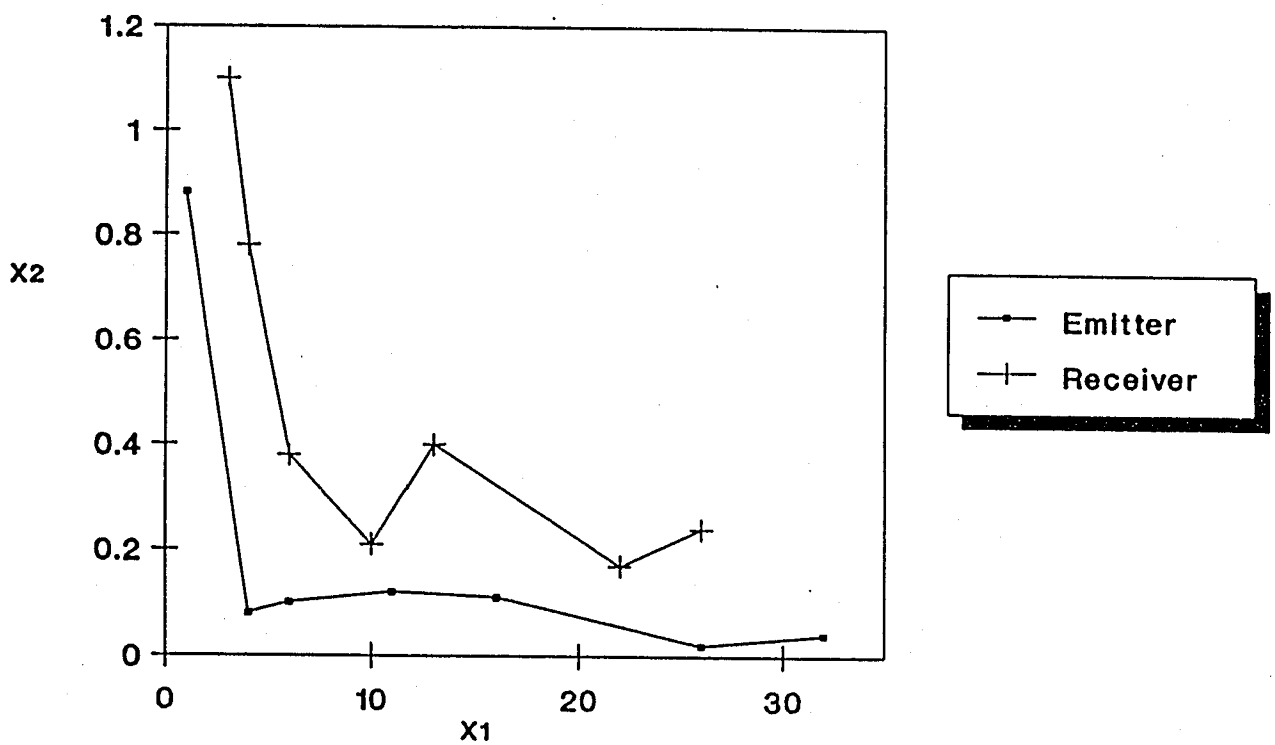

X1 : Contact-pressure applied to transducers in KPa.
X2 : Coefficient of variation of Ringdown Stress Wave Factor.

Figure 3.6. Sensitivity of AU measurements to contact-pressure applied to transducers. Coefficient of variation of Ringdown Stress Wave Factor, as the ratio of standard deviation to mean of the measure values, versus contact pressure. (From Russell-Floyd,R. and Phillips,M.G., [45]).

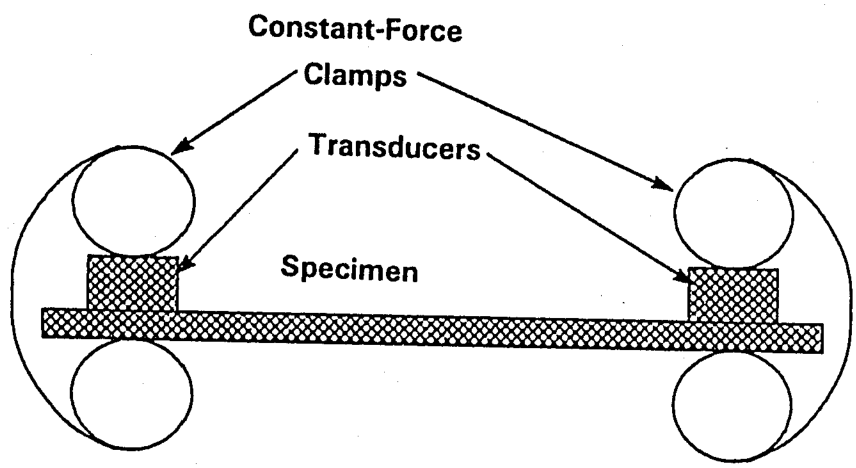

Figure 3.7. Constant-force clamp configuration to apply relative contact pressure between the transducers and the specimen in an Acousto-Ultrasonics experiment.

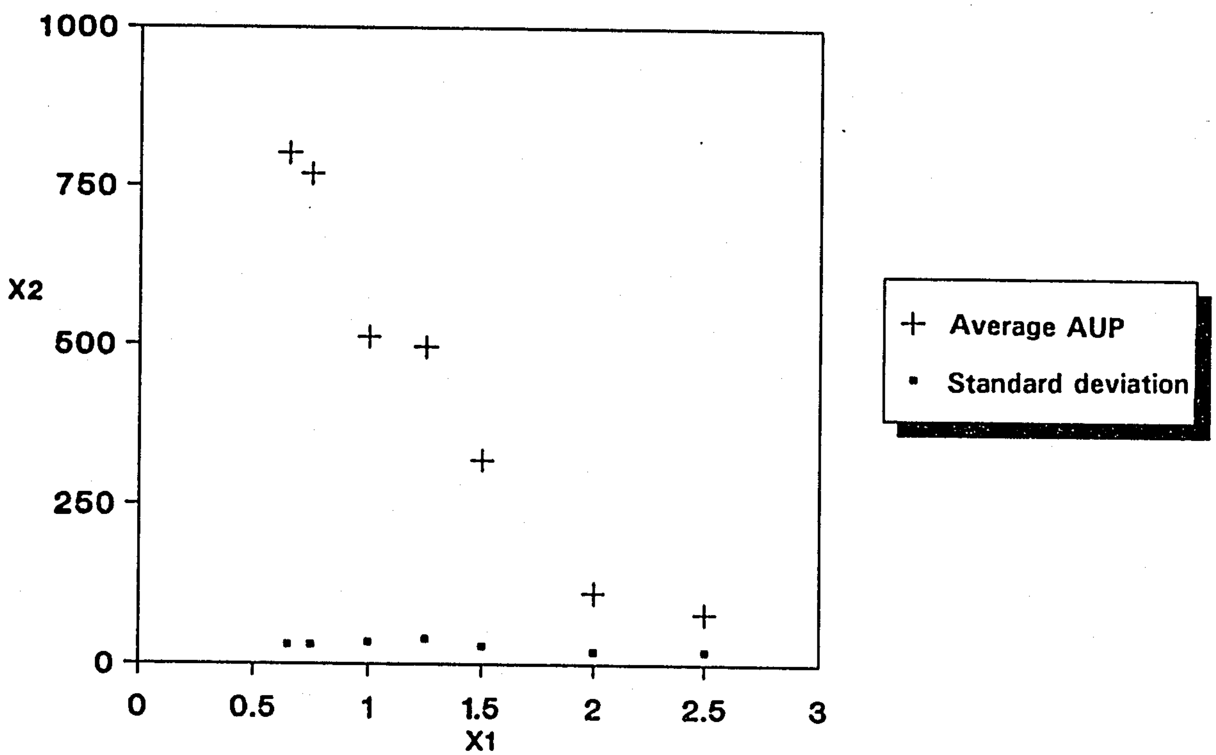

X1 : Central frequency of the ultrasonic pulse input in MHz.
X2 : Acousto-Ultrasonics Parameter in mVolts.

Figure 3.8. Sensitivity of AU measurements to the ultrasonic input frequency. Acousto Ultrasonics Parameter versus frequency of the emitted ultrasonic pulse for polyvinylchloride specimens.

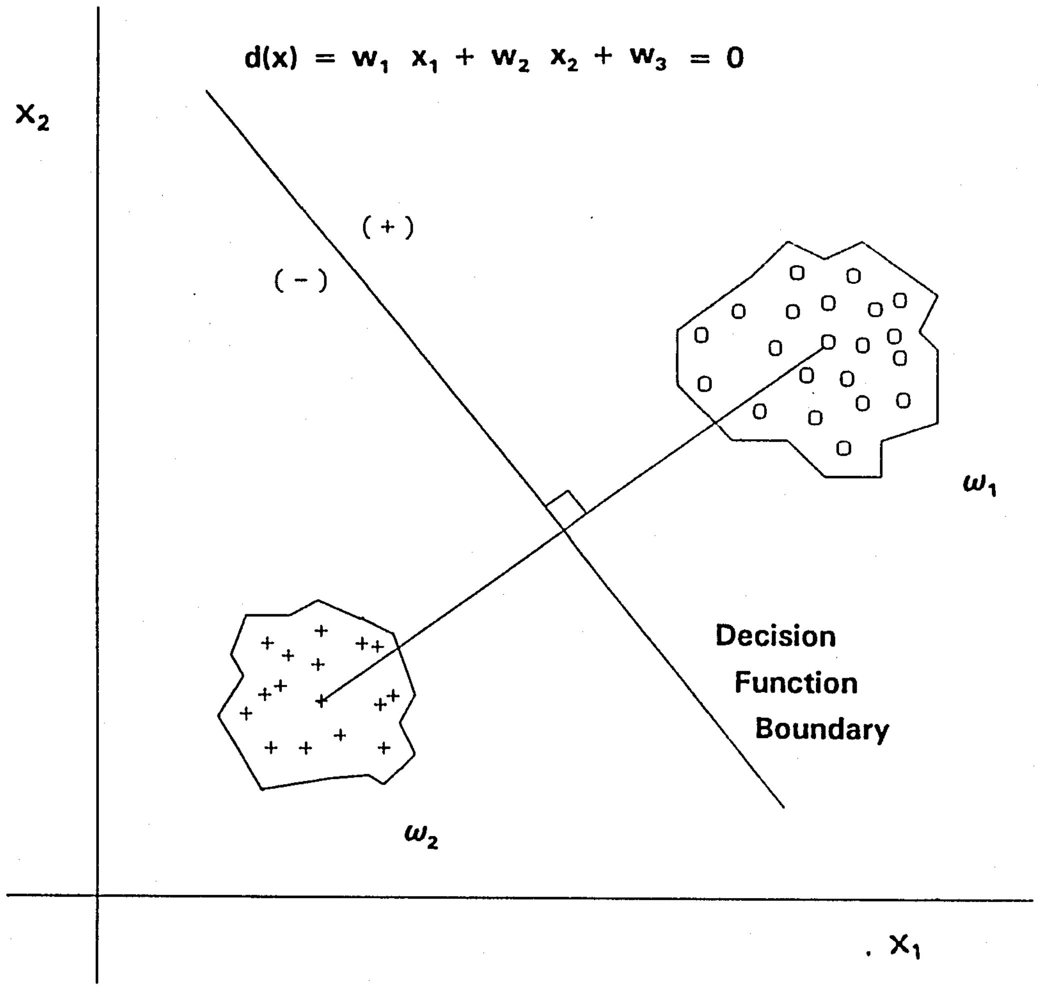

x_1 : Coordinate values of feature 1
x_2 : Coordinate values of feature 2

Figure 4.1. Linear Discrimination Decision Function d(x) for two classes in a two-dimension feature-space. Each class is characterized by a single prototype pattern.

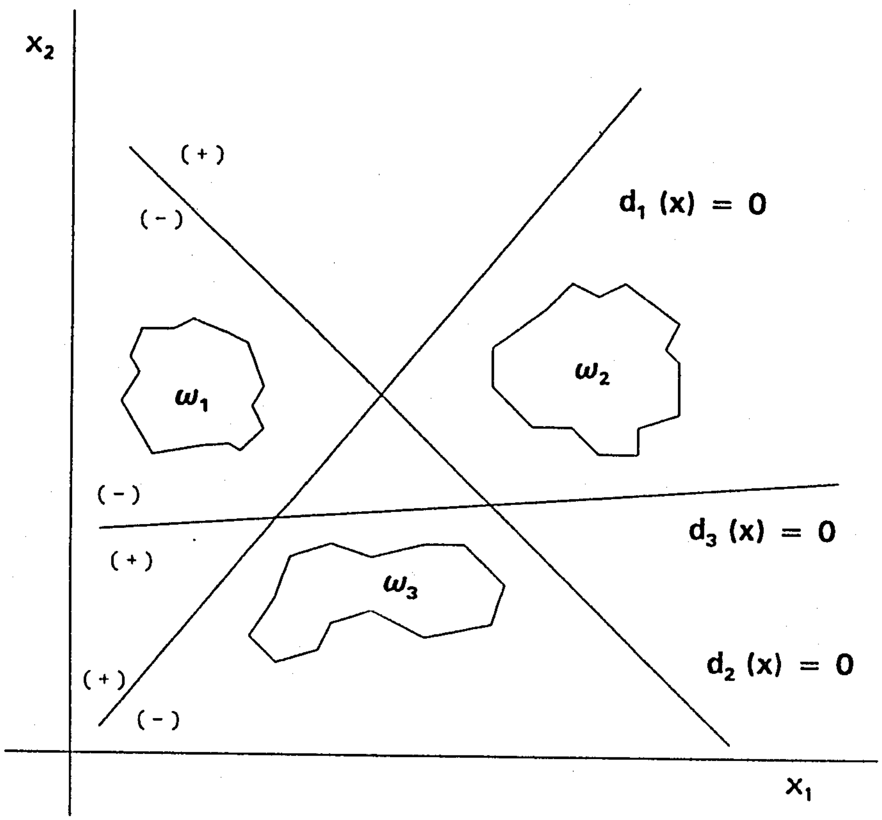

x_1 : Coordinate values of feature 1
x_2 : Coordinate values of feature 2

Figure 4.2. "First Case" of Linearly Separable Classes in a two-dimension feature space. The three classes are separated by linear boundaries pertaining to linear discriminant decision functions $d_i(x)$. Each class is characterized by a single prototype pattern.

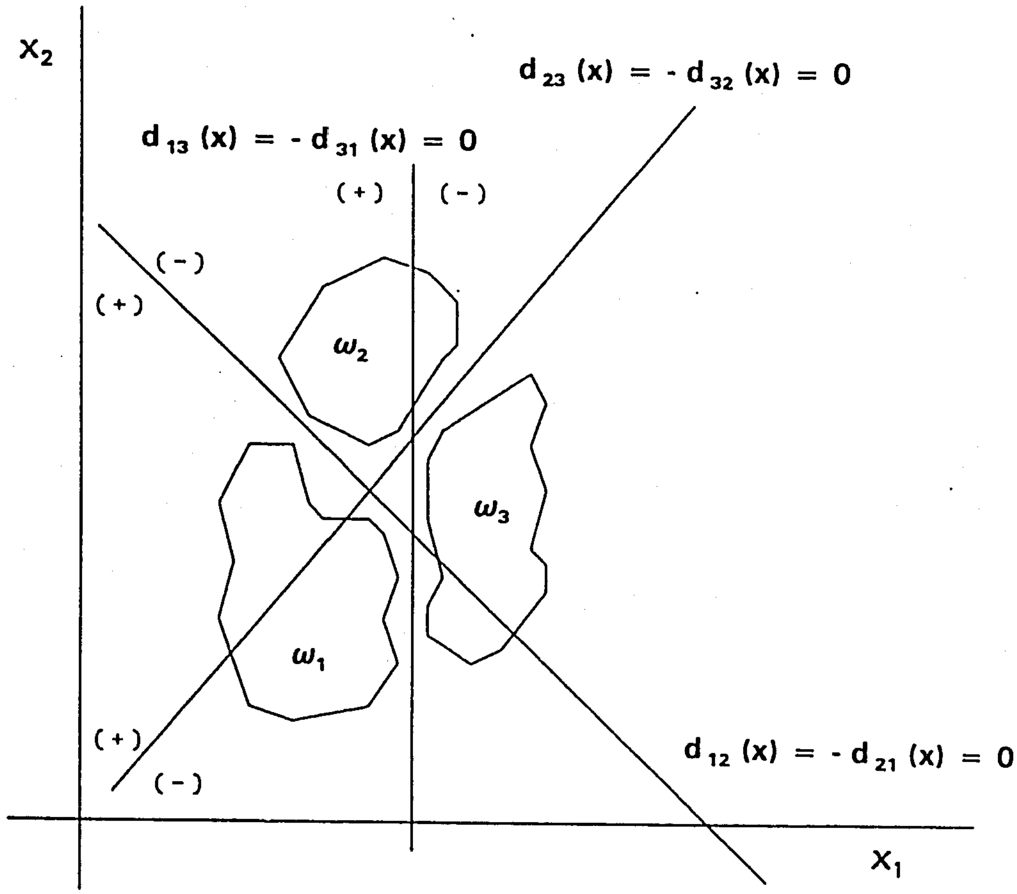

x_1 : Coordinate values of feature 1
x_2 : Coordinate values of feature 2

Figure 4.3. "Second Case" of Linearly Separable Classes in a two-dimension feature space. Each of the three classes is separated by two linear boundaries pertaining to linear discriminant decision functions $d_i(x)$. Each class is characterized by a single prototype pattern.

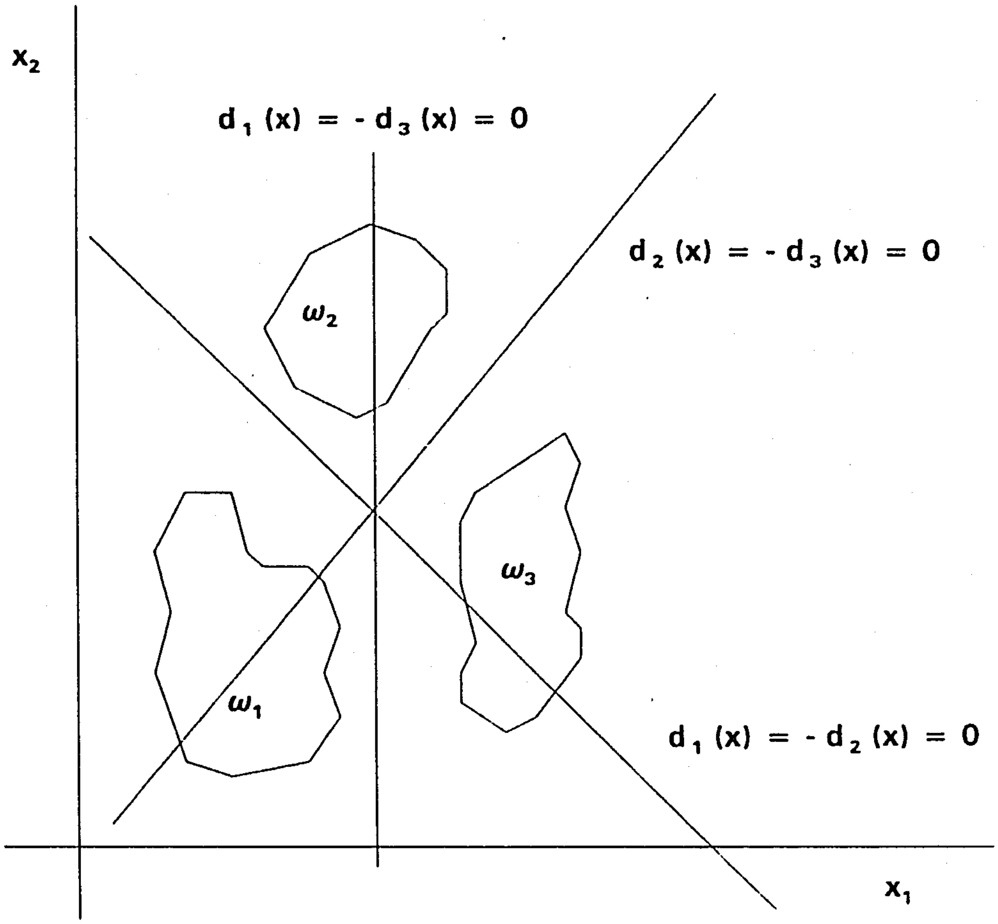

x_1 : Coordinate values of feature 1
x_2 : Coordinate values of feature 2

Figure 4.4. "Third Case" of Linearly Separable Classes in a two-dimension feature space. Each of the three classes is separated by two linear boundaries pertaining to linear discriminant decision functions $d_i(x)$. Each class is characterized by a single prototype pattern.

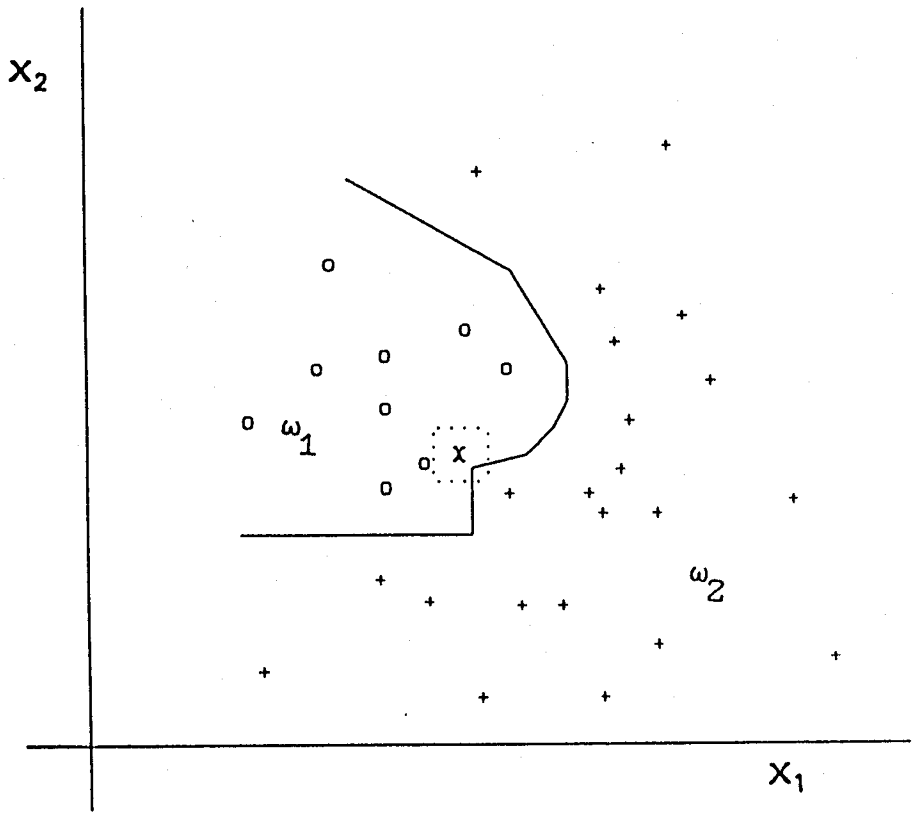

x_1 : Coordinate values of feature 1
x_2 : Coordinate values of feature 2

Figure 4.5. One-Nearest Neighbour Classification of pattern 'x' for two classes ω_1 and ω_2 in a two-dimension feature-space.

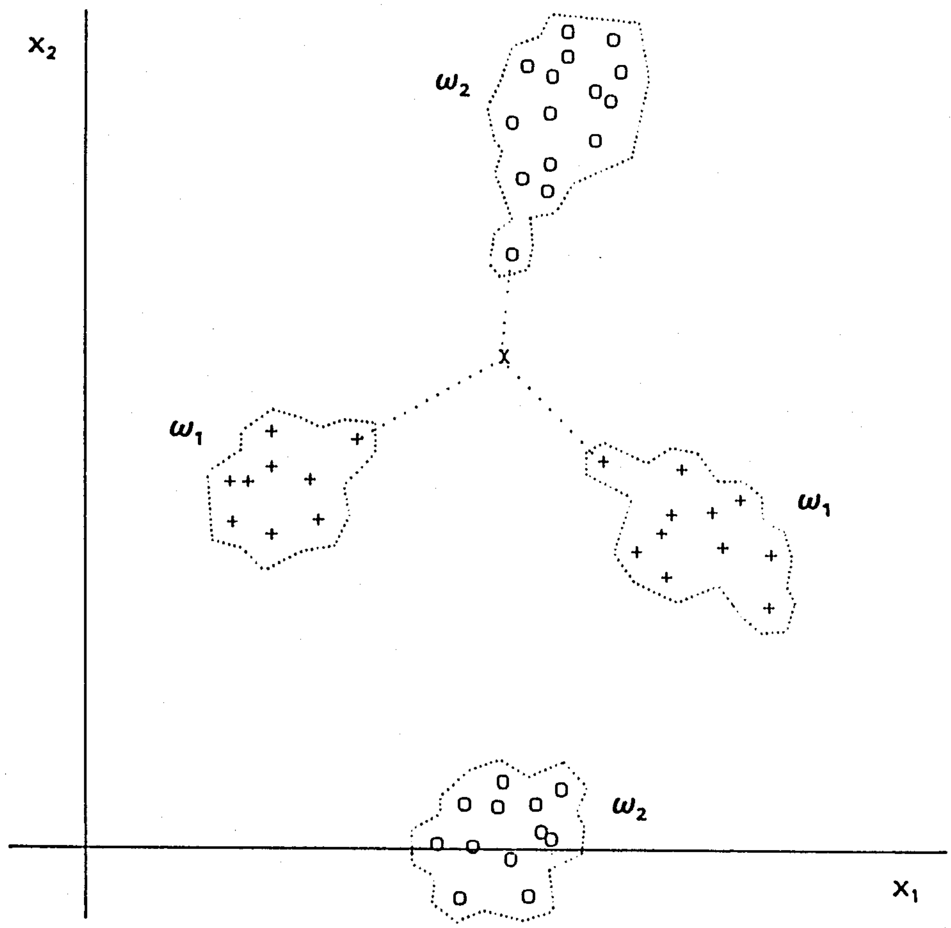

x_1 : Coordinate values of feature 1
x_2 : Coordinate values of feature 2

Figure 4.6. Three-Nearest Neighbour Classification of pattern 'x' for two classes ω_1 and ω_2 in a two-dimension feature-space.

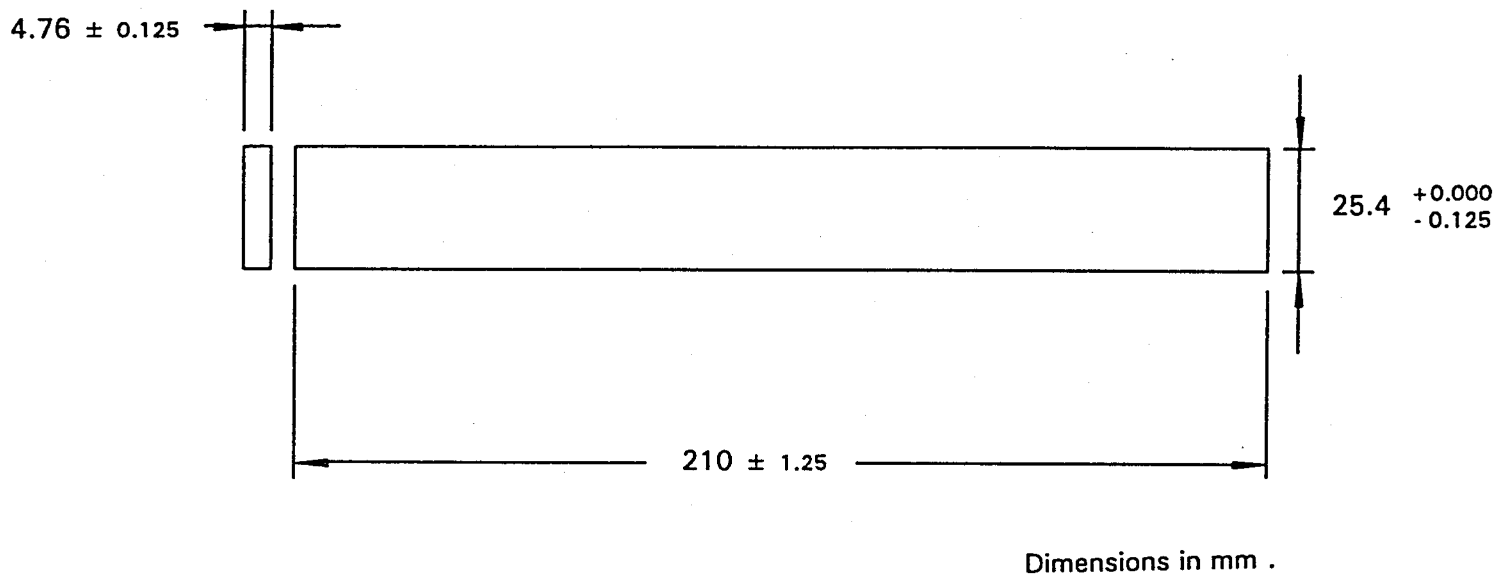

Figure 6.1. Polyvinylchloride specimen for the evaluation of repeated-impact damage.

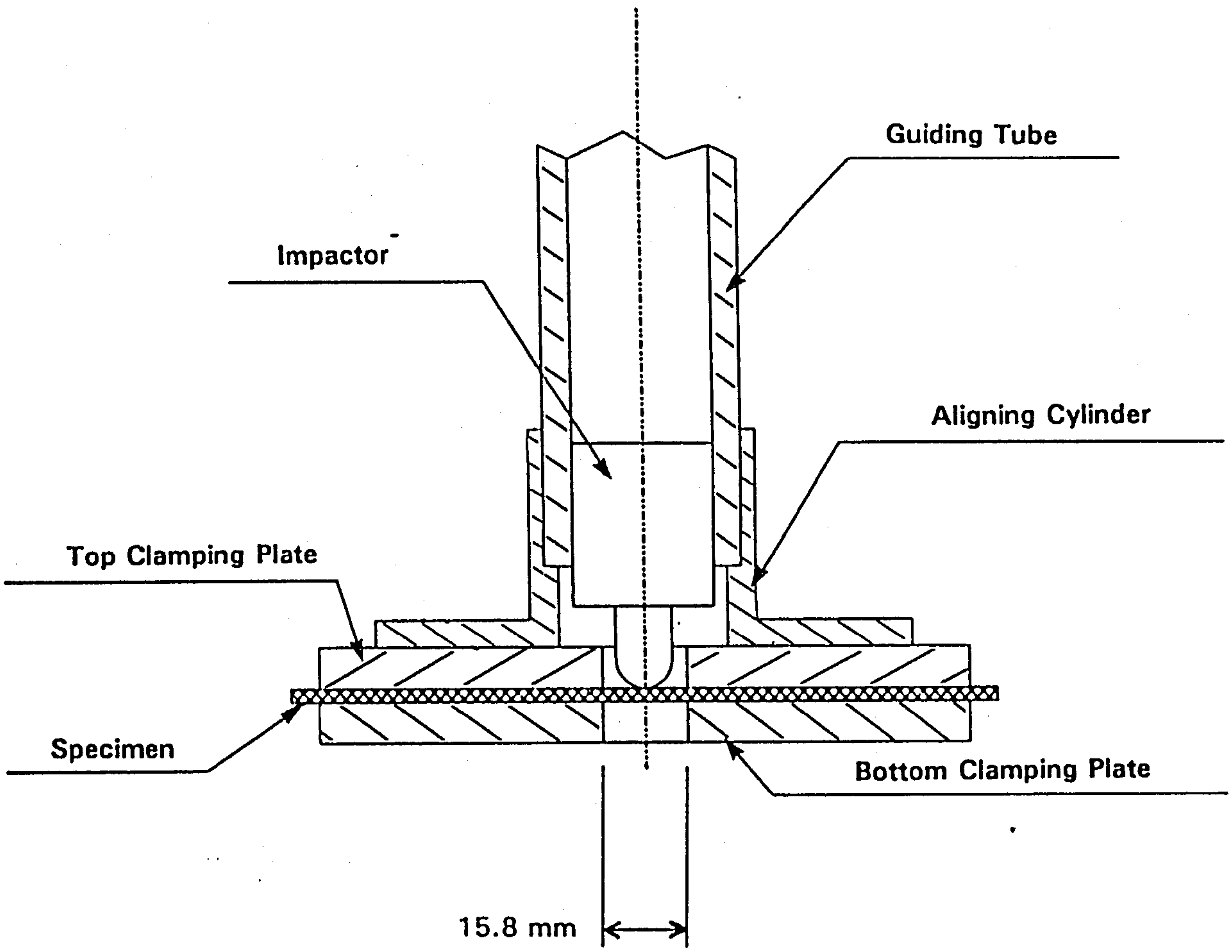

Figure 6.2. Experimental apparatus for the controlled repeated-impact procedure.

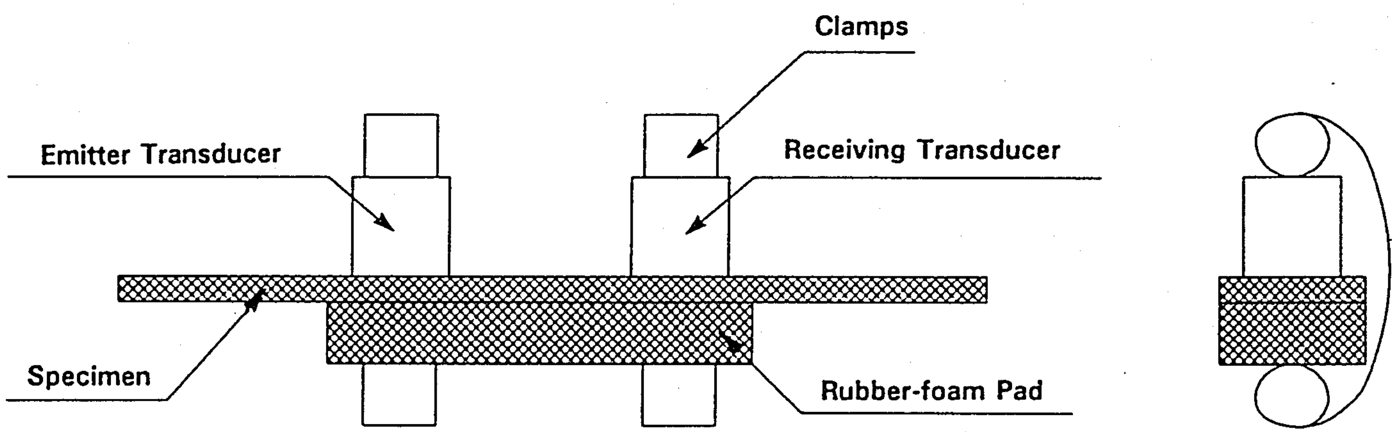

Figure 6.3. Transducer setup for the Acousto-Ultrasonics evaluation of repeated-impact damage in polyvinylchloride specimens.

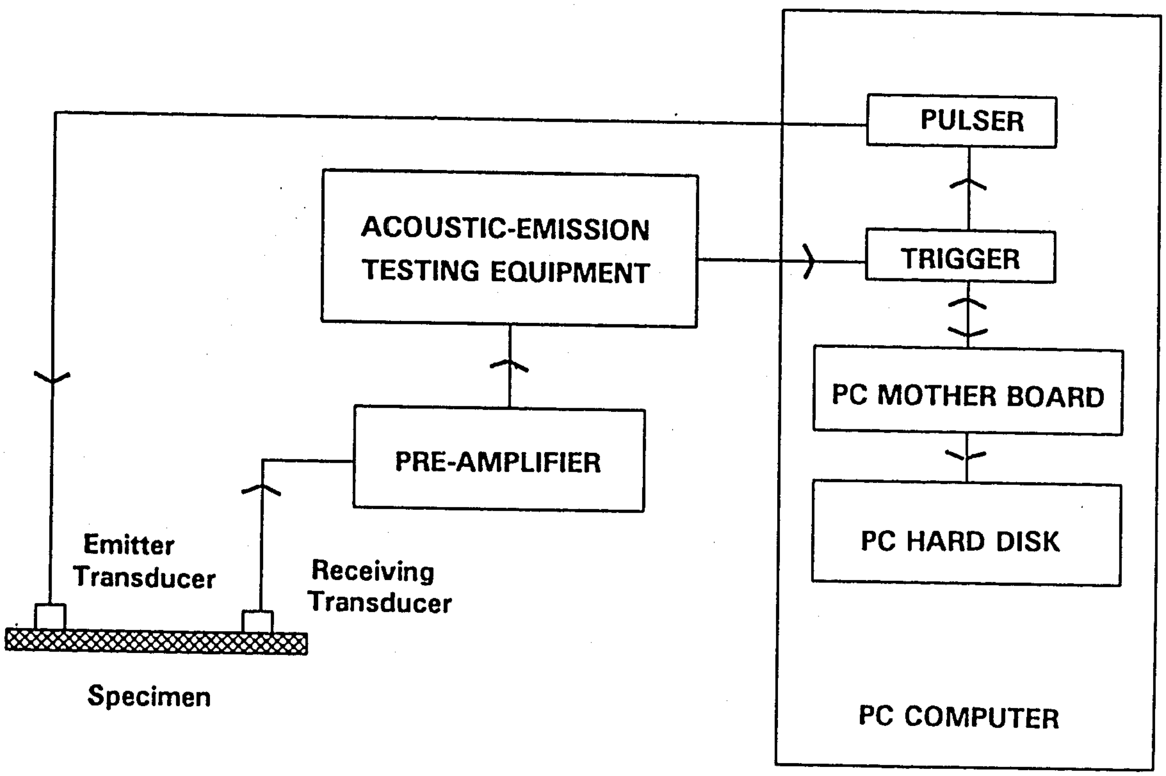

Figure 6.4. Acousto-Ultrasonics equipment and setup for AU-data acquisition.

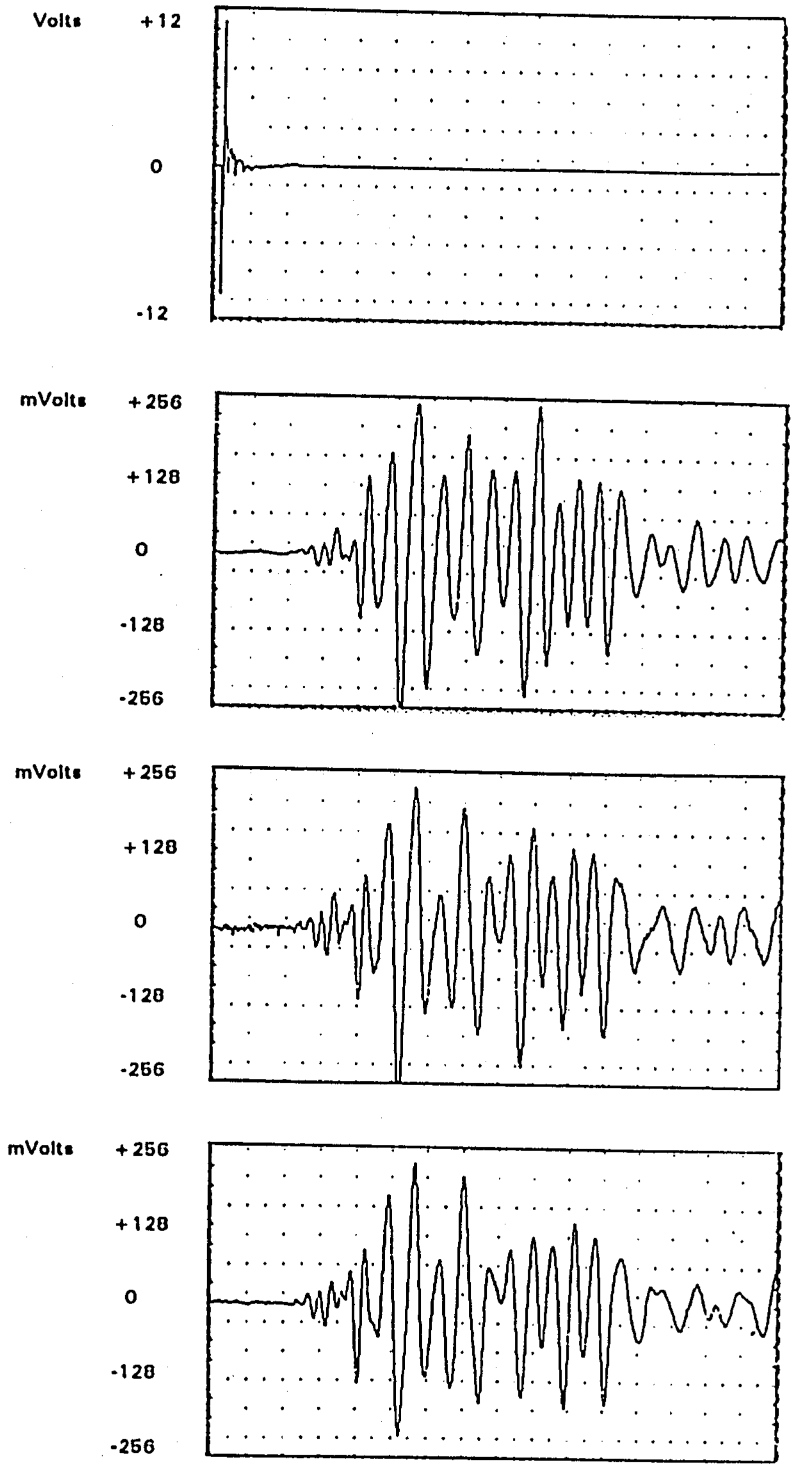

Figure 6.5. Ultrasonic pulse input and Acousto-Ultrasonics readings for different levels of repeated-impact damage in polyvinylchloride specimens.
From top to bottom: - Ultrasonic pulse input.
- AU reading for five-impact damage level.
- AU reading for ten-impact damage level.
- AU reading for twenty-impact damage level.

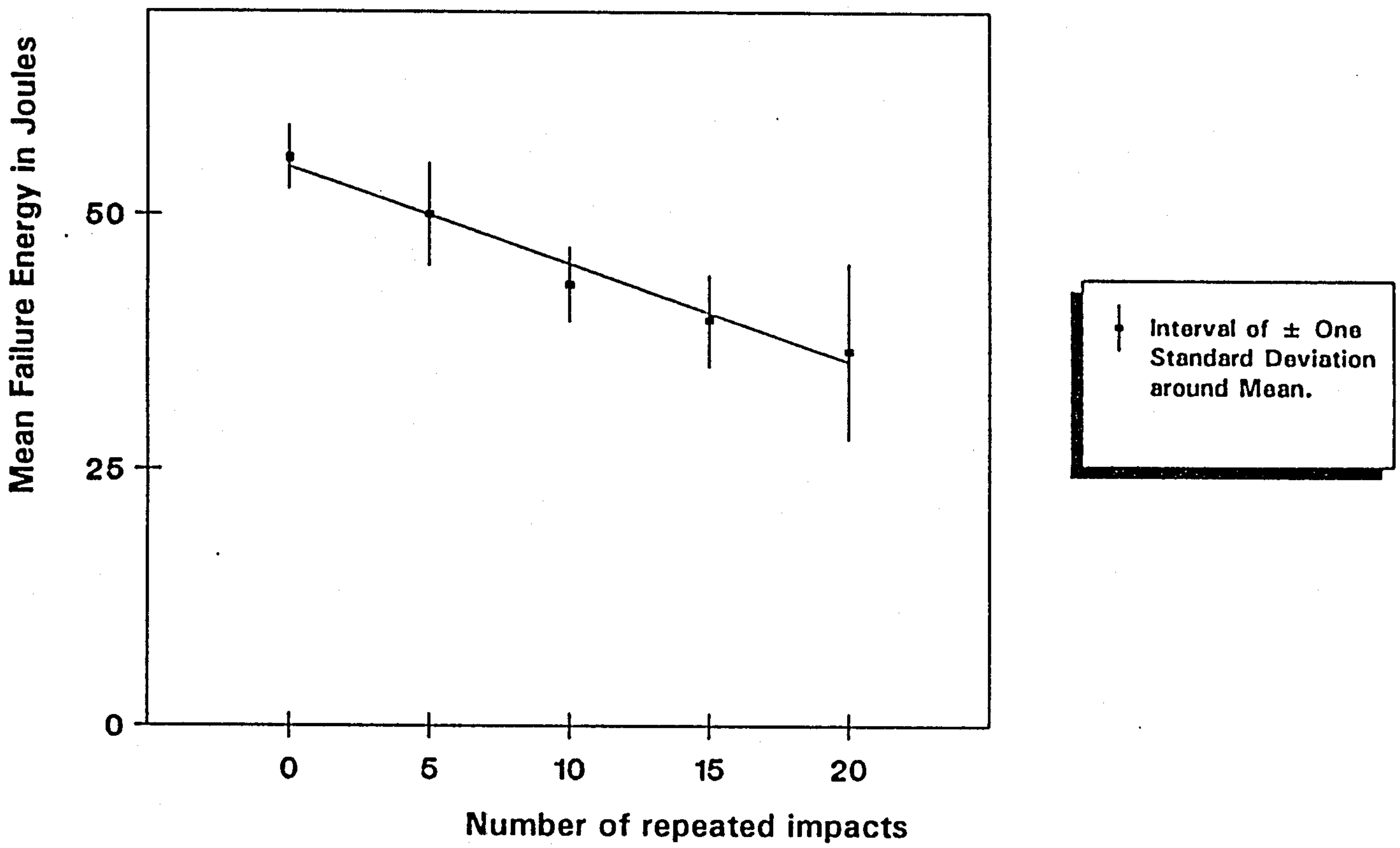

Figure 6.6. "Mean Failure Energy" versus number of repeated-impacts for polyvinylchloride specimens.

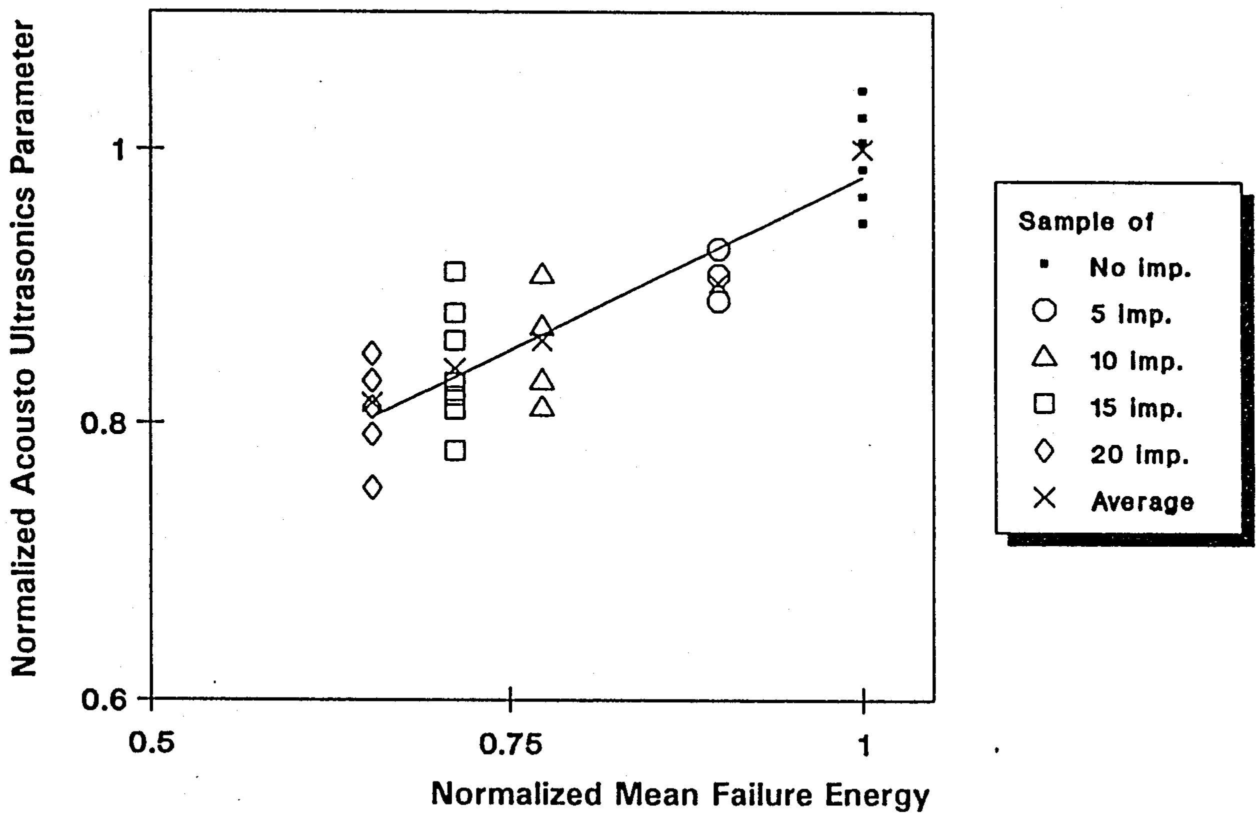

Figure 6.7. "Normalized Acousto-Ultrasonics Parameter" versus "Normalized Mean Failure Energy" for polyvinylchloride specimens.

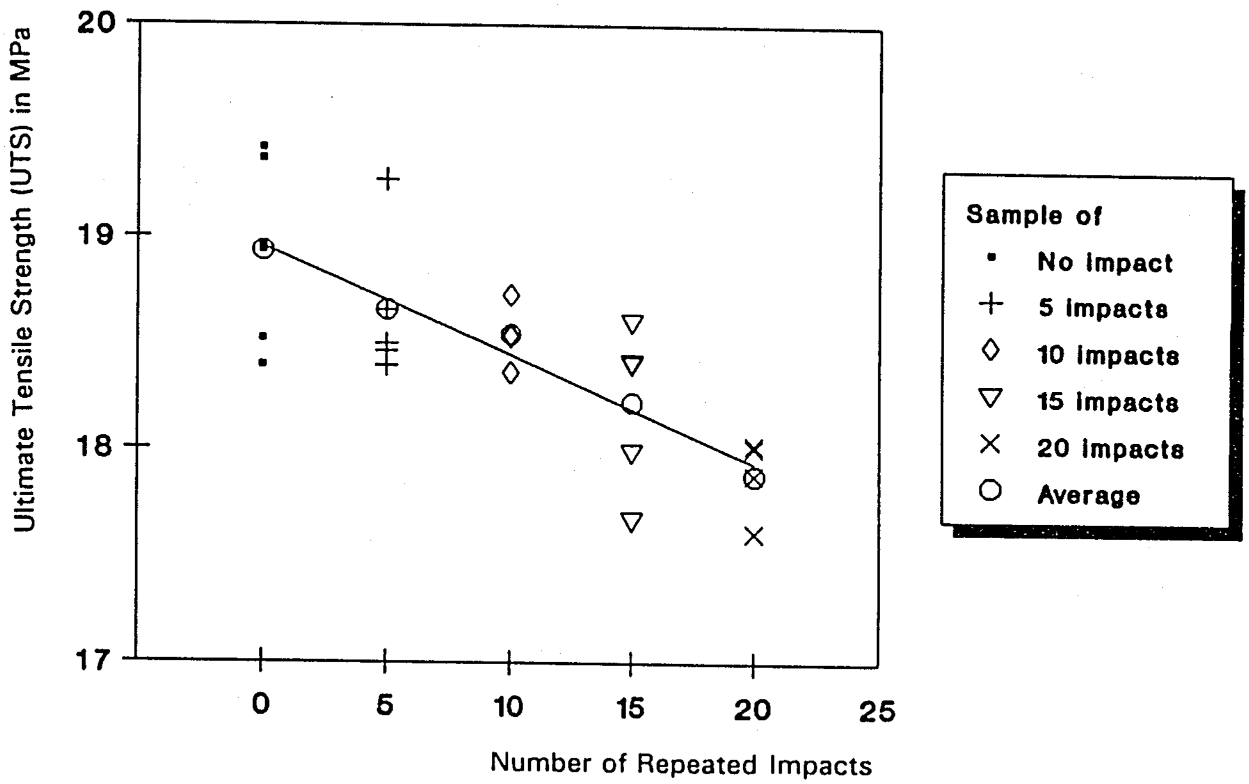

Figure 6.8. Ultimate Tensile Strength versus number of repeated impacts for polyvinylchloride specimens.

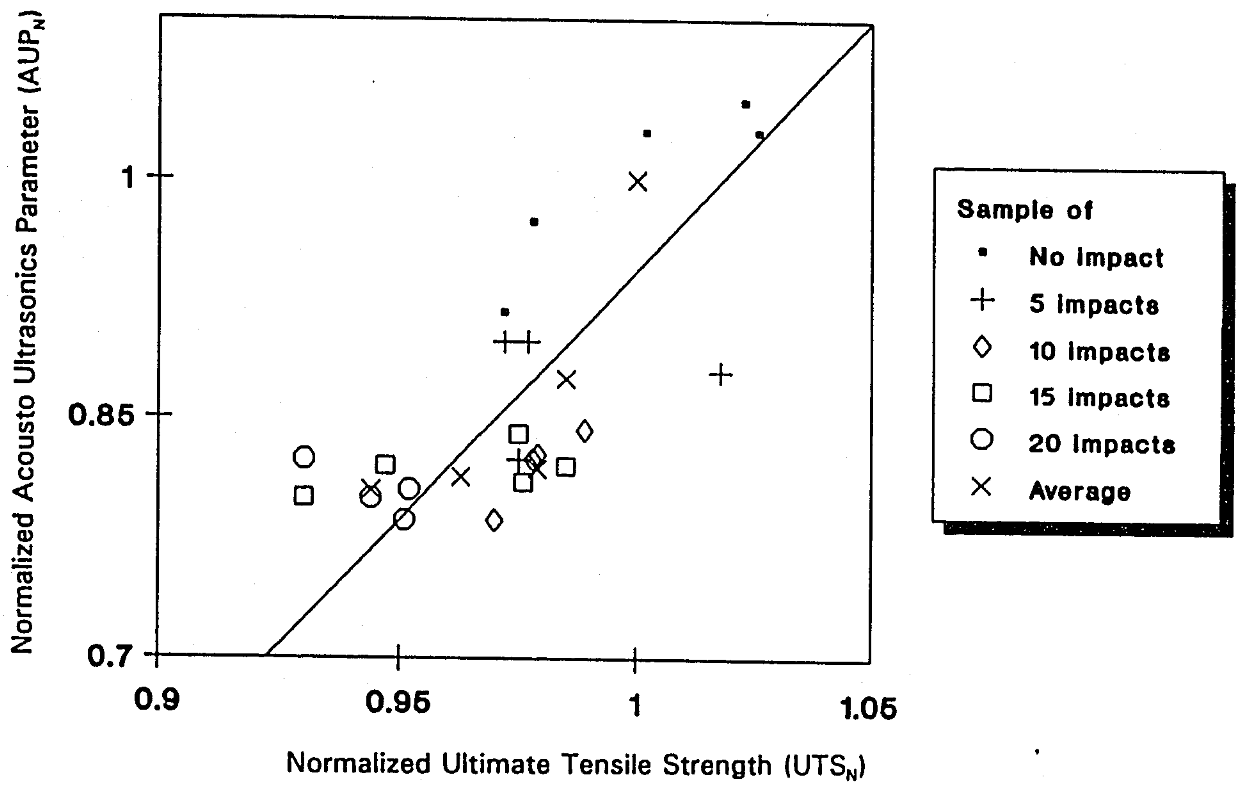

Figure 6.9. "Normalized Acousto Ultrasonics Parameter" versus "Normalized Ultimate Tensile Strength" for polyvinylchloride specimens.

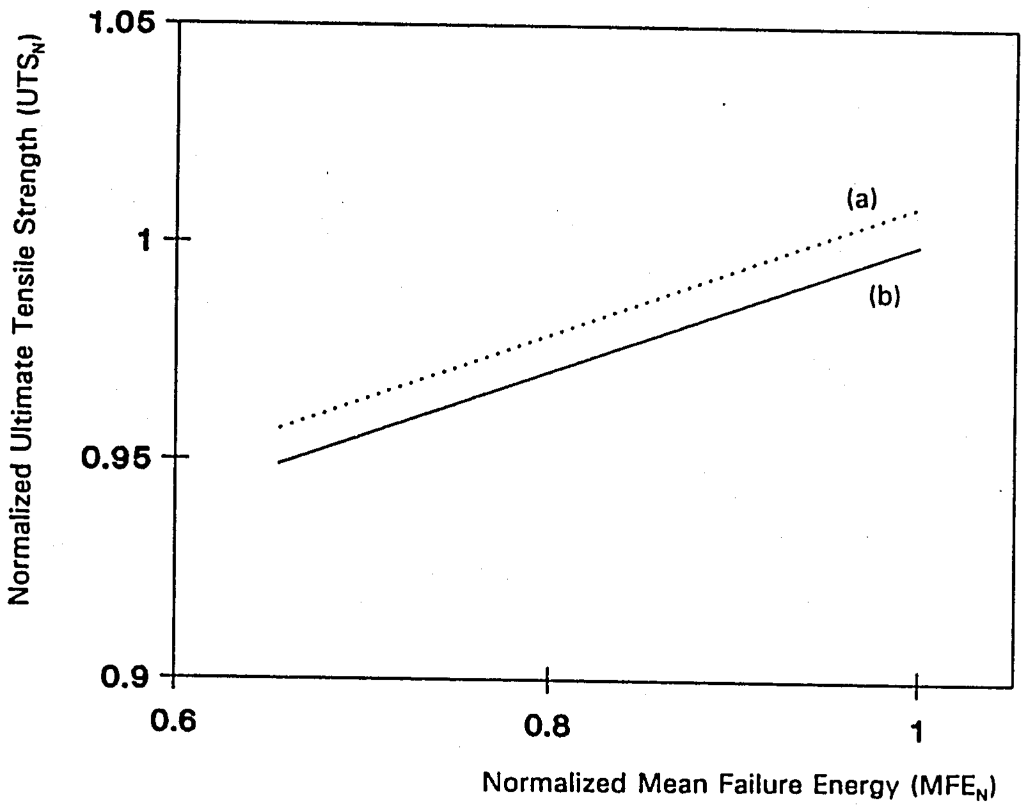

Line (a) corresponds to Expression (6.6).
Line (b) corresponds to Expression (6.7).

Figure 6.10. Comparison of the two expressions (6.6) and (6.7) relating "Normalized Mean Failure Energy" to "Normalized Ultimate Tensile Strength" in polyvinylchloride specimens.

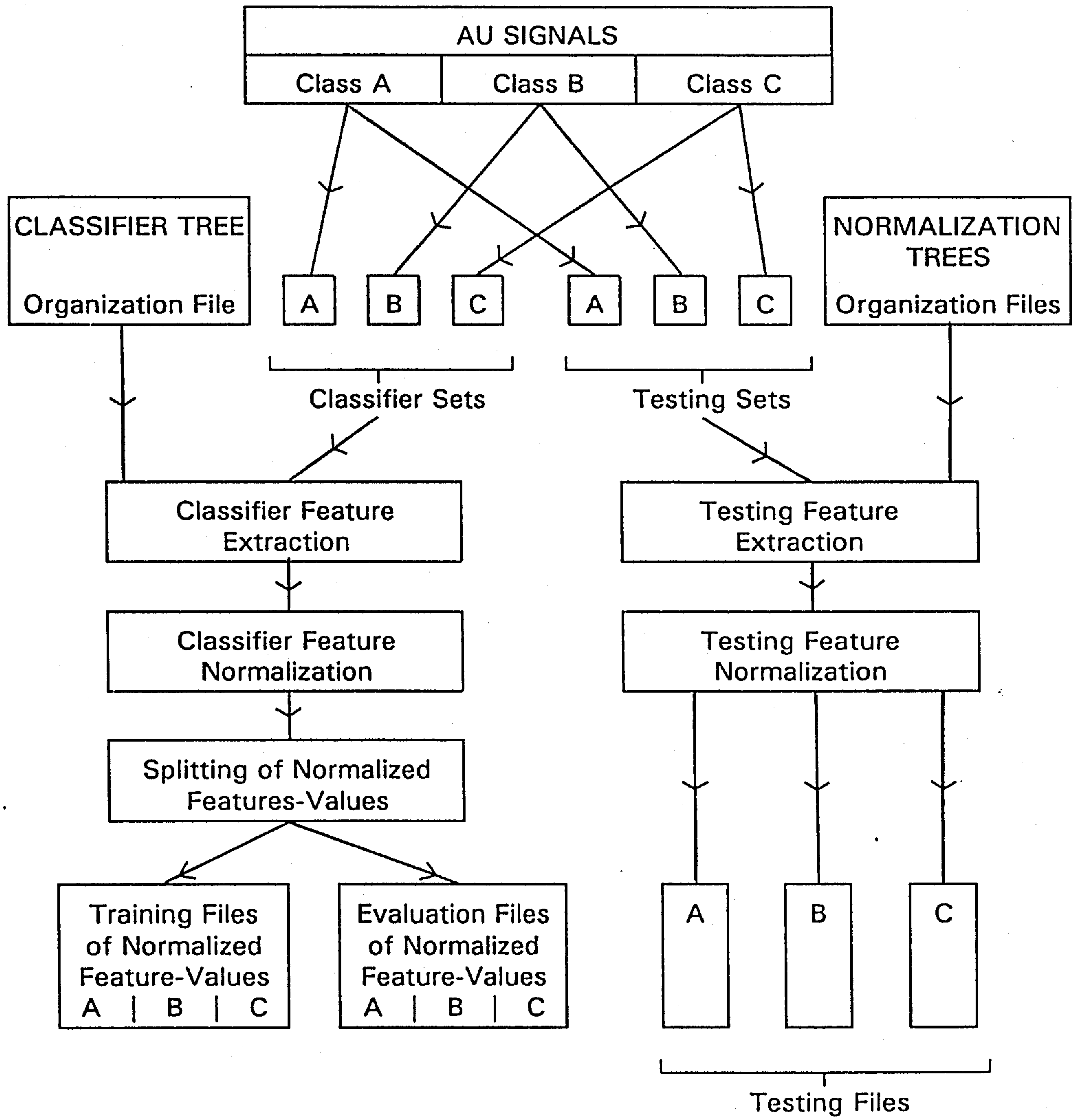

Figure 7.1. Schematics of the feature extraction, feature normalization and feature-value splitting for Acousto-Ultrasonics data.

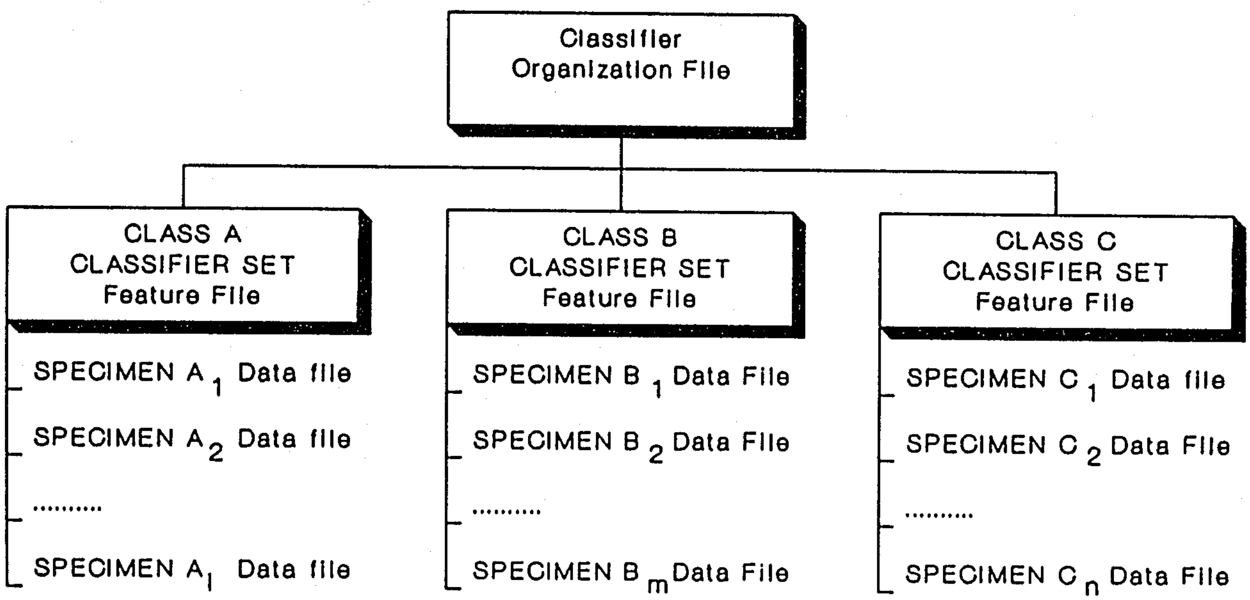

Figure 7.2. Classifier Tree. Arrangement of Acousto-Ultrasonics data files pertaining to repeated-impact damage classes of polyvinylchloride specimens.

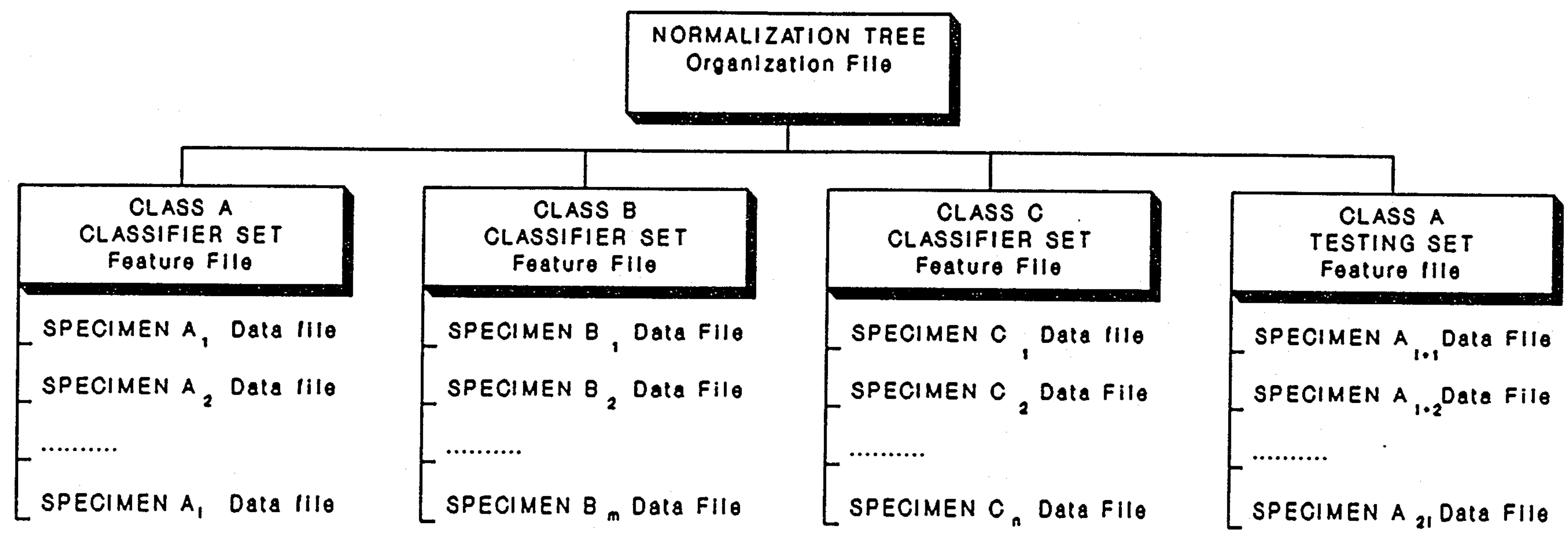

Figure 7.3. Normalization Tree file-arrangement for feature extraction and normalization of Classifier sets pertaining to polyvinylchloride specimens.

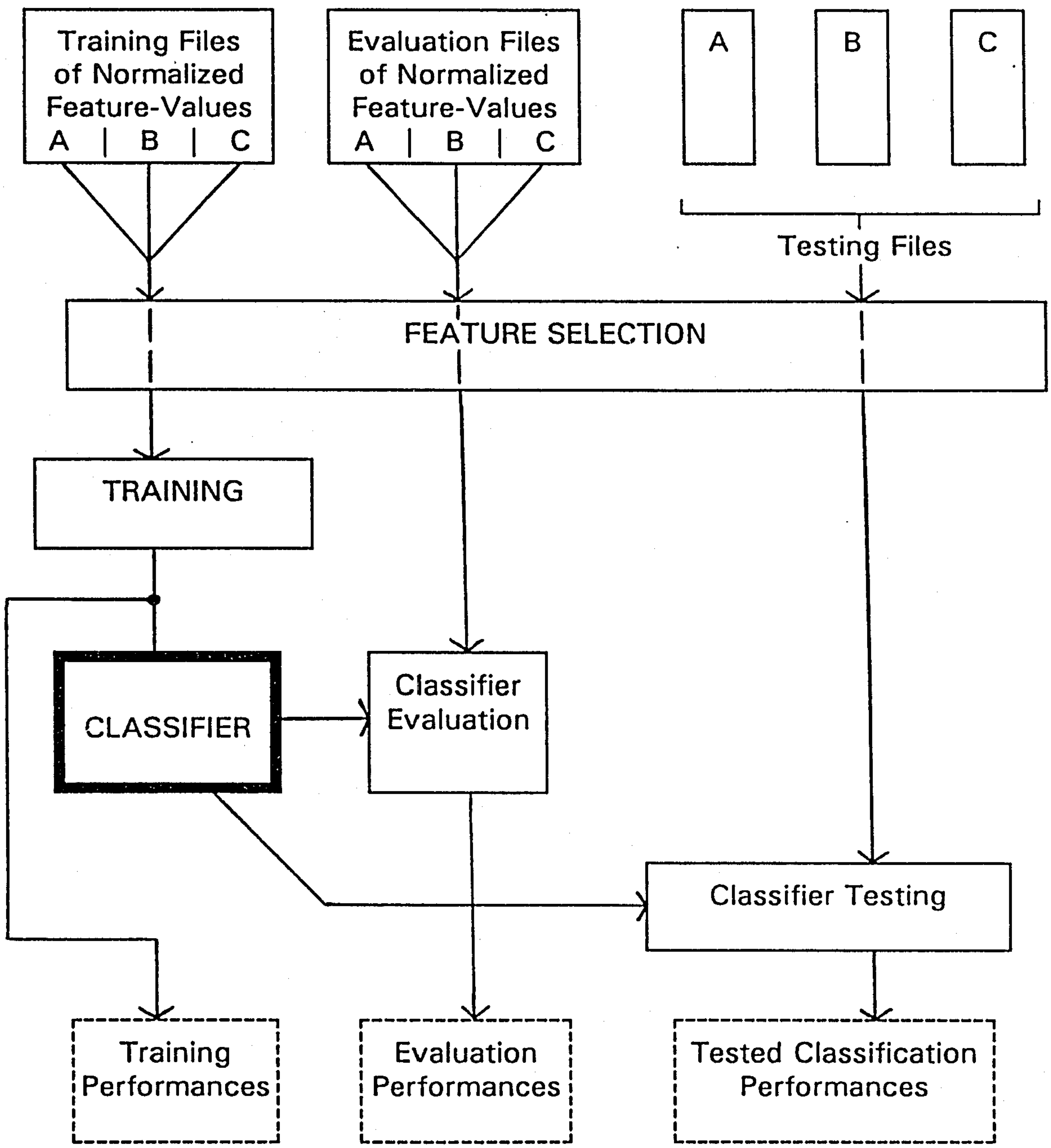

Figure 7.4. Schematics of the building and testing of the AU-Classifiers from files of normalized feature-values.

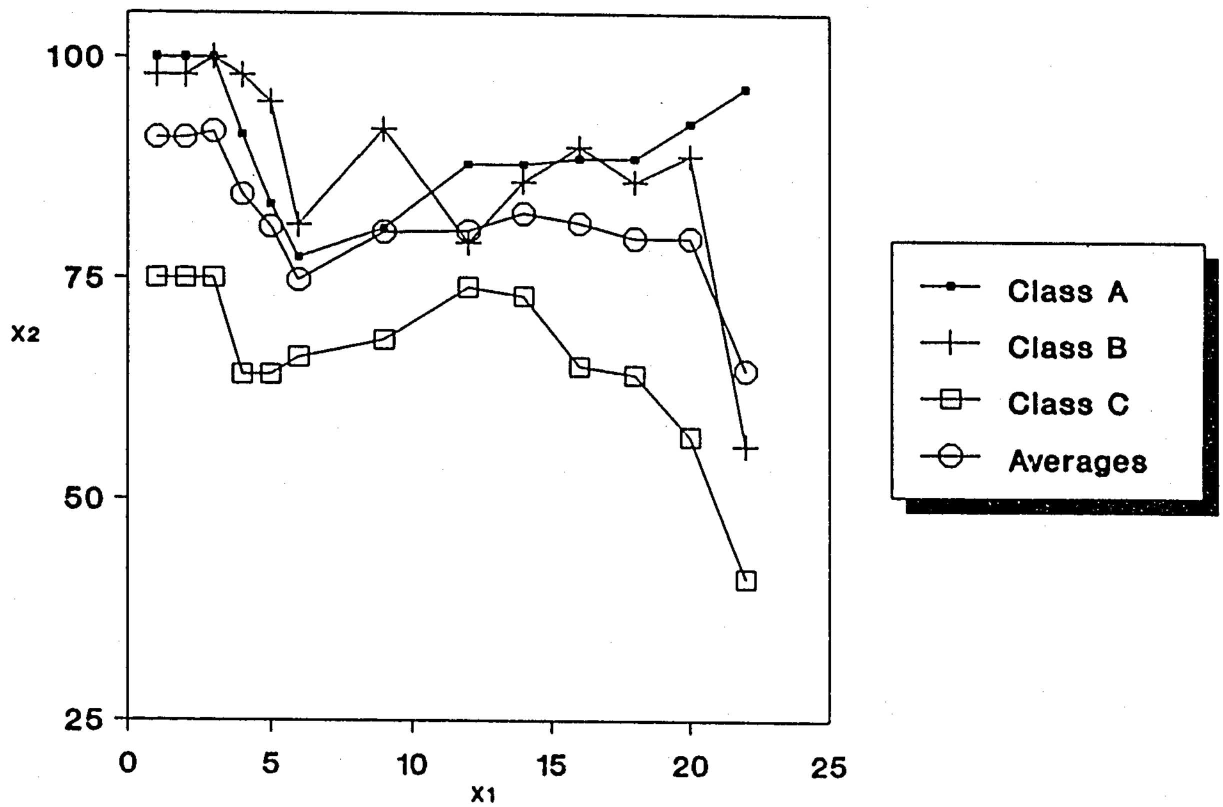

X1 : Number of used features as ranked by Fisher Discrimination Ratio.
X2 : Classification Performance in % of correctly classified AU-signals.

Figure 7.5. Classification performances for **Empirical Bayesian Classifiers** pertaining to the number of features used for Classifier building.

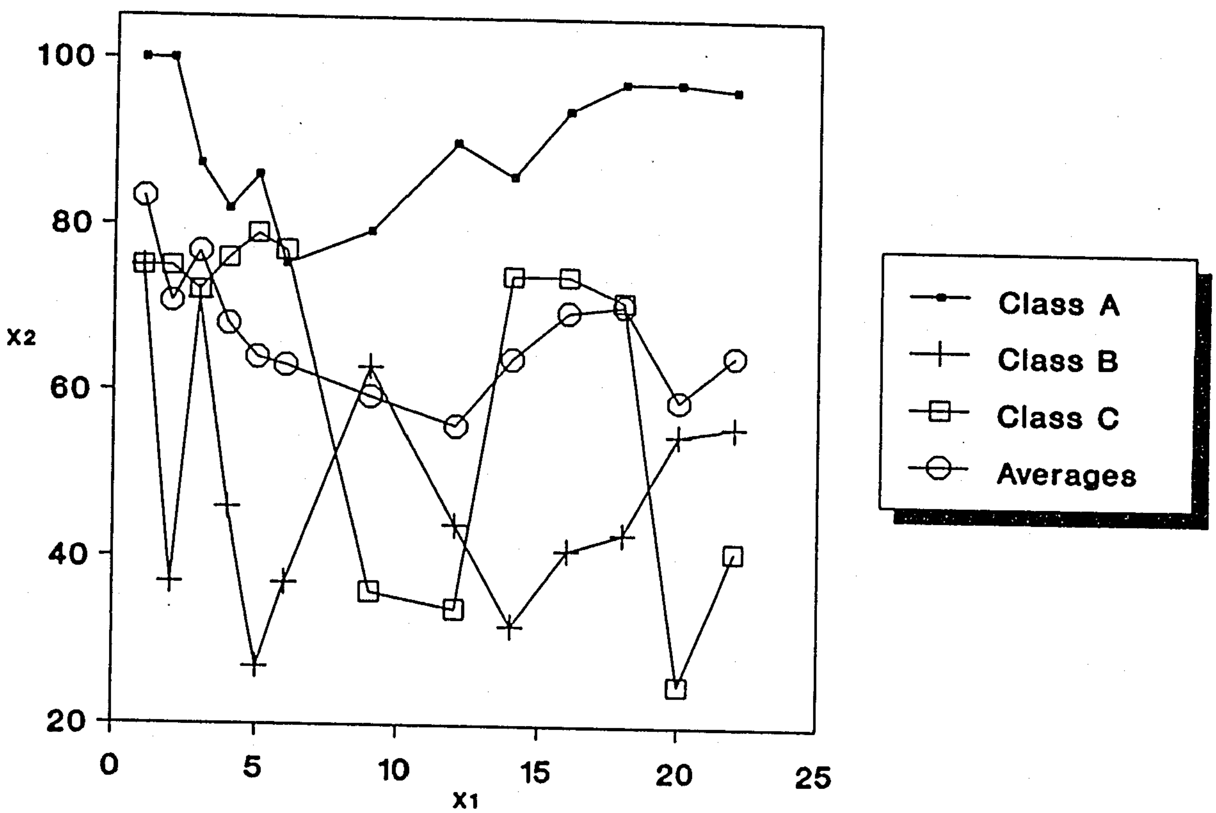

X1 : Number of used features as ranked by Fisher Discrimination Ratio.
X2 : Classification Performance in % of correctly classified AU-signals.

Figure 7.6. Classification performances for **Linear Discriminant Classifiers** pertaining to the number of features used for classifier building.

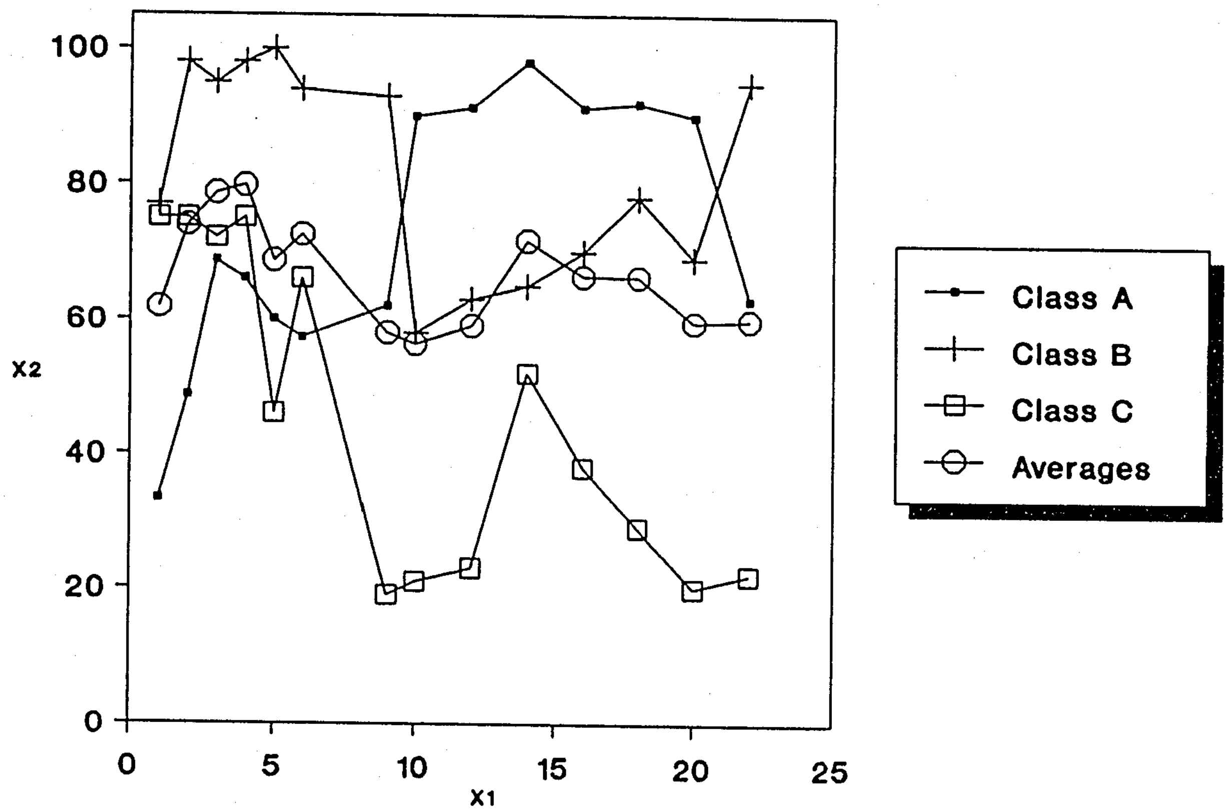

X1 : Number of used features as ranked by Fisher Discrimination Ratio.
X2 : Classification Performance in % of correctly classified AU-signals.

Figure 7.7. Classification performances for **K-Nearest Neighbour Classifiers** pertaining to the number of features used for classifier building.

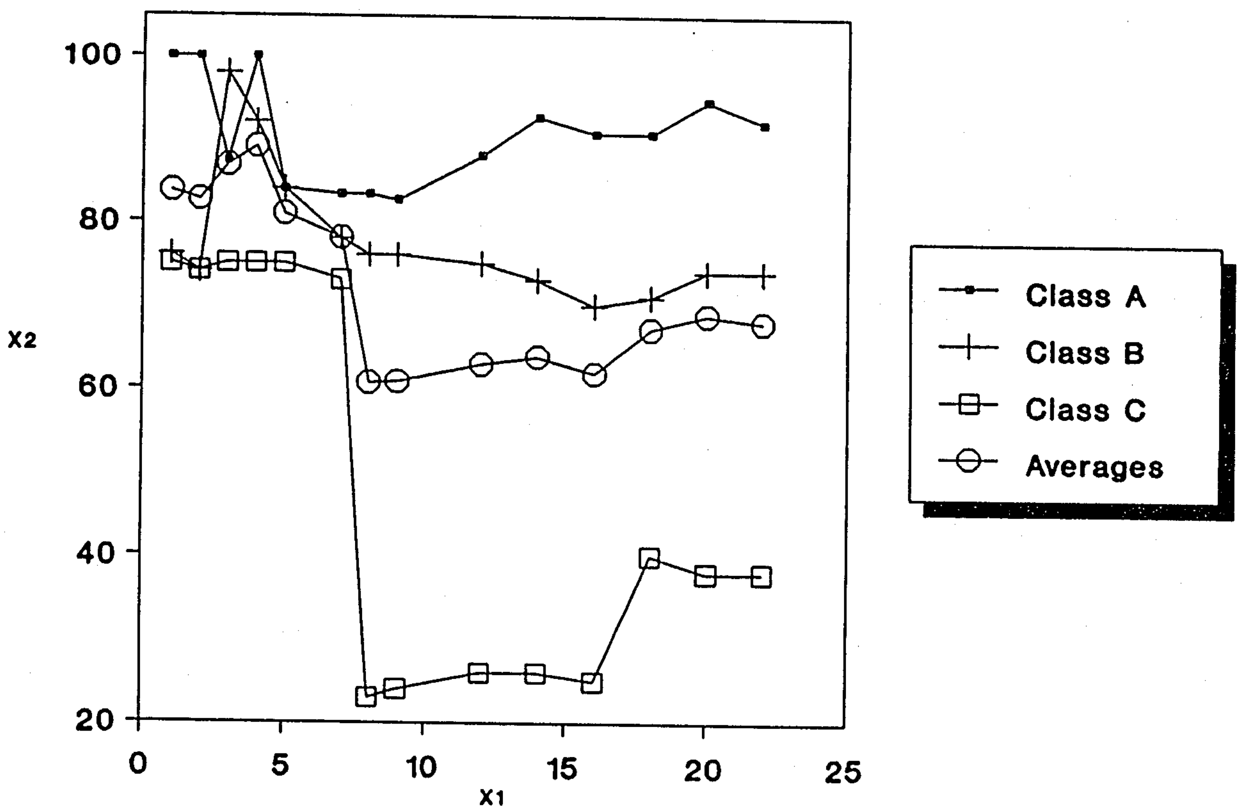

X1 : Number of used features as ranked by Fisher Discrimination Ratio.
X2 : Classification Performance in % of correctly classified AU-signals.

Figure 7.8. Classification performances for **Minimum Distance Classifiers** pertaining to the number of features used for classifier building.

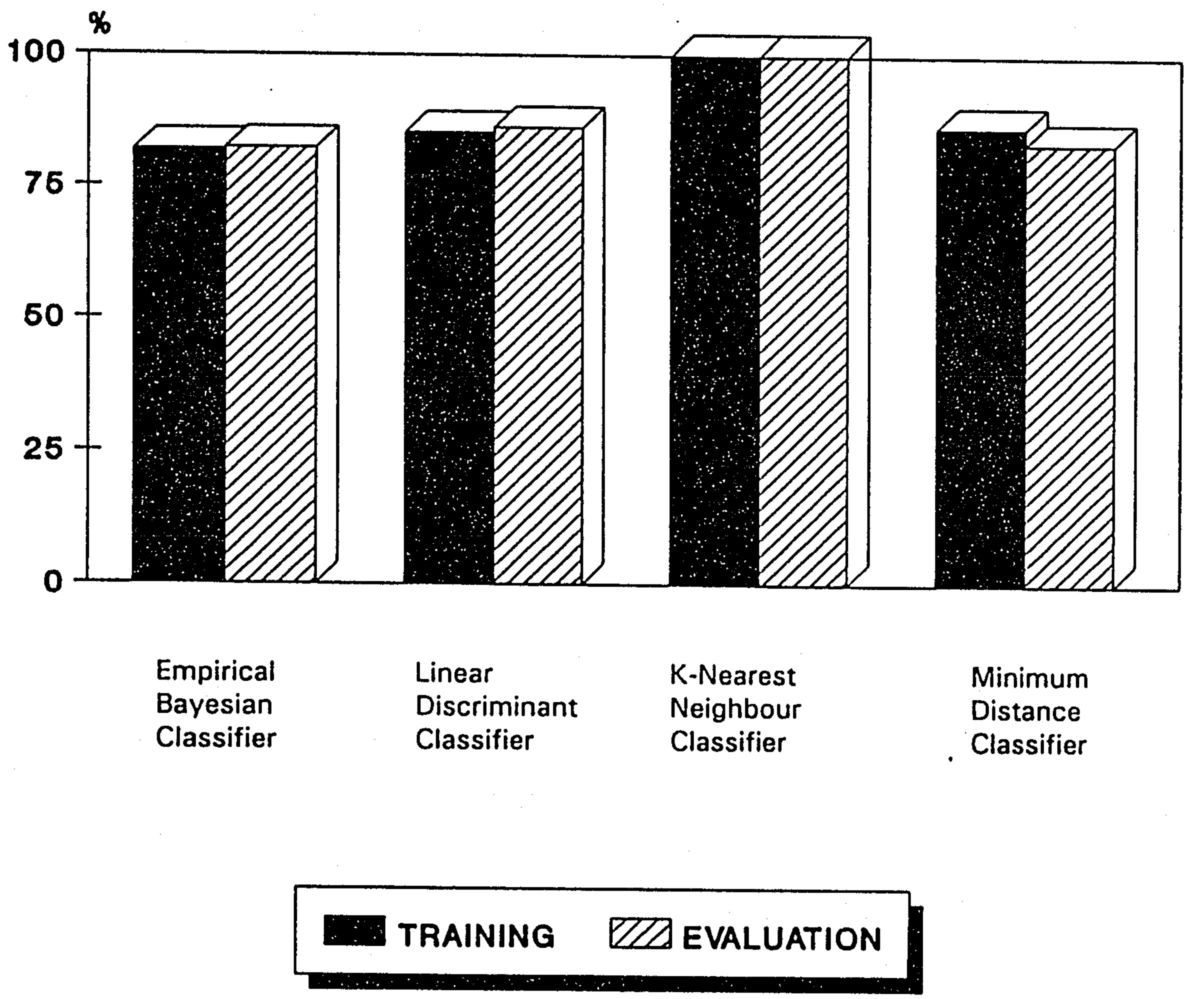

Figure 7.9. Training and Evaluation performances in % of correctly classified AU-signals for the four designed classifiers of Acousto-Ultrasonics signals pertaining to repeated-impact damage classes of polyvinylchloride specimens.

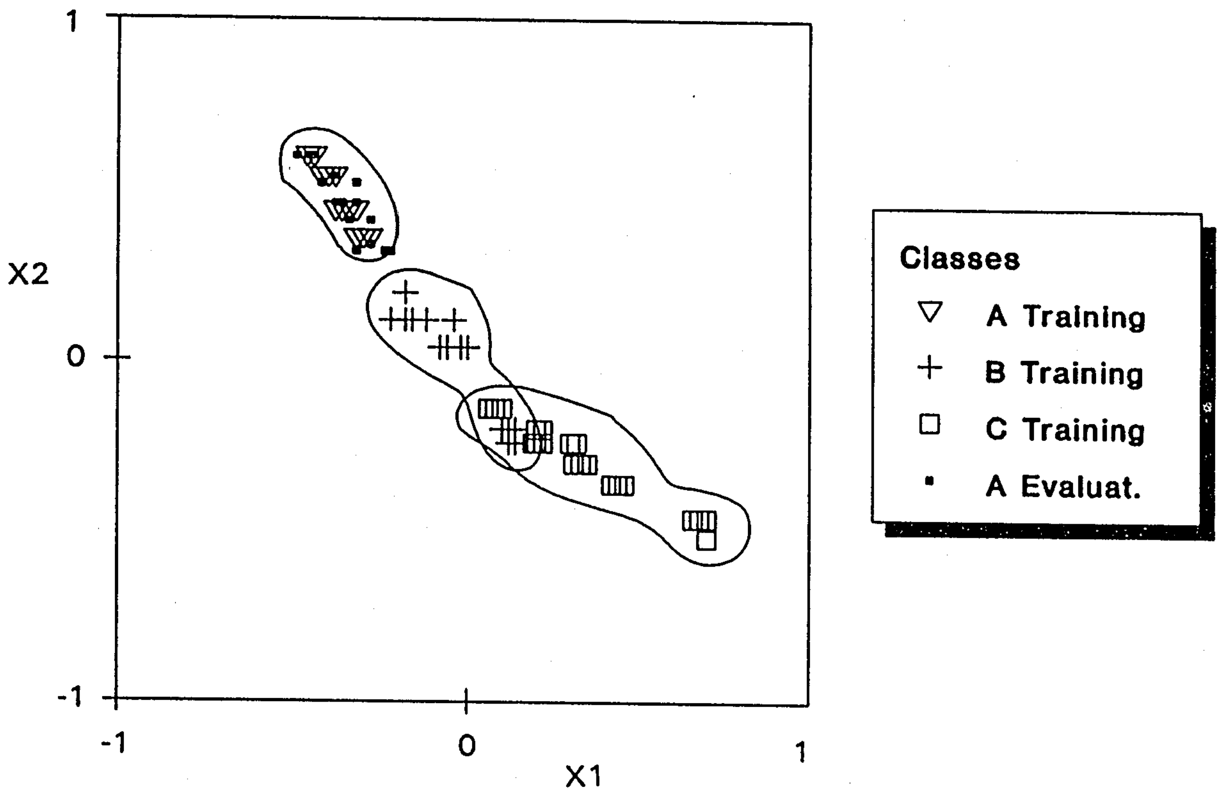

X1 : Normalized feature values of second-ranked feature.
X2 : Normalized feature values of first-ranked feature.

Figure 7.10. Normalized values of the two best-ranked features for Training and Evaluation Sets of Acousto-Ultrasonics data pertaining to repeated-impact damage levels in polyvinylchloride specimens.

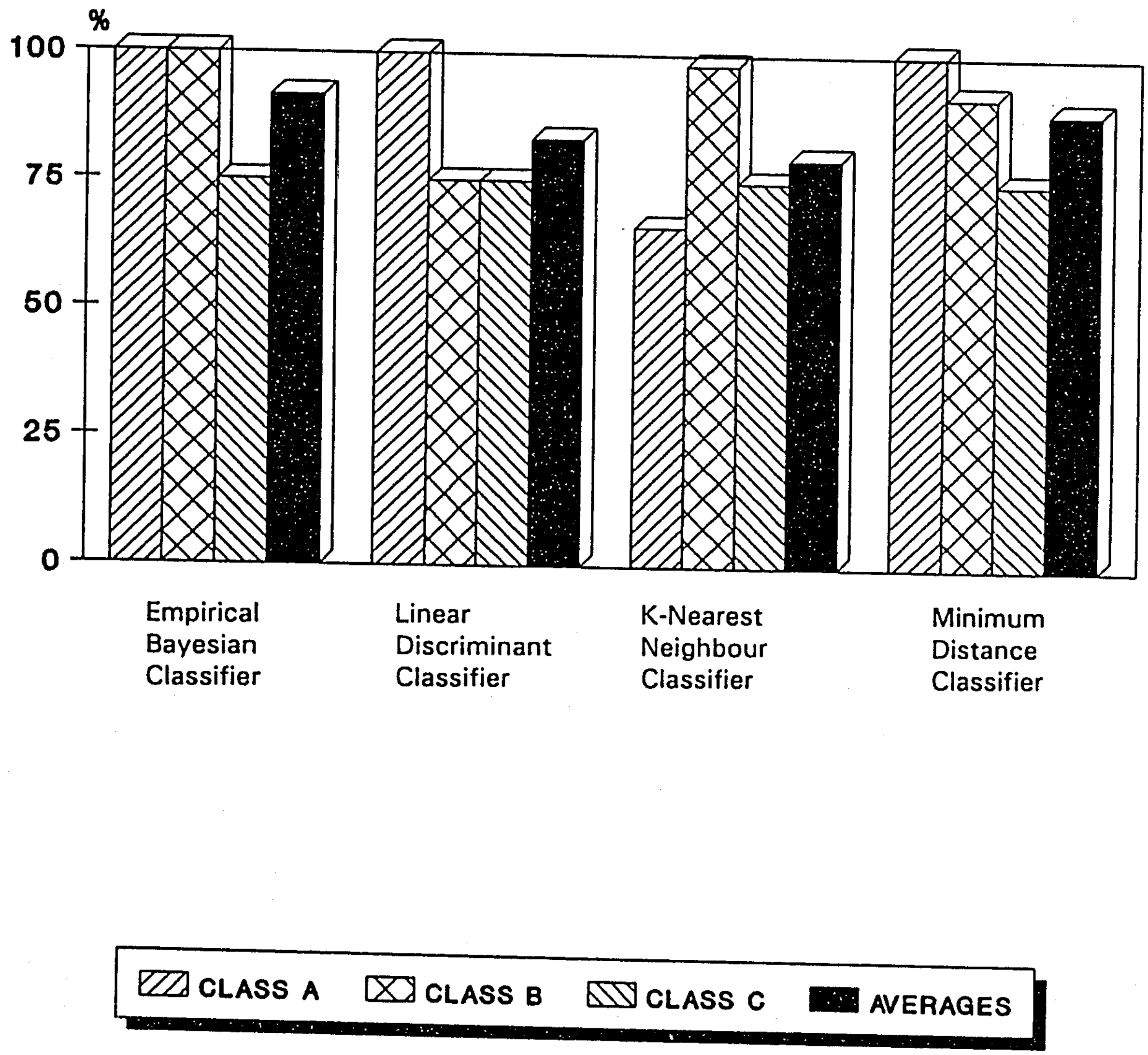

Figure 7.11. Classification performances in % of correctly classified AU-signals for the four designed classifiers of Acousto-Ultrasonics signals pertaining to repeated-impact damage classes of polyvinylchloride specimens.

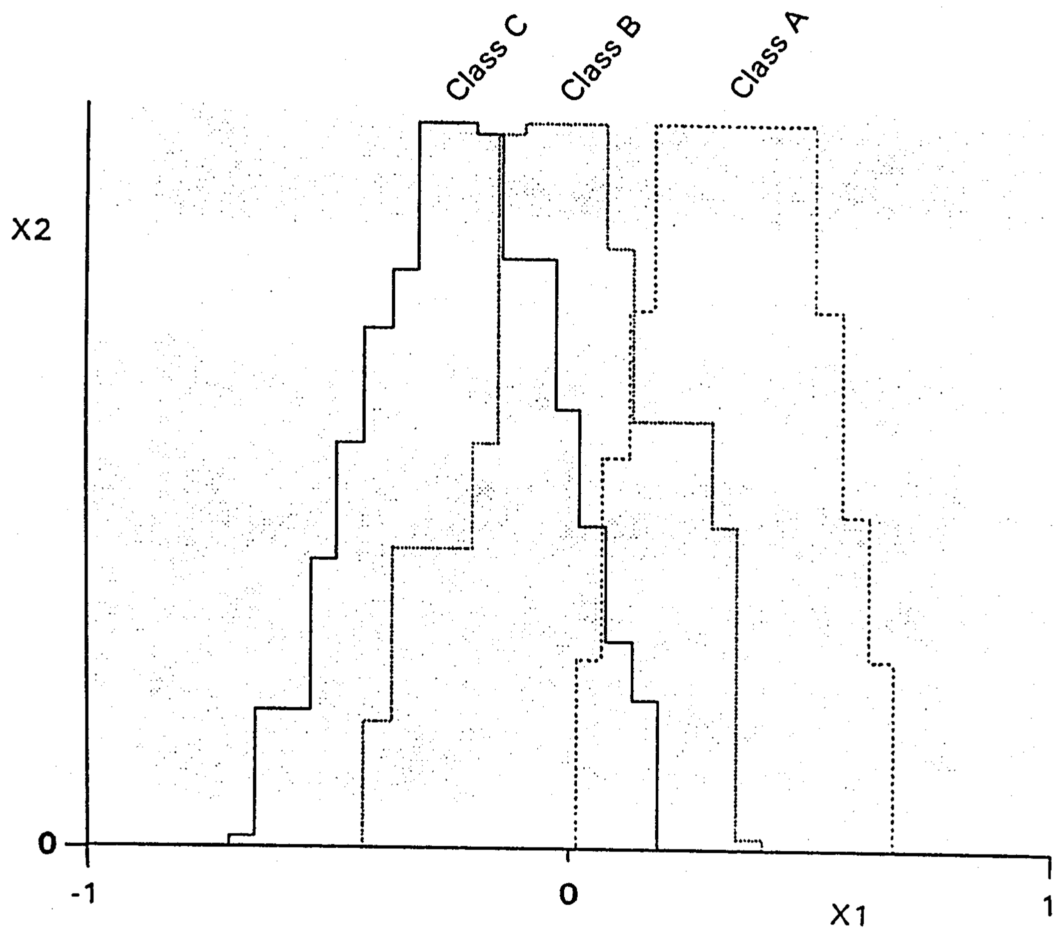

X1 : Normalized feature values of first-ranked feature.
X2 : Probability of ocurrence.

Figure 7.12. Probability Density Functions of the first ranked feature for Acousto-Ultrasonics data pertaining to repeated-impact damage classes of polyvinylchloride specimens.

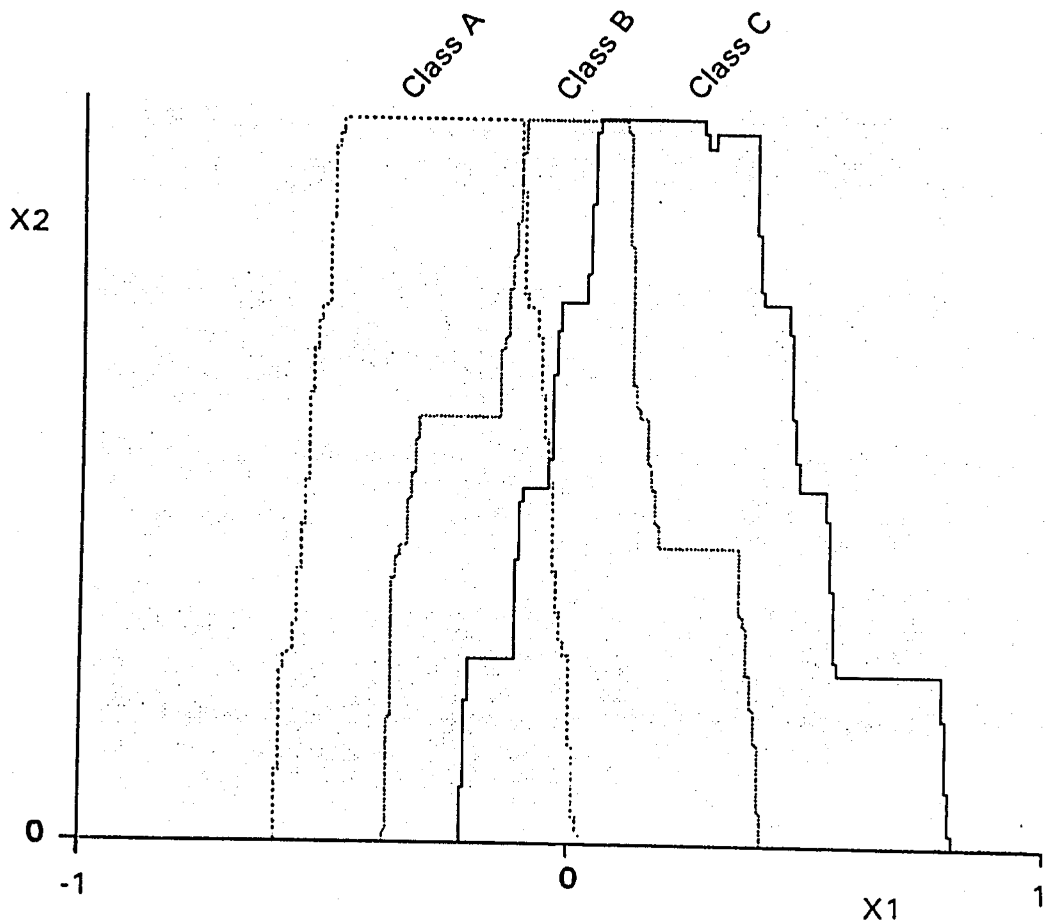

X1 : Normalized feature values of second-ranked feature.
X2 : Probability of ocurrence.

Figure 7.13. Probability Density Functions of the second ranked feature for Acousto-Ultrasonics data pertaining to repeated-impact damage classes of polyvinylchloride specimens.

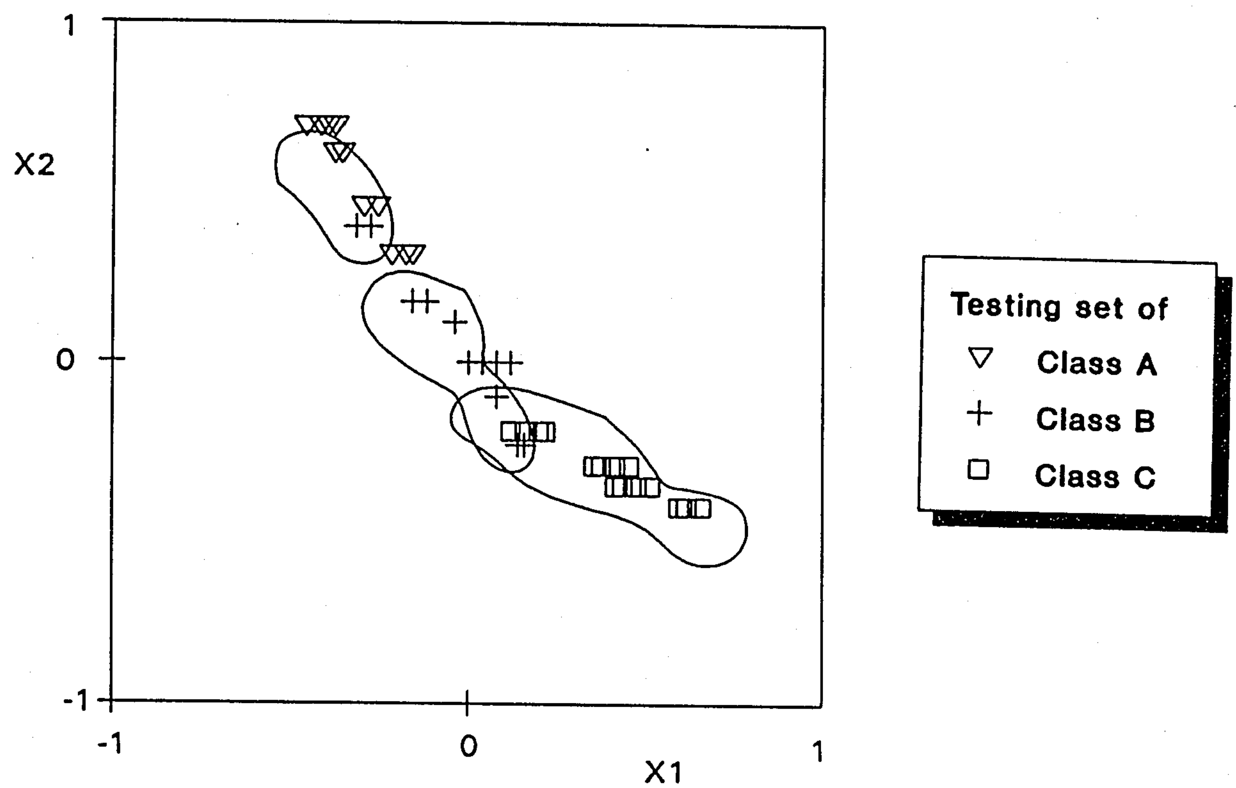

X1 : Normalized feature values of second-ranked feature.
X2 : Normalized feature values of first-ranked feature.

Figure 7.14. Normalized values of the two best-ranked features for Testing Sets and Classifier-Set boundaries for Acousto-Ultrasonics signals pertaining to repeated-impact damage levels of polyvinylchloride specimens.

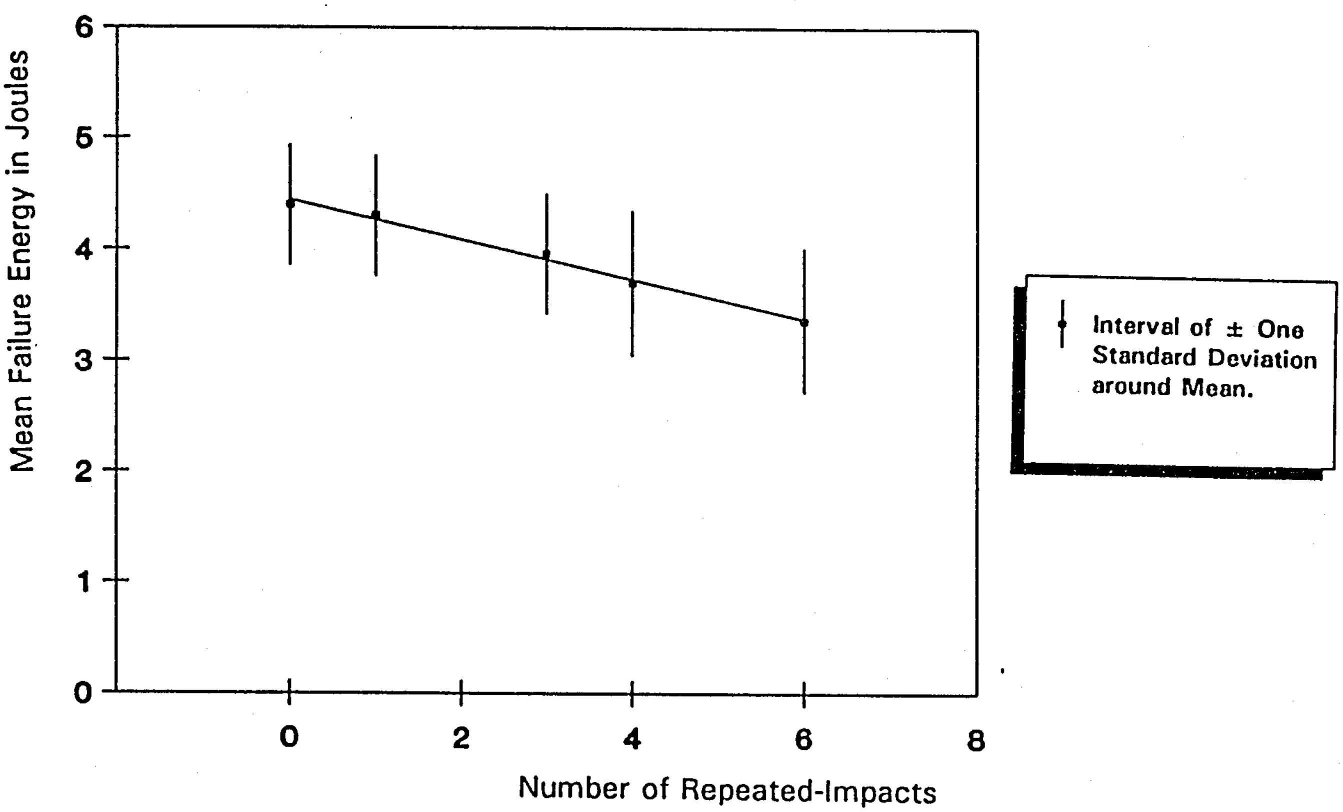

Figure 8.1. "Mean Failure Energy" versus number of repeated impacts for graphite/polycarbonate composite specimens.

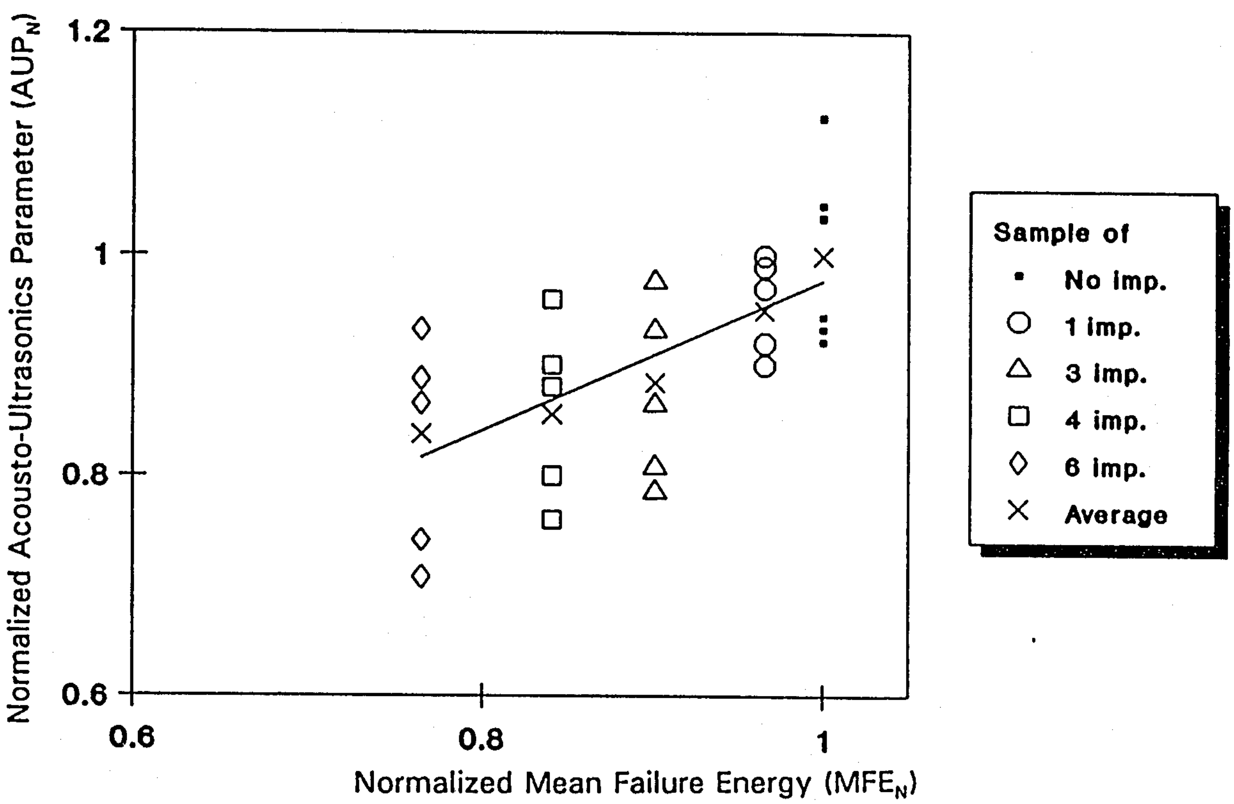

Figure 8.2. "Normalized Acousto-Ultrasonics Parameter" versus "Normalized Mean Failure Energy" for graphite/polycarbonate composite specimens.

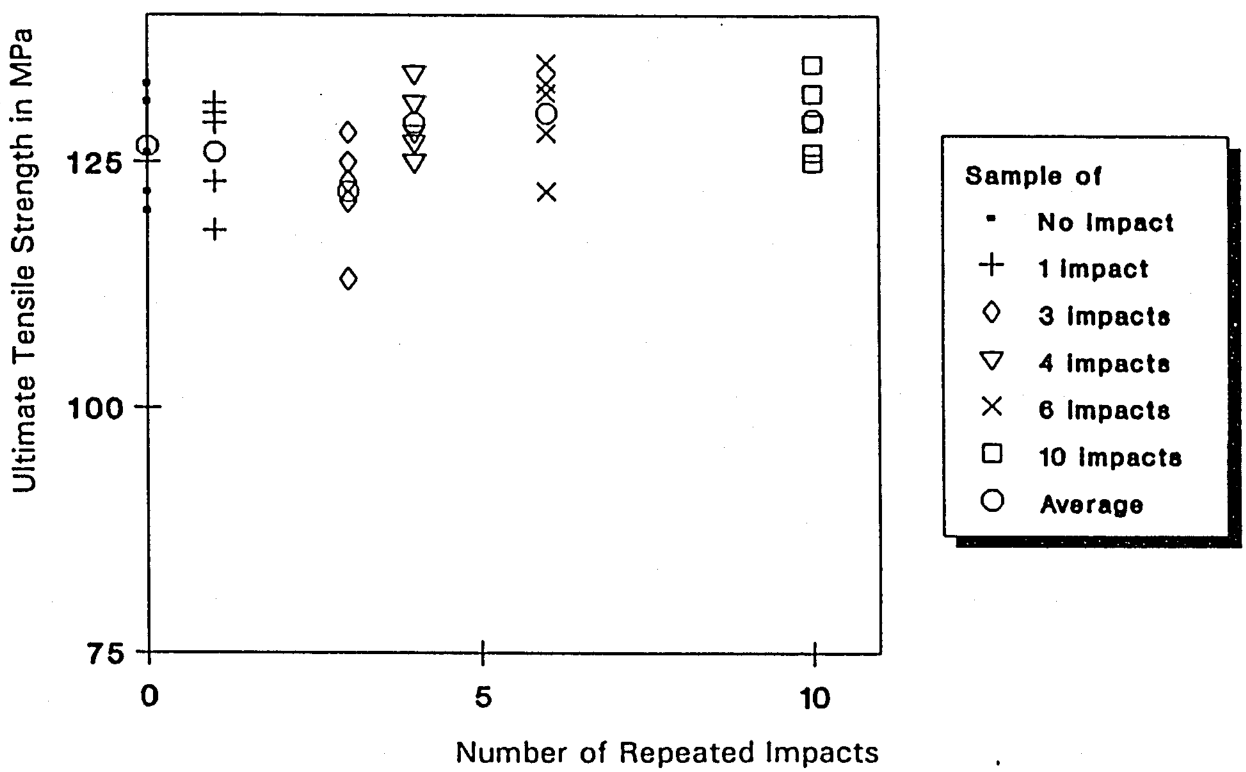

Figure 8.3. Ultimate Tensile Strength versus number of repeated impacts for graphite/polycarbonate composite specimens.

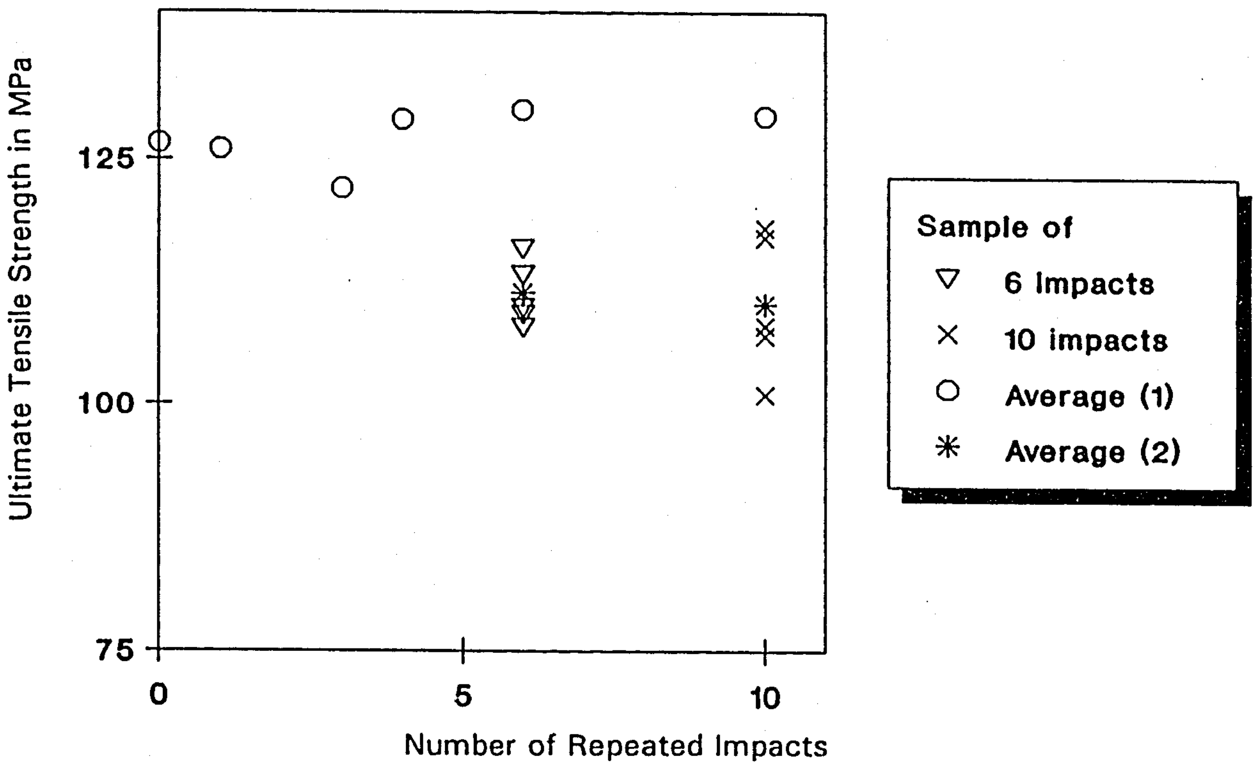

Average (1) Average Ultimate Tensile Strength for the samples of "surviving" composite specimens.

Average (2) Average Ultimate Tensile Strength for the samples of "failed" composite specimens.

Figure 8.4. Ultimate Tensile Strength versus number of repeated impacts for "failed" and "surviving" graphite/polycarbonate composite specimens

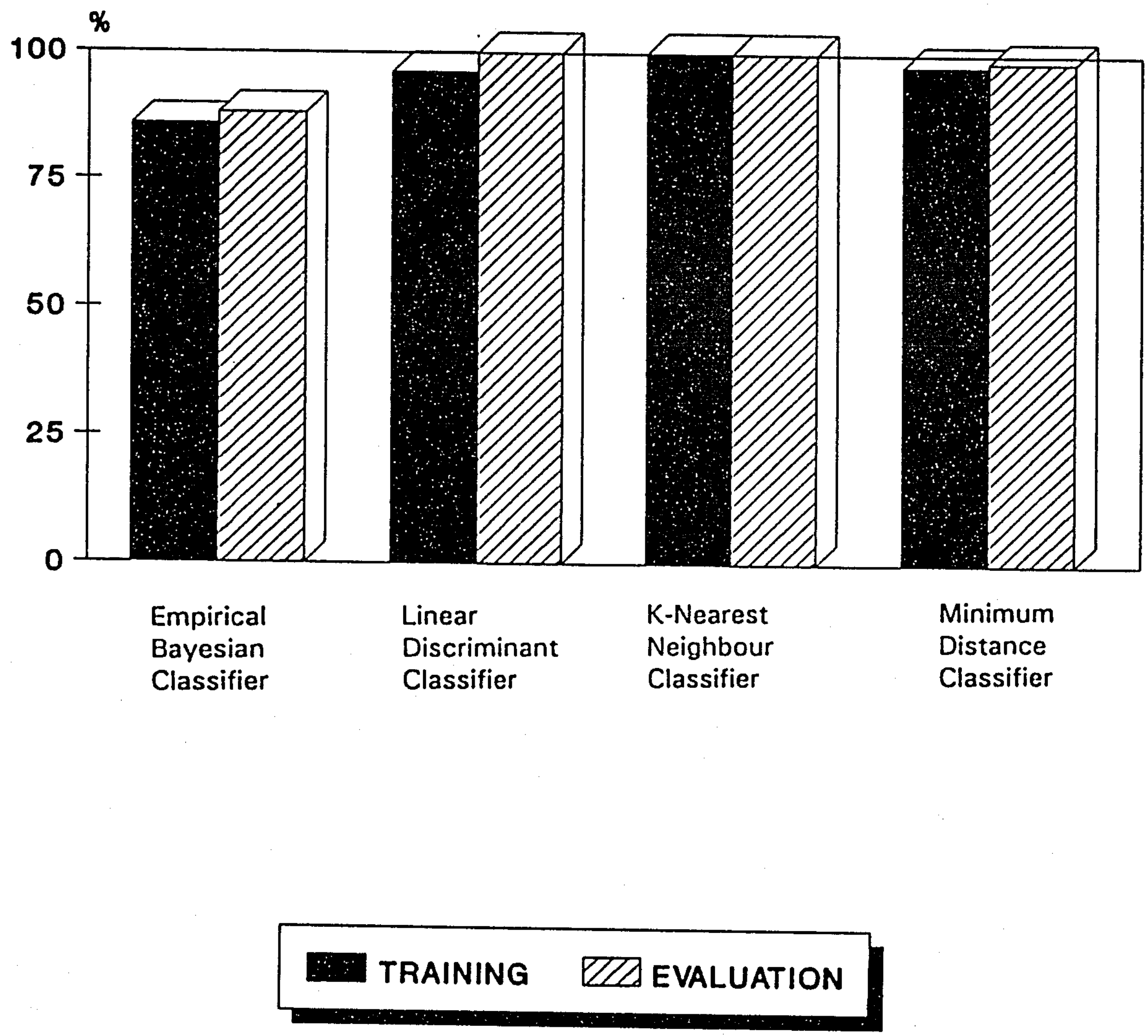

Figure 8.5. "Training" and "Evaluation" performances in % of correctly classified AU-signals for the four designed classifiers of Acousto-Ultrasonics signals of graphite/polycarbonate composite specimens.

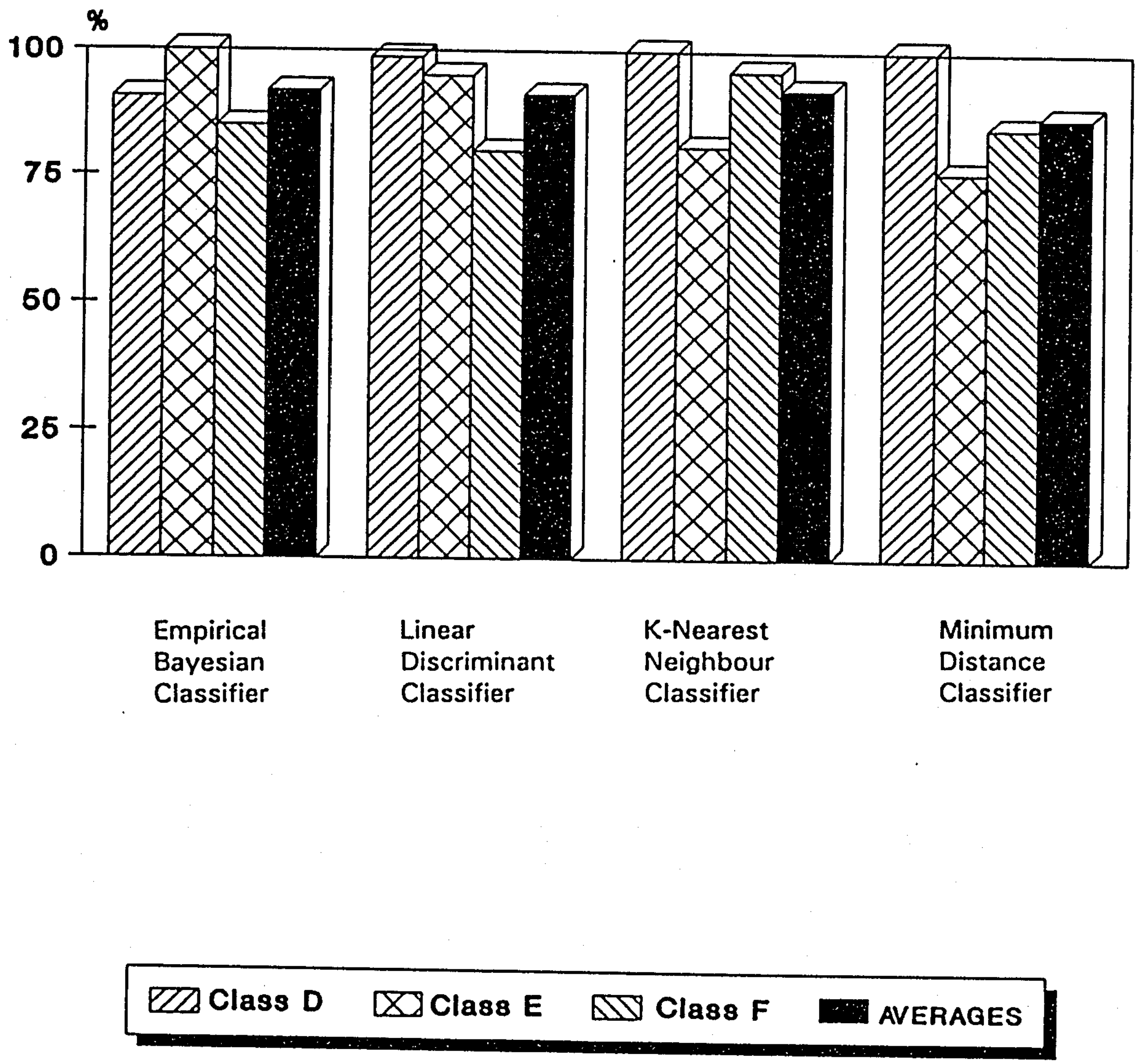

Figure 8.6. "Classification" performances in % of correctly classified Acousto Ultrasonics signals for the four designed classifiers of graphite/polycarbonate composite specimens.

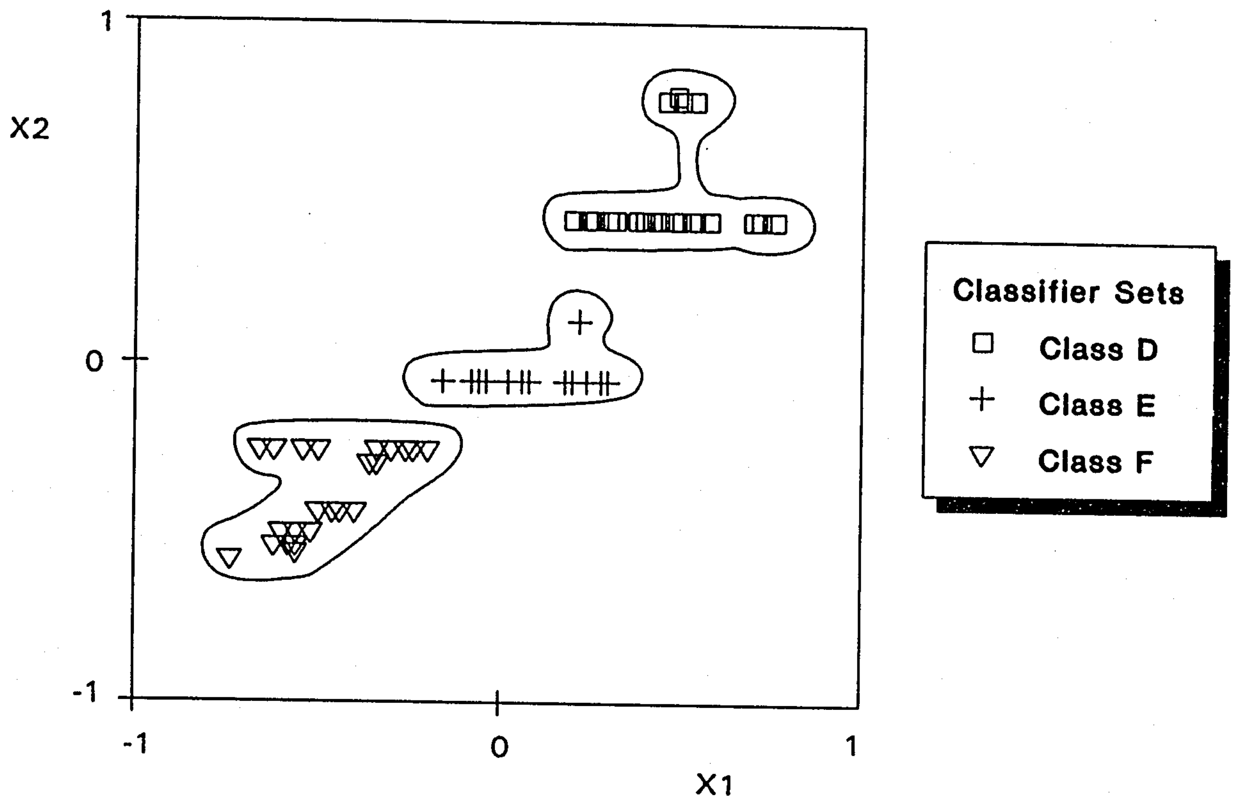

X1 : Normalized feature values of second-ranked feature.
X2 : Normalized feature values of first-ranked feature.

Figure 8.7. Normalized values of the two best-ranked features from Acousto Ultrasonics signals pertaining to repeated-impact damage levels in graphite/polycarbonate composite specimens.

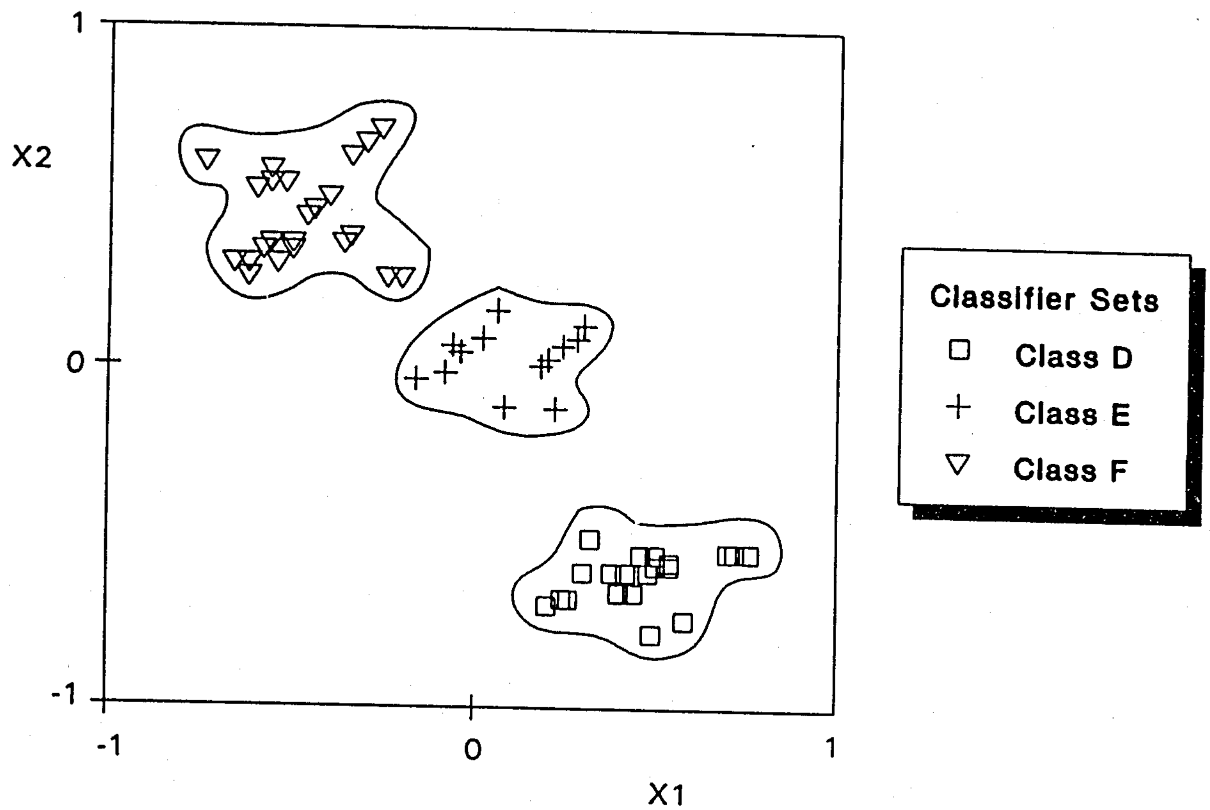

X1 : Normalized feature values of second-ranked feature.
X2 : Normalized feature values of third-ranked feature.

Figure 8.8. Normalized values of the second and third best-ranked features from Acousto-Ultrasonics signals pertaining to repeated-impact damage levels in graphite/polycarbonate composite specimens.